Radiosurgical dosimetry and the CyberKnife system: studies in verification, optimisation and comparison

Dr Alexander Martin

A thesis submitted for the degree of Doctor of Medicine (Research) at Queen Mary, University of London

June 2012

The Harley Street Clinic, and Barts Cancer Institute

Statement of Originality

I confirm that the work presented in this thesis is my own, unless otherwise indicated.

Abstract

Safe and effective delivery of radiosurgery demands a steep dose fall-off outside the target, in addition to highly conformal treatment and sub-millimetre overall accuracy. This thesis concerns the CyberKnife system - an image-guided radiosurgery system capable of treating both intra- and extracranial targets. Plan-specific QA performed using an ionisation chamber and radiochromic film confirmed that the dose distributions produced by MultiPlan software accurately reflect the treatment delivered, and therefore subsequent dosimetric studies using MultiPlan are valid. The relationship between prescription isodose value and external dose gradient (measured by the Gradient Index) was explored for solitary intracranial spherical targets, and then irregularly-shaped lesions. For smaller targets the steepest dose fall-off was achieved by prescribing to as close to the 50 % isodose as could be achieved. For larger targets the effect of changing the prescription isodose value was less marked but the optimum value was in the range 60 – 70 %. A planning method to optimise dose fall-off whilst maintaining other aspects of plan quality has been proposed. An additional study looked at optimising dose fall-off on one aspect of a target situated close to the brainstem. It was demonstrated that using "VOI" hard limits in treatment planning can reduce the brainstem dose substantially without any significant compromise on other important plan parameters. Finally, a dosimetric comparison between CyberKnife and the Gamma Knife system was performed for solitary intracranial targets. Overall, there was no significant difference in conformality and external dose gradient across the lesions studied. However the results suggested that Gamma Knife dosimetry may be superior for small lesions, and CyberKnife for larger ones. Whilst the experimental findings in this thesis relate to intracranial dosimetry, they may also be relevant to extracranial treatment planning using the CyberKnife system: this is a suggested area of future research.

Contents

Acknowledgements

Firstly I would like to thank HCA International for providing me with the opportunity to undertake this research, and for funding me fully during this period. In particular, thanks to Bernadette Stack and Aida Yousefi for their support during my research fellowship.

Thank you to my two supervisors, Nick Plowman and Amen Sibtain, for their many ideas and helpful discussions on the planning and execution of my research. Thank you also for providing me with very useful feedback on my draft chapters.

This thesis would not have been possible without the help and collaboration of a number of people more intelligent than me. I am indebted to Ian Cowley and Kelvin Hiscoke in the physics department at The Harley Street Clinic, for introducing me to the joys of radiotherapy QA and to various aspects of radiosurgery treatment planning. Ian, your "varied" iTunes music selection made those many treatment planning sessions much more interesting! Thank you also to Ian Paddick for collaborating with me on the dosimetric comparison study and for answering my many Gamma Knife questions.

Finally, to my wife Kinnary who has provided me with love and support throughout the last two and a half years, whilst also producing (and looking after) two beautiful children. This thesis is for you.

Abbreviations used in this thesis

ANOVA	Analysis of variance
AVM	Arteriovenous malformation
BED	Biologically effective dose
CCD	Charge-coupled device
CFR	Conventionally fractionated radiotherapy
CGI	Conformity Gradient Index
CI	Conformity Index
CK	CyberKnife
CT	Computerised tomography
CTV	Clinical target volume
DD	Dose difference
DICOM	Digital imaging and communications in medicine
dpi	Dots per inch
DRR	Digitally reconstructed radiograph
DTA	Distance to agreement
DVH	Dose volume histogram
EQD2	Equivalent dose in 2 Gy fractions
FSD	Source to focus distance
gEUD	Generalised equivalent uniform dose
GI	Gradient Index
GK	Gamma Knife
GTV	Gross tumour volume
HDR	High dose rate
ICRU	International commission on radiation units and measurements
IMRT	Intensity modulated radiotherapy
IPEM	Institute of physics and engineering in medicine
KV	Kilovoltage
LED	Light-emitting diode
Linac	Linear accelerator
LQ	Linear Quadratic

MeV	Megaelectron volt
MLC	Multi-leaf collimator
MRI	Magnetic resonance imaging
MU	Monitor units
MV	Megavoltage
MVD	Microvascular (surgical) decompression
nCI	New Conformity Index
OAR	Organ at risk
OMU	Optimise monitor units
PET	Positron emission tomography
PRI	Post-radiosurgery imaging
PTV	Planning target volume
QA	Quality Assurance
QDI	Quarter Dose Index
QUANTEC	Quantitative analyses of normal tissue effects in the clinic
RTSS	Radiotherapy structure set
SBRT	Stereotactic body radiotherapy
SCD	Semi-conductor diode
SRT	Stereotactic radiotherapy
SSD	Source to surface distance
TBD	Target boundary distance
TSS	Trans-sphenoidal surgery
V12	12 Gy Volume
V20	20 Gy Volume
VMAT	Volumetric modulated arc therapy
VOI	Volume of interest
WBRT	Whole brain radiotherapy

Index of Figures

Index of Tables

Chapter 1 - Introduction

Radiosurgery refers to the use of large single fractions of radiation, delivered with high accuracy to small, well-localised targets in the head or body. The term is often used interchangeably with Stereotactic Radiotherapy (SRT), although radiosurgery usually implies a single fraction treatment, whereas SRT may comprise a single or small number of high-dose fractions. In fact, "stereotactic" is no longer an all-embracing adjective for radiosurgical technologies as some systems now use sophisticated image guidance techniques instead of stereotactic coordinates for targeting and tracking during treatment.

Radiosurgery is conceptually different to conventionally-fractionated radiotherapy (CFR). In CFR, the planning target volume (PTV) comprises the target together with a margin of normal tissue. This margin is required to account for any inaccuracies in patient setup and treatment delivery. Treatment planning aims to cover as much of the PTV as possible with the prescription isodose line, and therefore a reasonable volume of normal tissue will inevitably receive the prescribed dose. CFR uses fractionation to exploit the different radiobiological behaviour shown by many tumours, relative to the normal tissue also encompassed by the prescription isodose line. This results in an improved therapeutic ratio (the degree of tumour cell kill for a given degree of normal tissue toxicity).

In contrast, radiosurgery uses little or no PTV margin around the target, and harnesses the ablative power of a large single dose of radiation. The safe and effective delivery of

radiosurgery therefore requires the utmost accuracy in patient immobilisation, target localisation (which may involve fusion of different imaging modalities), and treatment delivery. Consequently most modern radiosurgery systems have demonstrated "sub-millimetre" accuracy in phantom studies, as will be discussed later. However, radiosurgery also requires the ability to produce treatment plans in which the prescription isodose line conforms very closely to the target outline, outside which there is a steep dose fall-off (external dose gradient). Both conformality and a steep external dose gradient serve to reduce the volume of normal tissue receiving a clinically significant dose. These dosimetric parameters – in particular the optimisation of external dose gradients – form the basis of the experimental work carried out in this thesis.

History of radiosurgery

Stereotactic mapping of the brain was first described by Victor Horsley and Robert Clarke in 1906. They developed a method of accurately locating deep-seated brain lesions by assigning coordinates in three planes to neuroanatomical structures, based on cranial landmarks. They used their "stereotaxic apparatus" to explore the anatomy and function of the cerebellum in cats and monkeys (1). However the variable relationship between skull landmarks and cerebral structures in humans prevented the use of this technique in patients. In 1946 Spiegel and Wycis (2) developed a technique of relating intracranial targets to landmarks within the brain, namely the pineal gland and foramen of Monro, which were visualized using a pneumoencephalogram. Central to the design was a custom-made plaster head cap known as a stereoencephalatome, and a frame based 3-dimensional coordinate system relative to this. This became the first stereotactic apparatus used routinely on patients.

Meanwhile, following the discovery of x-rays by Roentgen in 1895, the new medical discipline of radiology was born. The best documented early report of the therapeutic use of x-rays was by Freund (3) in 1897, who treated a large pigmented naevus on the back of a five year old girl. The term "radiotherapy" came into use in the 1920s, around the time that diagnostic and therapeutic radiology were emerging as distinct specialties. Early radiotherapy practitioners used radium, with teleradium units appearing in the 1930s. Around the same time, the first therapeutic kilovoltage X-ray tubes became available, in which photons are produced using thermionic emission. Cobalt beam units and then megavoltage linear accelerators were introduced in the 1950s. The higher energy of these techniques enabled more effective treatment of deeper targets within the body.

Lars Leksell, a Swedish neurosurgeon, was the first person to marry the two developing fields of stereotaxy and radiotherapy, and introduced the term "radiosurgery" in 1951. He had developed a stereotactic system for performing image-guided surgery on deep brain structures. The surgical "tool" was mounted on an arc, which was in turn attached to a stereotactic head frame fixed to the skull. Imaging was obtained with the frame in place, and the arc positioned so that the target coincided with its centre. Instruments inserted from any point along the arc would be incident on the target (Figure 1.1). He realised that narrow x-ray beams delivered from multiple points on the arc would result in a high dose to the target, and a substantially lower dose to surrounding tissue (4). He initially employed multiple orthovoltage tubes (photon energy approximately 250 KV) but found they were of both insufficient energy and accuracy for targeting deep brain lesions. In 1967 he developed the first Gamma Knife prototype using 179 individual

Figure 1.1 Image showing the Leksell stereotactic frame. The frame is afixed to the skull using four screws. A needle is attached to an arc which, in turn, is fixed to the frame. Movement of the needle relative to the skull is possible in Anterior-Posterior, Left-Right and Superior-Inferior directions, with x,y and z coordinates for any needle position.

Cobalt-60 sources, each emitting gamma rays of energy 1.17 and 1.33 MeV, and all incident on the target. Over the last forty years the system has undergone a number of modifications, although the principles remain the same. The latest model, Gamma Knife Perfexion (Elekta, Stockholm, Sweden) is described in detail in Chapter 2.

The first radiosurgical treatments were functional ablations in patients with intractable pain, with target response assessed clinically, and later at post-mortem. Treatment was then expanded to include vascular obliteration of brain arteriovenous malformations (AVMs) and growth arrest of acoustic neuromas, since these targets could be accurately visualised using angiography and plain tomography respectively. The development of computed axial tomography (CAT, or CT) by Hounsfield in the early 1970s (5) allowed treatment planning based on axial imaging, thus expanding the range of intracranial targets which could be localised for radiosurgery. Also, together with the development of computers, CT enabled the use of 3-dimensional dose distributions, which is now central to most modern radiotherapy systems. The advent of Magnetic Resonance Imaging (MRI) followed a few years after CT, offering enhanced resolution of many intracranial targets. This is now the preferred method of target delineation for most solid tumours in the brain.

The early 1980's saw the adaptation of linear accelerators (linacs) for intracranial stereotactic delivery, with the earliest published reports from Argentina (Betti et al) (6) and Italy (Colombo et al) (7). The required accuracy was again achieved using a pinned stereotactic head frame, and radiation was administered via multiple non-coplanar arcs around the patient using the linac gantry. This was followed quickly by the development of specialist radiosurgical dosimetry software eg X-Knife (Radionics, Boston, MA).

Linacs dedicated to delivering radiosurgery started to appear in the 1990's, and modern examples include Novalis TX (BrainLAB, Munich, Germany) and Elekta Axesse (Elekta). Recent developments include increased conformality through the use of both micro-multi-leaf collimators (micro-MLCs) and modulated arc therapy/tomotherapy.

Whilst a pinned stereotactic frame provides (near) absolute immobilisation, its use is limited to the treatment of intracranial targets, which show negligible movement relative to the skull. It is also limited to single fraction treatments. Relocatable stereotactic frames have been used by some centres to allow fractionation of treatment, usually for larger tumours where there may be concerns over using a single fraction. For example the Gill-Thomas-Cosman frame uses a mouthbite together with vertical brackets to achieve the required immobilization and reproducibility. Its introduction in the UK in 1989 allowed fractionation of radiosurgery for the first time (8). However, relocatable frames are now being replaced by modern image guidance as described below.

Extracranial targets do not share the same fixed relationship with any external body contour, and there can be both inter- and intra-fraction target and critical organ movement. This has historically limited the use of single fraction radiation treatment to targets outside the skull. However, over the last fifteen years, advances in "on-line" radiotherapy image guidance technology mean that many extracranial targets can now be tracked with the required accuracy to deliver radiosurgical doses safely. Modern systems use either volumetric imaging (eg cone-beam CT or in-room CT-on-rails), or planar imaging together with implanted fiducial markers or bone-tracking software. As a result of this improved technology, "Stereotactic" Body Radiotherapy (SBRT) has

emerged as a new treatment, and its use has been increasing steadily over the last decade.

CyberKnife (Accuray Inc, Sunnyvale, CA) is an example of a modern image-guided radiosurgery system. It was first conceived in 1990 by John Adler, a neurosurgeon at Stanford University, with the first patients being treated a few years later (9). A compact X-band linac is mounted on a six-joint robotic arm, allowing delivery of multiple non-coplanar beams from a wide range of angles around the patient. Image guidance is achieved by virtue of two kilovoltage x-ray sources positioned at 90 degrees to each other. The use of planar imaging allows intra-fraction image guidance with repeat imaging (and adjustment if necessary) after each beam delivered. Thus the system can deliver "frameless" radiosurgery to both intracranial and extracranial targets. Additionally, since no frame is needed, treatment can be fractionated where appropriate. A detailed description of the CyberKnife system components follows in the next chapter.

Clinical use of intracranial radiosurgery

There are now over forty years' published data on the use of intracranial radiosurgery. Most of this experience has come from the Gamma Knife system, although there have also been important publications from centres using gantry-based linacs and, more recently, the CyberKnife system. As stated above, the first radiosurgery treatments were for functional disorders such as trigeminal neuralgia, and whilst the technique was temporarily abandoned for this indication in the 1970's-80's, the availability of high quality MR imaging led to a re-emergence of use in the 1990's, and there have since

been some encouraging reports. For example, Régis et al (10) presented prospective data from one hundred patients treated with a single maximum dose of 70 – 90 Gy using Gamma Knife. At minimum twelve months follow-up, 83/100 were pain-free and 58 had stopped taking medication. There was a 10 % incidence of mild facial paraesthesia or hyperaesthesia. However, the authors acknowledge that microvascular surgical decompression (MVD) should be considered as the first-line treatment in most cases.

There is a large body of published experience of the use of radiosurgery for the treatment of arterio-venous malformations (AVMs), and it is now regarded as the standard of care for many of these patients. High-dose irradiation causes progressive stenosis, luminal closure and eventual obliteration of the AVM nidus. The University of Pittsburgh Gamma Knife centre has been a regular contributor to the literature. For example, Flickinger et al (11) reported a 75 % nidus obliteration rate in 351 patients treated with a single marginal dose of 12 – 30 Gy (median 20 Gy). On dose-response modelling, there was an estimated 88 % maximum obliteration rate, for doses in the region of 22 – 25 Gy. There was no evidence for any benefit of dose escalation beyond 25 Gy. The same authors had also performed multivariate analysis on the data from 307 AVM patients, investigating risk factors for developing post-radiosurgical imaging (PRI) changes predictive of symptomatic complications. The 12 Gy volume (V12) was the only parameter showing a significant correlation with development of PRI changes (12). In a further publication (13), these authors have produced V12 graphs for different parts of the brain, which predict the risk of complications, and which are used by many centres as an aid to radiosurgical treatment planning (Figure 1.2).

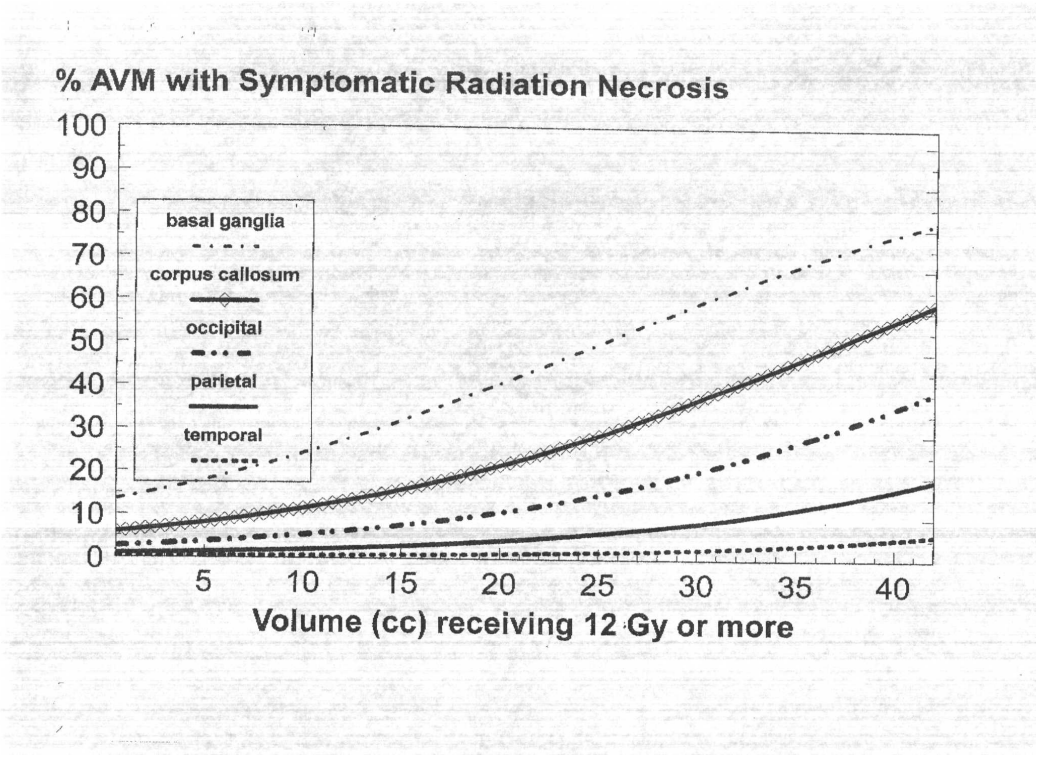

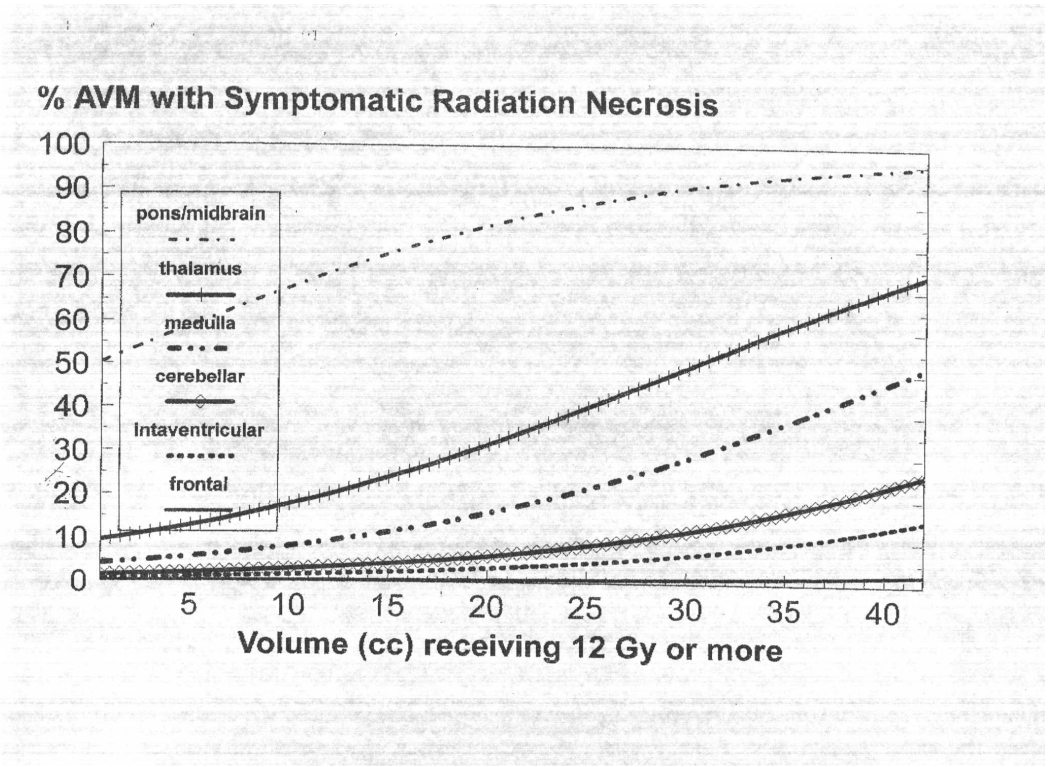

Figure1.2 Graphs showing the percentage risk of symptomatic radiation necrosis against the volume of brain receiving 12 Gy or more, with different plots for the different areas of the brain. Graphs produced from Pittsburgh Gamma Knife Center patient data(13).

The treatment of small (< 3-4 cm diameter) acoustic neuromas (vestibular schwannomas) is another area where many people now regard radiosurgery as the standard of care. The radiation dose required to give long-term tumour control is lower than orginally predicted, and so prescribed doses have come down (eg 12.5 – 13 Gy in one fraction or 18 Gy in three fractions), in turn leading to improved complication rates. When compared to most surgical series, modern radiosurgery gives comparable local control and improved hearing preservation, together with reduced treatment-related morbidity. Lunsford et al (14) presented a retrospective review of fifteen years' experience, treating 829 patients with a median marginal dose of 13 Gy using Gamma Knife. In the 252 patients with more than ten years' follow-up, long-term local control was 98 %, although local control was defined as "absence of the need for further intervention". The 5-year actuarial rates of hearing preservation and speech preservation were 69 % and 86 % respectively. It has been suggested that fractionating treatments may result in less cranial nerve damage (for example, 18 Gy in 3 fractions is favoured by Stanford CyberKnife centre (15)) although superiority over single fraction regimens remains to be proven.

Surgery remains the best treatment for many intracranial meningiomas, however tumours located near the base of skull are very difficult surgical targets, and the risk of complications is much higher, even with modern microsurgical techniques. Radiosurgery has emerged as a very good treatment option for small meningiomas, especially in surgically hazardous locations such as the cavernous sinus and optic nerve sheath. The biggest single retrospective analysis of the results of benign meningiomas treated with radiosurgery has been performed recently by Santacroce et al (16). 5300 tumours in 4565 patients were treated across fifteen participating Gamma Knife centres,

using a median marginal dose of 14 Gy. Local control was 93 % with median five years radiological follow-up. This comprised a decrease in tumour volume in 54 %, and stable appearances in the other 39 %. The permanent morbidity rate was 6.6 %. Colombo et al (17) have reported on 199 meningioma patients treated with CyberKnife using 2 – 5 fractions. Local control was 92 % with median 30 months follow-up. Approximately 30 % of these patients had tumours which would have been considered too large for single fraction radiosurgery.

Trans-sphenoidal surgery (TSS) is the preferred primary treatment for most pituitary adenomas and, in the case of secreting tumours, patients can feel better in a matter of hours. CFR is usually offered as adjuvant treatment, for example, if secreting hormone levels do not come down satisfactorily. Radiosurgery is sometimes used in the adjuvant setting, but has a more established role in the salvage of patients with small, discrete local recurrence. Pituitary tumours are often situated very close to the optic apparatus, and the steep external dose gradients produced in radiosurgery are especially important here. Mingione et al (18) reported on one hundred consecutive patients with residual or recurrent non-secretory pituitary macroadenoma, treated with a single median marginal dose of 18.5 Gy (range 5 – 25 Gy). There was 92 % local control with median 45 months radiological follow-up, with tumour volume decreasing in 66 %. The incidence of hormonal deficit in patients with fully-functioning glands was 20 % at median four years follow-up. Recent UK data have established the usefulness and safety of radiosurgery for treating focal relapse of pituitary adenoma in patients who have already received CFR (19).

The management of brain metastases is a controversial area. Unlike the above conditions, these patients generally have a very poor prognosis. Median overall survival is approximately seven months, although this can be stratified using the disease-specific graded prognostic assessment (20) in order to identify patients most likely to benefit from intervention. Surgery, radiosurgery and whole brain radiotherapy (WBRT) are all treatment options, and can be used in combination. The published literature contains many different permutations and can appear confusing.

Patchell et al (21, 22) have provided two small randomised trials involving the use of surgical resection in patients with single brain metastases. Firstly, the addition of surgical resection to WBRT resulted in a significant overall survival advantage (40 weeks vs 15 weeks) and greater preservation of functional dependence, compared to WBRT alone (21). A second trial used surgery +/- post-operative WBRT, again for single brain mets. This showed a significant decrease in recurrence, both locally and in the rest of the brain, in the arm receiving WBRT. There was no overall survival difference, although the trial was underpowered to detect this (22). More recently there has been interest in the use of radiosurgery to the post-operative resection cavity (23), thus removing, or at least delaying, the need for WBRT.

Andrews et al (24) have provided level 1 evidence of increased local control and overall survival from the addition of a radiosurgery boost to patients who have undergone WBRT for a single metastasis. However, there was no significant benefit in patients with multiple metastases. Chang et al (25) explored the benefit of adding WBRT to radiosurgery in 58 patients with up to three metastases. One-year local control rates were lower, and distant brain recurrence rates higher, in the radiosurgery-only arm, with

a greater number requiring salvage treatment. However, overall survival was actually higher in this arm, and cognitive decline (as measured using verbal memory tests) was less at four months post treatment.

The above clinical situations represent the most common indications for radiosurgery, although other lesions are also treated, such as craniopharyngiomas and skull base chordomas and sarcomas.

Radiobiological considerations in radiosurgery

The Linear Quadratic model is the most commonly used mathematical model of the response of different tissues to different doses of radiation (26):

$$Surviving\ fraction = e^{(-\alpha d - \beta d^2)}$$

where d = dose per fraction, and α and β indicate the tissue sensitivity to lower and higher doses of radiation respectively. Attempts to form a mechanistic justification for the mathematical model include the postulation that the linear component is due to single radiation track lethal events, and the quadratic component due to two-track events. The α/β ratio determines the "bendiness" of the log cell survival curve (Figure 1.3), and therefore the tissue sensitivity to changes in fraction size. Many malignant tumours have a high α/β ratio (eg 10 – 20 Gy for squamous cell carcinoma of the lung) and most late normal tissue effects have a low α/β. This provides the rationale for conventional fractionation (1.5 – 2 Gy per fraction), in order to improve the therapeutic ratio, when tumour and normal tissue are both contained within the PTV. In addition to fraction size, there are further factors which influence the response of tissues, such as

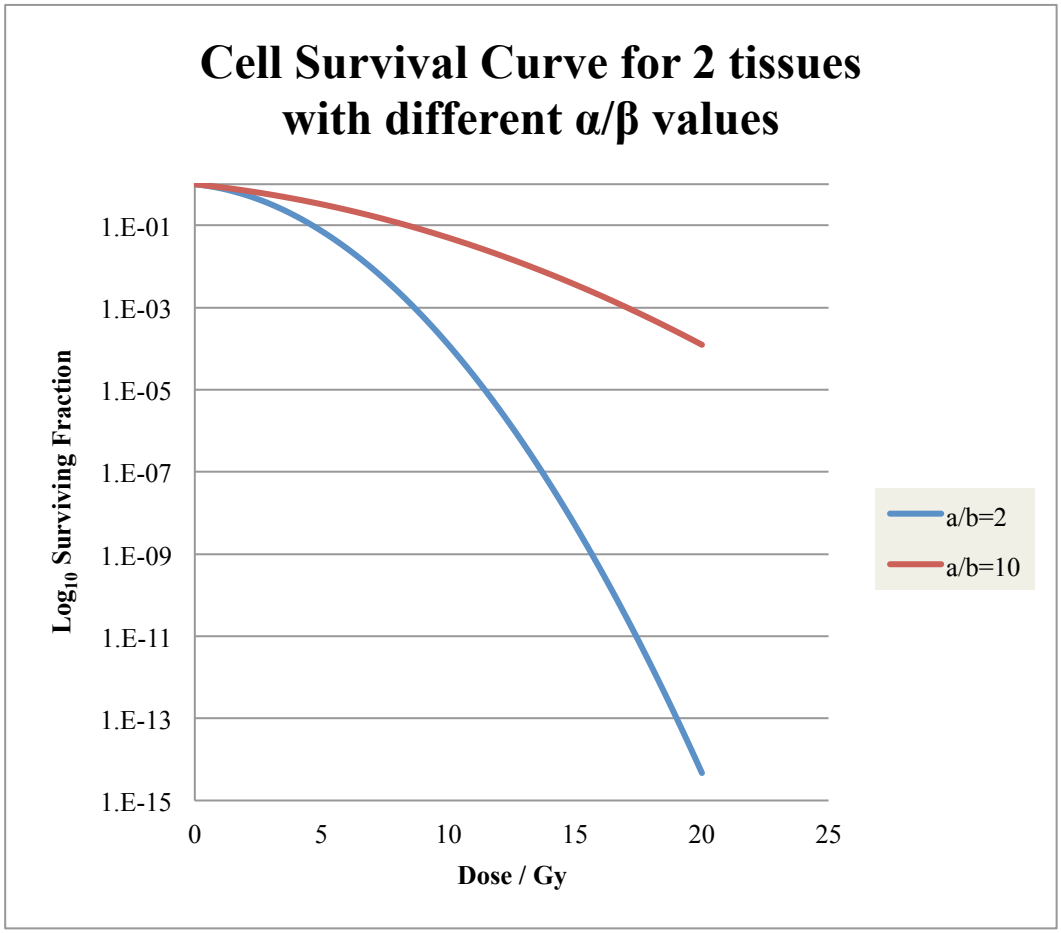

Figure 1.3 Graph of Log_{10} Surviving Fraction against Dose (Gy) for two different tissues, as predicted by the Linear Quadratic Equation. The tissues have different α/β values, giving rise to the different shapes seen. The red curve corresponds to α/β = 10, which is often used to model rapidly-proliferating tumours eg squamous cell carcinoma of the head and neck. The blue curve corresponds to α/β = 2, which is often used to model late normal tissue effects such as spinal cord myelopathy.

Withers' (27) "4 Rs": Repair, Repopulation, Reoxygenation and cell cycle Reassortment (Radiosensitivity is often added as a fifth "R"). Hypofractionation is the use of any fraction size larger than 2 Gy. Moderate hypofractionation (for example, doses in the range 2.5 – 7 Gy per fraction), as with conventional fractionation, corresponds to the curved "shoulder" of the log cell survival curve (Figure 1.3), where both linear and quadratic components contribute to the effect. DNA repair and the other "Rs" are therefore still important in this dose range. Extreme hypofractionation (for examples, doses greater than 8 Gy per fraction) corresponds to the exponential (linear) part of the cell survival curve. Radiosurgery uses one large single fraction, and therefore represents the most extreme form of hypofractionation. At doses of this magnitude, there is a high probability of disrupting both clonogenicity (the ability of cells to form colonies by cellular division) and cellular function: this is often referred to as ablation. The radiobiological considerations important in conventional fractionation, such as the "5 Rs", become less significant at these doses. Normal tissue is protected by virtue of the highly conformal prescription isodose line encompassing a target volume containing negligible normal tissue, and the steep external dose gradient outside of this.

In extra-cranial stereotactic radiotherapy (SBRT), slightly larger PTV margins are often required in order to account for intra-fraction target movement. Also the targets treated may be larger eg prostate gland. This means that a greater volume of normal tissue will lie inside (and immediately outside) the PTV. SBRT is often delivered in 3 – 5 fractions, acknowledging the need for at least some degree of normal tissue recovery. Since hypofractionation will usually lower the therapeutic ratio relative to conventional fractionation, SBRT only makes logical sense in certain clinical situations. Firstly, when the α/β of the tumour is thought to be lower than that of the surrounding tissue late

effects, then hypofractionation will actually improve the therapeutic ratio. Secondly, when the surrounding normal tissue is a parallel organ then small volume normal tissue ablation will not cause any loss in tissue function. This is discussed in more detail below. Thirdly, when the PTV and OAR(s) are a sufficient distance apart, then the steep external dose gradient results in a safe dose to the OAR. This distance may only need to be a few millimetres.

Whilst the linear quadratic equation models tissue response accurately over the range of doses used in conventional fractionation and moderate hypofractionation, there have been questions raised about its accuracy when very large fraction sizes are used. The LQ equation has a continuously bending shape, and may overpredict the effects at large doses. There have been a number of proposed modifications in order to increase the accuracy at larger doses, such as the Modified Linear Quadratic model by Guerrero and Li (28) and the Universal Survival Curve by Park et al (29). However, Fowler (30) has suggested that for rapidly-proliferating tumours, increasing the α/β from 10 to 20 straightens the curve sufficiently over the dose ranges used in radiosurgery and SBRT.

Radiobiology can inform us about normal tissue structural tolerance, however it is functional radiation tolerance which is more relevant to the patient. Functional tolerance depends on tissue organisation as well as cellular radiosensitivity. A distinction can be made between so-called “serial” and “parallel” OARs (31). In a serial organ, damage to a small volume may cause loss of function of the whole organ. Spinal cord is often considered to be the best example of a serial organ, as function is dependent on the integrity of the entire length of the nerve fibres within. From an intracranial perspective, the brainstem is the largest serial structure. It is continuous with spinal cord, and is

believed to share many radiobiological similarities. Additionally, with regard to hypofractionated radiotherapy, spinal cord and brainstem are believed to have a low α/β ratio (a value of 2 is often used), and are therefore especially sensitive to large fraction sizes.

The radiation tolerance of serial organs is consequently usually defined in terms of maximum dose to any part of the organ, for example 50 Gy in 25 fractions, or 15 Gy in 1 fraction, for brainstem. However, modern planning systems can provide the "point" maximum dose to one voxel (often < 1 mm^3) of the OAR. It is not entirely clear whether it is most useful to apply dose constraints to this tiny volume, or rather the dose to some larger, but still very small, volume. Radiosurgical treatment plans often contain steep dose gradients, such that the maximum dose to a single voxel can be substantially higher than the dose even to a very small volume such as 10 – 20 mm^3. A greater understanding of the dose-volume effects in serial organs would therefore be of use to the radiosurgical community. This is discussed further in Chapter 6, which concerns optimising external dose gradient on one side of targets close to (or abutting) the brainstem.

Parallel organs (eg lungs, liver) are comprised of multiple subunits which all have the same function, and which function independently of each other. Functional damage will therefore only occur if a critical volume of tissue is damaged. Dose constraints in treatment planning are therefore usually defined in terms of the volume of organ receiving a certain threshold dose. For example, V20 (volume receiving at least 20 Gy) < 30 % volume is a common lung constraint in 2 Gy/fraction radical radiotherapy. In SBRT, when the target lies within the parenchyma of parallel organs, a small volume of

organ tissue within (and immediately adjacent to) the PTV will be destroyed. However, extreme hypofractionation may still be a safe treatment, provided that the target volume (and therefore the volume of normal tissue affected) is sufficiently small.

In intracranial radiosurgery, as with the lungs and liver, the target may lie entirely within an OAR. It is usually accepted, therefore, that a small rind of normal brain surrounding the target is at risk of damage, notwithstanding the steep external dose gradient. Brain tolerance limits are often defined in terms of the volume receiving a certain dose. For example, as discussed above, the 12 Gy volume (V12) has been shown to correlate with post-radiosurgery complications. However, in spite of this no part of the brain can be viewed as truly parallel, since even damage to a very small volume of cerebral cortex can have profound consequences. The V12 graphs described above demonstrate that certain parts of the brain need to be especially respected (Figure 1.2). Small targets and a steep external dose gradient will both reduce the V12, and are therefore critical to the safe delivery of intracranial radiosurgery. Optimising the dose fall-off evenly around the target using the CyberKnife system is covered in Chapters 4 and 5.

Dose rate has been shown to be a very important variable in radiobiology (32). The dose rate effect is likely to be important in radiosurgical practice since fraction times can vary significantly across the different modern radiotherapy systems. For example, the duration of a single 18 Gy fraction to an intracranial lesion would usually be 30 – 60 minutes using CyberKnife, but could be as short as 10 minutes using modulated arc therapy. It is therefore not clear to what extent 18 Gy delivered using the two different techniques actually differs in biological effect. For example, 18 Gy in 1 fraction

delivered over “x” minutes may be comparable to 20 Gy in 1 fraction delivered over “y” minutes using a different system. However, the effect of dose rate is currently not really considered when discussing and comparing radiosurgical treatment plans in everyday clinical practice. More research is needed in this area, as will be discussed later.

Dosimetry in radiosurgery

Radiation dosimetry is the calculation of absorbed dose in matter as a result of exposure to ionising radiation. This covers radiotherapy system Quality Assurance (QA), and all aspects of radiotherapy treatment planning. The general principles of treatment planning are the same for radiosurgery as for CFR: the goal is to minimise dose to normal tissue (or the volume receiving a particular dose) for a given dose to the target. There are, however, some important differences between radiosurgery and CFR in the area of dosimetry.

Perhaps the most obvious difference is the much smaller field sizes that are commonly used in radiosurgery, which is a direct consequence of the smaller targets treated. This has implications with regard to QA, since specialist apparatus (and experience) is required to perform small field dosimetry appropriately. The Institute of Physics and Engineering in Medicine (IPEM) have recently produced guidelines for small field dosimetry (33), but the area remains controversial. Chapter 3 will include an appraisal of the different techniques and apparatus that could be potentially used in small field QA.

Another important difference is the selection of the isodose which covers the target – the marginal isodose. In CFR, dose is prescribed to the 100 % value on the treatment plan. Most plans conform to ICRU 50 and 62 recommendations (34, 35), such that the 95 % isodose covers the whole PTV, and the maximum dose on the plan is < 107 %. Consequently the dose heterogeneity within the PTV is usually less than 12 %. However, in radiosurgical planning 100 % represents the maximum dose delivered, and the treatment dose is prescribed to the marginal isodose. Common radiosurgical practice is to use lower marginal isodose values, resulting in greater dose heterogeneity inside the target (the choice of marginal isodose is central to much of the experimental work in this thesis). A consequence of target dose heterogeneity is that it is harder to be sure of the true "effective" dose delivered. Additionally, there is considerable variation in practice across different radiosurgical systems (and across different centres using the same system!). For example, common Gamma Knife practice is to use marginal isodoses in the range 40 – 60 %, whereas CyberKnife and gantry-based linac publications usually show the use of isodoses in the range 60 – 90 %. This implies that the integral dose to the target for two plans with the same prescribed dose can be very different, and therefore comparing results between different centres can be problematic.

Radiotherapy clinicians are familiar with using Biologically Effective Dose (BED) or Equivalent Dose in 2 Gy fractions (EQD2) (both of which are derived from the linear quadratic equation) to compare treatment regimens of different fractions, and can perform these calculations by hand. However no attempts are usually made to account for the effects of a different marginal isodose in radiosurgery or SBRT. The generalised Equivalent Uniform Dose (gEUD) has been proposed by Niemierko (36) as a method of

reducing a heterogenous dose distribution across a target to a single dose which, if delivered uniformly across the target, would have the same biological effect:

$$gEUD = \left(\frac{1}{N}\sum {D_i}^a\right)^{1/a}$$

where Di is the dose to a voxel i of the volume, N is the total number of voxels and a is a tissue-dependent factor. However, even though this formula is a simplification of the original EUD equation proposed, it is still too complicated to be calculated by clinicians in everyday practice. It would be useful, therefore, if this formula could be incorporated into future treatment planning software, so that appropriate plan comparisons can be made.

A further difference between CFR and radiosurgery is the very steep external dose gradient outside the target which is seen in radiosurgical plans. As stated above, this is critical to the safe delivery of ablative doses of radiation. External dose gradient is therefore an important radiosurgical parameter, together with target conformality and coverage. There have been a number of proposed measures of both external dose gradient and conformality, and these are discussed fully in Chapter 4. Optimising external dose gradients in CyberKnife radiosurgical planning is the central goal in three of the experimental chapters in this thesis. In particular, the relationship between the choice of marginal isodose value and external dose gradient is explored in detail.

Outline of thesis

This chapter has provided a background of the historical, clinical and radiobiological aspects of radiosurgery. It has also introduced the subject of radiosurgical dosimetry, which will be the main focus of this thesis.

Chapter 2 will describe the G4 CyberKnife and Gamma Knife Perfexion systems in detail. There will be a summary of 3-dimensional radiotherapy planning techniques, focusing on the planning software used with the above two systems.

Chapter 3 will seek to verify that treatment plans produced by MultiPlan (the CyberKnife planning software) accurately reflect the actual treatment delivered, and that subsequent work based on MultiPlan dose distributions is therefore valid.

Chapter 4 will explore the effect of the prescription (marginal) isodose value on the external dose gradient, as measured by Gradient Index, for solitary spherical virtual targets of different diameters, using two different optimisation algorithms in MultiPlan.

Chapter 5 will continue the work of the previous chapter, but now using irregularly-shaped lesions from patients treated at this centre. On the basis of these results, a method for the planning of solitary intracranial lesions using MultiPlan will be proposed.

Chapter 6 will consider the situation where an intracranial target lies close to, or abutting, the brainstem – where the external dose gradient is therefore especially important on one aspect of the target. Once again, spherical virtual targets of different sizes will be used.

Chapter 7 will describe a dosimetric comparison of the CyberKnife and Gamma Knife systems. Identical target contours will be planned using each system, and various important planning parameters compared.

In Chapter 8, all the results of the experimental chapters will be brought together and summarised. There will be a general critique of the experimental methods, and areas for future research will be proposed.

Chapter 2 - Materials and Methods

The vast majority of the work in this thesis has been carried out using the CyberKnife system, and therefore this chapter contains a detailed description of the main system components. The key components of Gamma Knife hardware and software are also summarised, as a planning comparison of the two systems forms part of the experimental work which follows. Radiosurgery planning is at the heart of the thesis, and so this chapter also covers the various planning techniques and optimisation algorithms used in the experimental chapters.

Overview of the radiosurgery systems used

CyberKnife

CyberKnife is a radiosurgery system which uses robotics and image guidance to deliver radiotherapy with "stereotactic" accuracy (9). As discussed above, radiosurgical systems have traditionally relied upon immobilisation via a rigid stereotactic frame in order to treat with the required sub-millimetre accuracy. For frame-based systems stereotactic space is within the frame and hence clinically confined to the cranium. The ability of CyberKnife to achieve this accuracy without rigid immobilisation allows the system to deliver radiosurgery to both intracranial and extracranial targets. Unlike gantry-based linear accelerators, there is no fixed isocentre. For each patient, an align centre within the patient is chosen during the treatment planning stage, and beam

coordinates are relative to this. Figure 2.1 is a picture of a G4 CyberKnife, with the different system hardware components labelled.

X-band Linear Accelerator (Linac)

In a linear accelerator, electrons produced by thermionic emission gain megavoltage energy by being accelerated through multiple electromagnetic fields within a waveguide. The required length of the waveguide is dependent on the frequency of the electromagnetic field used to accelerate the electrons. The majority of conventional linacs use frequencies within the S-band (2-4 GHz) range. In the last twenty years, advances in technology have enabled the production of linacs which use electromagnetic fields within the X-band (8-12 GHz) range. This reduces the required length of the waveguide by two thirds, leading to a much more compact and lightweight design. The G4 CyberKnife system uses a 6 MV X-band linac with a dose rate of 800 MU/minute, mounted on the robotic arm.

(Secondary) Collimators

In CyberKnife, both fixed and variable aperture (Iris) collimators are available, which dictate the field size of the radiation beam. The fixed collimators are tungsten inserts with conical holes, creating a circular beam with a penumbra (20 – 80 %) of approximately 3.8 mm. There are twelve different fixed collimators with field sizes between 5 mm and 60 mm. They are housed on an exchange table, allowing the robot to

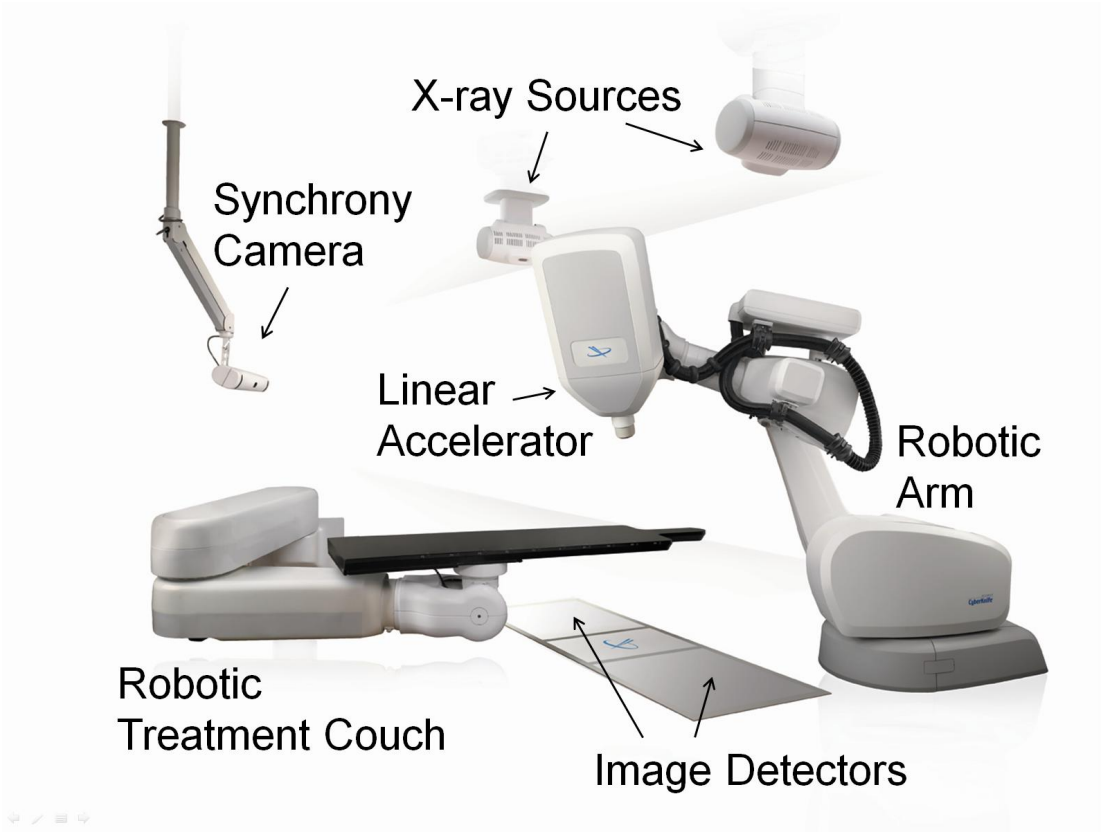

Figure 2.1: Picture of the G4 CyberKnife system, with the key system components labelled.

exchange automatically collimators as required during treatment. Up to three different fixed collimators can be used for each treatment. The Iris collimator is a more recent development which was introduced with the G4 CyberKnife. It contains two stacked hexagonal banks of tungsten segments, offset by 30 degrees to each other. This produces a radiation beam in the shape of a dodecagon. The segments move to adjust the size the aperture, with all twelve segments being driven by a single motor. In this way, the collimator can approximate all 12 fixed collimator circular field sizes, with a mechanical reproducibility of less than 0.1 mm. The Iris collimator allows any combination of the twelve different field sizes to be used for each treatment. This can substantially reduce the overall treatment time and, in some cases, improve the quality of the plan.

Robotic manipulator

The manipulator arm is a KUKA KR 240-2 (Series 2000) industrial robot (KUKA Robot Group, Augsberg, Germany). It has a payload (carrying capacity) of 240 Kg. The maximum reach is 2.7 m, and it has 6 joints, which enables the beam to be pointed in any 3-dimensional angle, from every position within the reach of the manipulator. This setup produces a large non-coplanar workspace around the treatment couch, from which radiation beams can be delivered. The arm has a reproducibility of 0.12 mm, and a rapid response time, enabling anticipatory movement of the beam head to track respiratory movement, where appropriate.

Treatment Couch

The couch consists of a flat carbon fibre top mounted on an additional six joint KUKA robotic arm, which enables movement in the 3 translational (left-right, superior-inferior, anterior-posterior) and 3 rotational (roll, pitch, yaw) planes. This allows the couch to correct for any tumour (or patient) movement which is beyond the pre-specified robot limits, without the need to reposition the patient. This can be especially useful when treating certain tumour sites (eg prostate) where there may be significant, but variable intra-fraction tumour movement.

Kilovoltage X-ray sources and flat panel image detectors

Two kilovoltage x-ray sources are mounted on the ceiling of the treatment room, with x-ray beams at an angle of 45 degrees to the patient and 90 degrees to each other. The beams cross at the imaging centre. Each source has a corresponding in-floor mounted flat amorphous silicon image detector. The detectors have a 20 x 20 cm field of view and a resolution of 1024 x 1024 pixels. Pairs of images are obtained throughout patient setup and treatment. They are compared with the digitally reconstructed radiographs (DRRs) generated from the planning CT, and the error for each of the six degrees of freedom is calculated. The robotic arm can move the beam head to compensate for errors within a certain tolerance; beyond this, the treatment couch must realign the patient by moving appropriately, before treatment can resume.

Synchrony camera

The Synchrony camera array consists of 3 charged couple device (CCD) detectors oriented towards the patient. Together they can track the 3-dimensional position of light emitting diodes (LEDs) placed on the patient's chest. As the chest wall moves with breathing, real-time information on chest wall position is fed to the Synchrony software, and a breathing model is generated. The Synchrony software is used in conjunction with fiducial-based tracking (see below). Several static KV images are obtained at different points in the breathing cycle, and the software correlates fiducial position with breathing. A predictive algorithm is generated which enables the radiation beam to track the tumour continuously. This obviates the need for respiratory gating.

Tracking

A key aspect of CyberKnife radiosurgery is the ability to track the position of the target (or some surrogate for target location) accurately, both during initial treatment setup and throughout treatment delivery. As described above, the KV x-ray sources enable near real-time image guidance through comparison with the DRRs. As they are planar images, most solid tumours are not visible. The treatment system therefore has a number of different tracking methods which are used depending on the treatment site. Data on the accuracy of these methods have been published previously (37-42).

6D Skull tracking

This is the method of tracking for all intracranial lesions and some head and neck tumours which are felt not to move relative to the skull. The skull is a rich source of distinctive bony anatomical features easily seen on planar imaging. The 6D skull software compares the images obtained during setup and treatment with the DRRs, and can adjust for displacement in the 6 directions of movement using rigid transformation, with a demonstrated total system accuracy of 0.44 - 0.48 mm (37, 42). The patient is fitted with a thermoplastic shell, to ensure any head movement is limited to a few mm – comfortably within the corrective tolerance of the robot.

Xsight Spine tracking

The spine is a similarly rich source of bony anatomical features. However, unlike the skull, the individual vertebrae move independently of one another during treatment, therefore rigid transformation between live images and the DRR is not valid. Instead the software performs non-rigid image registration based on a bony region of interest near the target. The total system accuracy when using Xsight Spine tracking has been measured at 0.52 - 0.61 mm (38, 39). It can be used to treat most spinal tumours, and selected soft tissue tumours which are within a few cm of the spinal column, and which are not likely to move relative to the spine.

Fiducial-based tracking

This method is used in most cases where neither 6D skull nor Xsight Spine tracking is appropriate. Small gold cylindrical fiducial markers are inserted into (or close to) the tumour, and act as a surrogate for tumour position. Fiducial insertion occurs under radiological guidance, via a percutaneous, trans-rectal (prostate tumours) or endoscopic (selected thoracic and abdominal tumours) approach. This software relies on rigid

transformation, therefore if a fiducial has migrated more than 1.5 mm between planning CT and treatment, it cannot be used, and there must be a minimum of 20 mm between each marker. Additionally, fiducials which overlap in either 45 degree imaging plane cannot be used. A minimum of 3 fiducials are required to apply both translational and rotational corrections; a single fiducial is sufficient for translational corrections alone. Phantom studies have shown the accuracy of fiducial tracking to be 0.68 +/- 0.29 mm when used alone for stationary targets (40), or 1.5 mm as part of the Synchrony system for targets moving with breathing (41).

Xsight Lung is a recent development which can track selected lung tumours without the need for implanted fiducials, thus avoiding a procedure which carries the risk of pneumothorax. The tumour must be visible on both 45 degree KV images and larger than 15 mm in maximum diameter.

MultiPlan Treatment Planning System

MultiPlan (Accuray Inc) is the system software which manages all aspects of CyberKnife treatment plan generation. The tasks are arranged into six sections which are displayed as tabs across the top of the page (Figure 2.2). The workflow passes logically through each section in turn, the final result being a deliverable treatment plan which can be exported to the treatment delivery system.

1. Load. New plans are created here by importing the planning CT dicom files, together with any additional imaging datasets as appropriate. Pre-existing plans can be loaded for further work.

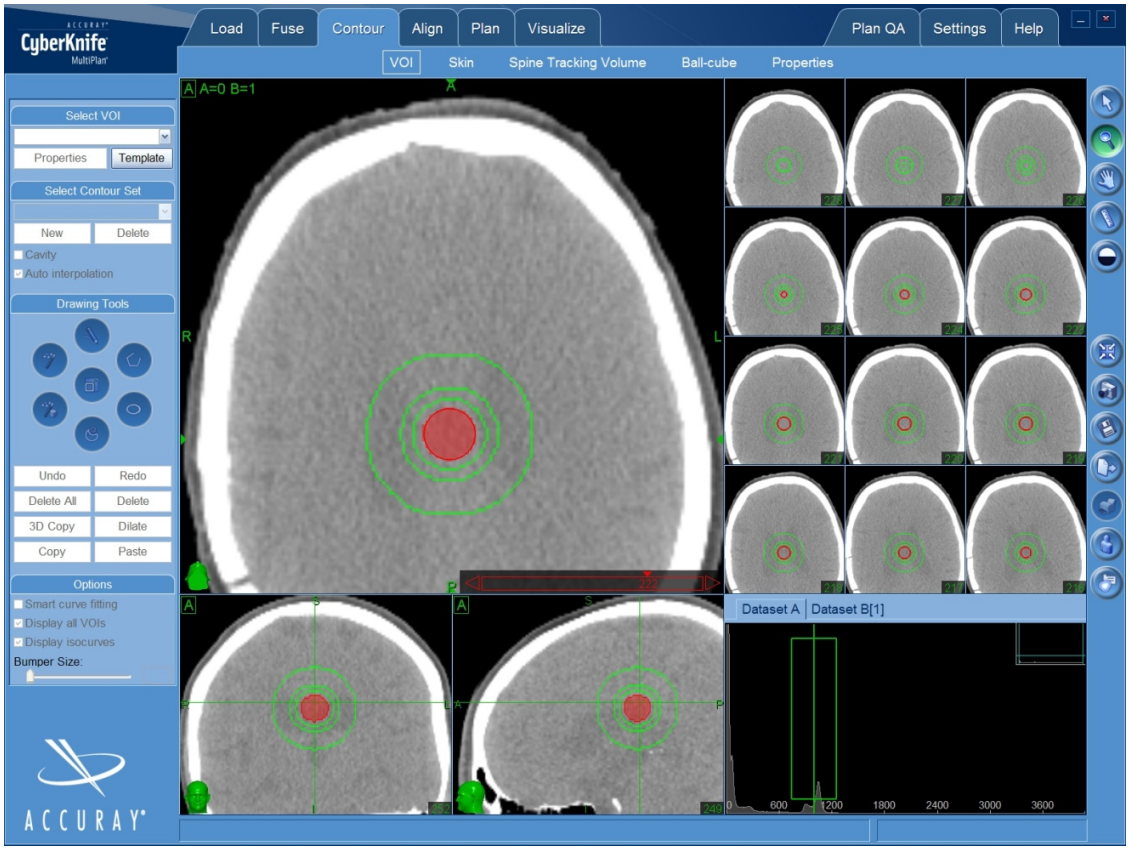

Figure 2.2: Screenshot showing the layout of MultiPlan version 3.5.1 software, with the tabs at the top of the screen subdiving the various planning taks. In the screenshot the "Contour" window is shown, which allows axial, sagittal and coronal views to be reviewed simultaneously. A "virtual" spherical target has been drawn, toghether with 3 optimisation shells at 3, 6 and 15 mm distance from the edge of the target.

2. Fuse. This tab displays tools for registering the primary (planning CT) image series with any secondary series imported to aid target delineation, such as contrast-enhanced CT, MRI or PET. Common anatomical “seed points” (eg spinous process) are selected on both image sets, and an initial transformation is carried out. The system can perform an intensity-based registration process to improve the accuracy of fusion. The results can also be adjusted manually with reference to axial, sagittal and coronal planes. The accuracy of image fusion is critical to the total system accuracy, and therefore the importance of this step should be stressed.

3. Contour. Targets and Organs at Risk are created here using a variety of contouring tools. Each “volume of interest” (VOI) is contoured in axial, sagittal or coronal plane, with options to expand or erode VOIs as required. The “ball-cube” function allows the creation of a spherical target, the location and diameter of which can then be adjusted as appropriate. This function will be used in Chapters 4 and 6.

4. Align. As previously mentioned, there is no fixed isocentre in the CyberKnife system. Before treatment planning can begin, an align centre must be chosen, which will also be the imaging centre for the plan. This point is selected such that all the anatomical information required to track the target is included in the DRRs (and subsequent in-room KV images). For example, with 6D skull tracking, the align centre will be a point within the brain selected so that as much skull anatomy as possible is visible in the 20 x 20 cm DRRs. For fiducial tracking, the align centre is usually the mid-point between all fiducials present. All beam coordinates are now relative to this fixed point. The number of fractions, tracking method, and choice between using Iris or fixed collimators are all decided at this stage.

5. Plan. In this section treatment plans are generated, evaluated and modified, and can be saved at any point during this process. MultiPlan has the option of both isocentric and non-isocentric planning techniques.

In isocentric planning, a point within the target is chosen as the isocentre, and beams from each location in the treatment path are selected, all of which converge on that point. Whilst this is a quick and relatively simple method of planning, it lacks the flexibility inherent in the non-isocentric planning techniques, and is therefore only used rarely.

In non-isocentric planning, whilst all the beams are convergent on the target, they do not meet at a single point. There are a huge number of potential beams which could be selected for each plan, and multiple other variables to consider, and therefore inverse planning optimisation algorithms are used here (see below). MultiPlan has a choice of three different optimisation algorithms: Simplex and Iterative (conformal planning algorithms), and Sequential optimisation. Radiotherapy treatment planning techniques and, in particular, the Simplex and Sequential algorithms are discussed in more detail below.

MultiPlan uses a Ray-Tracing algorithm as the standard method of dose calculation. The algorithm traces a straight line from each beam to each point in the patient. The "equivalent path length" is calculated based on the distance to that point and the density of the tissue traversed in reaching it (based on the CT number of each pixel in the

beam's path). Using the equivalent path length, the dose delivered to that point is calculated based on the known depth-dose data for the beam.

Ray-Tracing produces accurate results when tissue density is more or less uniform, but will tend to overestimate the dose delivered when the beam passes through an area of relatively lower density within the body, such as nasal cavity/sinuses or the lungs. This is because the algorithm fails to take into account the reduced secondary electron production in the lower density region, relative to the higher density region upstream. Consequently, inaccurate results may be obtained near boundaries of significant density change.

Monte Carlo is regarded as the gold standard radiotherapy dose calculation algorithm. It simulates the probable particle interactions of each photon delivered (and every secondary electron produced) during treatment. Until recently, use of Monte Carlo in radiotherapy planning systems was limited due to the processing power needed to perform the calculation. However, the current MultiPlan versions are now capable of performing Monte Carlo dose calculation. Whilst it is still time-consuming, it would be recommended to recalculate plans using Monte Carlo where there is significant tissue heterogeneity as described above.

Experimental work in this thesis concerns targets within the brain parenchyma, where tissue density is largely homogenous. In this situation, Ray-Tracing has been shown to produce accurate dose calculations. Ray-Tracing will therefore be the dose calculation algorithm used in this thesis.

6. Visualise. Within this tab are further ways to visualise the plan before approving it, such as viewing multiple slices of the isodose arrangement simultaneously, and a 3-dimensional viewing option. Exporting DICOM files and 3-dimensional dose information is also possible here, as will be used in Chapter 7.

Gamma Knife

Gamma Knife is a dedicated radiosurgery system which delivers a single high dose of radiation to targets inside (or very close to) the skull. Central to the accuracy of radiation delivery is the use of a rigid frame which is fixed to the patient's skull using metal screws. Thus, any target which does not move relative to the skull is effectively immobilised with this technique. Additionally, the frame defines the stereotactic space which is used for patient setup and treatment delivery. The system comprises the least possible number of movable components in order to preserve the accuracy achieved through immobilisation. Studies of overall system accuracy, including every step from frame immobilisation through to delivered treatment plan, have shown an accuracy of 0.48 – 0.70 mm (43, 44). A consequence of the frame is that unlike CyberKnife, the whole procedure, from image acquisition right through to treatment, needs to be performed in a single session. Another difference is that the system uses live radiation sources (Cobalt-60) which must be shielded adequately when not in use. The most recent system version is the Leksell Gamma Knife Perfexion, and this is the model which has been used in this thesis. The main components are summarised below.

Sources

An array of 192 Cobalt-60 sources is arranged in a cone section configuration. All sources emit radiation which, via collimators, converge at a single point (isocentre), with a source to focus distance (FSD) varying from 374 to 433 mm. The resultant aggregate beam is referred to as a "shot". The sources are subdivided into eight independently-movable sectors, each with 24 sources, mounted on the collimator body. Cobalt-60 emits gamma rays with energies of 1.17 and 1.33 MeV (and low energy beta particles which are easily shielded). The decay half life is 5.27 years, and cobalt sources should be replaced at least every three years to maintain adequate dose rate. The whole radiation unit sits in a cast iron body, and steel shielding doors are closed when treatment is not ongoing. Additionally, in the "Beam off" position, the sources are withdrawn from the collimators and not aligned with the collimator holes, thereby providing further shielding.

Collimators

Unlike previous Gamma Knife models, there is a single, 120 mm thick, tungsten collimator array with 576 collimator channels. This allows automatic change of collimator size during treatment. There are three different collimator sizes: 4 mm, 8 mm and 16 mm. The tray housing the sources moves to align them with the appropriate collimator size during treatment (Figure 2.3). The eight independently movable groups of sources can be aligned with different size collimator channels, and there is also the

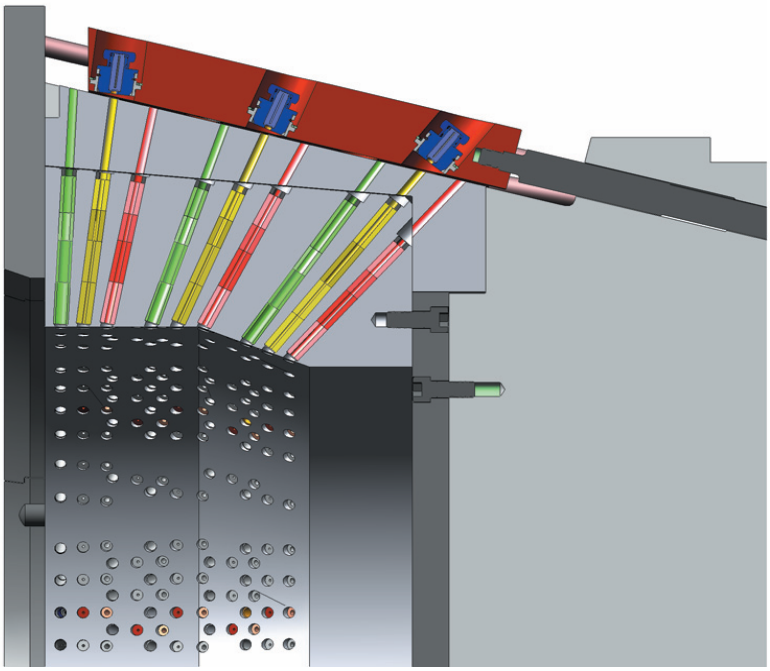

Figure 2.3: Cross-sectional diagram through the Gamma Knife Perfexion collimator assembly. Three Cobalt-60 sources (blue) are housed on a source tray (red) which can move along horizontally so that the sources align with the appropriate collimators. The 4, 8 and 16 mm collimators are shown here in yellow, green and red respectively. In the diagram the sources are aligned to the 4 mm collimator.

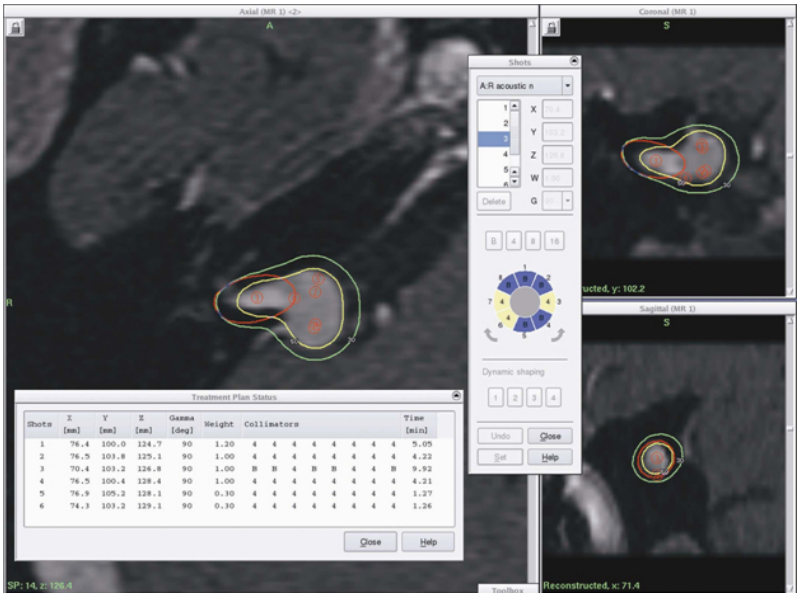

Figure 2.4: Screenshot from GammaPlan showing the treatment plan for an acoustic neuroma, consisting of six shots. Five of the shots are spherical, but shot 3 (shown in red) is non-spherical due to the blocking of segments 1,2,4,5 and 8. This allows the shot to conform more closely to the shape of the lesion, as shown in the axial, sagittal and coronal views.

option of blocking each individual sector of sources. These refinements allow the generation of a non-spherical shot, where desirable (Figure 2.4).

Patient positioning system

The patient lies on a flat couch and the frame is attached to a docking device which immobilises the frame (and skull) relative to the couch. The couch then moves the patient into the beam delivery unit, and sets the position according to the x, y and z spatial coordinates defined in the treatment plan.

Leksell Coordinate G Frame

This is a rectangular aluminium frame with engraved, scaled rulers which provide x, y and z coordinates. It is fixed to the skull by means of four screws, each of which pass through one of the four rigid corner posts. The zero point of the coordinate system is superior, lateral and posterior to the frame on the patient's right side. The radiation beam coordinates are relative to this point in stereotactic space. Indicator boxes specific to the imaging modality (CT, MRI or Angiography) are attached to the frame prior to scanning, and they impose reference fiducials which facilitate image registration.

Leksell GammaPlan Treatment Planning System

GammaPlan deals with all aspects of image import, target delineation and treatment planning for the Gamma Knife system. It can handle CT, MR and PET images, in addition to projectional images from angiograms. Since all imaging is usually acquired with the frame in-situ, and the appropriate imaging box attached, accurate image registration can be performed easily. As with MultiPlan, the target and organs at risk can be contoured using a variety of different tools, and with access to axial, sagittal and coronal planes during this process. Unlike CyberKnife, a CT is not a requirement for treatment planning (although it may be desirable in some cases), since the CT number (density) of different tissues inside the skull is not taken into account. The patient's skull contour is measured manually and uniform density is assumed for all tissue inside this contour.

Gamma Knife treatment planning is a forward-planning process which involves the manual positioning of one or more shots in such a way as to maximise tumour coverage with the prescription isodose and minimise dose to normal tissue. This is discussed in more detail below.

3-dimensional radiotherapy planning

Before the implementation of axial scanning for radiotherapy, treatment planning was performed either by hand or with simple 2-dimensional computer dose calculation.

There was no compensation for inhomogeneity of tissue density, and much less flexibility to adjust established beam arrangements. In the 1990s, CT planning arrived in the UK together with more sophisticated computer dose calculation software capable of processing the increased information obtained. Since then, computer planning systems have continued to evolve with ever greater complexity. Within 3-dimensional radiotherapy planning, the different planning techniques can be broadly divided into two categories: forward and inverse planning.

Forward Planning

In the case of forward planning for traditional 3-dimensional conformal radiotherapy, the planner has control over the number, direction, size, shape and weighting of individual beams (and in some cases the intensity across each beam). The planner attempts to produce a solution which best meets the clinical requirements by manipulating these variables. Often the number of beams and basic beam arrangement will be largely consistent for a particular treatment site (eg anterior and two opposed lateral beams for prostate radiotherapy), but patient-specific optimisation relies on fine-tuning the remaining variables, and recognising when the "standard" beam arrangement needs to be modified.

Gamma Knife planning is another example of forward planning in that the size, position, number and shape of the shots used is manually adjusted on a trial and error basis, in order to come up with a plan in which tumour coverage, conformality and dose fall-off outside the target have been optimised. Whilst occasionally a single shot is

sufficient to cover a lesion adequately, usually the planning process involves the positioning of multiple shots within the PTV and then fine-tuning the positions and weightings to optimise plan parameters.

Similarities have been drawn between the Gamma Knife planning process and mathematical "sphere packing" problems, where the goal is to fill as much of a defined space as possible with a number of identical spheres. However, there are a few key differences, which have limited the ability to find "best solutions" through mathematical modelling. The standard sphere packing problems deal with identical, non-overlapping spheres inside a regularly-shaped space. In Gamma Knife planning, the spheres can be of different sizes, they can overlap inside the PTV, and the PTV itself is irregularly-shaped. Additionally, with the advent of Gamma Knife Perfexion, non-spherical shots can now be used. The "composite shot" feature enables the generation of a single shot composed of different beam diameters. This, together with the ability to block specific sectors of sources, means that a wide variety of different shapes can be generated (Figure 2.4). Whilst such new features have made it easier to produce isodose arrangements which conform well to the targets, the quality of the plan produced remains largely dependent on the experience of the planner. Indeed, planning experience is a major potential confounding factor in any comparative study of different radiosurgical techniques, as will be discussed in Chapter 7.

Inverse Planning

In the last twenty years, 3-dimensional planning has become more sophisticated with the emergence of Intensity-Modulated Radiotherapy (IMRT) and radiosurgery systems with huge flexibility, such as CyberKnife. With increased sophistication usually comes an increase in the number of variables which impact on the plan parameters. For example, with IMRT, in addition to the number, direction and weighting of beams, the fluence across the beam can be varied to improve dosimetry. Consequently in many situations it may not be possible to manipulate all these variables effectively with a forward planning technique. Inverse planning algorithms have therefore been developed with the processing power required to deal with this increased complexity.

In inverse planning, the planner sets a series of goals and constraints relevant to the clinical situation, usually with some way of prioritising these, such as a weighting measure. The planning system then comes up with a solution which best meets the original goals. Unlike forward planning, therefore, the planner has no control over the precise number, position or weighting of the beams, or indeed any of the other variables such as beam fluence.

An inverse planning optimisation algorithm will only attempt to achieve what it is specifically asked to, and if a particular set of goals are not possible to achieve, it may appear to "give up" rather than produce the nearest possible solution. Special care must therefore be paid when setting goals and constraints, and in addition, certain techniques are required to get the best out of the system.

Tuning structures are an important component of the inverse planning process as they give the planner increased control over the distribution of dose within a plan. The inverse planning goals which are set by the planner mainly apply to contoured structure sets. For example, a minimum dose to the PTV can be specified, together with a maximum dose to an OAR. Consequently, one may achieve a solution which meets the goals of PTV prescription isodose coverage and OAR constraints, but which still has undesirable features such as high dose in other areas, or shallow dose fall-off outside the PTV. Tuning structures are contour sets which do not relate to anatomical structures, but which the planning system recognises as structures with constraints attached. They can therefore help to guide the system to produce a plan with the best overall isodose arrangement.

An optimisation shell (also sometimes referred to as a ring structure) is one such tuning structure which is central to the planning technique for many inverse-planned radiosurgical systems, and is used extensively throughout this thesis. A shell consists of a narrow 3-dimensional ring of tissue around the PTV, at a distance from the edge of the PTV (Figure 2.2). The shell contour is usually generated by an isotropic expansion of the PTV boundary, and is therefore the same shape as the PTV. A series of 2 or 3 shells at different distances from the PTV boundary are often used together. Goals and dose constraints can be applied to the shells in the same way as any other volume of interest. For example, by setting a maximum dose goal to a shell, this will encourage the planning system to ensure the dose has fallen off to this value over the distance between the PTV boundary and the shell. “Pushing” the system by setting more challenging shell goals may result in a steeper dose fall-off, but may also negatively impact on other parameters such as conformality. This is discussed in more detail later in the thesis. In

general, for a given tumour coverage and conformality, the use of shells encourages steeper dose fall-off and helps to prevent high-dose fingers at a distance from the target (Figure 2.5).

CyberKnife treatment planning deals with a huge number of possible beams from a large 3-dimensional space, and each selected beam only comprises a small proportion of the overall dose to the target. Inverse planning is therefore usually necessary to generate the best beam arrangement for each clinical situation. As described above, there are three different inverse planning optimisation algorithms available in MultiPlan. Simplex and Sequential optimisation feature heavily in this thesis and are now discussed in more detail.

Simplex optimisation

Simplex is one of the two conformal planning algorithms. It requires the user to choose a desired minimum and maximum dose to the PTV, a maximum dose to other VOIs (organs at risk and optimisation shells), and a weighting applied to each of these values, based on their relative importance. The weighting can vary between 0 and 100, where 0 means that the constraint is ignored, and 100 means that it must be met. All constraints with weighting > 0 but < 100 are referred to as "inexact constraints". The planning system then aims a random selection of beams at different points on the PTV surface. The optimisation algorithm adjusts the delivery MUs of all the beams in order to minimise the total deviation away from the inexact constraints that have been set, and minimise the total MU delivered. In mathematical terms, the algorithm minimises

Plan A

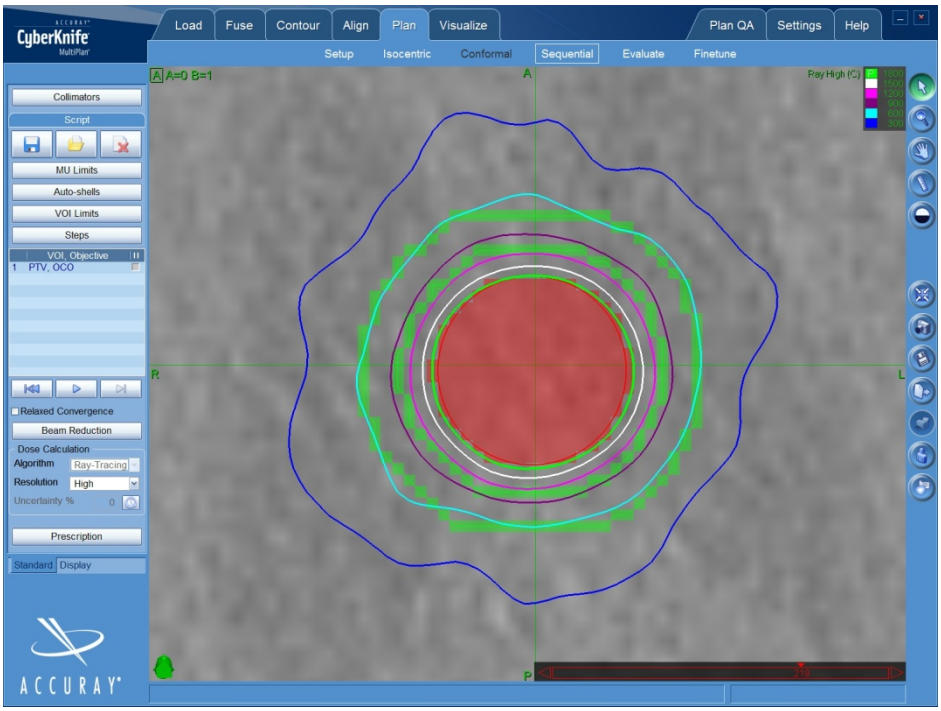

Plan B

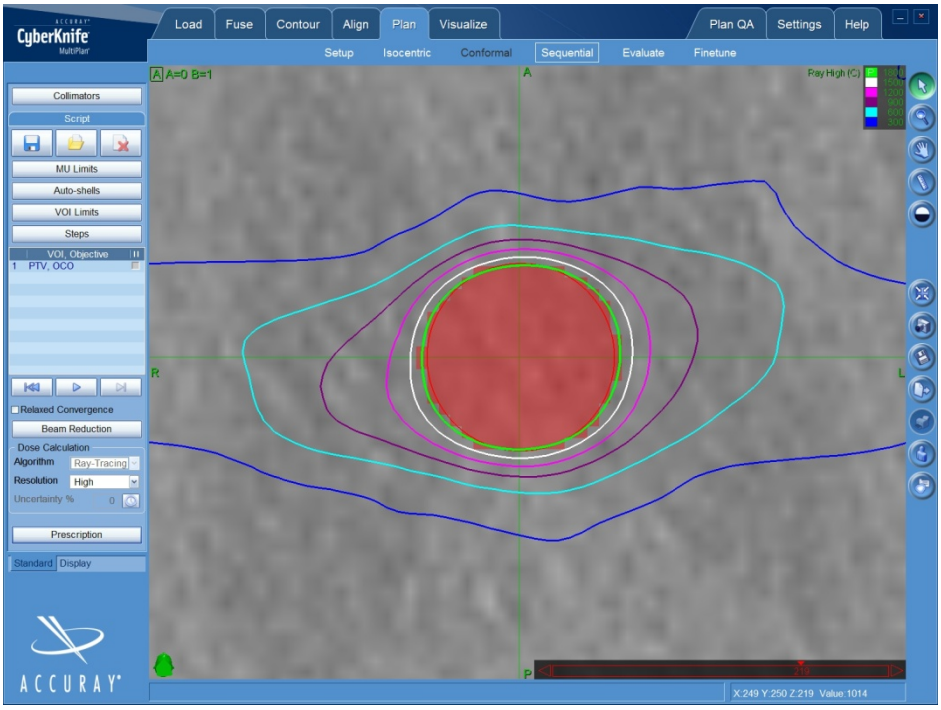

Figure 2.5: Two screenshots from MultiPlan version 3.5.1 each showing a different treatment plan. An identical virtual spherical target of 15 mm diameter has been planned in both cases. The Sequential optimisation plan settings were identical, except that in plan A two optimisation shells were used), and in plan B no shells were used. In plan A the shells are shown in green, positioned at 3 and 6 mm distance from the edge of the PTV. The isodosimetry is shown in each case, with the lines corresponding to the following doses: green = 18 Gy (prescription isodose line), white = 15 Gy, pink = 12 Gy, purple = 9 Gy, light blue = 6 Gy, dark blue = 3 Gy. The plans illustrate that optimisation shells can help to produce a steeper, more even dose fall-off outside the target, and reduce the amount of moderate dose distant to the target.

$$\sum \Omega_i \delta_i + \sum x_j$$

Where δ_i is the deviation factor for each constraint, Ω_i is the weighting for each constraint, and x_j is the MU for each beam. There is no feedback during the optimisation process; the algorithm simply produces the best solution at the end. It is usually necessary to modify the constraints and weightings a few times to get the best solution, but each time the algorithm must start from the beginning. Thus, simplex optimises multiple, potentially conflicting objectives in a single step.

Sequential optimisation

Sequential differs from the more conventional optimisation algorithms (such as Simplex) where multiple objectives are grouped together in a single cost function and optimised simultaneously. Instead the algorithm is executed sequentially as a series of individual optimisation steps, where each step corresponds to a clinical objective (Table 2.1). The steps are ordered in terms of clinical priority (rather than having weightings applied to them). It is argued that these features make the planning process more intuitive to the treating physician, thus encouraging more clinician input into the process.

The user initially sets "hard" maximum dose limits for all the VOIs (PTV, OARs and shells), and certain other limits such as the maximum total MU to be used and

	Objective	Description
Target		
	OMI	"Optimise Minimum Dose". Attempts to maximise the minimum dose to the whole target, bringing this up to as close to the desired prescription dose as possible.
	OCO	"Optimise Coverage". Attempts to maximises the % of the target receiving at least the desired prescription dose, bringing this up to as close to 100 % as possible.
	OHI	"Optimise Homogeneity". Attempts to cover the whole target with the prescription dose, whilst also minimising the dose variation inside the target.
Optimisation Shell		
	OCI	"Optimise Conformality". Attempts to minimise overall maximum dose to any point in the shell, as close to the goal value as possible.
Organ At Risk		
	OMA	"Optimise Maximum Dose". Attempts to give the smallest maximum dose to any point in the target, as close to the goal value as possible.
	OME	"Optimise Mean Dose". Attempts to give the smallest total dose to the selected OAR, as close to the goal value as possible
Overall Plan		
	OMU	"Optimise Monitor Units". Attempts to reduce as far as possible the total MU required to deliver the treatment, within the constraints applied by previous optimisation steps.

Table 2.1: showing the seven clinical objectives which can be used as individual steps during Sequential optimisation. Each step applies to a single specified structure eg PTV1, Shell1, or spinal cord (OAR). Each optimisation requires a minimum of one step; optimisation time will tend to increase as the number of steps increases.

maximum MU per beam. These limits will be respected during the optimisation sequence. The steps are then selected in order of importance. A goal value is specified for each step (for example, optimise coverage of the PTV by the 18.5 Gy dose line), together with a relaxation value. The relaxation value informs the system how much the result of the current step can be compromised in order to achieve any step further down the list.

For each step in turn, the result represents the optimal achievable value for that objective, given the existing constraints and relaxation values. Each result is applied as an additional constraint for each subsequent step. The plan is therefore built up one objective at a time, with gradual improvement seen after each step. Unlike Simplex, the planning process can be paused at any time to allow the adjustment of relaxation factors before being restarted at the same point. Reordering of the steps does however require restarting from the beginning.

There are a number of additional planning variables within MultiPlan which are not covered here, but which can have a big impact on the final result, such as Target Boundary Distance (in Simplex and Sequential) and the Sequential Beam Reduction step. These, and their effects on plan parameters, are discussed in Chapters 4 and 5.

This Chapter has provided a summary of the main features of both the radiosurgical systems which will be used in the experimental chapters, together with an introduction to the radiosurgical planning techniques which lie at the heart of this thesis. The following five chapters will describe and discuss the experimental work performed.

Chapter 3 – Assessing the concordance of planned and delivered dose distributions on the CyberKnife system, using plan-specific QA

Introduction

In later chapters, this thesis will explore ways to optimise the quality of radiosurgical plans produced with CyberKnife, and compare plans produced using CyberKnife and Gamma Knife systems. It is therefore important to verify that plans produced by the MultiPlan treatment planning software accurately reflect the actual treatment delivered, both in terms of the dose delivered and the spatial dose distribution. The purpose of this chapter is to establish the best method for doing this, and then to perform "plan-specific" Quality Assurance (QA) on treatment plans produced in MultiPlan and delivered on a solid water phantom.

QA refers to a program for the systematic monitoring and evaluation of the various aspects of a project, service, or facility to ensure that standards of quality are being met. QA is central to the safe and effective delivery of radiotherapy. It includes both the measurements performed during commissioning of a new radiotherapy system, and, for a working system, the regular checks to ensure that it continues to function with the required accuracy and reliability. Radiotherapy departments are responsible for designing and implementing appropriate QA protocols, which will specify both how often each test should be performed and the permitted tolerances in each case. These protocols are influenced by national QA radiotherapy guidelines, for example IPEM

Report No. 81 (45). Additionally, radiotherapy system manufacturers also often recommend a minimum set of procedures as being essential for safe use of their system.

Since the widespread introduction of CT planning in the 1990s, conventional radiotherapy planning has become increasingly sophisticated with movement from parallel opposed fields to multi-field conformal radiotherapy, and then to IMRT. In IMRT, the total treatment field is made up of multiple small beamlets, making it much harder to carry out the traditional "calculations by hand" which would be done to verify conventional plans. Also, IMRT often entails the use of moving multi-leaf collimator (MLC) leaves during radiation delivery. This adds an important potential source of error in terms of both dose delivered and spatial dose distribution. Consequently, IMRT treatment requires a more rigorous QA protocol. Many centres perform "patient-specific" QA of each IMRT plan before the course of treatment, which involves transferring the plan on to a phantom, delivering a fraction, measuring the dose delivered and comparing this with the planned dose. Patient-specific QA is not part of the Accuray recommended minimum QA for CyberKnife. However, some centres would consider this to be advisable, especially when using the Iris collimator, where the moving segments introduce the possibility of additional error in a similar way to the moving leaves of IMRT treatment.

Reference Dose Measurement

As mentioned above, two important aspects of radiotherapy quality assurance are the verification of dose, and the spatial accuracy achieved. Ionisation chambers represent the most accurate method of reference dose verification for radiotherapy centres. They measure the electrical charge generated by radiation-induced ionisation inside the chamber. This is converted to dose (units of gray or J/Kg) using a series of conversion factors specific to the beam quality and ionisation chamber. Individual field chambers must be regularly calibrated, showing "traceability" back to the "primary standard", which in the UK is held at the National Physical Laboratory. This is usually via a "secondary standard" ionisation chamber held at each centre.

Ionisation chamber readings are most reliable when a single radiation beam covers the chamber completely, as in this situation partial volume effects can be ruled out. This is the common setup when calibrating linac output during commissioning or routine QA. One potential problem with the use of ionisation chambers in radiosurgical plan QA is that multiple small beams are used, some of which may only partially irradiate the chamber. One cannot assume charged particle equilibrium at the beam edge, and the behaviour of the ion chamber is therefore less well characterised in this situation. Nevertheless, ionisation chambers are still likely to be the most accurate way for departments to measure the dose delivered in a radiosurgical plan. The Farmer chamber (PTW, Freiburg, Germany), with a measuring volume of 0.6 cm^3, is a commonly-used thimble chamber for reference dosimetry. The use of a smaller chamber such as a PinPoint chamber (PTW), which has a volume of 0.015 cm^3, would appear to be an

attractive option as there will be fewer beams which only partially irradiate the chamber. Indeed, the PinPoint chamber is specifically designed for stereotactic field measurements. However, smaller chambers produce a smaller signal, and therefore will be more affected by any "noise" in the system. This makes them potentially less accurate, and for this reason PinPoint chambers are generally not recommended for reference dosimetry. The Semiflex chamber (PTW), with a measuring volume of 0.125 cm^3, is a useful compromise providing both reasonable spatial resolution and reasonable dosimetric accuracy.

Semiconductor diodes (SCDs) provide an alternative means of measuring dose output. They are small and relatively easy to use, produce an instant reading, and provide a good measure of relative dose. However, they are less stable than ionisation chambers for measuring true dose delivered: whilst they can also be calibrated to a secondary standard, dose readings are much more prone to drift than with a field ionisation chamber.

Spatial Dose Distribution Analysis

Most radiotherapy centres assess spatial dose distribution by analysis of a 2-dimensional (2D) plane of dose within the 3-dimensional treatment plan. The delivered dose is measured over a series of points in the 2D plane and compared with the intended 2D distribution on the corresponding "slice" of the plan. The result is then assumed to be representative of the whole plan. Multiple ion chambers or SCDs can be arranged in a

2D array to enable measurement of the spatial dose distribution. However, in both cases the spatial resolution is limited by the gaps between the individual chambers or diodes, for example 10 mm with a PTW Seven29 ion chamber array (PTW). This array is commonly used for IMRT patient-specific QA, but the resolution is insufficient for use with small fields, and may not be the best way to measure dose in areas of steep dose gradient. Radiographic film has been widely used in the past, providing sub-millimetre spatial resolution. However, there are problems with using this technique. It requires post-exposure chemical processing to develop and fix the pattern on the film. This process introduces many potential sources of error and uncertainty into the analysis, and in the era of linac electronic portal imaging, many centres no longer have the necessary equipment and materials. Another problem is the sensitivity of radiographic film to any light, meaning that extra precautions must be taken with the film prior to processing.

Radiochromic film has become an increasingly popular tool for spatial dosimetry measurement. Once again it provides sub-millimetre spatial resolution, but unlike radiographic film it requires no chemical processing. It is also much less sensitive to room light. It can measure relative signal across a 2D plane, but only has limited accuracy in measuring true dose delivered. Gafchromic EBT2 (International Specialty Products Inc, Wayne, NJ) is the main commercially available radiochromic film suitable for plan QA, replacing EBT film in 2009. Using the original EBT film, Saur et al reported a dose uncertainty (with 95 % confidence) within 4 % for doses between 1 and 3 Gy (46). A recent study using EBT2 film estimated that dose could be measured with an overall accuracy of 4 - 5 % (47). On the basis of these results, any analysis of a spatial dose distribution using EBT2 film as a true measure of dose will not be able to

compare dose difference with a tolerance of greater than about 5 %. A more detailed discussion about EBT2 film will be provided later in this chapter.

In modern radiotherapy plan QA it is usually desirable to test the spatial accuracy of the radiotherapy dose distribution to a tighter tolerance than 5 % dose difference, and therefore film is often used as a measure of the relative dose across the 2D plane, rather than true dose. A single point on the film is normalised either to a previously measured reference dose at that point, or to the dose at that point on the planned dose distribution (48). The former method is usually favoured where possible, as this uses an independent measure of dose. On a gantry-based linear accelerator, the treatment plan is usually delivered twice on a solid water phantom, firstly with an ionisation chamber within the "PTV", and then with a portion of film positioned at the same point within the PTV relative to the isocentre. The signal on the relevant part of the film is then normalised to the ionisation chamber dose.

Unfortunately this technique would not be possible on the CyberKnife system using the solid water phantom available at this centre (Figure 3.1, and see below). The align centre for treatment is the mid-point of three metal fiducial markers embedded in the layer of solid water which contains the space for the ionisation chamber. Film is placed between layers of solid water, and it is therefore not possible to position it in the same location as the chamber, relative to the align centre. Whilst both the chamber and part of the film will be contained within the PTV, the dose within the PTV will vary by up to 50 % of the prescribed dose in the treatment plans used in this study. Consequently it is not possible to normalise a point on the film to the ionisation chamber. For relative dose

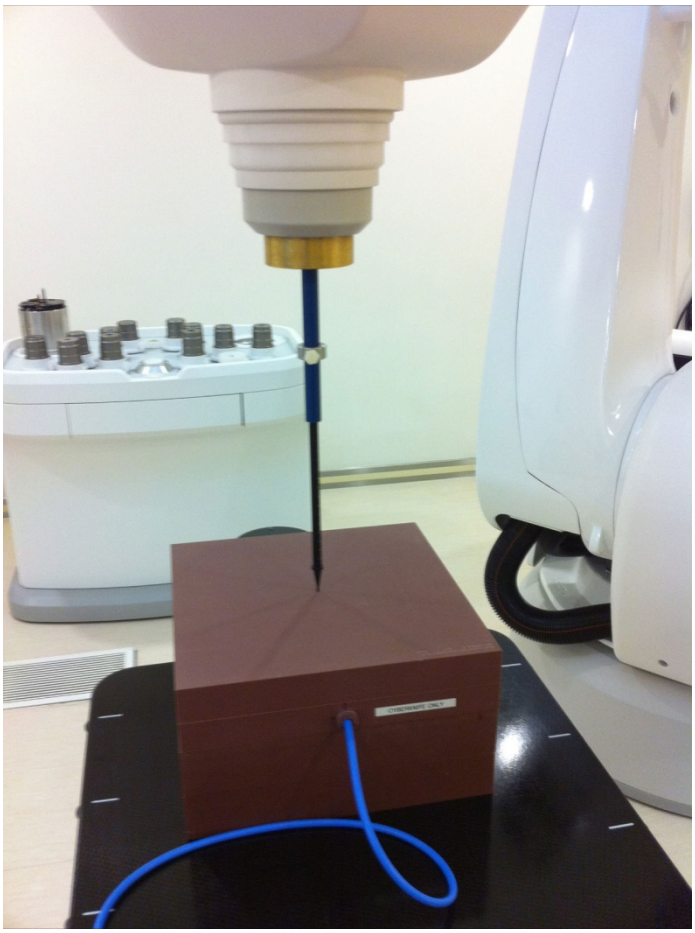

Figure 3.1: Photograph of the WT1 solid water phantom positioned on the CyberKnife treatment couch such that the centre of the phantom aligns with the centre of the beam. A measuring post is being used to verify that the source to surface distance (SSD) is 75 cm. The phantom consists of five individual layers stacked on top of each other. There is a purpose-built hole in the second layer down, into which a Farmer chamber has been inserted (blue cable attached). The chamber is at 5 cm depth within the phantom.

analysis, the only option with the equipment used here is to normalise to a point on the planned dose distribution. This technique unfortunately does not use an independent measure of dose delivered during treatment, and the results of spatial dose comparison will depend to some extent on the dose point chosen for normalisation.

Choosing a Dose Evaluation Metric and Appropriate Tolerances

Historically, various dose evaluation metrics have been proposed for comparison between planned and delivered spatial dose distribution. One simple approach is to calculate the dose difference between planned and delivered dose for each point. However in areas of steep dose gradient, a small spatial shift between intended and delivered plans may produce very large dose differences. Another approach is to overlay the planned and delivered dose distributions and calculate the shortest distance from a point on one distribution to the nearest point on the other with the same dose value. This "distance to agreement" method is useful in areas of the plan with a steep dose gradient, but in areas of shallow dose gradient, a small change in dose may correspond to a large distance to agreement. The Gamma Index (49) combines dose difference (DD) and distance to agreement (DTA) methods in a single index, thus largely avoiding the potential problems in areas of steep and shallow dose gradient. For each point on the delivered dose distribution, this evaluation method automatically finds the closest agreement with the planned distribution, on the basis of a vector combination of DD and DTA measures. If this agreement lies within the pre-specified tolerances then that point has "passed". The pass/fail status of each point can then be shown on the spatial dose distribution. The Gamma Index is not without its limitations (although a

detailed discussion is beyond the scope of this chapter). Nevertheless, it is now widely used in radiotherapy departments around the world.

Patient-specific QA in radiotherapy has become much more widely used since the implementation of IMRT, as mentioned above. Commonly quoted Gamma Index tolerances for IMRT QA using an ionisation chamber array are 3-4 % DD and 3-4 mm DTA. For example, IPEM Report 96 (48) provides examples of clinical tolerances in use in the UK. For head and neck IMRT, which often involves particularly complicated treatment plans, a tolerance of 4 % (DD)/4 mm (DTA) is cited, with the suggestion that at least 95 % of pixels inside the 10 % isodose region of interest should pass these criteria. Many centres would aim for tighter tolerances than this with modern radiotherapy systems.

As discussed above, radiosurgery, with its small fields and areas of steep dose gradient, requires sub-millimetre spatial accuracy, and therefore it can be argued that radiochromic film needs to be used to evaluate radiosurgical spatial dose distribution. It also seems appropriate that the distance to agreement tolerance for a radiosurgery plan should be 1 mm. With respect to dose difference, it would be desirable to follow the established IMRT practice and use a 3-4 % tolerance. Unfortunately, due to the current uncertainties of measuring true dose with Gafchromic film, it would not be possible to use a DD tolerance of less than 5 % in this situation. Indeed, a recent publication of radiosurgical QA on the Tomotherapy system used EBT film for reference dosimetry, and chose 5 % DD and 1 mm DTA as tolerance values (50). However, if using film to

measure relative signal by normalising to the planned dose distribution, then a 3 % DD should be achievable.

In summary, the purpose of this study is to verify that the treatment plans created using the MultiPlan treatment planning system are an accurate reflection of the radiotherapy treatment which would be delivered, by performing plan-specific QA. The following method is proposed. Treatment plans will be generated in MultiPlan and delivered on a solid water phantom. A Semiflex ionisation chamber placed inside the phantom will be used to measure the reference dose. With respect to reference dose, a plan will be deemed to have "passed" the QA test if the delivered dose is within 3 % of the dose calculated by MultiPlan. At the same time EBT2 film placed inside the phantom will be used for 2D spatial dose evaluation. The Gamma Index will be the chosen spatial dose evaluation metric. Analysis will be performed firstly by measuring reference dose across the film, with tolerances of 5 %/1 mm, and then measuring relative dose after normalising to the planned dose distribution, with tolerances of 3 %/ 1 mm. For the purposes of this verification study, any plan in which >/= 95 % points within the region of interest meet these tolerances will have passed the spatial dose distribution QA.

Methods

Treatment plans were generated using MultiPlan treatment planning system, version 3.5.1. A WT1 solid water phantom (St. Bartholomew's Hospital, London) was scanned using a GE LightSpeed 16 slice CT scanner (GE Healthcare, Buckinghamshire, UK). Prior to scanning, a 0.125 cm^3 Semiflex (ionisation) Chamber (PTW, Germany) was positioned inside the phantom, through the purpose-built hole in one of the layers. An 8 x 10 inch sheet of EBT2 film (with one triangular corner cut out to ensure correct orientation) was carefully placed between the first and second solid water layers and secured with tape. The axial slice thickness of the CT scan was 1.25 mm, as is standard for all CyberKnife planning CT scans at this centre. The scan was then imported into MultiPlan. A 3 cm diameter spherical "virtual" planning target volume (PTV) was created using the ball-cube function, and positioned in the phantom such that it contained the ionisation chamber thimble and a portion of the sheet of EBT2 film. The size of the target (3 cm diameter) was chosen as it could comfortably contain both the whole measuring volume of the chamber and a reasonable area of film. Within the PTV, the measuring volume of the chamber was contoured as a separate structure (Figure 3.2).

Ten treatment plans were produced, five using the simplex optimisation algorithm with 3 fixed collimators, and five using the sequential algorithm with the Iris variable aperture collimator. Ray-Tracing was used as the dose calculation algorithm. For each plan, a prescription dose of 3 Gy was used, and the variables were configured to produce a prescription isodose between 65 and 70 %. This meant that the maximum

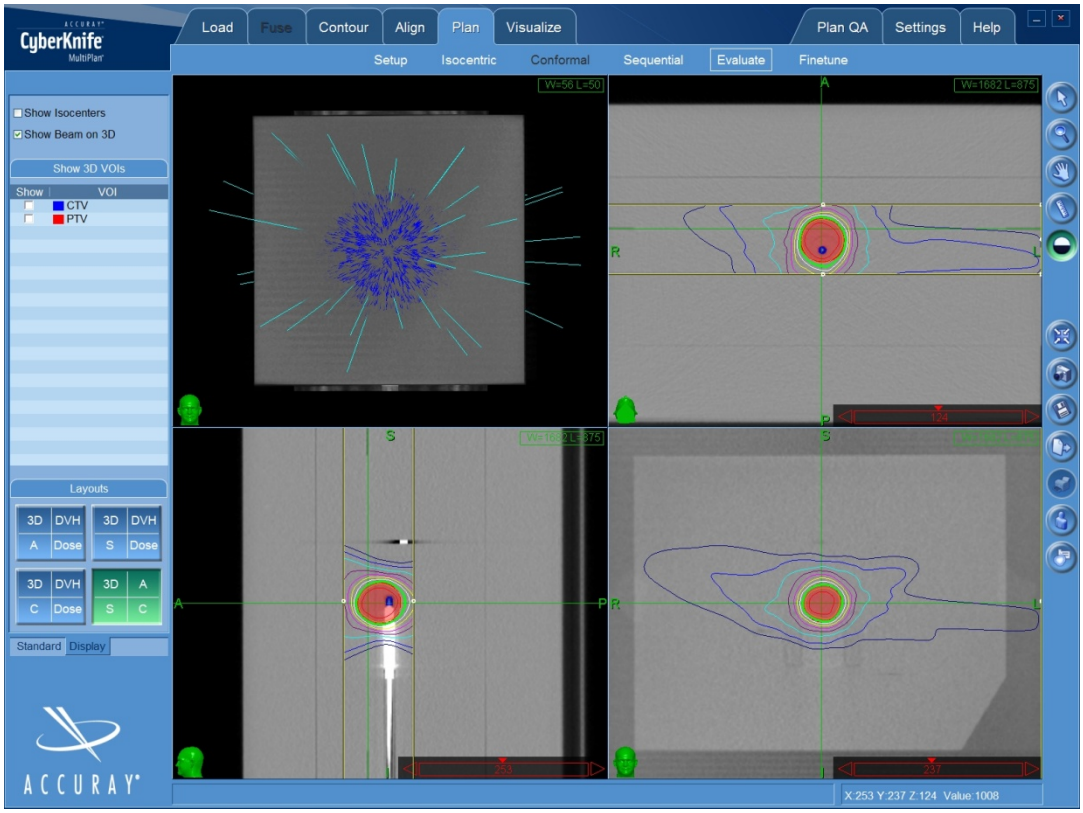

Figure 3.2: Screenshot from MultiPlan version 3.5.1 showing a treatment plan for the 30 mm spherical target (red overlay) produced using Sequential optimisation. Axial, sagittal and coronal views are shown, together with a "hedgehog" view of the beam arrangement (top left – beams are shown in light blue). The ionisation chamber can be seen in the sagittal view (bottom left), and the measuring volume of the chamber is shown in blue overlay inside the target. The outline of a piece of gafchromic film (with one corner chopped off) is seen in the coronal view (bottom right), positioned between two layers of the phantom for the planning CT.

dose to any point would be no more than 4.6 Gy, which is safely below the saturation level of the EBT2 film (approximately 8 Gy). Steps were taken during the planning process to minimise the heterogeneity of dose within the chamber measurement volume. For each plan, the mean, minimum and maximum dose to the measurement volume was recorded. Each plan was saved as "deliverable" and transferred to the treatment delivery console.

The solid water phantom was then moved to the CyberKnife bunker and positioned on the treatment couch. At the start and end of each treatment session, the CyberKnife linac output was measured using a 0.6 cm^3 Farmer chamber (PTW) positioned at 5 cm depth in the solid water phantom, with 75 cm source to surface distance (SSD) (Figure 3.1). 200 MU was delivered using the 60 mm fixed collimator, and the electrical charge in the chamber recorded on a Unidos Webline electrometer (PTW), with the polarity set at -400 V. If the output was different at the end of the session compared to the beginning, the average of the two readings was taken as the output during the treatment session.

For the treatments, the Farmer chamber was replaced with the Semiflex chamber and a new piece of EBT2 film positioned exactly as for the planning CT scan (Figure 3.3). Each batch of film had been previously calibrated against the Farmer chamber across a range of MU levels from 0-800. The calibration curve generated was subsequently used by the dose verification software (see below). A new piece of film was used for each treatment plan. Each of the ten plans generated was delivered once. For each plan the dose recorded with the ionisation chamber was compared to the mean chamber dose seen in the corresponding treatment plan: the percentage difference was recorded.

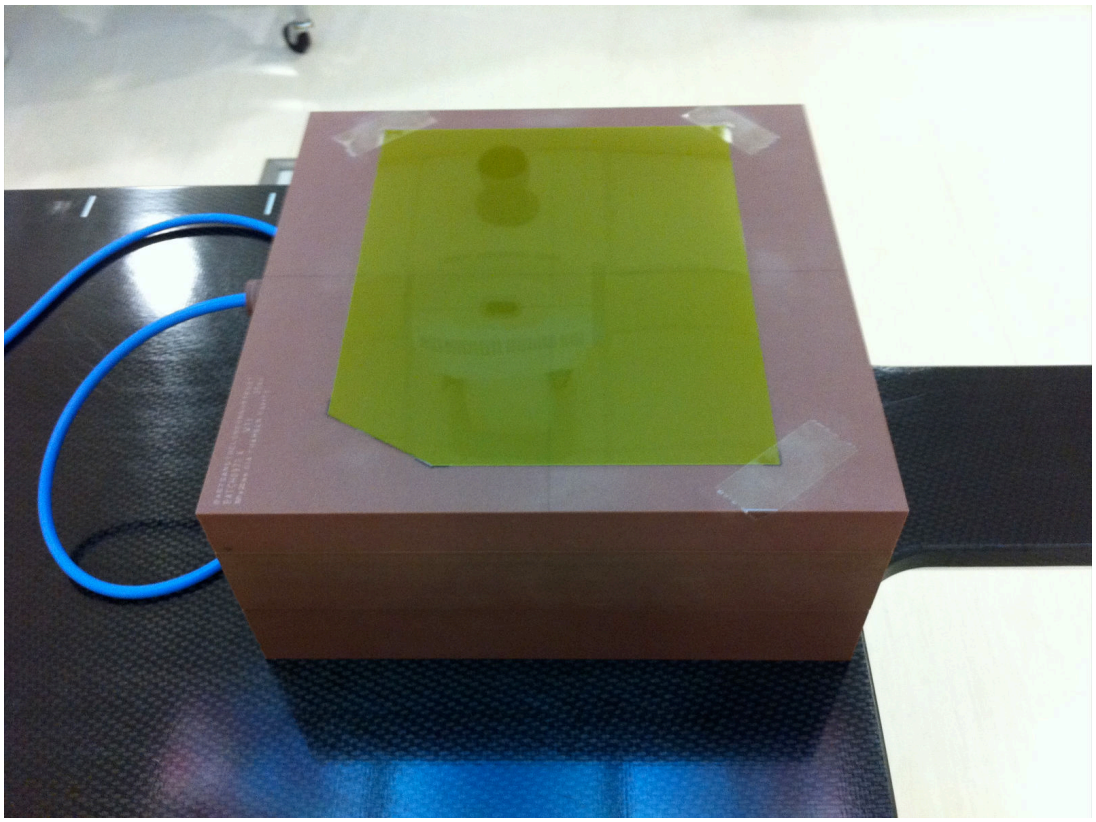

Figure 3.3: Photograph showing the bottom four layers of solid water positioned on the CyberKnife treatment couch. An 8 x 10 inch piece of Gafchromic EBT2 film with one corner cut off has been placed on top of the upper solid water layer, and fixed in place with tape. A Semiflex chamber has been inserted into the custom-built hole in the upper layer. A fifth and final solid water layer is placed on top of the four layers shown to complete the phantom setup.

The irradiated film was collected and stored for 48 hours to allow completion of the development process. It was then uploaded for analysis using an Epson Expression 10000XL A3 scanner (Seiko Epson Corporation, Japan). Care was taken to position each film in the same position on the scanner bed, as there is usually a non-uniform response across the scanner bed (Figure 3.4) (see discussion). Each film was also scanned in the same orientation, as there have been reports that EBT film shows a different response when scanned in different orientations (51, 52). The scan resolution was set at 72 dots per inch (dpi), giving the film a spatial resolution of 0.35 mm. The scanned images were imported into Verisoft (PTW) verification software, together with the corresponding plan dose distributions which were imported directly from MultiPlan. For each case, the planned and delivered dose distributions were overlaid using a translational movement such that the centre of the delivered dose distribution was on the centre of the planned dose distribution. The region of interest for comparison was the central 21 x 16 cm rectangle of the film, which allowed exclusion of approximately 2 cm on all sides around the edge of the film. This excluded areas where the film had been written on (labelled), handled, or cut, any of which would affect the reading.

Comparison between the planned and delivered dose distributions was then performed using the Gamma Index evaluation metric. The comparison was carried out twice for each plan. Firstly, the film was used as a measure of reference dose, with a factor applied to account for the machine output on the day the film was exposed. A Gamma Index analysis was then applied with tolerances of 5 %/1 mm. Secondly, the film was used for relative dose measurement, after normalisation to the planned dose distribution. An arbitrary dose point was selected in an area of relative dose homogeneity within the PTV and close to the prescription isodose line. The planned dose at this point and the

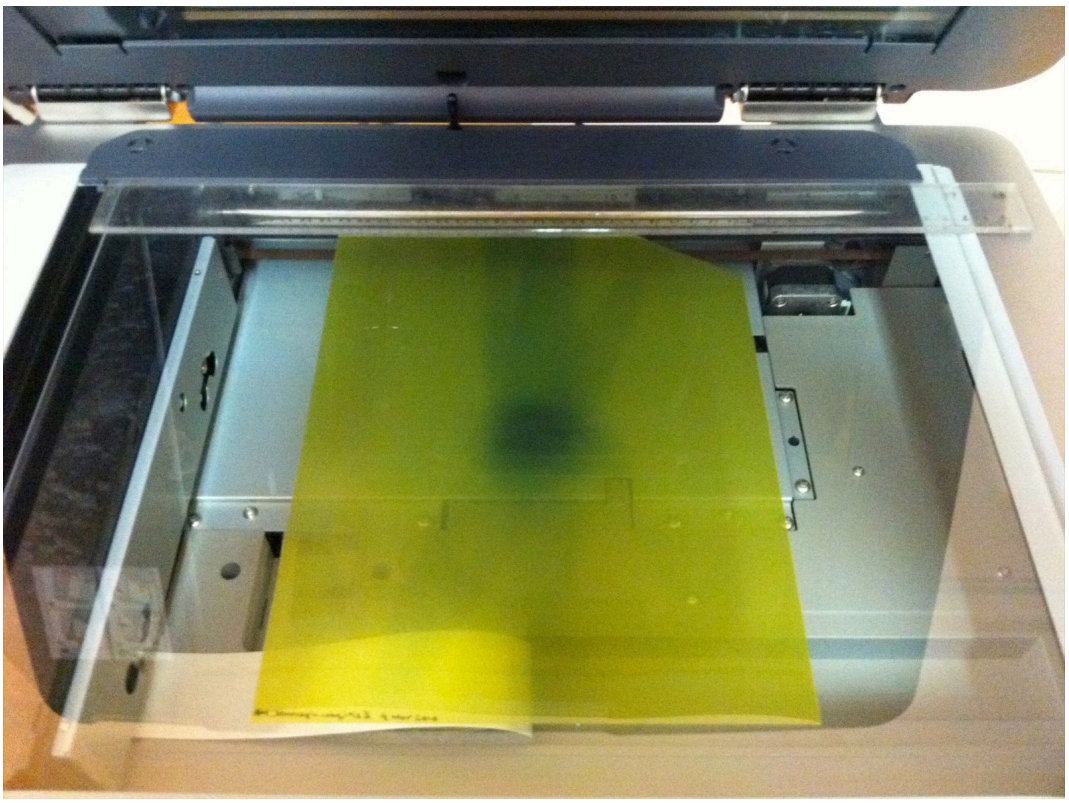

Figure 3.4: Photograph showing a piece of exposed EBT2 film placed on the flatbed scanner. A ruler has been placed up against two sides of the scan bed. The film is positioned according to the ruler measurements, to ensure that each successive film is scanned in exactly the same position.

coordinates of the point were recorded. The corresponding dose measured on the film was calculated by taking the mean dose of the nine dose points nearest to the coordinates (the film spatial resolution is 0.35 mm, compared to the 0.97 x 0.97 mm pixel size on the planning CT). An appropriate normalisation factor was then applied across the whole film, based on the planned dose and film dose at this point. Gamma Index analysis was then applied with tolerances of 3 %/1 mm.

Dose points on the planned distribution which were less than 5 % of the prescribed dose were excluded from analysis. Since dose difference tolerances (eg 3 %) are relative to the maximum dose on the plan, low dose points are much less likely to "fail" on this criterion. Restricting analysis to points over 5 % of the prescribed dose prevented the results from being "unrealistically" good, whilst still ensuring that there was a sufficiently large area of dose points for spatial analysis of the plan. Films on which < 95 % points passed the Gamma Index criteria were investigated qualitatively.

Results

Ionisation chamber reference dosimetry

The ionisation chamber dose measurements for the ten treated plans are shown in Table 3.1, together with the mean planned dose across the ionisation chamber and the percentage error of the plan, where:

$$\%\ error = \frac{|(measured\ dose - mean\ planned\ dose\ to\ chamber)|}{mean\ planned\ dose\ to\ chamber}$$

Table 3.1 also shows the minimum and maximum planned doses to the chamber in each plan, together with the percentage variation across the chamber, where:

$$\%\ variation\ = \frac{(planned\ chamber\ max.dose - planned\ chamber\ min.dose)}{mean\ planned\ dose\ to\ chamber}$$

The percentage error ranged from 0.4 % - 2.01 %, with mean 1.07 % and standard deviation 0.53 %. All measured doses were comfortably within 3 % of the planned dose, and were therefore acceptable in this regard. The mean error for the fixed collimator plans was 0.78 %, compared to 1.36 % for the iris plans. The distribution of error scores is not likely to be normally distributed, therefore the assumptions for performing a parametric test to compare the two groups of errors were not met. Using the Mann-Whitney U test to compare the two groups of data, there was no statistically significant difference in error between the two groups at the 5 % level ($p = 0.095$).

Plan Name	Planned chamber minimum dose (cGy)	Planned chamber maximum dose (cGy)	Variation in planned dose across chamber (%)	Planned chamber mean dose (cGy)	Measured dose (cGy)	Absolute dose error (%)
Fixed 1	397.54	428.57	7.46	416.17	417.85	0.40
Fixed 2	411.00	441.18	7.06	427.36	423.36	0.94
Fixed 3	425.26	454.55	6.64	440.89	444.32	0.78
Fixed 4	403.00	428.57	6.11	418.28	422.10	0.91
Fixed 5	410.82	441.18	7.10	427.65	424.01	0.85
Iris 1	407.07	422.34	3.68	415.28	417.66	0.57
Iris 2	411.57	437.37	6.05	426.69	434.97	1.94
Iris 3	413.13	438.89	6.03	427.41	436.00	2.01
Iris 4	403.82	432.15	6.72	421.54	425.60	0.96
Iris 5	422.54	456.16	7.60	442.30	448.05	1.30

Table 3.1: Comparison of the planned dose to the ionisation chamber with the dose measured on delivering the treatment, for each of the ten treatment plans produced.

Table 3.2 shows the percentage of points in each treated plan which passed the Gamma Index analysis, firstly at 5 %/1 mm tolerance using dose measured by the film, and then at 3 %/1 mm after normalising to a point on the planned dose distribution. In all ten plans, >/= 95 % of points within the region of interest "passed" at 5 %/1 mm. Figure 3.5 shows a summary of one of these results. At 3 %/1 mm, nine of the ten plans exceeded the required 95 % pass rate. In the remaining plan, "Fixed 2", only 92.9 % points passed the analysis. The ionisation chamber dose error result for this plan (0.94 %) was well within the pre-specified tolerance, as was the Gamma Index result using measured dose at 5 %/1 mm tolerances (99.8 %). Nevertheless a more qualitative analysis of the Gamma Index results for this plan was carried out.

Figure 3.6 shows the isodose lines of the "Fixed 2" planned dose distribution, with the delivered dose distribution overlaid. The spatial arrangement of the 7.9 % failed points is also shown. There is no clear pattern to the arrangement of the failed points. However, a large proportion of them lie in one small area of the region of interest. Visual inspection of the film did not show any obvious damage in this area. These failed points are hot (the measured dose was higher than the planned dose), and therefore could represent a treatment overdose in this area. Whilst this portion of film corresponds to a low dose area of the plan, where doses are less than 20 % of the prescription dose, the clinical acceptability would depend on the nature of the tissue being overtreated. The area of steep dose gradient outside the PTV is relatively free of failed points, which is important as this is often the area where organ-at-risk tissue most

	Reference dosimetry	*Relative dosimetry*
Plan Name	**% points passed at 5 %/1 mm**	**% points passed at 3 %/1 mm**
Fixed 1	99.6	98.4
Fixed 2	99.8	92.9
Fixed 3	99.8	95.1
Fixed 4	99.6	97.9
Fixed 5	99.7	97.9
Iris 1	99.1	97.6
Iris 2	95.8	97.7
Iris 3	95.5	96.6
Iris 4	100.0	99.5
Iris 5	99.8	98.8

Table 3.2: Percentage of dose points passing the Gamma Index analysis for each of the ten plans produced. Results are shown for two different tolerance levels: 5 %/1 mm with no normalisation, and 3 %/1 mm after normalising the film to a point on the planned dose distribution. The value shown in red failed the pre-specified 95 % pass rate

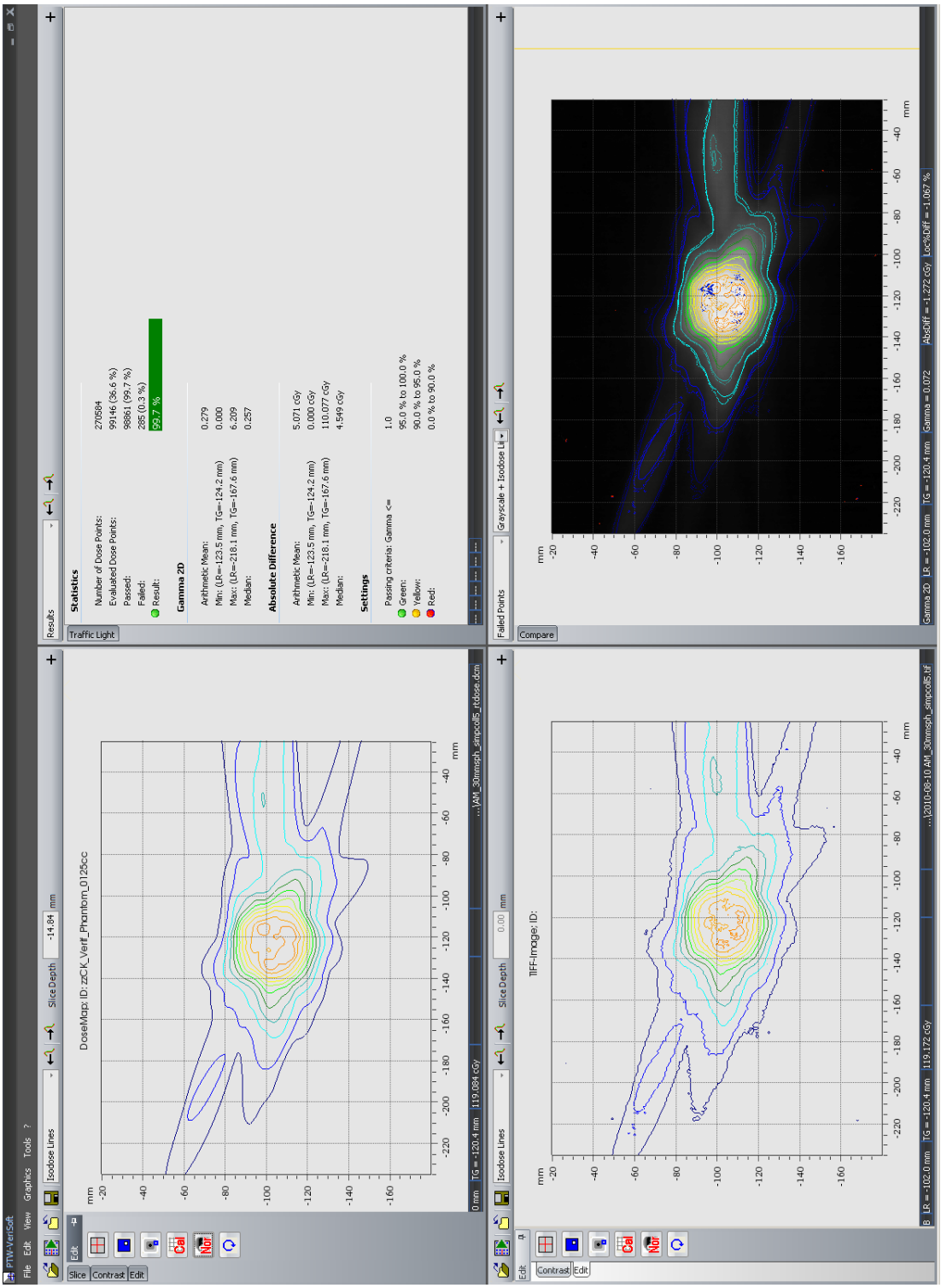

Figure 3.5: Screenshot from Verisoft software, showing the results of a Gamma Index analysis performed on the "Fixed 5" treatment plan using 5 %/1 mm tolerance levels. The planned and delivered dose distributions are shown in the top left and bottom left windows (landscape view) respectively. The top right window shows the plan statistics including the overall pass rate (highlighted in green). The bottom right window shows the planned and delivered dose distributions superimposed.

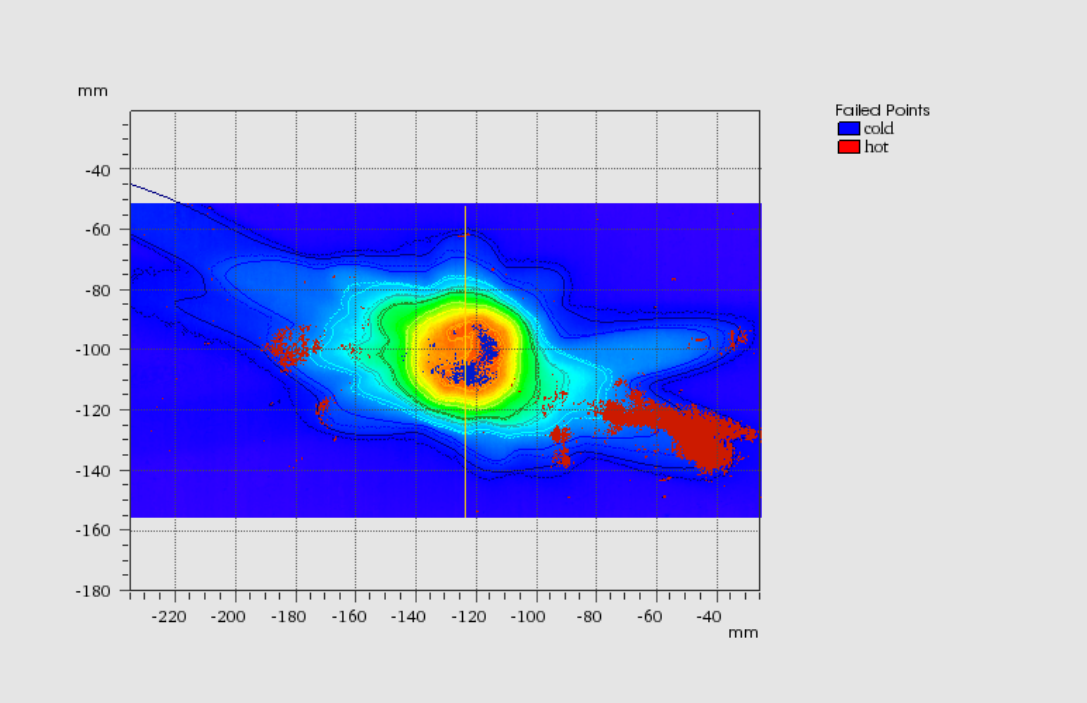

Figure 3.6: Image taken from Verisoft software showing the planned and delivered dose distributions of the "Fixed 2" plan overlaid. A colourwash has been applied showing more broadly the dose distribution across the film. Additionally, the dose points on the film which failed the Gamma Index analysis at 3 %/1 mm tolerance are shown in red and blue for "hot" and "cold" points respectively. The majority of hot points are in one area at the bottom right of the film. The majority of cold points are inside the PTV.

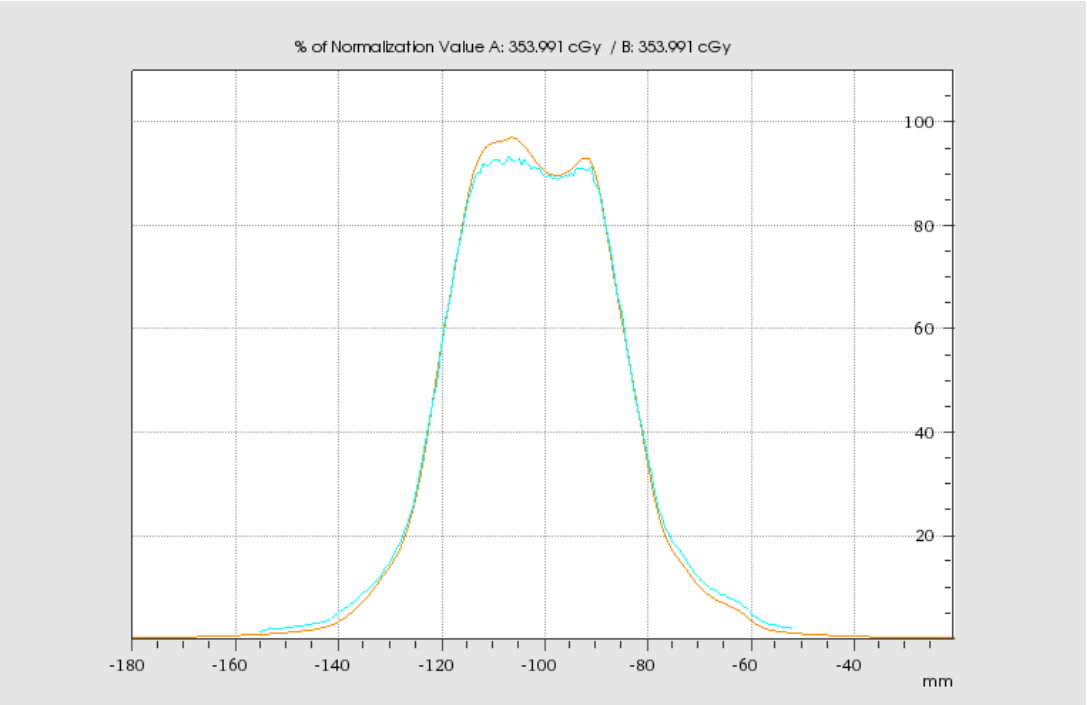

Figure 3.7: Image taken from Verisoft software showing the planned (orange curve) and measured (blue curve) doses for points on a one-dimensional line through the PTV, as shown in yellow in Figure 3.6. The y axis numbers show the dose as a % of the maximum dose on the plan.

at risk of damage is located. Within the PTV there are a number of failed points which are cold (measured dose lower than planned dose). Figure 3.7 shows a comparison of the planned (orange curve) and measured (blue curve) doses for points on a one-dimensional line through the middle of the PTV, as shown in yellow on Figure 3.6. The y axis scale runs from 0 - 100 % dose; the prescription isodose for this plan is 68 %. The graph shows that in the area where the measured dose is "cold", the dose points are still receiving substantially more than the prescription dose, and therefore these failed points within the PTV are unlikely to be clinically significant if this was a real treatment plan.

Discussion

CyberKnife treatment plans are usually complex, consisting of multiple small, non-coplanar beams incident on a small target. The ionisation chamber reference dosimetry results here show that the system is able to deliver such plans with dose accuracy comfortably within the pre-specified 3 % error value. Although there was a trend towards smaller errors with the fixed collimator plans, there was no statistically significant difference between the two groups. Whilst a bigger sample size may have shown a significant difference, the error values seen with the iris collimator plans were still easily within 3 %.

With respect to spatial dose distribution analysis, all of the ten plans "passed" the Gamma Index analysis with tolerances of 5 %/1 mm without normalising the film, and nine out of the ten passed at 3 %/1 mm, after normalising the film dose to the planned dose distribution. In the one plan which did not pass at 3 %/1 mm ("Fixed 2"), a qualitative analysis revealed that this plan would probably be a borderline case in terms of acceptability. The significance of the failed points in the low dose area would depend on the tissue being irradiated here. As will be discussed later, it is not clear to what extent the failed points in this analysis were due to inaccuracy at some step in the treatment process, or to problems with intra-film variability in response to radiation.

Radiotherapy QA can be performed using a variety of different techniques and tools. In the introduction section of this chapter, many of these different techniques were

discussed, and a method for performing CyberKnife plan-specific QA was proposed. Whilst care was taken to ensure that this method was reasonable given the nature of the task and the techniques available, there are still a number of limitations and possible sources of error which will now be discussed.

The biggest source of error in the results obtained is likely to be the use of EBT2 film. There is no doubt that a meticulous, consistent technique is critical to film dosimetry (as it is for all radiotherapy QA), but even with this in place there is still a large potential for error using this film. Original EBT film was introduced in 2004, consisting of two identical active transparent layers which darken on exposure to radiation, and which are sandwiched between two protective surface layers. As discussed previously, it is easier to handle than radiographic film and is self-processing. Unfortunately it has been shown that even with the use of a high quality scanner and appropriate scanner technique (discussed below), including a flattening correction, there was still uncertainty of absolute dose measurement in the region of 4 % (46). The manufacturer attributes this, in the main part, to intrinsic variation of the thickness of the active layer. Whilst it may be expected that different batches of film will differ in the active layer thickness, unfortunately this variation can be seen across different films in the same batch, and even across an individual sheet of film.

EBT2 film was introduced in 2009 with the aim of improving the accuracy of dose measurement. A radiation-insensitive yellow dye was added to the active layer which causes attenuation of the signal in the scanner's blue channel, and thus provides a measure of the thickness of the active layer. In theory, therefore, the variation in

thickness across the film can be corrected for by measuring the signal from the standard red channel, together with the signal from the blue channel. Unfortunately, the correction protocol is extremely complicated, and at the time of writing only one brand of commercial dose verification software ("Film QA" (International Specialty Products)) is capable of processing this information. Also it involves measuring signal through the blue channel, which is not usually recommended for dosimetry. Without this correction in place, EBT2 is no more accurate than EBT at measuring dose, and unfortunately shows greater intra-sheet inhomogeneity. For example, Hartmann et al (53) reported intra-sheet inhomogeneities increasing from +/- 1 % with EBT to +/- 3.7 % with EBT2. This is fairly consistent with results obtained at this centre, using the equipment described. A single piece of film was cut into four pieces and each placed in turn at 5 cm depth within the solid water phantom. 400 MU were delivered from above, through a single 60 mm beam. The measured dose was found to differ from the ionisation chamber reference dose by -1.6 %, -3.0 %, -3.7 % and -4.2 % for the four pieces of film.

For Gamma Index analysis of radiosurgical spatial dose distribution, tolerances of 3 %/1 mm would seem appropriate. When using EBT2 film, due to the above problems, it is not possible to use a DTA tolerance of 3 % without normalisation either to a ionisation chamber point dose or to a point on the MultiPlan dose distribution. Even with normalisation, the intra-film inhomogeneity means that results must still be interpreted with caution. Whilst normalising to the planned dose distribution could be criticised as being less robust than using an independent dose measurement, the problems of intra-film inhomogeneity remain with either technique. More work needs to be done to improve both the accuracy and reliability of dose measurement with EBT2. It is hoped

that either the EBT2 correction protocol becomes more widely-usable (and more manageable) or an alternative product is developed without the above problems.

The scanner provides an additional source of error related to film analysis. In this study, a high quality professional flatbed charge-coupled device (CCD) scanner was used. A relative flattening correction was applied within Verisoft to account for non-uniformity across the scanner, as documented by Devic et al (54), amongst others. Also, care was taken to ensure consistency across different films with respect to the position and orientation on the scanner bed, as this too has been reported as a source of error (51, 52). Films were scanned in "landscape" mode, as this is recommended by the EBT manufacturers, and has been shown to have less pronounced non-uniformity in the direction of the CCD array, when compared to scanning in portrait mode (46). In spite of these measures there may be further possible error. For example, Lynch et al showed that with repeated scans, the temperature of the scan bed will increase, and this increased temperature can affect the optical density of the film on the scan bed (51). However, any residual error related to the scanner is likely to be small in comparison with the film-related uncertainty discussed above.

The size of ion chamber (0.125 cm^3) was chosen as it provided a reasonable compromise between spatial resolution and dosimetric accuracy. It could be argued that the measuring volume was too large to provide a meaningful value for comparison with the planned dose. In this study, the chamber reading was compared against the mean dose delivered to the measuring volume on the treatment plan. However, the planned dose within the measuring volume varied by as much as 7.6 % of the mean dose, across

the ten plans generated (Table 3.1). It would be good to have a smaller volume chamber which produces sufficient signal to maintain dosimetric accuracy. Liquid ionisation chambers produce greater signal than air chambers for a given measuring volume. MicroLion (PTW), with a measuring volume of 0.0017 cm^3 is an example of one such chamber designed for stereotactic QA. However, one possible disadvantage is that the irradiation direction is axial, compared to the radial direction of the air chambers used in this study. In other words it is designed to measure radiation which enters directly through the end of the chamber, as opposed to the whole cylindrical circumference as with the air chambers. One can predict that with a CyberKnife treatment plan, involving multiple non-coplanar beams originating from a wide space around the patient, it will not be possible to ensure that all beams are incident on the chamber in the appropriate way. In any case, a liquid ion chamber was not available for use in this study.

Only one size (and shape) of target (30 mm sphere) was used. This size was chosen as it allowed the Semiflex chamber and a section of the film both to be contained within the virtual PTV, and also ensured that most of the area inside the 10 % isodose was included in the film region of interest. Using targets significantly bigger or smaller than this would have caused a problem in these respects. Keeping to a single size and shape of target also allowed a fair comparison between the performance of fixed and iris collimators. However, the size of the target did mean that fixed collimators larger than 30 mm were not used, and the iris aperture size similarly did not go above this size. The accuracy of the larger collimator sizes has therefore not been verified here. However, it was felt that any small errors in field size would have more effect on the smaller collimator sizes/iris settings, as they would represent a greater proportion of the overall field size. Nevertheless, a continuation of this project, performing ionisation chamber

and film analysis on treatment plans of real lesions of varying shapes and sizes would be useful, perhaps once EBT2 film analysis can be easily performed with greater dosimetric accuracy.

Summary

Based on this study, the CyberKnife system is able to deliver treatment plans using either fixed or Iris collimators with an ionisation chamber reference dose accuracy well within 3 %. With regard to spatial dose distribution, it is more difficult to make firm conclusions based on the results here, because of the problems obtaining reliable results using EBT2 film. It is acknowledged that there is a need for improved film dosimetry in CyberKnife QA, and possible ways to improve the method have been discussed. However, the analyses performed here did not reveal any results which would be a major cause for concern.

For the purpose of this thesis, on the basis of the work carried out, it is reasonable to conclude that the calculated dose and spatial dose distribution produced by MultiPlan accurately reflect that which is administered during treatment. Dosimetric planning studies which rely heavily on MultiPlan dose calculation algorithms can now be carried out with reasonable confidence that the plans produced are realistic in terms of patient treatment.

Chapter 4 – Establishing the relationship between prescription isodose value and external dose gradient for spherical intracranial targets

Introduction

Radiosurgery uses the ablative power of very high doses of radiation with the intention of destroying all tissue within the PTV. In order to achieve this safely, the volume of normal tissue receiving a high dose of radiation must be minimised. There are three main ways in which this is achieved.

Firstly, the volume of normal tissue contained within the PTV should be minimised. Within the PTV the gross tumour volume (GTV) represents the macroscopic extent of the tumour as visualised on the appropriate axial imaging. The clinical target volume (CTV) consists of the GTV together with a margin added on all sides to account for any subclinical tumour spread. This margin depends on the tumour type and location, and can vary from 0 mm in certain benign brain tumours up to as much as 25 mm in conventional radiotherapy for glioblastoma multiforme. A margin is then added to the CTV on all sides to account for inter- and intra-fraction tumour and organ motion, and inaccuracies of patient setup and treatment delivery: the resultant volume is the PTV(34, 35). Reducing the CTV - PTV margin will therefore reduce the volume of normal tissue within the PTV. One of the main differences between conventionally-fractionated radiotherapy (CFR) and radiosurgery is the size of the CTV - PTV margin required. For example, even though intracranial tumours show negligible movement, a margin of 3 - 5

mm is still usually recommended in CFR to the brain in order to account for setup and delivery inaccuracy, and any patient head movement within the (relatively) firm-fitting thermoplastic shell. However, radiosurgery systems can treat intracranial tumours with sub-millimetre accuracy, either through rigid immobilisation with a pinned stereotactic frame or, as in the case of CyberKnife, accurate alignment using near real-time image guidance (37, 42). As a result, a CTV - PTV margin of 0 - 2 mm is standard practice in intacranial radiosurgery, depending on whether any image fusion needs to be accounted for. This substantially reduces the volume of normal tissue within the PTV, compared to conventional radiotherapy treatment (Figure 4.1). It should be reiterated here that simply choosing smaller targets will also reduce the normal tissue volume within the PTV, which is why target size is such an important consideration in radiosurgery.

The second way to minimise the volume of normal tissue receiving a high dose of radiotherapy involves the creation of a treatment plan where the dose distribution follows the contour of the PTV as closely as possible. The term “conformality” refers to the degree to which the prescription isodose line “conforms” to the PTV contour, and is an important radiosurgical parameter. Whilst it is clearly important that the prescription isodose line should cover as much of the PTV as possible (this is known as PTV coverage), it is also important to minimise the coverage of normal tissue lying immediately outside the PTV. Indeed, the safe delivery of obliteratively high doses of radiation requires a very conformal treatment plan. The perfect treatment plan, in terms of conformality, would be one where 100 % of the PTV is covered by the prescription isodose line, and 0 % of normal tissue outside the PTV is covered.

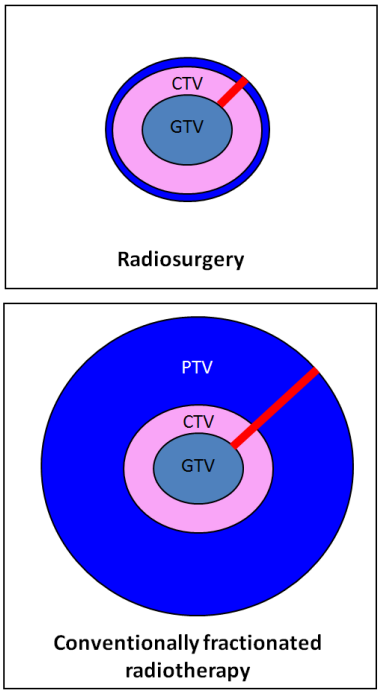

Figure 4.1: Diagram showing the different volumes used in radiotherapy planning, as per ICRU 50 and 62 guidelines. The different margins required in radiosurgery and conventionally fractionated radiotherapy are illustrated.

It is useful to have a universal measure of conformality, for example when comparing potential treatment plans on an individual patient, or comparing plans produced by different radiosurgery systems. A number of different measures have been proposed. Shaw et al (55) proposed the PITV ratio as a conformity index (CI):

$$CI = \frac{PIV}{TV}$$

where PIV is the volume contained within the prescription isodose line (prescription isodose volume) and TV is the target volume. Whilst this is easy to calculate, it is only a valid measure if it is assumed that the centre of the PIV is positioned at the centre of the (P)TV, and that the PIV and PTV are the same shape. If not, then this index can give inappropriate values, as illustrated by Figure 4.2. Knoos et al (56) in their work on conventional radiotherapy, proposed an index which is broadly equivalent to:

$$CI = \frac{TV_{PIV}}{TV}$$

where TV_{PIV} is the volume of the target which is contained within the prescription isodose volume. Unfortunately, whilst this corrects the flaws present in the Shaw index, there is another problem. Any plan where the PIV covers the TV completely will give a perfect score of 1, regardless of how much normal tissue is contained within the PIV (Figure 4.3).

Paddick (57) proposed an alternative index which appears robust to the above problems:

$$CI = \frac{(TV_{PIV})^2}{(TV \times PIV)}$$

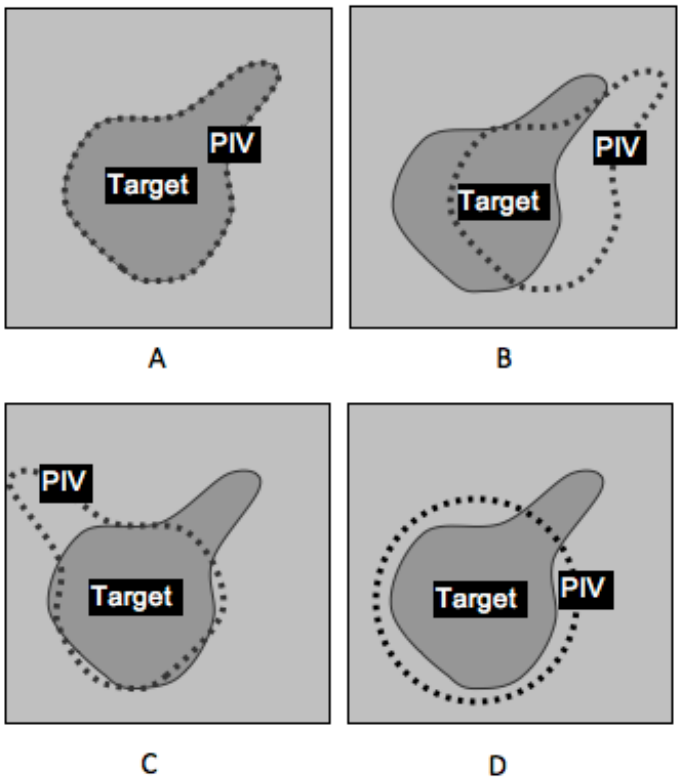

Figure 4.2: Four diagrams, each showing the same radiosurgical target, but with different prescription isodose lines containing the prescription isodose volume (PIV). The PIV has the same volume as the target in each case, and therefore the conformality index (CI) would be a perfect score of 1, using the measure proposed by Shaw et al (55). This score would be appropriate for diagram A, but not for diagrams B (wrong position), C (wrong orientation) or D (wrong shape). Reproduced from Paddick (57) with permission.

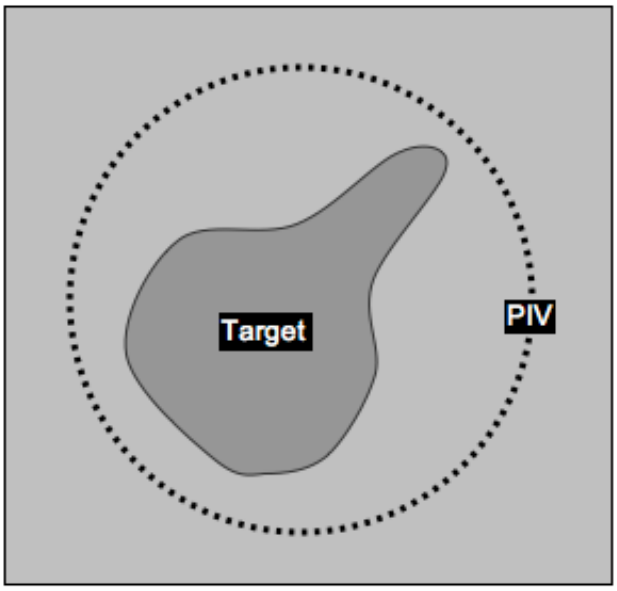

Figure 4.3: Diagram showing a radiosurgical target fully covered by the prescription isodose line, containing the PIV. The conformality index (CI) would be a perfect score of 1, using the measure proposed by Knoos et al (56), which is inappropriate since a large volume of tissue outside the target is also contained within the prescription isodose line. Reproduced from Paddick (57) with permission.

Using this index, a conformity index of 1 represents the perfect radiosurgical plan, with lower values corresponding to progressively worse conformality. The reciprocal of this measure has been incorporated into the MultiPlan system as an automatically generated value for every plan produced. It is referred to as the new Conformity Index (nCI), and is the conformality measure chosen for use in this study. An nCI of 1 still represents perfect conformality, but now the value increases as conformality worsens.

The third strategy used in radiosurgery to reduce the volume of normal tissue receiving a high dose of radiation is the generation of a steep dose fall-off outside the PTV. This strategy is very important in intracranial cases where the target is often surrounded by normal brain tissue. In this situation a steep dose fall-off on all sides is required. Sometimes an especially radiosensitive organ lies close to the target on one side. Here, whilst a steep dose gradient on all sides is desirable, it is especially important to achieve steep fall-off on the side which is closest to the critical organ. This situation will be examined in Chapter 6. Radiosurgical treatment plans use multiple small beams (or multiple arcs), all incident on the target, which results in a steeper dose gradient away from the PTV than can be achieved with CFR. Furthermore, the CyberKnife system can select from a very large number of non-coplanar beams which reduces beam overlap outside the PTV, thus further increasing the external dose gradient.

As with conformality, it is useful to have a measure of external dose gradient to allow comparison of different treatment plans and technologies. Once again a number of measures have been proposed. The volume of tissue within the 12 Gy isodose line (V12) is a widely used parameter as it has been shown to correlate with normal tissue

complications in radiosurgery for AVMs (12) and intracranial tumours (58). However, whilst it is very useful clinically, it is not a pure measure of dose gradient per se, as it will also depend on both the prescribed dose and the size of the PTV. Liscak et al (59) used the following measure of gradient:

$$Gradient = \frac{volume\ within\ the\ (x - 20)\ \%\ isodose\ line}{volume\ within\ the\ x\ \%\ isodose\ line}$$

where x = the chosen prescription isodose of the plan. The authors found a positive correlation between this value and risk of cranial nerve complications in a group of patients with acoustic neuromas. Whilst this demonstrates the importance of a steep external dose gradient, once again it is not an ideal measure, as it is influenced by the choice of prescription isodose in each plan. For example, if x = 40 % in one 18 Gy treatment plan, then (x-20) corresponds to the 9 Gy isodose line. However if x = 60 % in another plan of the same dose, then (x-20) corresponds to the 12 Gy isodose line. A comparison of the two plans using this measure of external dose gradient would not be fair.

Paddick and Lippitz (60) have proposed a gradient index which is independent of the chosen prescription isodose:

$$Gradient\ Index = \frac{volume\ within\ \left(\frac{x}{2}\right)\%\ isodose\ line}{volume\ within\ x\ \%\ isodose\ line}$$

where x = prescripton isodose of the plan (Figure 4.4). This index is therefore a measure of the speed of dose fall-off from prescription dose to half this dose, and can be used to compare plans with different chosen prescription isodoses. When comparing two plans, the plan with the lower gradient index (GI) value has a steeper dose fall-off.

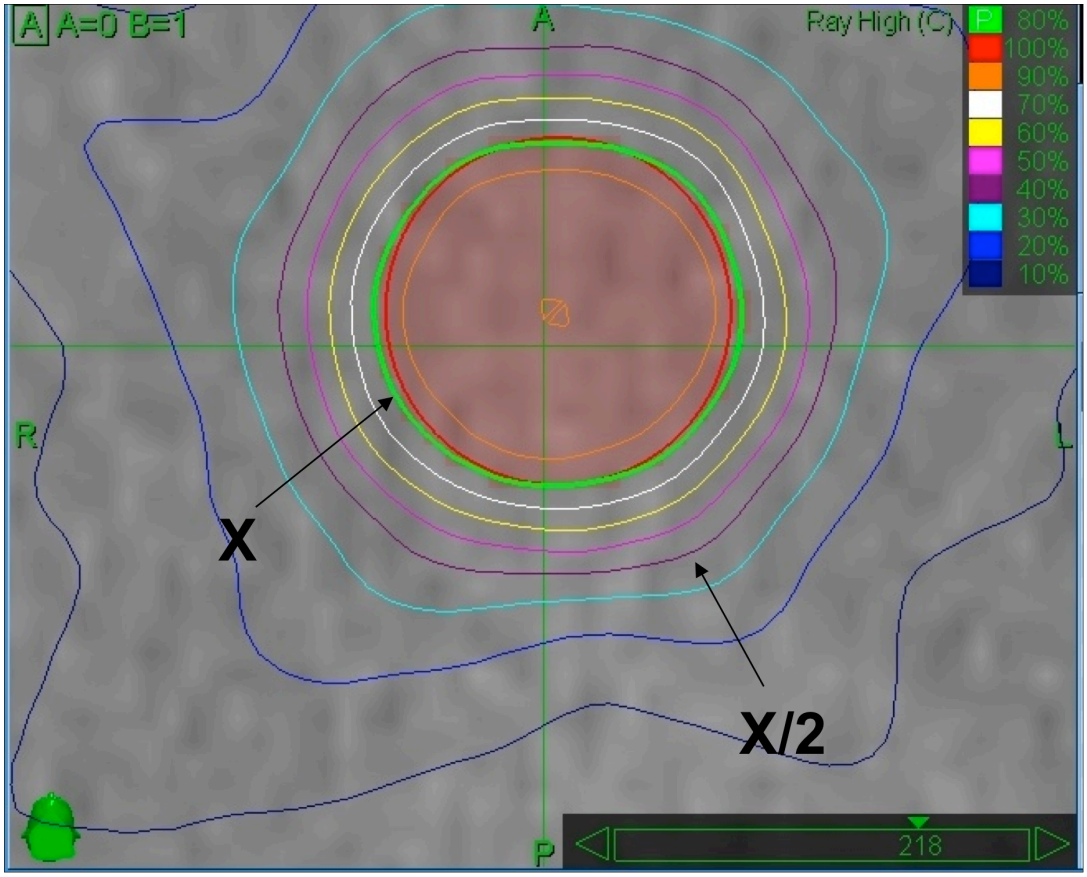

Figure 4.4: Screenshot (zoomed in) of the isodose arrangement in a treatment plan for a spherical target (red overlay) prescribed to the 80 % isodose. In this example the gradient index (GI) (60) is calculated by dividing the volume within the 40 % (purple) line by the volume within the prescription isodose line (green).

Paddick and Lippitz used their GI in a retrospective analysis of 50 multi-isocentre acoustic neuroma treatment plans created on the Gamma Knife system. The chosen prescription isodose % was varied in each of the 50 plans in order to observe the effect of this on the GI. The prescription isodose which optimised the GI was noted for each lesion. The mean optimal prescription isodose was found to be 39.8 % (median 38 %, range 30-61 %). This was considerably lower than expected. Indeed, the mean prescription isodose originally chosen for these treated plans was 49.4 %, and 48 of the 50 plans would have benefited from choosing a lower prescription isodose. However, it should be noted that in the above analysis the plans were not adjusted to maintain the same conformality, and in some cases an optimised GI came at the expense of worse conformality (60). Table 4.1 shows the details of five Gamma Knife publications selected from the period 2008 - 2009 (61-65). The prescription isodose is most commonly in the 40-60 % range, and some centres aim to prescribe to the 50 % isodose for most/all lesions, although the work by Paddick and Lippitz raises some questions as to whether this is necessarily the best approach.

Table 4.2 shows the details of five CyberKnife publications selected from the same period (2008 - 2009) (17, 61, 66-68). In these series, the prescription isodose is largely in the 60-90 % range. It is not entirely clear why a higher prescription isodose value tends to be used for CyberKnife treatment plans when compared to Gamma Knife plans. Prescribing to a lower prescription isodose will inevitably result in greater inhomogeneity of dose within the PTV. In the past, there has been concern raised about the possible effects of PTV dose inhomogeneity on treatment-related toxicity (69). However several larger, more recent analyses have not shown this to be a risk factor for complications following radiosurgery (12, 70, 71). Indeed, most radiosurgery long-term

Author	Centre	Lesions	Median Target Volume and Range (cm^3)	Prescription Isodose (%)
Wowra	Munich	single metastasis	Mean 5.2 +/- 5.5 (1 sd)	Mean 53 +/- 7 (1 sd)
Kased	San Francisco	one or more mets	0.22 (0.01 – 13.2)	Median 55 (38 – 96)
Haselsberger	Graz	meningioma	19.0 (5.4 – 42.9)	Median 45 (30 – 60)
Kano	Pittsburgh	haemangioblastoma	0.72 (0.08 – 16.6)	50 % for most lesions
Lasak	Wichita	acoustic neuroma	1.5 (0.09 – 6.1)	50 % for all lesions

Table 4.1: Selected Gamma Knife radiosurgery publications over the period 2008 – 9, showing the choice of prescription isodose. Abbreviations: mets = metastases; sd = standard deviation.

Author	Centre	Lesions	Mean Target Volume and Range (cm^3)	Prescription Isodose (%)
Wowra	Munich	single metastasis	5.1 +/- 7.6 (1 sd)	Mean 67 +/- 5 (1 sd)
Colombo	Vicenza	meningioma	7.5 (0.1 – 64.0)	70 - 90
Hara	Stanford	one or more mets	1.5 (0.02 – 35.7)	Median 80 (65 – 98)
Gwak	Seoul	one or more mets	12.4 (0.2 – 58.3)	Mean 80 (65 – 84)
Ju	Taipei	acoustic neuroma	5.4 (0.1 – 25.0)	Mean 83 (80 – 89)

Table 4.2: Selected CyberKnife radiosurgery publications over the period 2008 – 9, showing the choice of prescription isodose. Abbreviations: mets = metastases; sd = standard deviation.

toxicity data have come from Gamma Knife experience, where the well-established practice of using low prescription isodoses shows no signs of changing. An alternative explanation for the use of higher prescription isodoses in CyberKnife is that the practitioners are predominantly clinical oncologists with extensive experience of CFR. For these professionals, a prescription isodose of 60 - 90 % represents an ideological mid-ground between the 95 %-plus conventions set out in ICRU 50/62 (34, 35) for conventional radiotherapy, and the low prescription isodoses used in Gamma Knife practice.

To the author's knowledge there has not been a study looking at how the choice of prescription isodose affects the external dose gradient for radiosurgical plans using CyberKnife. The objective of this study is to explore this for spherical targets of different sizes, across the range of prescription isodoses comfortably achievable with the planning software. Whilst CyberKnife has the capability of treating both intracranial and extracranial targets, the study will be carried out on intracranial targets as this is the traditional radiosurgical treatment site.

Methods

The study used MultiPlan versions 3.1.0 and 3.5.1 (a software upgrade being carried out partway through the project). The unenhanced brain CT scan images of a previously-treated patient were used as the baseline CT dataset, with axial slice thickness of 1.25 mm. All previously contoured structure sets were deleted from the plan. An intracranial spherical "virtual" target was created using the ball-cube function. Four different plan baselines were created, each with a sphere of different diameter centrally located within the brain. Previous planning studies have found that plan parameters are largely independent of the (intracranial) location of the target (72, 73). It was therefore decided that a single central intracranial location would be sufficient for this study, using the same location for each target used. Spheres of 8 mm, 15 mm, 30 mm and 50 mm diameter were chosen as being reflective of the range of lesions commonly treated (although it is acknowledged that a 50 mm intracranial target would not be treated in a single fraction). As this was a dosimetric exercise aiming to optimise the dose fall-off on all sides of the target, the target was positioned such that it was comfortably away (> 3 cm) from particularly radiosensitive structures such as brainstem or optic apparatus, and therefore no specific organs at risk needed to be considered in the optimisation steps. For each target, two optimisation shells were produced: an inner shell approximately 2.5 - 3 mm away from the edge of the PTV, and an outer shell approximately 5 – 8 mm away.

The main study objective was to observe the variation (if any) in gradient index (GI) when comparing plans produced with different prescription isodose values. Four

different prescription isodoses were selected: 50, 60, 70, and 80 %. These cover much of the range of prescription isodoses which can be achieved by the MultiPlan system, based on preliminary investigation, and on experience of clinical cases treated at this centre. Whilst a prescription isodose of < 50 % or > 80 % can be achieved in certain situations, this may not be possible depending on tumour size and shape. At initial setup, the planning variables were adjusted in order to try to produce a plan which would have a marginal isodose of one of these four percentages. For every plan produced, the prescription isodose was selected as the one which resulted in the best conformality (nCI) whilst also achieving > 95 % PTV coverage. If this turned out to be, for example, 49 % or 51 %, then the plan was not accepted for further analysis. This was to prevent prescribing up or down to reach eg 50 %, at the expense of conformality or coverage.

Each spherical target was planned using two different optimisation algorithms: Simplex and Sequential. These algorithms were discussed in detail in Chapter 2. The Simplex algorithm is used solely with fixed collimators, and allows a maximum of three collimator sizes to be used. For the larger sphere sizes (30 mm and 50 mm), where there are a number of possible collimator sizes to select from, a minimum of two combinations of three collimator sizes was tried for each target. The Sequential algorithm can be used either with the fixed collimators or the Iris collimator. For this study, the Iris collimator was used as this provides a greater range and flexibility of collimator sizes for each plan. In either case the basic planning setup was performed as described above. The optimisation variables were then manipulated over multiple inverse-planning iterations, in order to find the solution with the steepest dose fall-off, as measured by GI. For each solution, the following plan characteristics were recorded:

prescription isodose, number of beams, number of monitor units (MU), conformality (nCI), PTV coverage (%) and GI. Each of these values is automatically produced by the MultiPlan system except for GI, which was calculated from the dose volume histogram (DVH) produced.

One of the main goals of the study was to provide information which may influence the CyberKnife planning technique for future patients at this centre. It was therefore important to make this a clinically accurate and relevant dosimetric project. To this end, care was taken to make this as clinically realistic as possible. All beams which would pass through the orbits to reach the target were disallowed, so that the system could not select them as part of the treatment plan. The plan was setup to deliver a single fraction of 18 Gy to the PTV, a common prescription dose for intracranial lesions. High resolution optimisation and calculation was used in order to produce a high quality, accurate and deliverable plan. As high resolution optimisation takes substantially longer than the low resolution option, the calculation grids were made just large enough to cover the PTV and shells, and PTV skip factors were used for the larger targets. This is done routinely in normal clinical practice in order to produce a plan within a reasonable amount of time, but may have a minor effect on the conformality achieved, as will be discussed later. Candidate plans then underwent high dose calculation with a much larger calculation grid to allow a more qualitative analysis, such as the detection of high (iso)dose “fingers” away from the target which may render a plan clinically unacceptable.

Overall treatment time is a very important aspect of radiosurgery, in terms of both patient and departmental resource factors. It was therefore felt that there should be a limit on the number of beams and monitor units allowed for an accepted treatment plan in this project. For the G4 CyberKnife (linac output of 800 MU/minute) with 6D skull tracking, the following equation can be used to estimate the treatment time:

$$Treatment\ time\ (minutes) = \frac{Number\ of\ beams}{6} + \frac{Number\ of\ MU}{800}$$

For example, a plan using 180 beams and 16000 MU would take 50 minutes to deliver. It was decided that the maximum treatment time for acceptable plans should be 60 minutes. Finally, whilst the external dose gradient is an important feature of radiosurgical plans which should be optimised, this should not be at the expense of other important parameters such as PTV coverage and conformality, as was observed by Paddick and Lippitz (60). As explained above, all clinically acceptable plans had > 95 % PTV coverage by the prescription isodose line. In addition, it was felt that conformality should be maintained for plans generated throughout this study. Plans for each spherical target were therefore only accepted if the conformality (nCI) was within 0.03 of the best (lowest) nCI value achieved for that target using the same optimisation algorithm. Preliminary analysis showed that with spherical targets, > 90 % of plans generated had a nCI within 0.03 of the best value that can be achieved consistently. Applying more challenging constraints to certain planning variables will lead to nCI values outside this range. Whilst the GI may sometimes (but by no means always) improve as a result, these plans were not considered valid solutions. Thus there were rigid criteria to ensure that the GI achieved was not at the expense of coverage or conformality.

Statistical analysis

For each spherical target, multiple plans were produced for each of the four prescription isodose values. The ten "clinically acceptable" plans with the best (lowest) GI values were selected for each isodose and compared. This was done using Simplex and Sequential algorithms in turn. Whilst the selection of the ten best plans in each group (as opposed to selecting ten plans at random) may introduce the possibility of selection bias, this method was chosen as it makes the comparative process more relevant to real clinical practice, where a treatment plan is often chosen after a comparison between two or more of the best candidate plans generated. This will be discussed further below.

The ten best plans for each of the four isodose values (50, 60, 70 and 80 %) were compared, with the null hypothesis being that there is no difference in GI between the four groups. If the null hypothesis was rejected, further pre-specified analysis would compare 50 % vs 60 %, 60 vs 70 % and 70 % vs 80 %. The Bonferroni correction (74) would be used to address the potential problem of multiple comparisons.

Results

Multiple treatment plans were generated as described above, and the results analysed. Table 4.3 shows the mean and range of the ten best GI values for plans prescribed to each isodose, for each sphere/optimisation algorithm combination. The range of nCI values of the plans produced is also shown. nCI values for the 30 mm and 50 mm sphere were slightly higher than for the two smaller targets. One would normally expect the values to be at least as good for the larger targets, but the results were due to the fact that skip factors were applied to the larger targets for optimisation. This allows treatment plans to be generated within an acceptable amount of time, but may result in worse conformality since not every point within the target is used for optimisation.

For the 8 mm target it was not possible to obtain a prescription isodose of 50 %, regardless of how the planning variables were adjusted. This is probably due to the fact that the system is unable to generate sufficient internal dose gradient for such a small target, in order to achieve a marginal isodose as low as 50 %. For this target, therefore, only results at 60, 70 and 80 % are shown.

Figure 4.5 shows graphs of mean GI score (for the ten best plans) against prescription isodose for each target. For the 8 mm and 15 mm targets, a positive trend is observed between prescription isodose and GI, with both optimisation algorithms, over the range of prescription isodoses 50 – 80 % (60 – 80 % with the 8 mm sphere). In other words the GI score increases (dose fall-off becomes less steep) as the prescription isodose

Target	Vol. (cm^3)	Algorithm	nCI range	Mean GI (and range) from 10 best plans produced at each isodose:			
				50 %	60 %	70 %	80 %
8 mm sphere	0.3	Simplex	1.01 – 1.04	-	3.18 (3.11 – 3.27)	3.75 (3.63 – 3.87)	4.40 (4.26 – 4.51)
		Sequential	1.01 – 1.04	-	3.35 (3.32 – 3.39)	3.98 (3.92 – 4.05)	4.66 (4.57 – 4.76)
15 mm sphere	1.8	Simplex	1.02 – 1.05	2.54 (2.53 – 2.55)	2.72 (2.69 – 2.75)	2.91 (2.86 – 2.94)	3.25 (3.23 – 3.30)
		Sequential	1.01 – 1.04	2.57 (2.55 – 2.58)	2.64 (2.63 – 2.66)	2.75 (2.73 – 2.76)	3.05 (3.02 – 3.09)
30 mm sphere	14.1	Simplex	1.03 – 1.06	2.37 (2.36 – 2.39)	2.38 (2.36 – 2.40)	2.44 (2.41 – 2.48)	2.71 (2.60 – 2.77)
		Sequential	1.03 – 1.06	2.46 (2.41 – 2.50)	2.44 2.40 – 2.47)	2.43 (2.40 – 2.48)	2.50 (2.45 – 2.52)
50 mm sphere	65.4	Simplex	1.06 – 1.09	2.38 (2.30 – 2.53)	2.27 (2.25 – 2.31)	2.32 (2.27 – 2.35)	2.63 (2.56 – 2.70)
		Sequential	1.04 – 1.07	2.37 (2.33 – 2.39)	2.36 (2.33 – 2.39)	2.31 (2.25 – 2.35)	2.40 (2.33 – 2.46)

Table 4.3: Mean and range of ten best Gradient Index scores for clinically acceptable plans produced for each target/prescription isodose/optimisation algorithm combination. Abbreviations: Vol. = volume; nCI = new Conformity Index; GI = Gradient Index

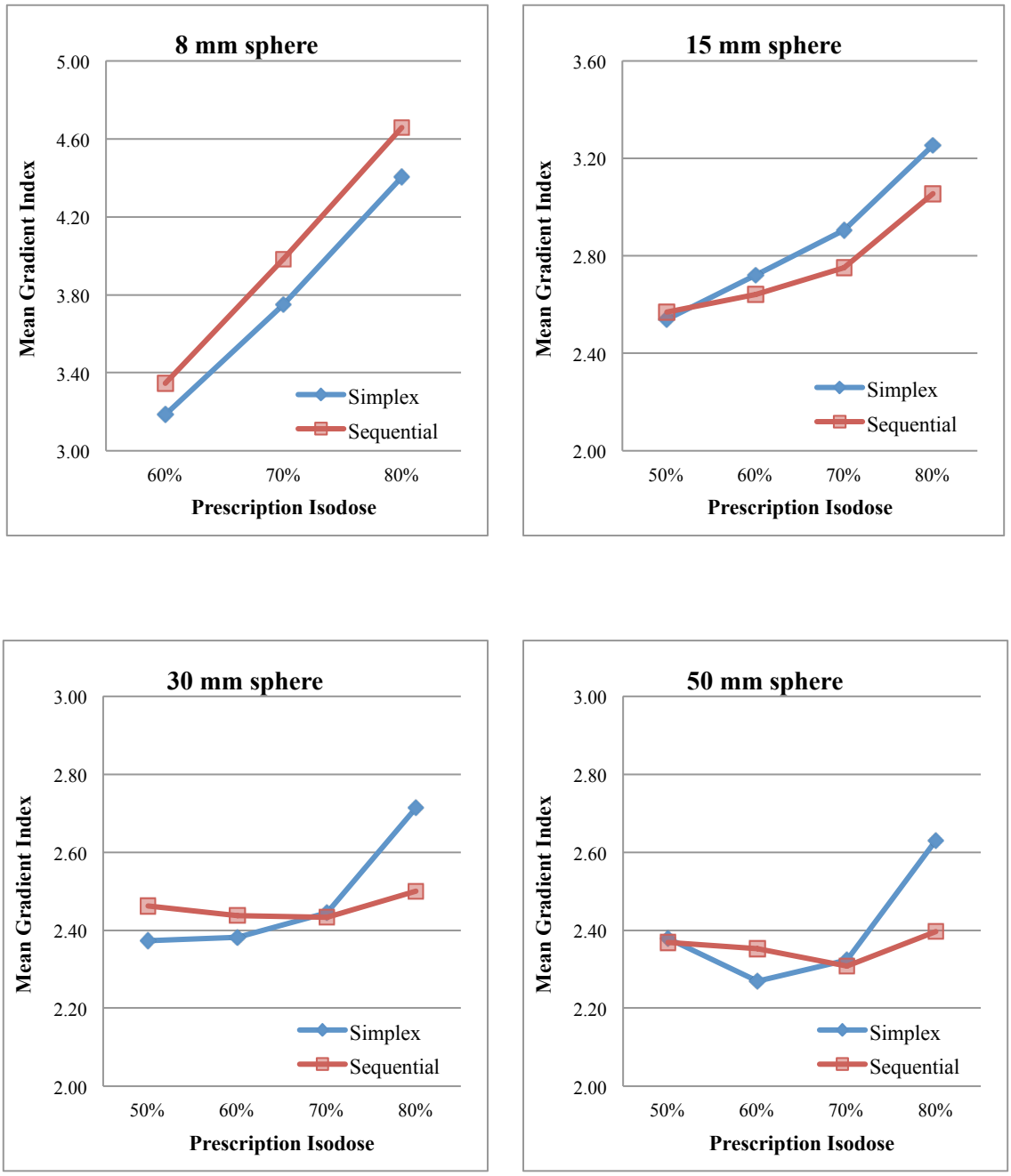

Figure 4.5: Graphs showing the mean Gradient Index of the ten best clinically acceptable plans, plotted against prescription isodose, for each sphere and using both Simplex and Sequential optimisation.

increases, over the range plotted. For the 30 mm and 50 mm targets, the effect of prescription isodose on GI is less marked, and the relationship a bit more complicated, but once again, the worst GI score in each case was obtained with the 80 % isodose value.

The distribution of GI values across the clinically acceptable plans was found to be right-skewed for each of the target/isodose value/optimisation algorithm combinations. As an example, Figure 4.6a shows a frequency plot of the GI values obtained in plans for the 15 mm sphere, prescribed to the 80 % prescription isodose, using Sequential optimisation. This is not surprising when one considers the underlying planning process. There is a limit to how low a GI value can be obtained, due to the limitations of the treatment system. On the other hand, there is a larger range of potential GI values that are worse than the mean value, leading to a long right-sided tail of data. A logarithmic transformation was applied to the data to see if a normal distribution could be obtained, but the resulting data were not normally distributed (Figure 4.6b). Parametric statistical comparison of the groups using Analysis of Variance (ANOVA) was therefore not appropriate, and non-parametric testing was used instead.

The results of the statistical analysis are summarised in Table 4.4. For each target and each optimisation algorithm a statistically significant difference between the isodose groups was detected using the Kruskal-Wallis Test with $\alpha = 0.05$, and the null hypothesis was therefore rejected in each case. The pre-specified individual comparisons (50 vs 60 %, 60 vs 70 % and 70 vs 80 %) were performed using the Mann-Whitney U Test. The Bonferroni correction was applied, resulting in $\alpha = 0.0167$ for

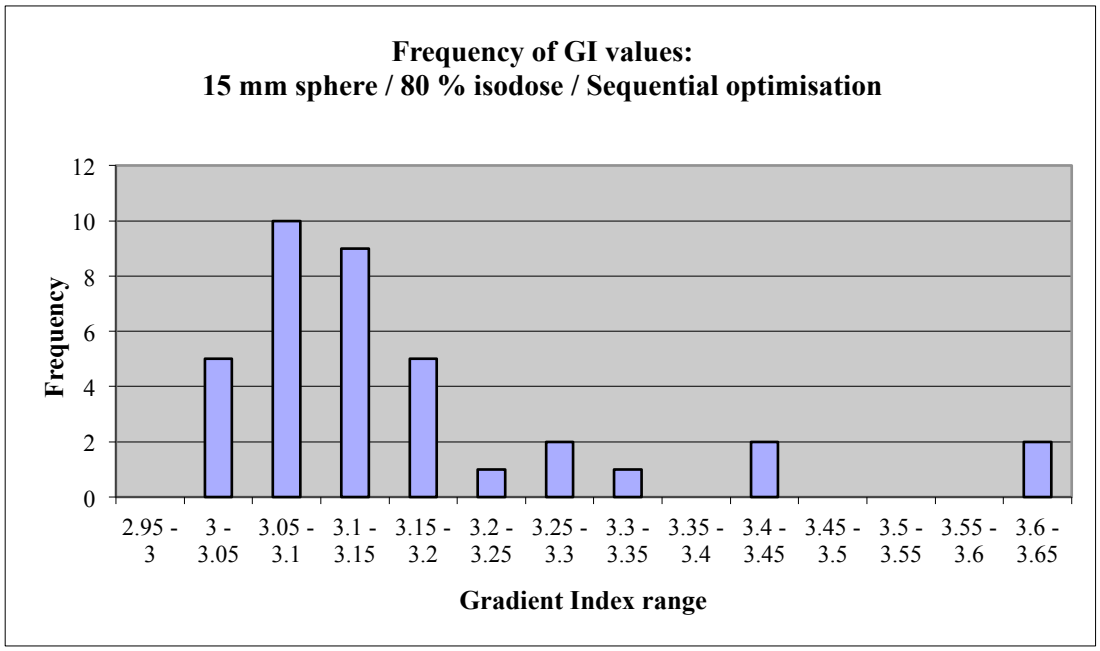

Figure 4.6a: Frequency plot showing the range of GI values from clinically acceptable plans of the 15 mm spherical target, prescribing to the 80 % isodose, and using Sequential optimisation.

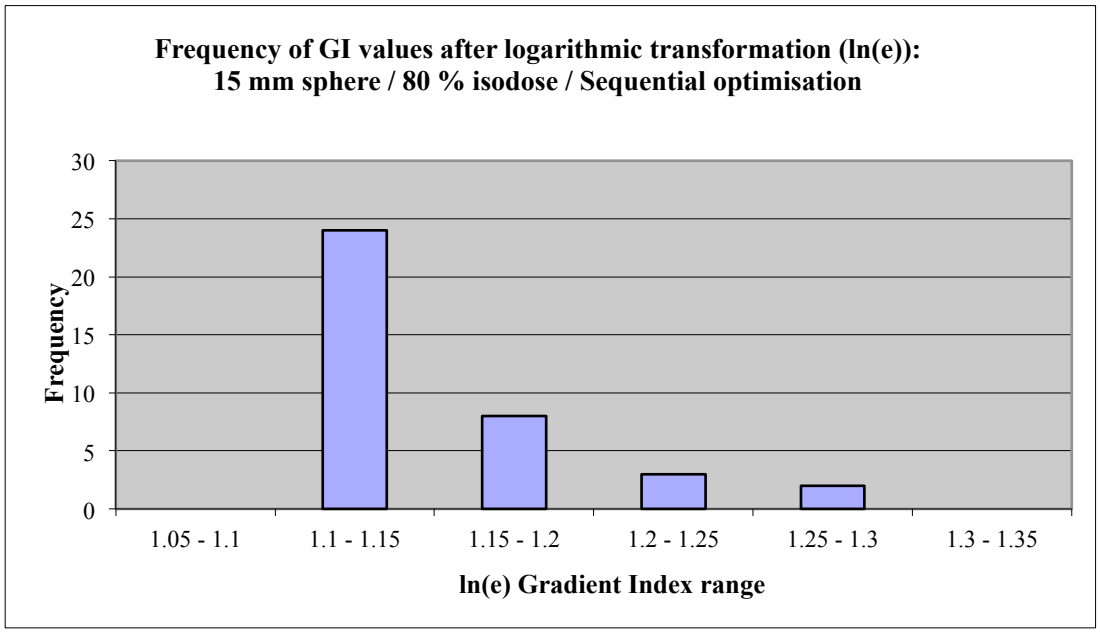

Figure 4.6b: Frequency plot of the GI values plotted in Figure 4.6a, but following logarithmic transformation using the natural logarithm (ln(e)).

Target	Algorithm	Overall p value	p value of comparisons between 2 isodoses		
			50 vs 60 %	60 vs 70 %	70 vs 80 %
8 mm sphere	Simplex	< 0.0001		0.0002	0.0002
	Sequential	< 0.0001		0.0002	0.0002
15 mm sphere	Simplex	< 0.0001	0.0001	0.0001	0.0001
	Sequential	< 0.0001	0.0001	0.0001	0.0001
30 mm sphere	Simplex	< 0.0001	0.1313	0.0001	0.0001
	Sequential	< 0.0001	0.0616	0.6701	0.0002
50 mm sphere	Simplex	< 0.0001	0.0002	0.0008	0.0002
	Sequential	< 0.0001	0.4181	0.0006	0.0003

Table 4.4: Results of statistical comparison between the ten best GI scores for each prescription isodose value, for each target/optimisation algorithm combination. Overall comparisons were performed using the Kruskal-Wallis test, with $\alpha = 0.05$. Comparisons between 2 isodoses were performed using the Mann-Whitney U test, with $\alpha = 0.0167$ (Bonferroni correction applied). Values in colour are statistically significant. The red values indicate a significant result where the lower GI score was obtained with the lower isodose value. The blue values indicate a significant result where the lower GI score was obtained with the higher isodose value.

each of the three comparisons (such that overall $\alpha = 0.05$ for all three comparisons together).

For the 8 mm and 15 mm targets there was a statistically significant difference in each of the pre-specified comparisons. There is therefore a significant positive relationship between prescription isodose and GI across the explored range of isodose values, using both optimisation algorithms. For the 30 mm and 50 mm targets, the GI values for the 80 % isodose were significantly higher than at 70 %, again using both algorithms. In these two larger targets, the optimum prescription isodose appeared to be somewhere in the 60-70 % range.

Figure 4.5 also shows the relative results of simplex and sequential algorithms for the four targets. Generally, the differences between the two algorithms are relatively small, in comparison to the main effect being studied (choice of prescription isodose). Neither algorithm consistently out-performed the other in terms of GI values across the four targets. For example, whilst the GI values for the 8 mm target were generally slightly lower using Simplex, the opposite was the case with the 15 mm target. When comparing the nCI values achieved by both algorithms (Table 4.3), again there is little difference, with the same range for 8 and 30 mm targets, although Sequential optimisation (with the Iris collimator) did perform slightly better with the 15 and 50 mm targets.

Discussion

Radiotherapy planning studies are often complicated by the fact that when it comes to assessing candidate treatment plans there is no single correct answer. It is not immediately clear for any given solution whether the plan parameters could be improved yet further by making small adjustments to the planning variables. This is especially the case with inverse planning algorithms where multiple variables influence the resultant plan parameters. Indeed, as planning algorithms have become more complicated, it is increasingly hard to be confident that a "best possible plan" has been reached. In clinical practice there are guidelines which help to identify plans as being clinically acceptable (eg ICRU 50 and 62 for conformal radiotherapy (34, 35)). Additional time spent on a clinically acceptable plan is likely to improve it further (especially with inverse planning), but it may take significantly longer to produce a plan only marginally better. In busy clinical departments, whilst a plan is rarely accepted if it does not meet the criteria for being "clinically acceptable", the time available to improve clinically acceptable plans even further is usually limited by departmental resources and patient workload.

The purpose of this study was to optimise the external dose gradient of CyberKnife treatment plans, without compromising on other plan parameters, and to explore how dose gradient is affected by the choice of prescription isodose. The data obtained have come from a very thorough and systematic approach to the manipulation of the optimisation variables. The study was designed to keep the planning process as simple as possible: a single spherical target with no organs at risk to consider. In spite of this,

for the above reasons, one cannot be certain that these results are the best solutions achievable with CyberKnife for the targets used. However, by gaining an understanding of the effect of the different variables on the gradient index and other parameters, we can be confident that the results are likely to be very close to the best obtainable**.** It is intended that this experience can now be carried over for use in future studies, and in the routine departmental planning of clinical cases.

The appropriate use of optimisation shells is of critical importance when attempting to optimise the dose fall-off in CyberKnife treatment plans. When using the Simplex algorithm, decreasing the maximum dose constraint to the optimisation shells will produce a plan with a steeper dose fall-off. It will also tend to lower the prescription isodose, but this can usually be compensated for (to keep at the desired prescription isodose %) by reducing the value of the maximum PTV dose constraint. The harder the shell dose constraints are "pushed", the lower is the GI of the resultant plan. However, beyond a certain point, this is usually achieved at the cost of gradually worsening conformality, and therefore a compromise must be reached.

The same can be observed with Sequential optimisation when hard limits are applied to the shells. Decreasing the shell hard limit doses will lower the GI, but ultimately at the expense of plan coverage and conformality. Alternatively, instead of pushing the shells with hard limits, Sequential has the option of setting shell optimisation goals. Whilst this more flexible approach may be a better method in more complex situations where there are multiple organ-at-risk optimisation steps, it does not usually create as steep a

dose fall-off as when using shell hard limits in the clinical situation relevant to this study ie solitary intracranial lesion > 3 cm away from brainstem and optic apparatus.

The experience of this study has shown Target Boundary Distance (TBD) to be another important variable when attempting to optimise the GI, using either of the two planning algorithms. TBD allows the planner to specify a virtual boundary either outside (positive) or inside (negative) the PTV, which all beams must pass through. For these four spherical targets, using a negative TBD always improved the GI, compared to a TBD of 0, and usually resulted in a smaller number of beams and MU. However, the optimum negative TBD varied depending on the size of the target and optimisation algorithm used, and was established by trial and error for each target in this study. An additional effect of a negative TBD is that it in some situations it can push down the prescription isodose. It may therefore not be possible to use the optimum negative TBD and still produce a plan with the desired prescription isodose. For example, when using the Simplex algorithm for a 15 mm spherical target, and aiming for a 80 % prescription isodose, the optimum TBD in terms of GI would be -6 mm, but it is not possible to use a TBD of less than -1 mm and still prescribe to the 80 % isodose.

Both algorithms may generate plans with a large number of beams and MU, especially when planning larger targets. The resultant plans may be high quality in terms of conformality and external dose gradient, but not feasible in terms of overall treatment time. In order to stay within the 60 minute treatment time restriction, planning variables which lead to a reduction in the number of beams and MU sometimes had to be exploited. Four ways of reducing the beams and/or MU have been identified. Firstly, as

discussed above, using a negative TBD appropriately can help to reduce beams and MU, especially with the 8 and 15 mm targets. Secondly, in Sequential planning, an "Optimise Monitor Unit" (OMU) step can be selected, usually as the final optimisation step. This will lower MU and to a lesser extent the beam number. Whilst this is usually achieved with no worsening of conformality, it almost always has a negative effect on the external dose gradient. It should therefore be avoided unless necessary. As discussed previously, MU optimisation is already built into the Simplex algorithm, and so there is no equivalent additional variable here. Thirdly, using larger collimators will lower the number of MU, and will also tend to reduce beam number. When using the Iris collimator with Sequential planning, a similar effect is produced by disabling the smallest collimator size(s) from selection. In either case, this may lead to plans with worse nCI and GI values, but sometimes they can be relatively unaffected.

A fourth method is to remove beams from a plan which has already been produced. When using Simplex, this is a manual process whereby all beams delivering MU below a specified level are removed from the plan, and the dose distribution is simply recalculated. In other words, there is no re-optimisation of the remaining beams according to the original plan goals. If only a few beams (with small MU) are removed, there may be no real effect on the plan parameters. However, if a larger number are taken out it can have quite a dramatic negative effect on the coverage, conformality and dose fall-off. This obviously restricts the number which can be safely removed by this process. In Sequential planning, the "Beam Reduction" step allows re-optimisation after beams have been removed. Consequently it is a much more useful tool, and the number of beams in a plan can sometimes be reduced dramatically without any significant effect on coverage, conformality and dose fall-off. In Sequential planning it is therefore

always advisable to use beam reduction; OMU should be used only if the treatment time and/or MU of the plan is still unacceptable.

The results demonstrate a statistically significant positive relationship between prescription isodose and GI for the 8 mm and 15 mm diameter spheres. For the 8 mm target, this relationship was observed over the isodose range 60 – 80 %, since it was not possible to produce a plan with a 50 % prescription isodose. As stated above, this was probably because with a target as small as this, the planning system cannot generate sufficient internal dose gradient to produce a 50 % marginal isodose. Nevertheless, the results suggest that for very small targets, the best dose fall-off will be achieved by prescribing to the lowest isodose which can be reached.

For the 15 mm target, prescription isodose values throughout the range 50-80 % could be comfortably achieved, and it was possible to prescribe even lower than 50 %. In view of this, the study was extended to explore whether the observed relationship between prescription isodose and GI continued down to the 40 % isodose. Figure 4.7 shows an extension of the previously-presented data for the 15 mm sphere, with the data for plans prescribed to the 40 % isodose. For both algorithms, the results for the 40 % isodose were very similar to those obtained for the 50 % isodose, therefore there does not appear to be an additional benefit in prescribing down below 50 %. Preliminary analysis using a 90 % prescription isodose showed that GI values were substantially worse than even those achieved when prescribing to the 80 % line, so this was not studied further.

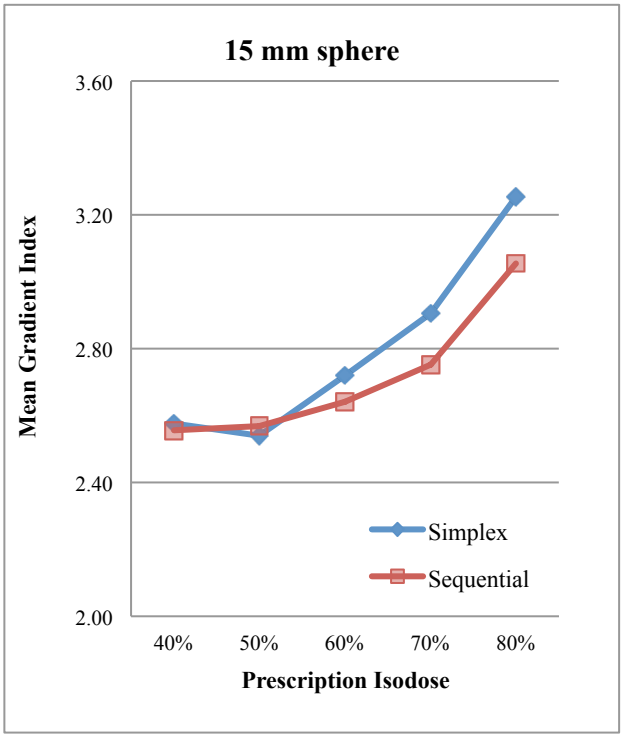

Figure 4.7: Extension of the graph previously shown in Figure 4.5 for the 15 mm spherical target, with additional data points added for plans prescribed to the 40 % isodose.

In the case of the larger two targets, the GI values were significantly lower when prescribing to the 70 % as compared to the 80 % isodose. In general, though, the effect of prescription isodose on GI was less marked in these targets. The relationship was also less consistent over the range 50 – 70 %, with the optimum prescription isodose likely to be somewhere around 60 % for the 30 mm sphere and 65 % for the 50 mm sphere.

The results suggest that when planning solitary intracranial targets, in terms of external dose gradient, it is not advisable to choose a prescription isodose above 70 %. Also, since most intracranial radiosurgery targets are likely to be less than 3 cm diameter, the optimum prescription isodose will usually be substantially lower than 70 %.

Table 4.3 and Figure 4.5 show that, compared to the effect of prescription isodose, the effect of optimisation algorithm on GI is quite small, with neither one consistently out-performing the other. Slightly improved conformality was seen with the Sequential algorithm/Iris collimator for two of the four targets. This is perhaps unsurprising since the Iris collimator allows more flexibility in choice of beam sizes for a given plan, compared to using Simplex, where a maximum of three fixed collimator sizes can be chosen per plan. Subsequent planning studies in this thesis will focus solely on Sequential planning using the Iris collimator.

Choosing a lower prescription isodose value will inevitably result in greater inhomogeneity of dose within the PTV. In the past, there have been concerns raised about the possible risk of complications associated with PTV inhomogeneity. For

example, Nedzi et al (69) reported that of sixty patients treated with radiosurgery, fourteen experienced complications, with median follow-up of 8 months. On univariate analysis, tumour dose inhomogeneity was found to be a risk factor for developing complications, as was tumour volume, and maximum dose to normal tissue. Consequently, PTV homogeneity has been viewed by some as an important radiosurgical parameter. However, more recent, larger analyses have specifically not shown any relationship between target dose inhomogeneity and post-radiosurgery complications (12, 70, 71). Instead, the following risk factors have been identified: tumour volume, prescription isodose volume, and volume of normal tissue inside prescription isodose (71); conformality (70), and V12 (12). Finally, most of the radiosurgical long-term follow-up data come from Gamma Knife practice, and these centres continue to use prescription isodoses of around 40 - 60 %, accepting target dose inhomogeneity with little concern.

Occasionally an organ-at-risk may lie inside the PTV, for example in some cases of acoustic neuroma and optic sheath meningioma. The use of a lower prescription isodose in this situation may increase the risk of delivering a dose higher than the prescribed dose to normal tissue contained within the PTV (and to normal tissue lying outside the PTV, but covered by the prescription isodose line). Choosing a higher prescription isodose would therefore appear attractive in this situation, although, as demonstrated in this project, this may result in a shallower dose gradient outside the PTV. However, the flexibility of CyberKnife planning allows the use of a low prescription isodose whilst at the same time optimising dose away from the critical structure in the middle of the target. This is illustrated by the “virtual HDR” prostate cancer planning technique

described by Fuller et al (75) (Figure 4.8), and now the subject of a multi-centre phase II trial in the USA.

The selection of the ten clinically acceptable plans with the lowest GI score at each prescription isodose leads to the possibility of selection bias – more specifically sampling bias. A more statistically sound method of sampling would have been to choose ten plans at random from all of those generated at each prescription isodose for subsequent comparisons. However this method was rejected as being less relevant to everyday clinical practice. The process of producing a clinical treatment plan usually involves the generation of multiple candidate plans. Each plan is reviewed, and variables are usually modified for the next iteration in an attempt to improve each subsequent plan produced. The selection of a final treatment plan then usually involves a comparison of the strengths and weaknesses of the two or three best plans generated. Some plans produced early on in this process may be "clinically acceptable" but clearly worse than others produced for the same target, and would therefore never be selected as the final treatment plan. In this study, the planning process was consistent across the different prescription isodoses so that, as far as possible, the only variable under investigation was the prescription isodose value itself. Nevertheless selection bias is still a possibility, and results need to be interpreted with this in mind.

In this study, statistical analysis involved the use of non-parametric tests (Kruskal-Wallis and Mann-Whitney U tests), as the criteria for performing parametric testing were not met. In general, these tests are less powerful than their parametric equivalents (ANOVA and unpaired t-test) since, instead of using all the information from the data,

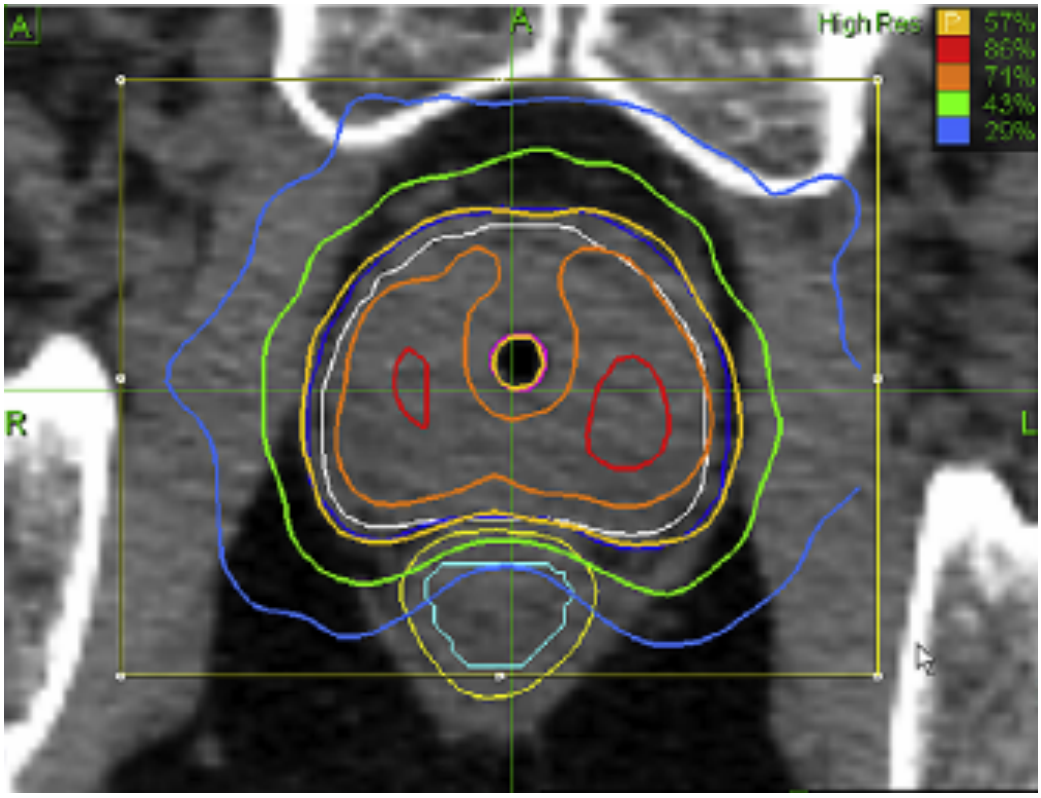

Figure 4.8: Axial slice of a prostate radiotherapy plan, showing the prostate (dark blue line), urethra (magenta line), and treatment isodose lines. The isodose values (%) are shown in the key at the top right of the image. The plan is prescribed to the 57 % isodose (yellow line), which covers the entire prostate conformally. "Hot" areas of 86 % dose (red line) are shown within the prostate, but the urethra is spared from doses above the prescription dose.

only the ranks of each data point are used in comparisons between the groups. This means that they are less likely to identify a statistically significant difference if there is one present. However, the analysis still yielded a number of significant results. The Bonferroni correction was used in the pre-specified comparisons between pairs of isodose values. This ensured that the probability of false positive results did not increase as a result of the multiple comparisons, but this came at the cost of a further reduction in the statistical power of the analysis. The significant results seen in the study have therefore been obtained in spite of these factors.

The study had a number of further limitations. Firstly, only four prescription isodose points were studied, with 10 % between each value. It can be hard to establish the precise relationship between prescription isodose and GI with only four data points for each target. Secondly, whilst the results give us an idea about the relationship between prescription isodose and GI, and how this relationship changes with the size of the target, only spherical targets were studied. It is not clear to what extent these results would also apply to non-spherical or irregularly-shaped targets.

Thirdly, the study only looked at one measure of external dose gradient: the Gradient Index. This was chosen as it is a pure measure of dose fall-off, being independent of the target volume or prescribed dose. However, it has not yet been shown to correlate with complications in the way that the V12 has, as discussed above. Also it only provides information on the dose fall-off to half the prescription dose. Whilst this covers the high dose area around the target, where normal tissue complications are most likely to occur, it provides no information on dose fall-off beyond half the prescribed dose. The volume

of normal tissue receiving a lower dose also has important implications, such as possible impact on the risk of radiation-induced malignancy. Finally, the results can only be applied directly to the planning of solitary intracranial lesions, and situations where an even dose fall-off on all sides of the target is desirable. Some of these limitations will be addressed by future work in this thesis.

Summary

This study has shown that in CyberKnife radiosurgery planning of solitary intracranial lesions, it is possible to produce plans with steep external dose gradients (as measured by the gradient index), without compromising on overall treatment time, conformality or PTV coverage. For smaller targets, inhomogeneity of dose within the PTV is the consequence of achieving the steepest dose fall-off possible. For larger targets it is not necessary to use such a low prescription isodose to maximise the GI, although an isodose as high as 80 % should be avoided unless dose homogeneity is a major requirement.

Chapter 5 – External dose gradient with irregularly-shaped targets: how do the results compare?

Introduction

The main purpose of this study is to explore further the relationship between prescription isodose value and external dose gradient in CyberKnife planning of solitary intracranial lesions, when an even external dose gradient on all sides is required. The aim is to build on the results of the previous chapter by addressing some of the limitations highlighted. Specifically, three of these limitations will be addressed in the design of this study.

Firstly, the previous study used spherical "virtual" targets centrally located in the brain, as the main aim was to observe the effect of prescription isodose value on dose fall-off, and effect of target size on this relationship. It was believed that any variation in target shape (and possibly location) might make the results harder to interpret, and it may have been more difficult to understand the effects of the individual planning variables on the resultant plan parameters. Having obtained the results described in Chapter 4, and gained some understanding of the above relationship, a logical step would be to see if this relationship is the same when real intracranial lesions (with irregular shape and variable intracranial location) are used. This study will therefore use a random selection of intracranial lesions previously treated at this centre.

Secondly, only four prescription isodose values were studied previously: 50, 60, 70 and 80 %. This was due to the time required to produce at least ten clinically acceptable plans for each isodose value, for each of the two different optimisation algorithms (Simplex and Sequential). Since the choice of algorithm had little effect on Gradient Index (GI) compared to the effect of prescription isodose value on the same parameter, it was decided that further studies would focus solely on the Sequential algorithm - the only one which supports the use of the Iris collimator. In this study, plans will be produced at each of six different prescription isodose values in the range 50 – 80 %, for each of the five intracranial lesions selected.

Thirdly, GI was chosen as the measure of external dose gradient, since it is independent of both target size and prescribed dose. However, there have not yet been any published data looking at the relationship between GI and post-radiosurgical complications. Also, GI only concerns fall-off from the prescribed dose to half this value. For the present study, therefore, two additional measures of external dose gradient will be calculated for each clinically acceptable plan produced. The volume contained within the 12 Gy isodose line (V12) was selected it has previously been shown to correlate with post-radiosurgical complications (12, 58). For the second additional measure, a new parameter is proposed: the Quarter Dose Index (QDI):

$$QDI = \frac{volume\ within\ \left(\frac{x}{4}\right)\%\ isodose}{volume\ within\ x\ \%\ isodose}$$

where x = prescription isodose value for the plan. So, for a prescribed dose of 18 Gy, this parameter provides a measure of dose fall-off down to 4.5 Gy.

For the present study, the GI will once again be used as the basis for selecting the best plans at each prescription isodose value. However, by also calculating the V12 and QDI for each plan, it will be possible to assess the degree to which these parameters correlate with the GI. This will provide more information as to whether or not GI should be used alone as the measure of dose fall-off when analysing CyberKnife radiosurgical plans.

A further aim of this chapter is to use the experience gained from both this study and the previous one to produce a stepwise method for the planning of solitary intracranial lesions using MultiPlan. This will apply specifically to situations where an even dose fall-off on all sides of the target is desired. By following the guidelines it should be possible to optimise external dose gradient without compromising on the other important plan parameters. The method will hopefully be a useful aid to the future planning of intracranial lesions at this and other CyberKnife centres.

Methods

The methods for this study were very similar to the previous chapter, but with some important differences which are now described. MultiPlan version 3.5.1 was used throughout the study. The intracranial solid tumours treated at this centre between February 2009 and May 2010 were examined. Twenty lesions were treated, of which eleven were > 2 cm away from brainstem or optic apparatus, and therefore fit with the study objective of producing an even dose fall-off around the target. From these eleven lesions, five were selected at random and used in this study. The unenhanced brain CT images, with axial slice thickness of 1.25 mm, together with the PTV and organ-at-risk contours, were used for each of the five lesions. As with the previous study, two optimisation shells were created around each lesion: one 2.5 - 3 mm away, and the second 5 – 8 mm away, depending on the size of the lesion. Sequential optimisation was used throughout, with the Iris collimator. For each lesion, the planning variables were adjusted to produce treatment plans with a prescription isodose of one of the following six values: 50, 56, 62, 68, 74 and 80 %. As previously, the planning variables were manipulated in order to optimise dose fall-off (as measured by Gradient Index (GI)) for the plans at each of the six prescription isodose values. In addition to GI, the V12 and QDI were also calculated from the DVH graph of each plan produced.

Multiple plans were produced for each lesion, but once again only "clinically acceptable" plans were accepted for further analysis. The criteria for clinical acceptability were the generally the same as in the previous study, including > 95 % PTV coverage by the prescription isodose line, and a treatment time of < 60 minutes, assuming the delivery of a single fraction of 18 Gy. There was, however, one difference

in the acceptability criteria. When using spherical targets, the New Conformity Index (nCI) for each plan had to be within 0.03 of the best achievable value for that particular target/prescription isodose value/optimisation algorithm combination. Preliminary analysis had shown that > 90 % of plans produced would lie within this range. Early work studying the real (irregularly-shaped) lesions found that there was a greater variation in nCI values across the plans produced, compared to the results with the spherical targets. > 90 % of plans produced had nCI values within 0.05 of the best achievable value for that target/prescription isodose value combination, and so the nCI criterion for clinical acceptability was increased from 0.03 – 0.05.

The ten clinically acceptable plans with the lowest GI scores for each target/isodose combination were selected for comparison. As before, the null hypothesis stated that there was no difference in GI across the isodose groups for each lesion. If the null hypothesis was rejected then pre-specified comparison of the following isodose values was performed: 50 vs 56 %, 56 vs 62 %, 62 vs 68 %, 68 vs 74 % and 74 vs 80 %. As before, the Bonferroni correction (74) would be applied to the α value to maintain an acceptable false-positive rate.

Results

The volume and maximum axial dimensions of the five lesions are shown in Table 5.1. The lesions were located within the brain as follows: left parietal lobe (lesions 1 and 4), left occipital lobe (lesion 2), left temporal lobe (lesion 3) and right frontal lobe (lesion 5). Table 5.1 also shows the mean and range of the ten best GI scores in clinically acceptable plans produced for each lesion/prescription isodose value combination, together with the range of nCI values achieved in each case. The nCI values ranged from 1.04 to 1.15 across the five lesions. This is slightly higher than that seen for the spherical targets in the previous chapter. This is unsurprising as one would expect the conformality to be slightly worse for irregularly-shaped targets. The table shows that for two of the five lesions (lesions 1 and 4) it was not possible to produce clinically acceptable plans prescribed to the 50 % isodose. Whilst these were not the smallest two lesions by volume, inspection of the contours showed that of the five lesions, these two had the smallest axial dimensions through at least part of the volume. Results were, however, obtained across the isodose range 56 – 80 % for all five lesions.

Figure 5.1 is a graph of the mean GI scores shown in Table 5.1, with the results for all five lesions displayed on the same graph. For the 3 smaller lesions (lesions 1 – 3) a positive relationship between prescription isodose value and GI was observed across the achievable range of isodose values. This resembles the results seen with the two smaller spherical targets in the previous chapter. For the two larger lesions (lesions 4 and 5), the effect of prescription isodose value on GI was not as great, as shown by the shallower gradient of these two curves. However, the worst GI scores for all five lesions were seen when prescribing to the 80 % isodose.

Target	Volume (cm^3)	Maximum Dimensions (mm)	nCI Range	Mean GI (and range) from 10 best plans produced at each prescription isodose value					
				50 %	56 %	62 %	68 %	74 %	80 %
Lesion 1	2.25	10 x 19	1.10 – 1.15	-	2.92 (2.86 – 3.00)	2.99 (2.94 – 3.03)	3.12 (3.05 – 3.19)	3.28 (3.22 – 3.33)	3.49 (3.43 – 3.53)
Lesion 2	2.95	18 x 19	1.08 – 1.13	2.77 (2.73 – 2.80)	2.82 (2.76 – 2.85)	2.87 (2.83 – 2.92)	2.93 (2.91 – 2.95)	3.04 (3.01 – 3.08)	3.17 (3.14 – 3.22)
Lesion 3	5.79	18 x 22	1.08 – 1.13	2.61 (2.58 – 2.66)	2.62 (2.58 – 2.66)	2.67 (2.64 – 2.71)	2.70 (2.65 – 2.74)	2.79 (2.75 – 2.82)	2.90 (2.87 – 2.93)
Lesion 4	9.61	15 x 38	1.09 – 1.14	-	2.83 (2.74 – 2.91)	2.81 (2.76 – 2.84)	2.83 (2.78 – 2.91)	2.92 (2.85 – 2.99)	3.03 (2.94 – 3.11)
Lesion 5	23.16	30 x 40	1.04 – 1.07	2.32 (2.29 – 2.34)	2.29 (2.26 – 2.32)	2.31 (2.27 – 2.36)	2.32 (2.29 – 2.34)	2.35 (2.33 – 2.37)	2.42 (2.40 – 2.46)

Table 5.1: showing the new Conformity Index (nCI) and Gradient Index (GI) scores for clinically acceptable plans produced for each target lesion used in this study.

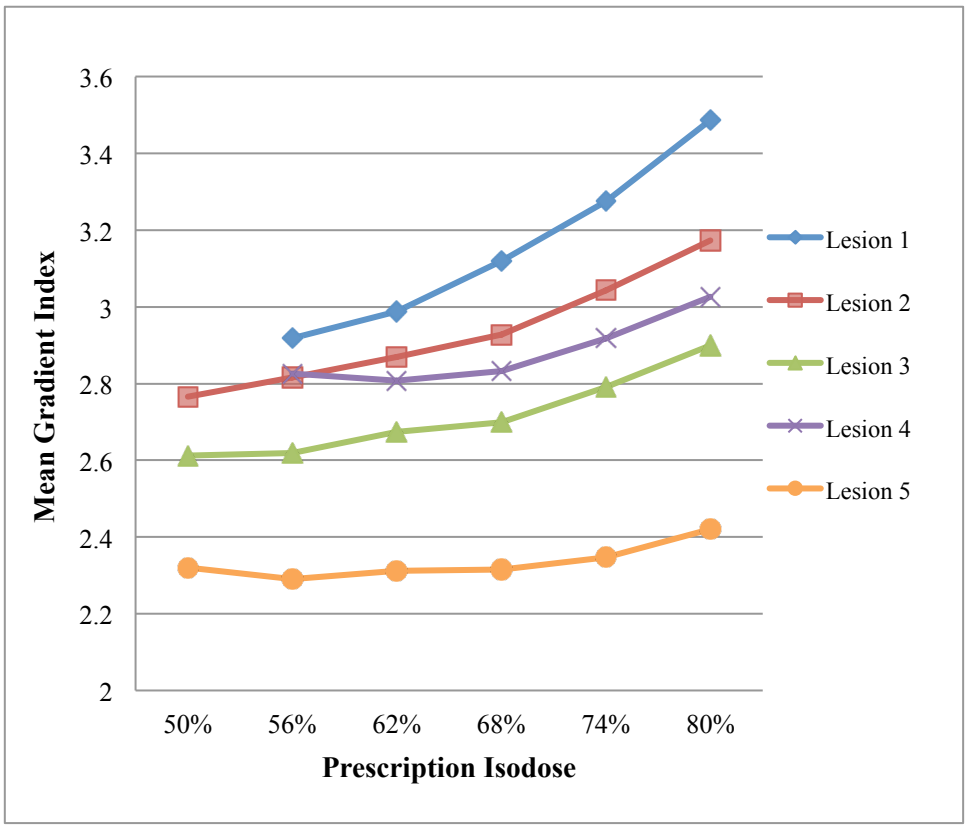

Figure 5.1: Graph showing the mean Gradient Index of the ten best clincally acceptable plans, plotted against prescription isodose for each of the five lesions.

Target	Overall p value	p value of comparisons between 2 isodoses				
		50 vs 56 %	56 vs 62 %	62 vs 68 %	68 vs 74 %	74 vs 80 %
Lesion 1	< 0.0001		0.0019	0.0002	0.0002	0.0002
Lesion 2	< 0.0001	0.0019	0.0015	0.0003	0.0002	0.0002
Lesion 3	< 0.0001	0.3643	0.0009	0.0963	0.0002	0.0002
Lesion 4	< 0.0001		0.4497	0.0963	0.0007	0.0004
Lesion 5	< 0.0001	0.0009	0.0963	0.5967	0.0019	0.0002

Table 5.2: Results of statistical comparison between the ten best GI scores for each prescription isodose value, for each lesion. Overall comparisons were performed using the Kruskal-Wallis test, with $\alpha = 0.05$. Comparisons between 2 isodoses were performed using the Mann-Whitney U test, with $\alpha = 0.01$ (Bonferroni correction applied). Values in colour are statistically significant. The red values indicate a significant result where the lower GI scores were obtained with the lower isodose value. The blue values indicate a significant result where the lower GI scores were obtained with the higher isodose value.

Table 5.2 summarises the results of the statistical analysis performed. Comparison across all the prescription isodose values together using the Kruskal-Wallis test showed a statistically significant difference in mean GI scores, for each of the five lesions ($p < 0.0001$). The null hypothesis was therefore rejected in each case, and the pre-specified comparisons between different pairs of isodose values were performed using the Mann-Whitney U test. For lesions 1 and 2 the positive relationship shown in Figure 1 was statistically significant across the whole range of values ($\alpha = 0.01$). For lesion 3, three of the five comparisons were significant (56 vs 62 %, 68 vs 74 %, and 74 vs 80 %). For lesions 4 and 5 there was no significant difference in GI across the range 56 – 68 %. However, as with the other three lesions, the rising GI values over the 68 – 80 % prescription isodose range were statistically significant.

Figure 5.2 contains a series of graphs illustrating the relationship between mean GI and the other two measures of external dose gradient, V12 and QDI, across the range of isodose values studied for each lesion. For lesions 1 – 3, the positive relationship between GI and prescription isodose described above is also seen for both V12 and QDI across the isodose range studied. In fact, V12 values also show a positive relationship across all values for lesion 4 and most of the range in lesion 5, with the lowest mean values being seen at the lowest prescription isodose values. However, for these latter two lesions, the lowest GI and QDI scores are observed somewhere in the range 56 – 68 %.

A more formal assessment of the association between GI and both the V12 and QDI values was also carried out. Spearman's Rank correlation coefficient values (r_s) were calculated for GI vs V12 and GI vs QDI relationships, using the ten best clinically

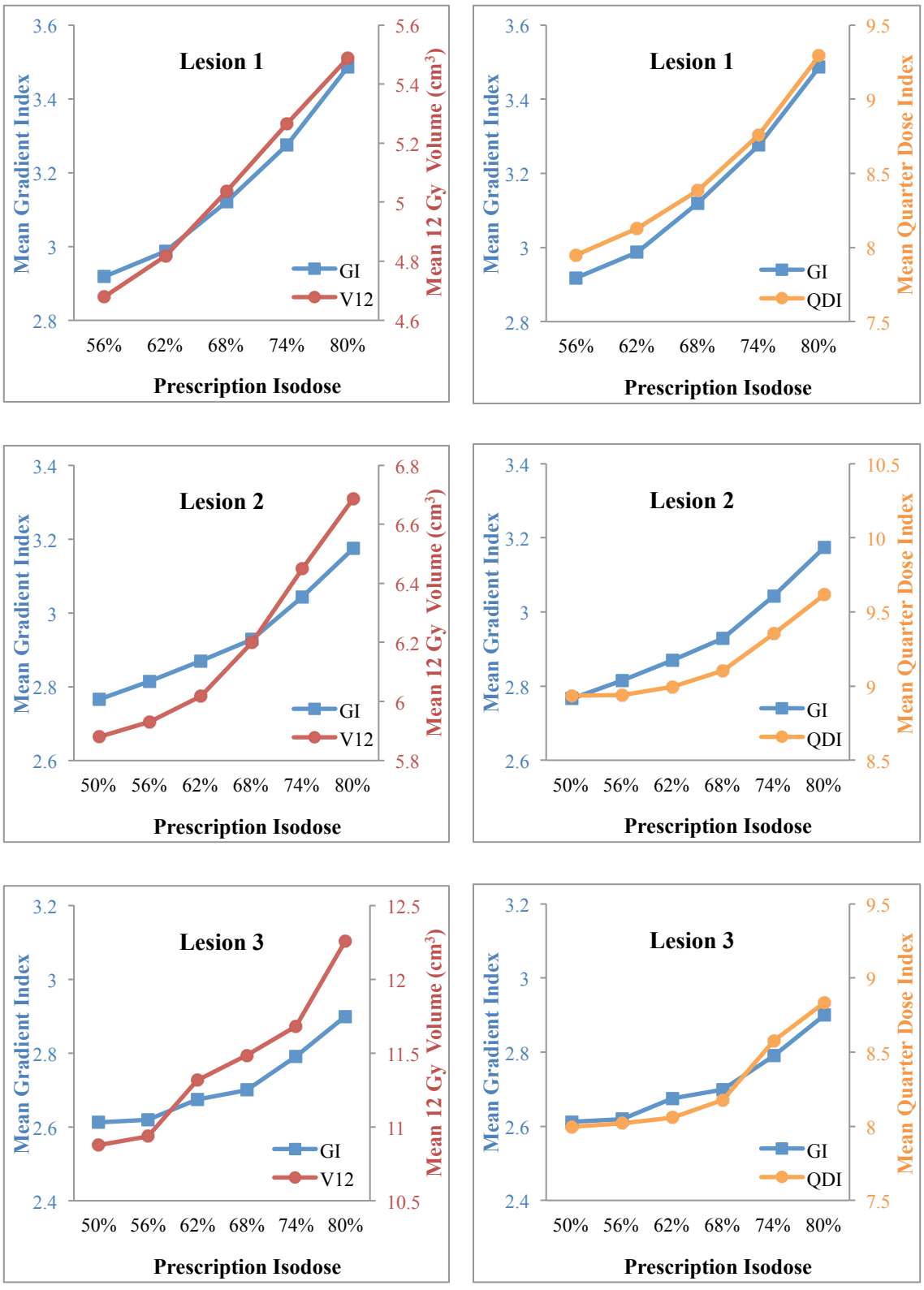

Figure 5.2: Graphs showing the effect of prescription isodose value on the Gradient Index (GI), 12 Gy volume (V12) and Quarter Dose Index (QDI) for each of the five lesions.

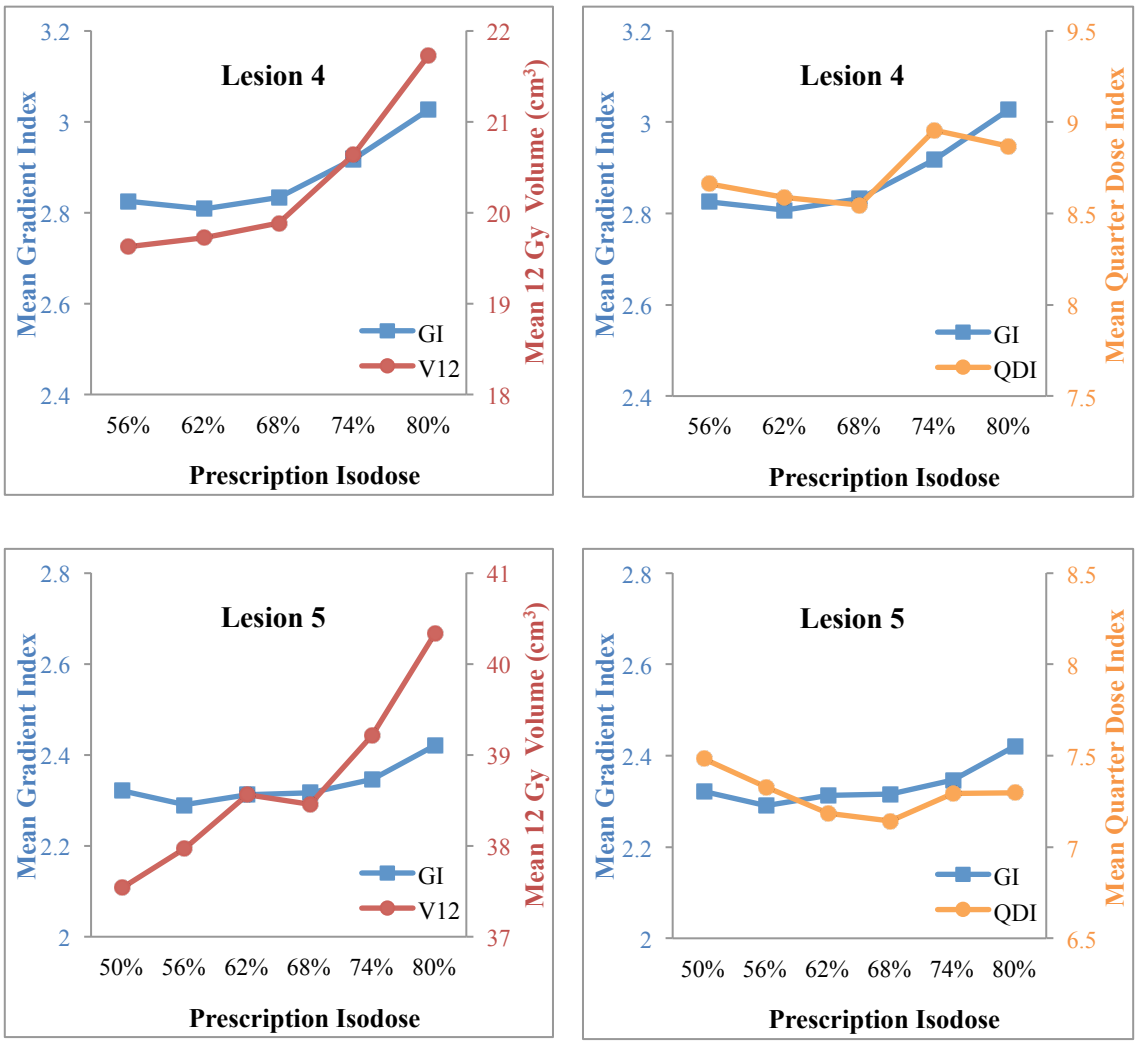

Figure 5.2 (continued): Graphs showing the effect of prescription isodose value on the Gradient Index (GI), 12 Gy volume (V12) and Quarter Dose Index (QDI) for each of the five lesions.

Parameters for correlation	Lesion 1	Lesion 2	Lesion 3	Lesion 4	Lesion 5
GI and V12	0.964	0.924	0.881	0.835	0.693
GI and QDI	0.973	0.705	0.750	0.455	0.197

Table 5.3: Spearman's Rank Correlation Coefficient (r_s) values for the association between Gradient Index (GI) and 12 Gy volume (V12), and between GI and Quarter Dose Index (QDI), using the ten plans with the lowest GI scores at each prescription isodose value. The table shows the results for each of the five lesions. Values in red are statistically significant (two-tailed p value < 0.05).

acceptable plans at each prescription isodose value. There were therefore 60 data points for lesions 2, 3 and 5, and 50 points for lesions 1 and 4 (no data at the 50 % isodose value). The results are summarised in Table 5.3. For lesions 1 – 3, there was a statistically significant strong positive association between GI and both V12 and QDI (rs 0.705 – 0.964), as might be expected from studying Figure 5.2. In the case of lesions 4 and 5, the association between GI and V12 is also relatively strong, and significant (r_s 0.693 – 0.835). However, the association between GI and QDI is less strong (r_s 0.197 – 0.455), and, for lesion 5, not statistically significant.

Discussion

This study can be viewed as an extension of the experimental method described and carried out in Chapter 4. Central to both studies was the development of an understanding of the effect of the individual planning variables on important radiosurgical parameters, such as PTV coverage, conformality, external dose gradient and treatment time. The planning variables exert their effects in a number of different ways, including, in some cases, by direct influence on the prescription isodose of the resultant plan. The key planning variables in both Simplex and Sequential optimisation algorithms, and their effects on these parameters, have already been discussed in depth in the previous chapter. The current study has focused on Sequential optimisation and, with regard to the effects of the planning variables, there do not appear to be any major differences when planning irregular lesions as opposed to spherical targets.

The main experimental aim for both studies was to establish the effect, if any, of prescription isodose value on external dose gradient, as measured by Gradient Index (GI). The results for the intracranial lesions studied here are generally consistent with those seen with the spherical targets, implying that the shape (and location) of the target does not influence the above relationship (and the effect of target size on this relationship) in any significant way.

It was not possible to produce clinically acceptable plans prescribed to the 50 % isodose for lesions 1 and 4, as was observed with the 8 mm spherical target in the previous chapter. It was suggested in the previous chapter that this may be due to the system

being unable to generate sufficient internal dose gradient to give a marginal isodose as low as 50 %. Lesion 4 had a volume of 9.6 cm^3 and lesion 1, whilst considerably smaller at 2.25 cm^3, still had a larger volume than that of the 15 mm sphere (1.8 cm^3), for which prescribing to the 50 % isodose (or even the 40 % isodose) was not problematic. This would suggest that it is the minimum diameter of the lesion, rather than the volume per se, which dictates the lowest marginal isodose value which can be reached.

This study demonstrated a statistically significant positive relationship between prescription isodose and GI over the range of achievable isodose values for the smallest two lesions (1 and 2). These results are the same as for the two smaller spherical targets studied previously. In the case of lesion 3, a similar positive relationship was observed, although the differences were not statistically significant throughout the whole range of values. Additionally, for these three lesions, a strong, statistically significant, positive association was demonstrated between GI and both the V12 and QDI measures of dose fall-off. This would justify the use of GI as a sole measure of external dose gradient when assessing any CyberKnife plan of a small solitary intracranial target.

The largest two lesions (4 and 5) show a statistically significant positive relationship between isodose value and GI over the range 68 – 80 %, but the differences in the range 56 – 68 % are non-significant, and generally smaller. Whilst the correlation between GI and V12 is moderately strong (and statistically significant) for these lesions, the V12 continues to get smaller as the prescription isodose is lowered right down to the lowest achievable value. On the other hand, QDI correlates less well with GI, and the optimum prescription isodose for QDI was 68 % in both cases.

Whilst acknowledging that caution should be shown before drawing firm conclusions from what is still a relatively small number of targets studied (four spheres and five irregular lesions), two groups of targets appear to have emerged:

1. Smaller targets, where the optimum dose fall-off is achieved by prescribing down to as close to 50 % as can be comfortably reached. In these targets, GI correlates well with both the V12 and QDI measures, and can therefore be used alone.

2. Larger targets, where the optimum GI is usually achieved by choosing a prescription isodose in the range 55 – 65 %. As volume increases, the optimum isodose value moves closer to 65 % (or even towards 70 % for very large targets). Additionally, choosing a value of less than 55 – 60 % may actually produce significantly worse results. The association between GI and both V12 and QDI is less strong in this group, although choosing an isodose in the 60 – 65 % range may often be the best compromise for all these different measures of dose fall-off.

It is important to know where the line between smaller and larger targets should be drawn. The best answer based on the results here is that lesions of volume < $5cm^3$ or maximum diameter < 20 mm will almost certainly fit in the group for smaller lesions. Targets of volume > 8 cm^3 or maximum diameter > 25 mm will probably fit in the larger lesion group. Targets in between these values could show mixed features of both groups. Reference is made to these two groups in the proposed method for planning solitary intracranial lesions described below.

The basic plan setup, as described in the methods section, involved the use of two optimisation shells. All plans produced were inspected qualitatively before being judged clinically acceptable. This involved expanding the calculation grid to cover the whole head, and observing the full isodose arrangement including low and medium dose areas. The addition of a third optimisation shell at a greater distance from the PTV (eg 15 – 25 mm) would probably have improved the overall plan dosimetry for larger targets. It is less important for smaller targets, as the overall dosimetry was usually excellent even without a third shell. The additional shell becomes especially important when a specific organ at risk on one side of the target is to be avoided, and will therefore be used in Chapter 6, where this clinical situation is explored.

The selection of the ten best "clinically acceptable" plans at each prescription isodose value followed the same method as the previous study. The rationale for this approach over choosing ten plans at random has previously been discussed: as stated in the previous chapter, the possibility of selection bias cannot be excluded, and results must be interpreted with this in mind.

Similarly, as in the previous study, statistical analysis here has involved non-parametric tests (Kruskal-Wallis, Mann-Whitney U, and Spearman's Rank correlation coefficients) since the GI scores (and other dose fall-off measures) for plans prescribed to a particular prescription isodose value are unlikely to be normally distributed. Whilst the tests are likely to be less powerful than their parametric equivalents, any statistically significant results obtained are just as valid.

Proposed planning method for solitary intracranial lesions using MultiPlan

The following is a proposed step-wise method for the planning of solitary intracranial lesions in situations where even dose fall-off on all sides of the target is desired. It enables optimising dose fall-off outside the target, whilst not compromising on other plan parameters. In situations where the target is very close to brainstem or optic apparatus, the best method is likely to be different, and this will be the subject of the following chapter.

Initial setup:

Set relatively strict maximum MU values per beam and node (eg 200 and 500 respectively). This will help to prevent the appearance of areas of moderately high dose distant to the target.

Use at least two optimisation shells in association with VOI limit values. The closest shell should be approximately 3 mm outside the PTV, and the second between 6 and 8 mm outside the PTV, depending on the PTV diameter (bigger margin for bigger target). This should result in the isodose line which is half of the prescription isodose lying somewhere between these two shells, for an optimised plan. A third shell positioned at approximately 15 – 25 mm outside the PTV will further help to reduce the areas of moderately high dose distant to the target. Select VOI limits for the two inner shells,

using values which straddle the half-prescription dose eg 13.5 Gy and 7.5 Gy for inner and second shells respectively if prescribing to 18 Gy.

Set the calculation grid to as small a size as can cover the target and shells. This will allow several iterations to be performed relatively quickly, whilst the optimum variable settings are established. The use of low resolution optimisation for the early iterations will also increase the speed, although results can be quite different when you change to high resolution optimisation.

Planning process:

1. Set the variables to achieve a prescription isodose of around 55 %, with a target boundary distance (TBD) of 0. MultiPlan should be able to achieve a 55 % prescription isodose for most lesions, and it will often be quite close to the optimum value.

2. Vary the TBD, starting at -1 mm and setting to increasingly negative values. Measure the gradient index (GI) for each result and find the value which gives the lowest GI score. This is likely to be between -1 and -4 mm for most lesions.

3. Start constraining the optimisation shells with increasingly tight VOI hard limits, through a series of further iterations. This will give steeper dose fall-off and may push the prescription isodose down. Eventually, as the shells are pushed further, conformality will start to worsen, and PTV coverage may also be affected. Establish the lowest

values which maintain conformality and coverage within your pre-specified desired range. > 95 % PTV coverage is a commonly used criterion, although it is often possible to achieve > 97 % coverage without any compromise. An nCI range of 0.05 will cover the large majority of plans produced for a given target.

4. For smaller targets (volume up to approximately 5 cm^3, or maximum diameter up to 20 - 25 mm), try changing settings to lower the prescription isodose down towards 50 % (if this has not already happened as a result of the above steps). This may further lower the GI. For larger targets, explore the prescription isodose range 55 - 65 %. In either case, find the value which gives the best solution with respect to dose fall-off, conformality and coverage.

5. Estimate the treatment time using the equation:

$$Treatment\ time\ (minutes) = \frac{Number\ of\ beams}{6} + \frac{Number\ of\ MU}{800}$$

Treatment time can be reduced if unacceptably long. In Simplex, manual beam removal will safely remove a small number of low-MU beams, but if further time reduction is required, it may be necessary to re-plan with larger collimators. This potential problem will usually be picked up earlier in the planning process. In Sequential, the Beam Reduction tool will usually be sufficient to reduce treatment time to an acceptable level. For best results run the process two or even three times, as low-MU beams may be added in the re-optimisation process. Beam Reduction can sometimes actually improve plan parameters (including GI) so when using Sequential it is worth trying it even if the treatment time is already acceptable.

6. Expand the calculation grid for the final plan produced in step 5, so that the whole brain and skull is included. Re-do the high dose calculation and perform a qualitative analysis, checking for any features which would make the plan clinically unacceptable, such as “fingers” of moderate/high dose away from the target. If this analysis finds no problems, save the plan as deliverable.

Summary

The choice of prescription isodose value does affect the external dose gradient in CyberKnife planning of solitary intracranial lesions, and this has been demonstrated both for spherical virtual targets (previously) and real intracranial solid tumours. The nature of this relationship is different in the case of smaller targets, as opposed to larger ones, as described above.

Gradient Index correlates very well with both the 12 Gy volume and Quarter Dose Index for smaller lesions, but less well for larger ones, therefore it may be advisable to use more than one measure of external dose gradient when assessing treatment plans for larger lesions.

On the basis of the results, a stepwise method for the planning of solitary intracranial lesions using MultiPlan has been proposed, to aid future treatment planning. The method seeks to optimise external dose gradient on all sides of the target, whilst not compromising on other important plan parameters.

Chapter 6 - Exploring ways to optimise dose fall-off on one aspect of a target, and the effects on overall plan quality

Introduction

The last two chapters have been concerned with creating clinically acceptable treatment plans with as steep a dose fall-off on all sides as possible. This is very important for many intracranial lesions, as cerebral cortex often surrounds the target. Whilst the dose to the cortex should always be as low as possible, within the skull there are some structures considered to be either especially radiosensitive or especially important in terms of function (or both). Brainstem, optic nerves and optic chiasm are the best examples here. For targets situated close to (or abutting) one of these structures, achieving an especially steep dose fall-off in that direction is often essential for the safe delivery of an ablative dose of radiation.

In radiotherapy planning, particularly favourable dosimetry on one side of a target is sometimes achieved at the expense of a significantly less favourable dose profile on the other aspects. This may be acceptable if the tissue on other sides is not considered to be particularly radiosensitive or functionally important. However, it is not really an acceptable solution for many intracranial lesions which are surrounded by cerebral cortex. Whilst the main priority may be to reduce the dose on one aspect, the radiation tolerance of the surrounding cerebral cortex must still be respected. The ideal solution will therefore be to optimise dose fall-off in one direction, but not at the expense of any substantial increase in dose to the cortex. A compromise will inevitably have to be made, due to the dosimetric limitations of the radiosurgery system being used. A

thorough understanding of the planning system (and optimisation algorithm) being used will enable the best compromise to be reached in any such situation.

The brainstem provides a connection between the cerebral cortex and spinal cord, with densely-packed nerve fibres comprising much of its volume. The nuclei for cranial nerves III – XII are also located here, as are centres controlling respiratory drive and cardiovascular homeostasis. Consequently brainstem damage is often life-threatening, and therefore when considering radiosurgery to any lesion close to the brainstem, the highest priority is usually given to obeying brainstem dose tolerances. This can be the dose-limiting factor in the planning of many skull base targets.

As discussed previously, the brainstem is an example of a serial organ in radiobiological terms. A high dose to a very small volume of brainstem could have major consequences. For this reason, the maximum dose to the brainstem is one important measure when assessing a radiosurgical plan. However, the point maximum brainstem dose on a plan corresponds to the highest dose to a single voxel, which in turn usually represents less than one cubic millimetre of brainstem volume (< 0.001 cm^3). In an area of steep dose fall-off, the dose to what may still be a very small volume of brainstem may be substantially lower than the point maximum dose. For example, in the treatment of trigeminal neuralgia, a dose of up to 90 Gy is delivered to a target only a couple of millimetres away from the brainstem. The point maximum brainstem dose may be as high as 40 Gy whilst the 12 Gy volume is usually well below 0.1 cm^3. This practice has been shown to be safe with regards to brainstem toxicity with long-term follow-up (76). On the other hand, Sahgal et al (77) performed retrospective analysis of five patients with myelopathy following spinal SBRT, comparing the treatment plans

with those from nineteen patients with no myelopathy. They found that the only spinal cord dose-volume endpoint with significant difference between both groups of patients was the point maximum dose.

This raises the question as to what is the most clinically useful serial organ dose-volume measurement when assessing a radiosurgical plan. Dose-volume studies on the spinal cord in animals have suggested that the spatial dose distribution may actually be more relevant to cord tolerance than simply the irradiated volume (78). If this were true for human spinal cord, neither DVH analysis nor absolute volume constraints will reliably predict complications. Nevertheless, until the relationship between dose distribution and tolerance is understood more clearly, dose-volume values should still be used. The recent QUANTEC (Quantitative Analyses of Normal Tissue Effects in the Clinic) recommendations for brainstem tolerance state that radiotherapy studies should at the very least report on point maximum dose, dose to 1 cm^3, and mean dose (together with dose per fraction, although this is not relevant for single fraction treatment) (79).

This study is a further dosimetric exploration of the CyberKnife system and concerns the radiosurgical planning of a solitary intracranial target which is largely surrounded by cerebral cortex, but is also situated very close to the brainstem on one side. As with the previous study, MultiPlan's Sequential optimisation algorithm will be used. This is the most widely used algorithm, and the only one which allows use of the Iris collimator. Sequential optimisation is discussed in more detail in Chapter 2. The most powerful way to limit dose to an organ-at-risk (OAR) in Sequential planning is to use a "VOI limit" (Volume of Interest limit). This can be applied to any contoured structure (or shell) and acts to limit the maximum dose to that structure according to the value

specified. It is selected during the setup of the initial plan variables, and is separate to the goal values specified in the optimisation steps. During optimisation, the algorithm works through the planning steps in order, trying to produce the best solution for each step in turn whilst attempting not to compromise on the solution to the previous step(s). However, it is also constrained even more strongly at each step by any VOI limits that have been specified.

When using a VOI limit, the only limit that can be applied is to the maximum dose to that structure. Limiting the maximum dose is clearly important for serial organs such as the brainstem, but as discussed above, it may not be the only consideration. It is not clear whether a VOI limit is also effective at limiting dose to, for example, 1 cm^3 volume, or even the mean dose to the structure. It also not clear to what extent the algorithm will be able to continue to lower the maximum dose to the OAR as the VOI maximum dose constraint is "pushed" progressively lower, and in what way other important plan parameters may be compromised in so doing.

The previous two studies have demonstrated that the choice of prescription isodose value affects the steepness of the external dose gradient when aiming for even dose fall-off on all sides of a solitary intracranial target. This effect is much greater for smaller targets than larger ones. It is not known whether the choice of prescription isodose will also influence dose fall-off when the priority is to spare dose to an OAR on one side of the target. This will also be explored in the current study.

In summary, the purpose of this study is to improve understanding with regard to the planning of solitary intracranial lesions located close to (or abutting) the brainstem, using Sequential optimisation in MultiPlan. More specifically, it is hoped that the experimental work will provide answers to the following questions:

1. When using a brainstem VOI limit, how much is it possible to reduce the brainstem dose whilst still producing a clinically acceptable plan?

2. Does the brainstem point maximum dose correlate with other dose-volume endpoints, such as the dose to 1 cm^3 or the mean dose, when a VOI limit is applied?

3. What is the relationship between brainstem dose and overall external dose gradient, as measured by gradient index (GI) and quarter dose index (QDI)?

4. Are the answers to the above questions affected by the choice of prescription isodose, the size of the target, or the distance from the target to the brainstem?

Methods

Certain parts of the experimental method are once again similar to that described in Chapter 4. The unenhanced CT scan (1.25 mm axial slice thickness) of a previously-treated patient was used as the baseline CT dataset, together with the contours of the main intracranial OARs. A spherical "virtual" target was created using MultiPlan's ball-cube function and positioned close to the brainstem. Two different spheres were created, with diameters of 15 mm and 30 mm. Results from chapters 4 and 5 suggest that the effect of prescription isodose on external dose gradient is different for "smaller" and "larger" targets, with the line between the two groups being drawn somewhere between 20 and 25 mm diameter. One smaller (15 mm) and one larger (30 mm) target were therefore selected here. Virtual targets were chosen rather than real lesions, as this allowed the distance between target and brainstem to be varied. Three optimisation shells were used around each target. They were positioned at 2.5, 6 and 15 mm outside the 15 mm sphere, and 3, 7 and 20 mm outside the 30 mm sphere.

Each sphere was placed at four different positions, with varying distance from the brainstem. The 2-dimensional distance between target and brainstem is measured by the planning system in terms of the number of CT pixels between the two structures. The CT images used in this study had an axial resolution of 512 x 512 pixels, and a 45 cm field of view. The axial distance across 1 pixel was therefore 0.88 mm. At the four different positions, the shortest 2-dimensional distances between target and brainstem were 12 pixels (10.5 mm), 6 pixels (5.3 mm), 3 pixels (2.6 mm) and 0 pixels (here the contours actually overlapped at the closest point). Thus eight plan baselines were created: four for each of the two spherical targets.

For each plan baseline, the method for planning solitary intracranial lesions proposed in the previous chapter was followed in order to produce a clinically acceptable plan with the steepest possible dose fall-off on all sides (as measured by the GI). The point maximum dose delivered to the brainstem was recorded in each case. This represented the maximum dose to the brainstem when no specific brainstem dose limit had been applied. Following this, a VOI limit was then applied to the brainstem. In the case of the 30 mm sphere, the initial maximum dose limit was set at the nearest 1Gy to the maximum brainstem dose just recorded. For example, if the point maximum brainstem dose had been 12.65 Gy, then the VOI maximum dose limit was set at 13 Gy for the next optimisation. The first clinically acceptable plan produced using this VOI limit was saved for further analysis. The brainstem VOI maximum dose limit was then lowered in steps of 1 Gy, with new optimisations at each new value, until a clinically acceptable plan could no longer be produced. The method for the 15 mm sphere was the same, except that the initial VOI limit was set at the nearest 0.5 Gy to the maximum brainstem dose initially recorded, and then subsequently lowered in steps of 0.5 Gy for each new optimisation. This was because the dose fall-off outside the smaller target is steeper in terms of absolute distance, therefore the maximum brainstem doses would be lower than for the larger target. Preliminary analysis showed that using steps of 0.5 and 1 Gy for the smaller and larger targets respectively would allow approximately 5 – 10 VOI limit steps in each case, which should be sufficient to obtain a reasonable picture of the relationship between VOI limit and maximum brainstem dose.

The following data were recorded for each accepted plan: target (PTV) coverage, new conformity index (nCI), GI, QDI, brainstem point maximum dose, dose to 0.1 cm^3 and 1 cm^3 of brainstem, and mean brainstem dose. Some of these values are automatically

generated by the planning system; the others were calculated using the DVH data and Microsoft Excel.

The above method was performed three times on each of the eight plan baselines, using one of three different prescription isodose values: 55, 65 and 75 %. Previous work in this thesis had explored the prescription isodose range 50 – 80 %. However for some lesions it was not possible to use a prescription isodose as low as 50 %. It was also observed that using an 80 % prescription isodose gave the worst dose fall-off for each lesion planned. For these reasons it was decided to explore the 55 – 75 % prescription isodose range, using these three different prescription isodose values.

As with the previous two studies, only treatment plans considered to be clinically acceptable were selected for further analysis. Once again, only plans with an estimated total treatment time of less than sixty minutes (delivering 18 Gy) were considered acceptable. In Chapter 4, using spherical targets, the nCI value had to be within 0.03 of the best achievable nCI for that lesion, to ensure that steep dose fall-off was not produced at the expense of conformality. For this study the acceptable nCI range was relaxed to within 0.05 of the best achievable value for each lesion. This is because in situations where brainstem sparing is an important requirement, a slightly greater compromise on conformality may be accepted.

Previously, clinically acceptable plans were required to have > 95 % PTV coverage by the prescription isodose. This is common practice in many radiosurgery centres. However, for this study the PTV coverage requirement was increased to > 97 %.

Experience with CyberKnife planning at this centre has shown that for most intracranial cases, > 97 % PTV coverage is an achievable objective. It is only really when there is significant overlap of the PTV with a radiosensitive OAR, or when the lesion is very close to more than one OAR, that PTV coverage drops below this level. Indeed, in a retrospective analysis of the all the clinically acceptable plans produced in Chapters 4 and 5 (where > 95 % PTV coverage was the requirement), 75 % plans actually had > 97 % PTV coverage. Increasing the coverage requirement to 97 % will bring all plans up to this level, and thus help to reduce the volume of PTV receiving doses less than the prescribed dose.

By introducing an OAR to be spared, this study provides a more difficult planning challenge than the previous two studies. Brainstem sparing will inevitably cause some deterioration in overall plan quality, such as the dose delivered to tissue a long way from the target. It was therefore necessary to try to quantify the peripheral dose distribution – something which is usually assessed in a more qualitative manner. For an 18 Gy treatment, the QDI provides a measure of the volume of tissue receiving >/= 4.5 Gy, and will therefore give some idea as to the effects of brainstem sparing on lower dose volumes. However, it was felt that there should be an additional measure of dose away from the target which would identify unacceptable “fingers” of moderately high dose. For this reason, volume of tissue outside the outer optimisation shell receiving >/= 6 Gy was calculated for each plan produced. In a clinically acceptable plan, this volume was required to be < 1 cm^3.

Results

Clinically acceptable treatment plans were produced for both spherical targets (15 and 30 mm), at each of four different distances from the brainstem, using the method described above. The maximum brainstem dose for each plan produced was plotted against the brainstem VOI limit value used, and the results for all eight sphere/distance combinations are shown in Figure 6.1. In each case, as the VOI limit was reduced, the maximum brainstem dose fell accordingly, and this continued until a clinically acceptable plan could no longer be produced. For the 15 mm target, a loss in conformality was always the first unacceptable feature to appear (ie nCI value outside the accepted 0.05 range). For the 30 mm target, in most cases conformality was maintained as the VOI limit was lowered, but ultimately at the expense of an unacceptable 6 Gy volume (ie > 1 cm^3) outside the outer shell. In seven of the eight graphs, the plots lie close to, but just above, the y = x line, showing that the plans produced come very close to achieving the specified VOI limit in each case. In the case of the 15 mm sphere overlapping the brainstem, the plots drift away from the y = x line, although the overall trend is still one of reducing brainstem maximum doses as the VOI limit is lowered.

Each graph in Figure 6.1 shows three separate plots for plans produced using the three different prescription isodose values (55, 65 and 75 %). The choice of prescription isodose value appears to have very little effect on the maximum brainstem dose for a given VOI limit. However, in some cases it does affect how far the VOI limit can be "lowered" whilst still producing a clinically acceptable plan. This is shown more clearly in Table 6.1. In the case of the 30 mm target, the range of VOI limit values is almost

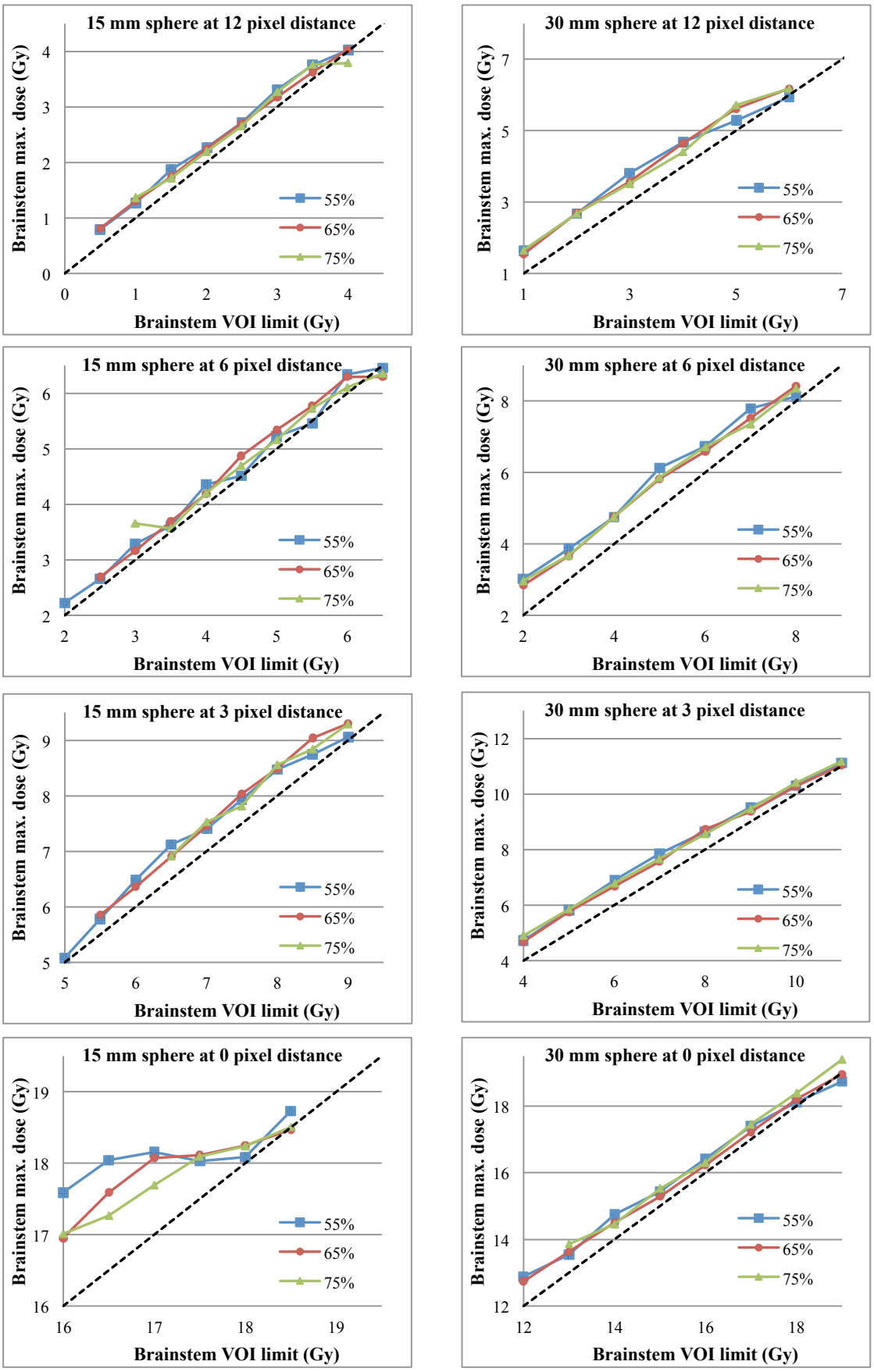

Figure 6.1: Graphs of maximum brainstem dose against brainstem VOI limit from treatment plans for each sphere, at each of four different distances from the brainstem. Plans produced with prescription isodose values of 55, 65 and 75 % are plotted separately on each graph. The dotted line shows y = x in each case.

		Range of brainstem VOI limit values (Gy) over which clinically acceptable plans could be produced			
Sphere size	**Prescription isodose**	**12 pixel distance**	**6 pixel distance**	**3 pixel distance**	**0 pixel distance**
15 mm	55 %	4.0 – 0.5	6.5 – 2.0	9.0 – 5.0	18.5 – 16.0
	65 %	4.0 – 0.5	6.5 – 2.5	9.0 – 5.5	18.5 – 16.0
	75 %	4.0 – 1.0	6.5 – 3.0	9.0 – 6.5	18.5 – 16.0
30 mm	55 %	6.0 – 1.0	8.0 – 2.0	12.0 – 4.0	19.0 – 12.0
	65 %	6.0 – 1.0	8.0 – 2.0	12.0 – 4.0	19.0 – 12.0
	75 %	6.0 – 1.0	8.0 – 2.0	12.0 – 4.0	19.0 – 13.0

Table 6.1: Showing the range of brainstem VOI limit values over which clinically acceptable plans could be produced, for each target size/brainstem distance combination.

identical for the three different isodose values. However, with the 15 mm target, using the 55 % prescription isodose value allowed the VOI limit to be lowered furthest, followed by the 65 % value, and then finally the 75 % value. This means that in many cases the lowest brainstem maximum doses (within clinically acceptable plans) were obtained using the 55 % prescription isodose value.

Tables 6.2a-c show Spearman's Rank correlation coefficients for the relationship between point maximum brainstem dose and the dose to 0.1 cm^3 (Table 6.2a), 1 cm^3 (Table 6.2b) and the mean brainstem dose (Table 6.2c). Once again, the results are shown separately for each target, at each of the four "target-brainstem" distances. The tables show a very strong (> 90 %), statistically significant positive correlation between maximum dose and all three brainstem dose-volume measurements. This applies to both targets when not actually overlapping the brainstem (ie at 3, 6 and 12 pixel distances). It also applies to the 30 mm target when overlapping the brainstem (0 pixel distance). In the case of the 15 mm target overlapping the brainstem, there is a significant moderately strong positive correlation (0.72) between maximum dose and the dose to 0.1 cm^3, but a very weak (and non-significant) correlation with both the dose to 1 cm^3 (0.07) and the mean brainstem dose (-0.03).

The relationship between brainstem maximum dose and overall external dose gradient in the plans produced is summarised in Figures 6.2 (Gradient Index) and 6.3 (Quarter Dose Index). The general trend in Figure 6.2 is that as the maximum brainstem dose is lowered (through progressively lower VOI limits), the Gradient Index (GI) increases. However, in the case of the 30 mm target, and to a lesser extent with the 15 mm target, the brainstem dose can be lowered some way before there is any significant

Table 6.2a	15 mm diameter sphere		30 mm diameter sphere	
Distance from brainstem	**Correlation Coefficient**	**p value**	**Correlation Coefficient**	**p value**
12 pixels	0.985	< 0.0001	0.988	< 0.0001
6 pixels	0.990	< 0.0001	0.987	< 0.0001
3 pixels	0.982	< 0.0001	0.990	< 0.0001
0 pixels	0.721	0.0028	0.989	< 0.0001

Table 6.2b	15 mm diameter sphere		30 mm diameter sphere	
Distance from brainstem	**Correlation Coefficient**	**p value**	**Correlation Coefficient**	**p value**
12 pixels	0.983	< 0.0001	0.983	< 0.0001
6 pixels	0.985	< 0.0001	0.986	< 0.0001
3 pixels	0.917	< 0.0001	0.967	< 0.0001
0 pixels	0.069	0.7718	0.968	< 0.0001

Table 6.2c	15 mm diameter sphere		30 mm diameter sphere	
Distance from brainstem	**Correlation Coefficient**	**p value**	**Correlation Coefficient**	**p value**
12 pixels	0.969	< 0.0001	0.971	< 0.0001
6 pixels	0.985	< 0.0001	0.973	< 0.0001
3 pixels	0.969	< 0.0001	0.949	< 0.0001
0 pixels	-0.03	0.8966	0.923	< 0.0001

Table 6.2a-c: Spearman's Rank correlation coefficients for the association between point maximum brainstem dose and the dose to 0.1cm^3 brainstem (Table 6.2a), 1cm^3 brainstem (Table 6.2b) and mean brainstem dose (Table 6.2c). Results are shown separately for treatment plans of the two different spherical targets, at each of the four different distances from the brainstem. All coefficients are statistically significant at p = 0.05 except for the values shown in red.

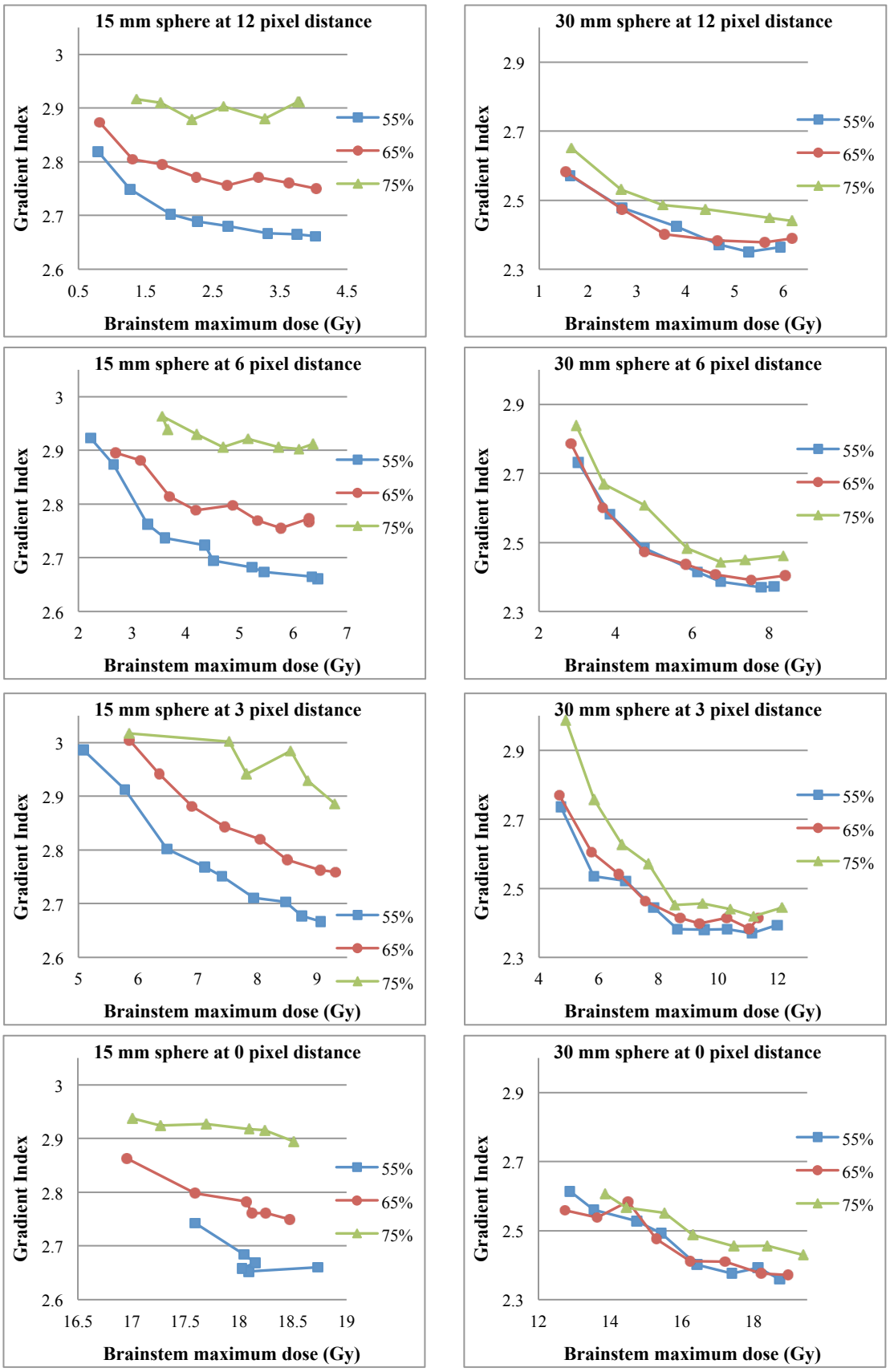

Figure 6.2: Graphs of Gradient Index against brainstem maximum dose, from treatment plans for the 15 mm (left) and 30 mm (right) spheres, at each of the four different distances from the brainstem. Plans were created using different brainstem VOI limit values. Results for the three different prescription isodose values (55, 65 and 75 %) are plotted on each graph.

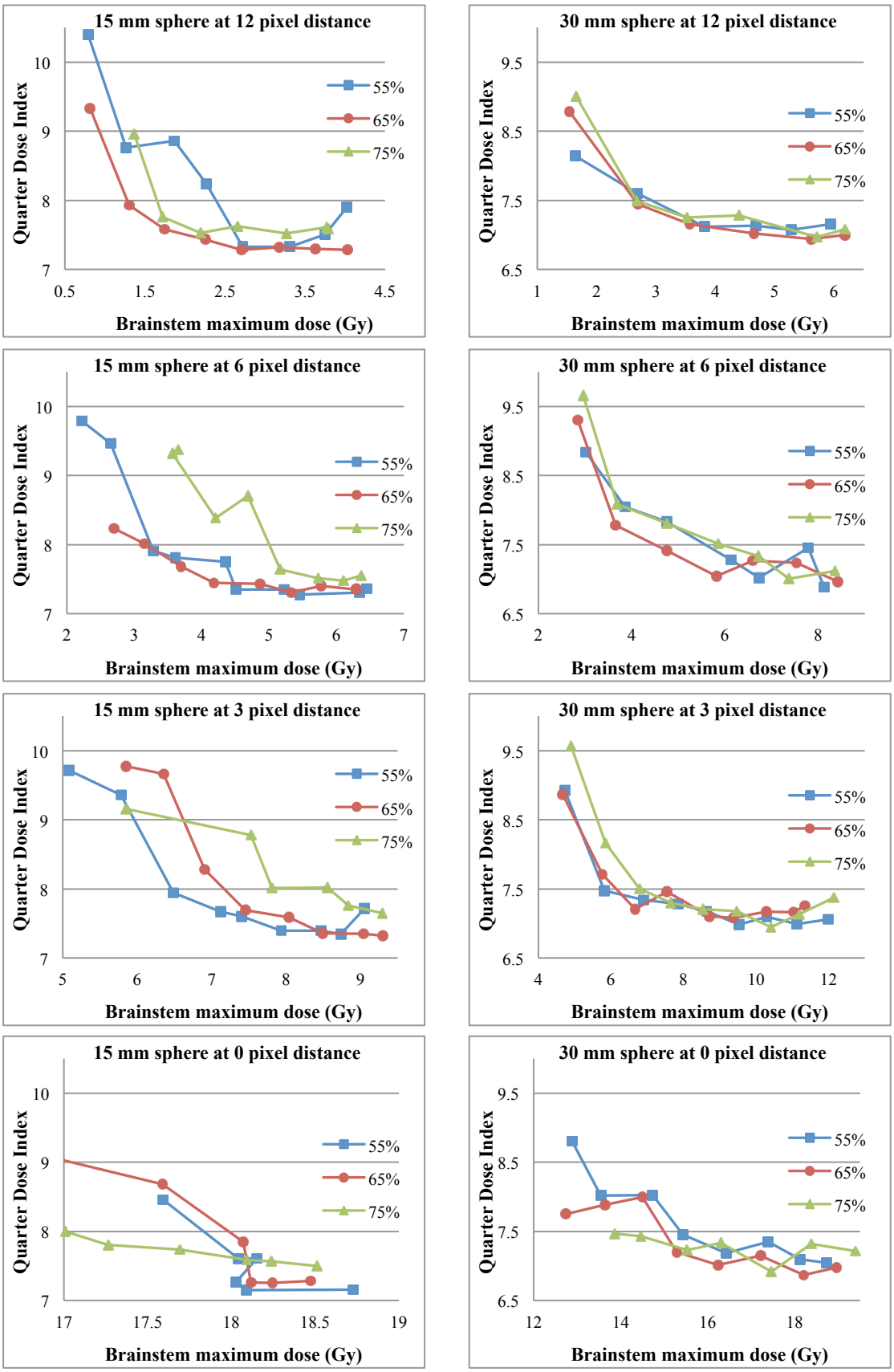

Figure 6.3: Graphs of Quarter Dose Index against brainstem maximum dose, from treatment plans for the 15 mm (left) and 30 mm (right) spheres, at each of the four different distances from the brainstem. Plans were created using different brainstem VOI limit values. Results for the three different prescription isodose values (55, 65 and 75 %) are plotted on each graph.

deterioration in GI. In fact with the larger target, at 3, 6 and 12 pixel distance, the GI initially falls as the brainstem dose falls, before levelling out and then increasing. There is a clear effect of prescription isodose on GI in the case of the smaller target, with GI values increasing as the prescription isodose increases from 55 % - 75 %. For the larger target this effect is less marked although using the 55 and 65 % isodoses consistently produced lower GI values than the 75 % isodose. All these results are in keeping with those from the previous two chapters.

In Figure 6.3, the relationship between maximum brainstem dose and QDI is demonstrated. As the brainstem dose is lowered the general trend is, once again, one of worsening external dose gradient. However, as seen with GI, in most cases there is a large fall in brainstem dose before any significant increase in QDI values. Indeed this is even more the case with QDI compared to GI. As before, this is seen especially with the larger target. For example, with the 30 mm target at 3 pixel distance from the brainstem, the brainstem maximum dose can be lowered from 12 – 6 Gy before the QDI rises above 7.5. Unlike in Figure 6.2 (with GI), there is a less clear relationship between prescription isodose and QDI in these graphs. Certainly with the 30 mm target, the 3 plots largely overlie each other. In the case of the 15 mm target, there is no clear pattern across the four different graphs.

Discussion

This study concerns the specific clinical situation of an intracranial target lying close to (or even overlapping) the brainstem on one side, and bounded on all other sides by cerebral cortex. This is a common clinical problem, and one that demands very steep dose fall-off towards the brainstem, without a significant detriment to the external dose gradient in all other directions, as well as other important plan features such as conformality and target coverage. The main purpose of the study was to improve CyberKnife radiosurgical planning of targets close to the brainstem, by exploring various relevant features of Sequential optimisation in MultiPlan.

The results confirm that the VOI limit is given a very high priority within Sequential optimisation, and the algorithm will generally try to meet the value chosen, even as this value is lowered further and further, eventually at the expense of some other aspect of plan quality. In the case of the 15 mm target, conformality was eventually lost as the VOI limit is lowered. However, with the 30 mm target, it was usually possible to maintain excellent conformality. This may be because, as there is more volume in inside the larger target, there is greater flexibility in terms of the number of possible plan solutions which can be generated. The algorithm therefore produces a solution which tries to the meet the VOI limit and maintains conformality, but ultimately at the expense of an increase in moderate dose areas away from the target (as measured by the 6 Gy volume outside the outer optimisation shell).

For targets close to (approximately 2.5 – 10 mm), but not overlapping, the brainstem there was a very strong, statistically significant positive correlation between the maximum brainstem dose and the three other brainstem dose endpoints (doses to 0.1 cm^3 and 1 cm^3, and mean dose). This applied to plans for both targets. Lowering the brainstem VOI limit in this situation serves to lower all of the measured brainstem endpoints, and not just the maximum dose. It has also been shown that lowering the brainstem dose eventually comes at the cost of a less steep overall external dose gradient, as measured by both Gradient Index and Quarter Dose Index. This is perhaps unsurprising given the inevitable limitations of any planning system. However, encouragingly, it appears that the use of a VOI limit can often lower the brainstem dose substantially before there is any significant change in GI and QDI. Whilst this applies to the planning of both targets, it is especially true in the case of the larger one.

The brainstem VOI limit is thus an extremely useful planning tool for targets located close to the brainstem. The decision regarding how hard to "push" the limit will vary from case to case, depending on the relative importance of brainstem dose, overall external dose fall-off, and other aspects of plan quality. Whilst the results have come only from the planning of spherical targets, on the basis of previous work in this thesis it is reasonably likely that planning of irregularly-shaped lesions will give similar results. However, there should be some caution when translating these results to the planning of targets close to other intracranial OARs (eg optic nerves or chiasm), as variations in shape and/or volume of an OAR may affect the relationship between maximum dose and other dose endpoints. It should also be noted that the brainstem maximum doses seen in Figure 6.1 for targets at 6 and 12 pixel distances from the brainstem are well within the perceived safe dose limit to this structure, and therefore one might question

the importance of studying the effects of lowering the brainstem dose yet further. However there will be some situations, such as patients who have received previous radiotherapy, where limiting the brainstem dose to even lower levels would be desirable.

Whilst the results discussed so far have been largely similar for the two different spheres, in the case of a target actually overlapping the brainstem (ie 0 pixel distance) different results were observed across the two targets. For the 30 mm sphere, maximum brainstem dose (and the other brainstem dose endpoints) continued to fall as the brainstem VOI limit was lowered over the range 19 – 12 Gy, in spite of the fact that the target and brainstem were overlapping, This was achieved at the expense of the minimum dose to the target, which also continued to fall accordingly from 17 Gy down to 10 Gy, although overall PTV coverage by the prescription isodose was maintained at > 97 %. In contrast, with the 15 mm sphere it was possible to achieve only a relatively modest reduction in maximum brainstem dose (approximately 1.5 Gy), and there was no correlation between maximum dose and either the dose to 1 cm^3 brainstem, or the mean brainstem dose. The difference in behaviour between the targets may once again be a consequence of the greater flexibility available for planning the larger volume, whereby the system can maintain conformality and coverage whilst substantially lowering brainstem maximum dose (albeit at the expense of PTV minimum dose). This is especially the case given the constraints of > 97 % coverage and nCI within 0.05 of the best achievable value. For the smaller target, these constraints leave very little room for manoeuvrability using the techniques described above.

Although reducing the minimum PTV dose is not ideal, if it allows brainstem dose sparing, and there is still > 97 % PTV coverage by the prescription isodose, then it may be the best compromise for a target overlapping the brainstem. As discussed, this was achievable for the 30 mm target, but not the 15 mm target using the above method. However, an additional technique which does allow further brainstem dose sparing for the 15 mm overlapping target is to create an "eroded PTV". The brainstem volume is grown by a small margin (eg 2 mm) which can then be eroded out of the original PTV, so that the new, eroded PTV is at least 2 mm away from the brainstem throughout the volume. This new PTV is used in the optimisation steps, but the plan measures (such as coverage, conformality and minimum dose) are still recorded for the original PTV. Creating this narrow "corridor" appears to allow the optimisation algorithm to cope better with the conflicting demands of PTV coverage and brainstem dose limits. This is illustrated in Figure 6.4, showing the results of plans prescribed to the 55 % prescription isodose. The original brainstem maximum doses were previously shown in Figure 6.1, and are now compared with the results obtained by optimising to the eroded PTV. When compared to the original results, the new technique leads to further brainstem dose reductions of approximately 1.5 Gy, without any significant further lowering of PTV minimum dose. However, the lowest point maximum brainstem dose is still 16 Gy using this technique, and for further reduction it is likely that there would have to be a compromise on the strict PTV coverage and conformality constraints used in this study.

The study also looked at the effect of prescription isodose value on the various dosimetric measures recorded, and the results are broadly similar to those seen in the previous two chapters. For the smaller target, there was once again an advantage in prescribing to the lowest isodose value (55 % in this case) as this yielded clinically

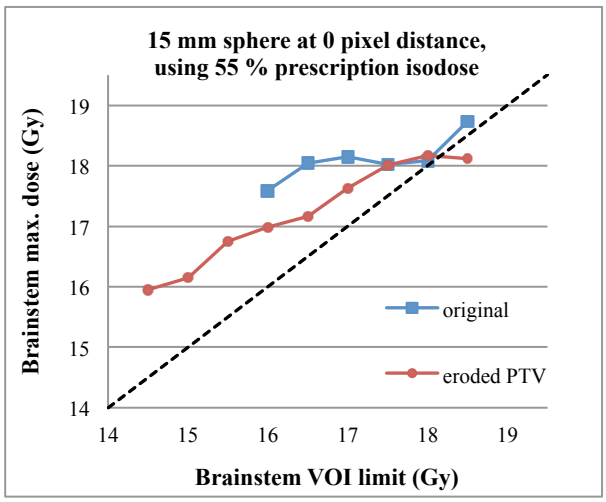

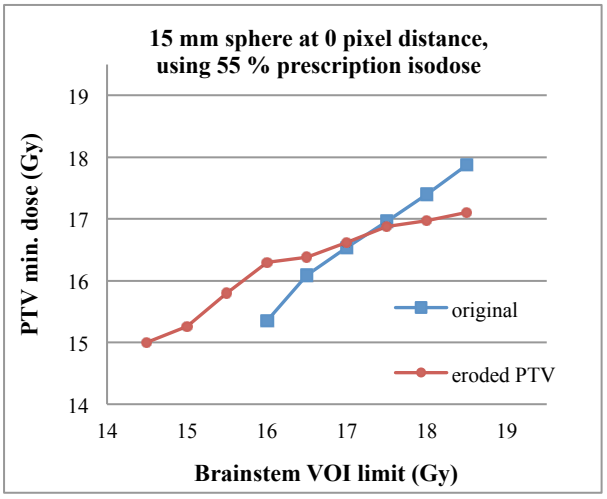

Figure 6.4: Graphs of brainstem maximum dose (upper graph) and PTV minimum dose (lower graph) against brainstem VOI limit, for plans produced for the 15 mm sphere overlapping the brainstem, using a 55 % prescription isodose. The two plots show the original results (blue) and the results obtained if the plan is optimised to an eroded PTV, with a 2 mm gap between brainstem and the new optimisation target (red). Each plot stops at the lowest brainstem VOI limit where a clinically acceptable plan could be produced. Abbreviations: max. = maximum; min. = minimum.

acceptable plans with the lowest GI scores and the lowest brainstem maximum doses. In the case of the larger target, the effect of prescription isodose value was once again less marked than with the smaller one. Brainstem maximum doses and QDI values were largely unchanged across the isodose range 55 – 75%, although the GI scores were consistently worse using the 75 % isodose, compared to the lower two values. Thus the best choice of prescription isodose appears to be the same whether the aim is to produce steep even dose fall-off outside the target or, as in this study, very steep fall-off on one side.

One limitation of this study was the use of the first clinically acceptable plan produced for each VOI limit value rather than selecting the best plan(s) from a selection (as with the previous two chapters), or even taking mean values across a set of plans. This meant that there was a reasonable amount of "noise" in the data collected, which reflects the inherent variability in dosimetric results seen in successive plans produced using the same plan settings. Unfortunately, due to the complicated design of the study, there was insufficient time to produce more than one clinically acceptable plan for each different combination of VOI limit/prescription isodose/target size/distance from brainstem. Whilst it was still possible to observe a number of important trends in the data collected, the results should be interpreted with this limitation in mind.

Summary

For intracranial targets located very close to the brainstem, the brainstem VOI limit is a very powerful tool for lowering dose to this organ. Moderate dose reductions can be achieved with no compromise on other measures of overall plan quality. Further brainstem dose reductions can be achieved, but at the expense of overall external dose gradient, and either conformality (15 mm sphere) or areas of moderate dose distant to the target (30 mm sphere).

When using a brainstem VOI limit with targets close to, but not overlapping, the brainstem, the maximum brainstem dose correlates very strongly (and significantly) with all other measured brainstem dose-volume endpoints, including mean dose.

In the case of targets overlapping the brainstem, creating a narrow "corridor" of tissue between PTV and brainstem by using an eroded PTV allows the brainstem dose to be lowered further whilst maintaining PTV coverage. However, reducing PTV coverage and PTV minimum dose may be necessary if the brainstem dose needs to be lowered even further.

Chapter 7 – A dosimetric comparison of CyberKnife and Gamma Knife systems in the treatment of solitary intracranial brain lesions

Introduction

The safe delivery of a radiosurgical treatment requires sub-millimetre overall system accuracy. This allows little or no PTV margin to be added, and thus reduces the volume of normal tissue within the PTV. There are a number of different modern radiosurgery systems, although they can be broadly divided into frame-based and non-frame-based technologies. Gamma Knife is the oldest radiosurgery system, and whilst it has undergone several important changes over the last 40 years, it still relies on absolute immobilisation achieved with a pinned stereotactic frame, and contains very few movable components in order to preserve this accuracy. Overall system accuracy has been shown to be 0.48 – 0.7 mm (43, 44).

CyberKnife is an example of a non-frame-based system which instead uses intra-fraction image guidance to achieve the required accuracy. Published results using the "End2End Test" (Accuray Inc.) have demonstrated a total system accuracy of 0.44 – 0.48 mm (37, 42) when tracking intracranial targets. However, it should be noted that this test does not include CT-MRI image registration, and therefore if the target is contoured using MRI then any error in registration will be additional to the quoted total system accuracy. This will be discussed in more detail later.

Radiosurgical systems must also be able to meet certain dosimetric requirements in the treatment plans produced. The prescription isodose line needs to conform very closely to the target contour so that target coverage is optimised whilst minimising the volume of normal tissue inside the line. There also needs to be a steep external dose gradient outside the target, and the ability to shape isodose distributions to avoid especially radiosensitive OARs. The previous three chapters in this thesis have explored ways to optimise these dosimetric parameters when using CyberKnife to treat solitary intracranial targets.

The importance of dosimetry in radiosurgery is illustrated by the large number of published dosimetric comparisons of the different radiosurgical techniques over the last twenty years. During this time a number of new systems have emerged. Additionally, most existing systems have undergone regular upgrades, improving their dosimetric capabilities or system accuracy (or both). Dosimetric comparisons continue, therefore, to be useful as the radiosurgical community attempts to reduce further the dose to normal tissue.

In one of the earliest comparisons of CyberKnife and Gamma Knife planning capabilities, Yu et al (80) used a solitary 25 x 35 mm ellipsoid target centrally positioned in a head phantom, constructed such that the target was visible on both CT and MRI imaging. CyberKnife and Gamma Knife treatment plans for the target were compared, together with plans produced using the following gantry-based radiosurgical techniques: multiple arcs, conformal static shaped fields and IMRT. All of the techniques were capable of achieving 100 % target coverage with comparable conformality as measured by Shaw et al's (55) conformity index. The CyberKnife plan

had the worst dose fall-off as measured by the ratio of the volume irradiated to half of the prescribed dose, to the target volume. However an 80 % prescription isodose line was used in the CyberKnife plan, and previous work in this thesis has shown that substantial improvements in dose fall-off can be achieved by using a lower prescription isodose. Also, the method was restricted to comparing results for the one ellipsoid target contained in the phantom.

Wowra et al (61) reported the Munich experience of radiosurgery using both Gamma Knife (between 1994 and 2005) and CyberKnife (2005 – 2007). They conducted a matched pairs comparison of dosimetric parameters and clinical outcomes from treating solitary cerebral metastases on both systems. Pairs were matched according to age, gender, performance status and primary tumour, but additionally target volumes had to be within 10 % or 0.25 cm^3. They observed statistically significant results in favour of CyberKnife with regard to conformality (as measured by the Shaw index) and the 10 Gy volume (after the target volume had been deducted). However, the mean conformality index in the matched Gamma Knife patients was 3.4. This is substantially worse than would be expected for most lesions treated at this centre, and may be in part due to the fact that these lesions were planned and treated on a model B Gamma Knife between 1996 and 2005.

Ma et al (81) performed a comparison of Gamma Knife, CyberKnife and Novalis radiosurgery systems. They developed an analytic model of dose fall-off characteristics near the target in radiosurgical treatment plans of solitary intracranial lesions. They then looked at ten different clinical cases previously treated using each of the three technologies (thirty cases in total), and assessed how well the plan characteristics fit

with their model. The model fitted very well in plans from all three systems, with correlation coefficients > 0.99 for each case. They also found no significant difference in dose fall-off between the systems, with mean Gradient Index (GI) values in the range 2.89 – 2.94. However, the target volumes ranged from 0.3 – 30.3 cm^3, and previous work in this thesis has shown that GI scores substantially lower than 2.9 can certainly be achieved for most lesions with volume > 1.5 cm^3 using CyberKnife. The scores are also higher than those achieved for most clinical Gamma Knife cases treated at this centre.

A fairer comparison would arguably use a number of identical targets planned on each system, rather than different cases as described in the above study. Perks et al (82) performed a comparison of Gamma Knife and gantry-based linac radiosurgery dosimetry using the same eight acoustic neuroma patients for each system. The target volume (the enhancing mass seen on MRI) was outlined on the same MRI images for each system in order to have targets as close to identical as was possible. However, even with the same person contouring the volume on each system, it is likely that there would still be some variation in the contour for each target across the two systems. This is important in a dosimetric comparison study as small changes in dimensions and volume can affect the radiosurgical parameters produced, especially in the case of very small targets.

A target contour can be saved as a "Radiotherapy Structure Set" (RTSS), which is a DICOM (Digital Imaging and Communications in Medicine) file associated with the CT or MRI DICOM files for the images on which the target was contoured. This RTSS file can be exported from and imported into radiosurgery planning systems together with the

associated CT or MRI image files. This allows a single identical target contour to be planned in different radiosurgical systems. Unfortunately, this method has traditionally not been possible for comparisons involving the Gamma Knife system, as GammaPlan software editions up to version 8 do not have the capability to import or export RTSS files. However, GammaPlan versions from 9.0 (2008) onwards do support DICOM RTSS import/export, albeit as an optional extra package.

Ma et al (83) used this new capability in their next dosimetric comparison of Gamma Knife with CyberKnife and Novalis (with micro-MLC), this time looking at treatment plans for multiple intracranial targets. They selected the single case of a patient with 12 brain metastases and created treatment plans for various subsets of target combinations (3, 6, 9 or 12 targets). The new Conformity Index (nCI)(57) scores were consistently lowest in plans produced using Gamma Knife, as was the volume of tissue outside the target irradiated to various different doses. They therefore concluded that the normal brain tissue dose in this clinical situation is apparatus dependent. At the time of writing there has been no published comparison of Gamma Knife and CyberKnife using identical contours for solitary intracranial targets. The aim of this study is to carry out such a comparison.

There are some additional problems when attempting to conduct a planning study of Gamma Knife and CyberKnife using identical lesions which may have been previously planned and treated on either system. The first problem relates to CT scanning. CT is essential for CyberKnife treatment planning (and indeed treatment planning for most modern radiotherapy systems) as the electron density information is used by the dose calculation algorithms. Furthermore the CT must cover the whole head including the

vertex and skin at the sides since the system will not allow any beams to enter through any part of the head where the skin contour is not known. In contrast, CT is not a requirement for Gamma Knife planning as long as a full head MRI has been performed, as the system assumes uniform electron density for all tissue inside the skin contour. If CT is required to assist contouring it is usually only acquired through the area of interest in the brain in order to reduce unnecessary radiation exposure. Consequently very few patients treated with Gamma Knife have had the full head CT which is required to plan the lesion with CyberKnife. A review of patients treated at two London Gamma Knife centres (St. Bartholomew's Hospital and The Cromwell Hospital) between 1999 and 2010 found only five patients (with seven intracranial lesions) who had had full head planning CT scans compatible with CyberKnife. Even in these cases, the CT had been acquired with a stereotactic frame fixed to the skull. This can produce considerable artefact which may affect the intracranial electron density values required for CyberKnife dose calculation.

An alternative approach would be to use CT and MRI imaging from patients previously treated on CyberKnife, and import the images for use in GammaPlan. However, these "frameless" images cannot be used for full planning and treatment in GammaPlan. This is because the stereotactic frame forms the fixed reference for the 3-dimensional coordinates used in planning and treatment. A "pre-planning" mode was introduced in GammaPlan version 7 (2006) which allows frameless images to be imported, contoured and planned, although 3-dimensional coordinates are not assigned and therefore certain functions such as collision checks cannot be performed. Additionally, planning cannot proceed without generating the full head contour which is usually done using a plastic helmet affixed to the frame. Fortunately the most recent software upgrade (version 10.0)

enables the skin contour to be produced from frameless CT images. Thus neither of the above approaches is perfect and this is reflected in the experimental method used in this study.

A major potential confounding factor in any dosimetric comparison of two different radiosurgery systems is the experience of the treatment planner(s) with each system. There is a considerable learning curve when a dosimetrist (or planning physicist) starts planning on a new radiosurgery system, especially since the planning techniques differ so much across the main systems in use. Also software upgrades often introduce new features, and it may take an experienced planner some time before the new features are used most efficiently. It would be unusual for a single planner to have the same experience using two different systems, which explains why most comparison studies are collaborative projects involving planners from two or more centres. Previous work in this thesis has given the author extensive experience of planning solitary intracranial lesions on CyberKnife. As with previous studies, the intention is for the author to collect as much of the experimental data as possible, creating treatment plans for all lesions in both MultiPlan and GammaPlan, and in so doing improve proficiency in Gamma Knife treatment planning. However it is acknowledged that this may not represent a fair comparison across both systems in view of the greater experience with CyberKnife. The decision was therefore made to collaborate with a Gamma Knife treatment planner (IP) with the greatest UK experience, who would also plan the lesions in GammaPlan.

Methods

Target lesions for the planning comparison were selected from intracranial cases previously treated at either the CyberKnife centre, London, or one of two London Gamma Knife centres (Barts and The London and The Cromwell Hospital). Cases of both solitary and multiple brain primary or metastatic tumours were reviewed to find appropriate targets, although in the case of multiple tumours only a single lesion would be planned at a time.

Ten target lesions were used, and were individually chosen such that they were representative of the range of solid tumours treated on both systems. The range of tumour histologies was as follows: metastases (five lesions), meningioma (two lesions), acoustic neuroma (two lesions), and chordoma (one lesion). Target volume was required to be less than 13 cm^3. This is the approximate volume of a sphere of 30 mm diameter, and it is generally accepted that Gamma Knife can comfortably treat targets up to approximately this size. Volume was also required to be greater than 0.5 cm^3. This is because with targets of very small volume, very small changes in the treatment plan arrangement can have an enormous impact on parameters such as conformality. This can make dosimetric comparison on the basis of such parameters difficult.

Five lesions (in four patients) had been previously treated using Gamma Knife, and therefore had CT and MRI scans performed with a stereotactic frame in-situ. These had been selected from the five Gamma Knife patients who had whole-brain CT scans which would be compatible with CyberKnife planning, as discussed previously. Five

lesions (in five patients) had been previously treated using CyberKnife, and therefore had CT and MRI images without a frame. Five of the lesions were “peripheral”, being located > 2 cm away from brainstem, cochlea or optic apparatus. In these cases, an even dose fall-off on all sides was required. The other five lesions were “central”, being < 2 cm away from one or more of these especially radiosensitive structures. Here, it was likely that a steeper dose fall-off towards these structures would be desirable.

Anonymised CT and MRI images for all ten targets were imported into MultiPlan v.3.5.1, and new patient files were created (patients 01 – 10). CT/MRI image fusion was performed, and then the CTV for each target was contoured with reference to both image sets. No margin was applied in producing the PTV from the CTV. This is common Gamma Knife practice. A small CTV – PTV margin of up to 2 mm is sometimes applied in CyberKnife planning, in order to account for any inaccuracies of CT/MRI registration. However it was not used in this study as the main goal was to compare the dosimetric capabilities of the two systems, and the fairest way to do this is with identical contours. Intracranial OARs were also contoured, including whole brain and (where appropriate) brainstem, optic apparatus and cochlea. All contours for each patient were then saved as an RTSS.DICOM file associated with the planning CT.

The CT images, together with the associated RTSS file, for each patient were then imported into GammaPlan v10.1, and new patient files were created. In the case of the five lesions originally treated on Gamma Knife, the original head frame/helmet measurements were used to generate the external skin contour. For the five lesions scanned without a frame, the skin contour was produced by applying the new auto-contour function to the CT images, followed by manual adjustment.

The ten targets were all individually planned on each system, with the goal of creating a plan which optimised external dose gradient and conformality. As with previous studies, plans were required to have an estimated treatment time of less than sixty minutes. This assumed a single fraction of 18 Gy for all targets except the two acoustic neuromas, for which a single fraction of 13 Gy would be delivered. Estimation of treatment time on CyberKnife has been previously discussed in Chapter 4. For Gamma Knife, treatment time is affected by the dose rate, which in turn is dependent on the activity of the cobalt sources which decay over time. GammaPlan gives an estimated treatment time for all plans produced, using an estimated dose rate for the system on that particular day. In this study, the treatment time shown was then adjusted in each case to give an estimated treatment time assuming an even dose rate of 3 Gy/minute for all plans. This was chosen as a reasonable average dose rate for most Gamma Knife systems.

It was decided that % PTV coverage for all plans should be controlled relatively strictly. This is because % coverage for a given plan has a direct effect on both the 12 Gy volume (V12) and the minimum dose to the PTV, both of which are parameters to be used for comparison. This is illustrated by the graph in Figure 7.1 which shows how the V12 can be lowered for a treatment plan simply by lowering the % PTV coverage (ie prescribing up to a slightly higher isodose value). The graph also shows that the consequence of prescribing up to reduce the V12 is a reduction in the minimum PTV dose. In Chapter 6, clinically acceptable CyberKnife plans were required to have > 97 % PTV coverage, which can be easily ensured as coverage for each plan produced on MultiPlan is given to the nearest 0.01 %. Unfortunately, GammaPlan only gives

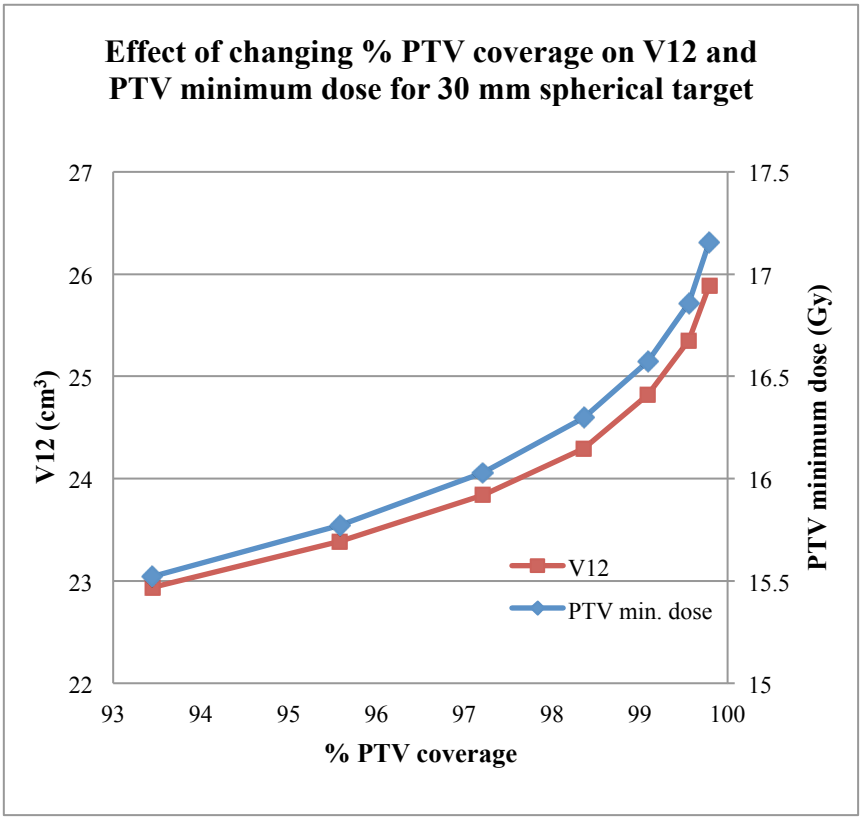

Figure 7.1: Graph showing the effect of changing the PTV coverage (by adjusting the prescription isodose) on the minimum dose to the PTV and the 12 Gy volume (V12). The data are taken from a single treatment plan produced for a 30 mm spherical target.

coverage to the nearest 1 % for plans produced. For this study, therefore, it was required that all plans for comparison should have a PTV coverage of 97 % to the nearest 1 %.

In the case of CyberKnife planning, multiple inverse-planned iterations were performed for each case, following the strategy developed in previous chapters of this thesis, until a plan was produced which appeared to give the best results in terms of the parameters under comparison. For Gamma Knife planning, the standard forward-planning approach was followed, whereby "shots" of variable diameter (and shape) are placed one by one, with real-time update of the plan isodosimetry. The position and weighting of each shot is then adjusted in order to optimise the plan parameters (see Chapter 2 for further details on Gamma Knife treatment planning). Each case was planned three times by the author (AM), and the best plan selected for comparison. Each case was also planned once by the leading UK Gamma Knife planning physicist (IP).

The following information was recorded for each plan, and formed the basis of the plan comparison: prescription isodose value, estimated treatment time, Conformity Index (CI) (Shaw et al), new Conformity Index (nCI) (see Chapter 4), Gradient Index (GI) (Paddick et al (60)), Quarter Dose Index (QDI), V12, and PTV point minimum and mean doses. These latter two values were then expressed as a percentage of the prescribed dose as there were two prescription doses being used in the study (18 Gy and 13 Gy). For the five "central" targets, the maximum and mean doses to any OARs within 2 cm of the target were also recorded. Comparisons were made between the CyberKnife plans, and the Gamma Knife plans produced by IP. As stated previously, this was to ensure that the person creating the plans on each system had extensive planning experience using that system. The Wilcoxon Signed-Ranks test was used to

compare each of the above plan parameters between the two groups. This is a non-parametric equivalent of the paired t-test, and is preferred to the t-test when the sample number (n) is less than 50. Similar comparisons were also made between Gamma Knife plans produced by AM with those produced by IP, in order to assess the effect of experience on Gamma Knife plan quality.

Results

Table 7.1 shows the characteristics of the ten target lesions used in this study. The lesions have been numbered 1 – 10 in increasing order of volume, as measured in MultiPlan. As previously stated, the targets were selected such that they were a reasonable representation of solid tumours treatable with both systems. The volume (measured in MultiPlan) ranged from 0.87 – 11.71 cm^3 (mean volume 3.18 cm^3). Surprisingly, whilst the target contours were identical, the target volumes were different when measured by the two different systems. The volume measured in GammaPlan was consistently smaller than that in MultiPlan, the median difference being 9.5 % (range 6 – 16 %).

The treatment parameters for all ten targets planned on both systems are summarised in Table 7.2. The table also shows the results of statistical comparison between the plans produced on each system, for each parameter, using the Wilcoxon Signed-Ranks test. With respect to the comparison between CyberKnife plans and Gamma Knife plans produced by IP, prescription isodoses were generally lower in the Gamma Knife plans, although this did not quite reach statistical significance at the 5 % level ($p = 0.0547$). Estimated treatment time was required to be </= 60 minutes, and within this restriction the range of treatment times was similar on both systems across the ten targets ($p = 0.9219$). Conformality was also similar across both systems, with the median Conformity Index (CI) slightly lower in the GK plans, and the median new Conformity Index (nCI) slightly lower in the CK plans; neither comparison reached statistical significance. The median value for both of the measures of external dose gradient (GI and QDI) was lower (ie steeper dose fall-off) in the CyberKnife plans, however again a

Target	Tumour type	Location	OARs within 2 cm	System treated on	Volume in MultiPlan (cm^3)	Volume in GammaPlan (cm^3)	Difference in volume
Lesion 1	Acoustic Neuroma	Central	Brainstem Cochlea	Gamma	0.87	0.73	16 %
Lesion 2	Meningioma	Central	Brainstem	Gamma	1.22	1.12	9 %
Lesion 3	Acoustic Neuroma	Central	Brainstem Cochlea	Cyber	3.04	2.7	11 %
Lesion 4	Metastasis	Peripheral		Cyber	3.08	2.59	16 %
Lesion 5	Chordoma	Central	Brainstem Chiasm	Gamma	3.09	2.91	6 %
Lesion 6	Meningioma	Peripheral		Gamma	3.27	3.03	7 %
Lesion 7	Metastasis	Peripheral		Gamma	4.12	3.89	6 %
Lesion 8	Metastasis	Central	Brainstem	Cyber	5.77	5.07	12 %
Lesion 9	Metastasis	Peripheral		Cyber	9.01	8.09	10 %
Lesion 10	Metastasis	Peripheral		Cyber	11.71	10.67	9 %

Table 7.1: Characteristics of the ten target lesions selected for the dosimetric comparison. Organs-at-risk (OARs) excludes whole brain. $\text{Difference in volume} = 100\left(\frac{\text{MultiPlan volume} - \text{GammaPlan volume}}{\text{MultiPlan volume}}\right)$.

Plan Parameter (Median and Range)	CyberKnife	Gamma Knife (IP)	Gamma Knife (AM)	p value CK vs GK (IP)	p value GK (IP) vs GK (AM)
Prescription isodose (%)	49.5 (48 – 61)	45 (40 – 54)	49.5 (46 – 50)	0.0547	0.0977
Treatment time (mins)	45.8 (21.5 – 58.9)	36.3 (28.8 – 60.0)	55.5 (37.6 – 59.2)	0.9219	0.0273
Conformity Index (CI)	1.07 (1.03 – 1.18)	1.06 (1.01 – 1.15)	1.08 (1.04 – 1.19)	0.1641	0.0039
new Conformity Index (nCI)	1.10 (1.06 – 1.21)	1.13 (1.07 – 1.24)	1.16 (1.11 – 1.27)	0.2500	0.0039
Gradient Index (GI)	2.53 (2.39 – 3.02)	2.54 (2.53 – 2.71)	2.60 (2.54 – 2.68)	0.6953	0.1289
Quarter Dose Index (QDI)	6.72 (6.35 – 9.31)	7.15 (6.94 – 7.6)	7.29 (7.09 – 7.46)	0.4922	0.0644
12 Gy volume (V12) (cm^3)	6.15 (1.18 – 19.84)	5.62 (0.94 – 19.61)	6.02 (0.95 – 19.83)	0.0020	0.0059
PTV minimum dose percentage (%)	85.3 (75.7 – 93.1)	65.8 (53.3 – 76.7)	71.4 (59.2 – 77.8)	0.0020	0.1055
PTV mean dose percentage (%)	140.9 (128.2 – 143.3)	143.1 (130.0 – 153.1)	144.4 (140.0 – 153.1)	0.1934	0.8203

Table7.2: Summary of the parameters for the treatment plans produced using CyberKnife and Gamma Knife systems. The median and range over the ten targets is shown for each system. Separate values are given for Gamma Knife plans produced by IP, and those by AM. PTV minimum and mean doses have been expressed as a percentage of the prescription dose. The results of the Wilcoxon Signed-Ranks Test comparison is shown for each parameter. CK = CyberKnife; GK = Gamma Knife.

statistically significant difference was not demonstrated. In contrast, the V12 values were significantly smaller in the Gamma Knife plans ($p = 0.002$), although PTV minimum doses were also significantly lower ($p = 0.02$). There was no significant difference in mean PTV doses ($p = 0.1934$).

The different external dose gradient and conformality scores for each of the ten target lesions planned on CyberKnife, and on Gamma Knife by IP were examined in more detail. The results are displayed in Figures 7.2 and 7.3 respectively. Whilst there was no significant difference in the overall Gradient Index and Quarter Dose Index scores, Figure 7.2 shows that for both of these measures, Gamma Knife tended to perform better for the smallest lesions and CyberKnife better for the largest ones. Gamma Knife plans showed better GI scores for the smallest two lesions, and better QDI scores for the smallest three lesions. Of note, for the smallest lesion, the Gamma Knife performance was substantially superior in terms of external dose gradient. However, CyberKnife plans showed better GI scores for the largest three lesions, and better QDI scores for the largest five lesions. A similar pattern (although slightly less clear) was seen in the conformality performance as shown in Figure 7.3. Gamma Knife plans had superior CI scores for the smallest three lesions, and better nCI scores for two of the smallest three lesions. Conversely, CyberKnife plans had superior CI scores for the largest three lesions, and better nCI scores for the largest four lesions.

Figure 7.4a shows the V12 scores for each lesion in CyberKnife and IP Gamma Knife plans. The V12 was smaller for each of the ten plans. However, as seen in Table 7.1, in spite of the identical contours, the target volumes were measured consistently larger in MultiPlan compared to GammaPlan. Figure 7.4b shows the V12 scores divided by the

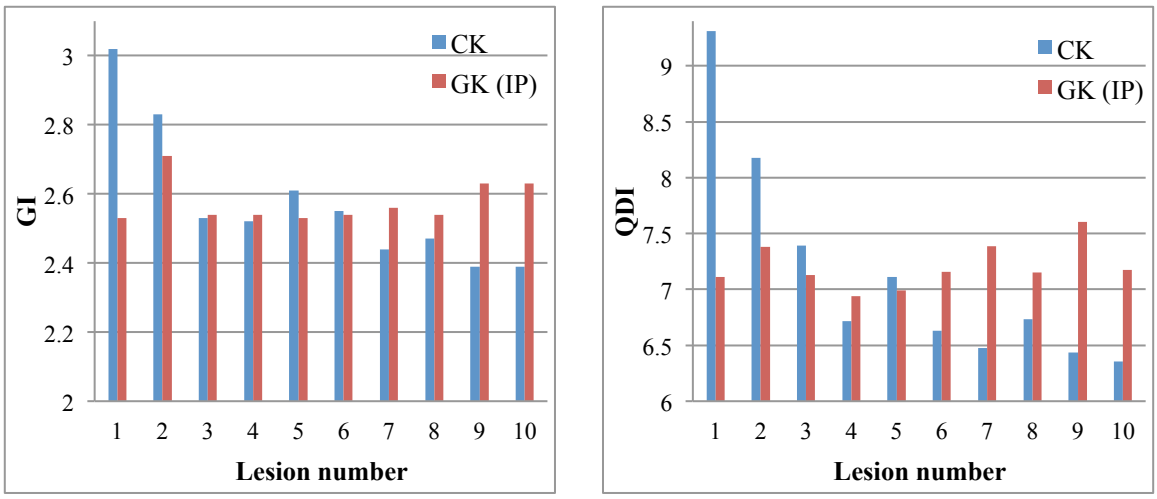

Figure 7.2: Graphs showing the different Gradient Index (left graph) and Quarter Dose Index (right graph) scores for each of the ten plans selected from the CyberKnife system (blue), and Gamma Knife system planned by IP (red).

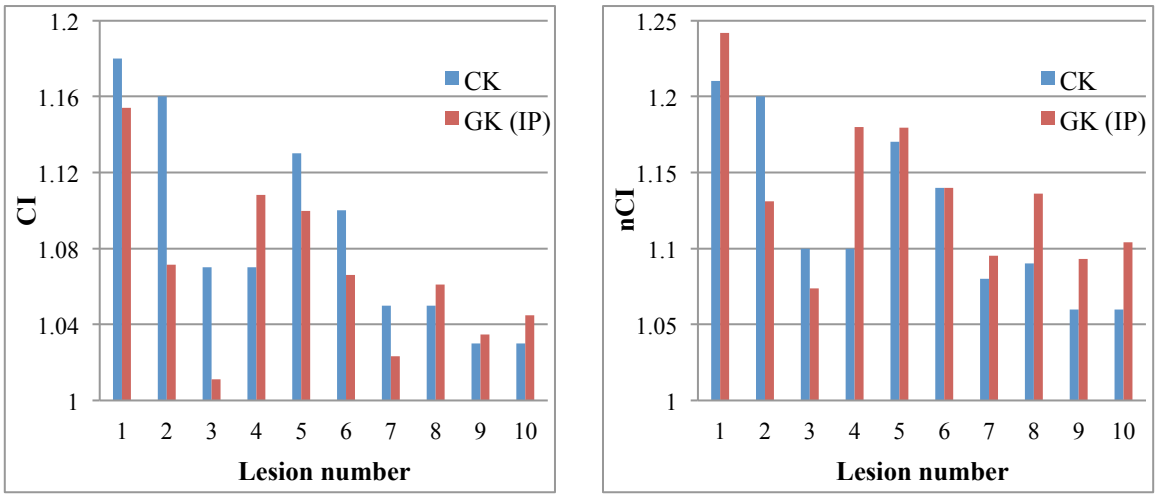

Figure 7.3: Graphs showing the different Conformity Index (left graph) and new Conformity Index (right graph) scores for each of the ten plans selected from the CyberKnife system (blue), and Gamma Knife system planned by IP (red).

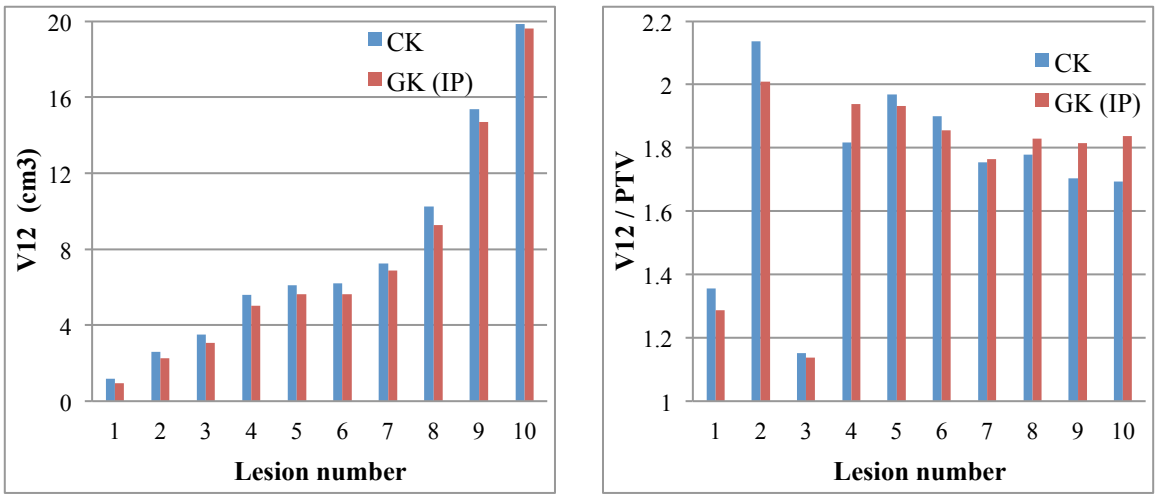

Figure 7.4: The left hand graph shows the different 12 Gy volumes (V12) for each of the ten plans selected from the CyberKnife system (blue), and Gamma Knife system planned by IP (red). The right hand graph shows the V12 values divided by the Target Volume (PTV) in each case.

Organ at Risk	CyberKnife		Gamma Knife (IP)		Gamma Knife (AM)	
	Minimum Dose (Gy)	Mean Dose (Gy)	Minimum Dose (Gy)	Mean Dose (Gy)	Minimum Dose (Gy)	Mean Dose (Gy)
Lesion 1 Brainstem	7.4	0.7	6.5	0.7	6.8	0.7
Lesion 1 Cochlea	5.4	3.1	3.9	2.2	4.0	2.4
Lesion 2 Brainstem	2.8	0.8	2.8	0.6	2.8	0.6
Lesion 3 Brainstem	10.3	1.2	9.1	1.2	9.2	2.3
Lesion 3 Cochlea	10.3	7.0	10.5	5.5	9.1	5.3
Lesion 5 Brainstem	16.8	2.1	15.5	2.2	14.8	3.0
Lesion 5 Chiasm	4.7	3.7	6.0	4.5	3.8	2.2
Lesion 8 Brainstem	11.6	2.1	12.2	0.8	10.4	0.9

Table 7.3: Showing the point minimum and mean doses to especially critical organs-at-risk within 2 cm of the "central" targets planned in this study. Results are once again shown for the chosen plans produced using CyberKnife, and Gamma Knife with two different planners (IP and AM).

PTV (as measured by the software creating the plan) for each target. In this graph, the results are similar to those described for external dose gradient and conformality. The V12:PTV ratio was lower in the Gamma Knife plans for the smallest three lesions, and lower in the CyberKnife plans for the largest three.

Returning to Table 7.2, and with respect to the comparison between Gamma Knife plans produced by IP with those created by AM, there was a significantly shorter treatment time in the IP plans ($p = 0.0273$). Conformality was also better in the IP plans, as measured by both CI ($p = 0.0039$) and nCI ($p = 0.0039$). External dose gradient was not significantly different as measured by GI ($p = 0.1289$) and QDI (0.0644). However, for both measures there was a non-significant trend towards steeper dose gradient in the IP plans, and the V12 was significantly smaller ($p = 0.0059$). On the other hand, there was a non-significant trend ($p = 0.1055$) towards lower minimum PTV doses in the IP plans.

The doses to OARs within 2 cm of the five central lesions are shown in Table 7.3. Firstly, comparing the CyberKnife plans with those produced by IP on Gamma Knife, the minimum OAR dose was lower in the Gamma Knife plans for four of the eight OARs, and lower in the CyberKnife plans for three, with one OAR receiving an equal dose on both systems. Overall there was no significant difference between the systems ($p = 0.375$). Results were similar for the mean OAR dose, with four doses lower on Gamma Knife, two on CyberKnife, and two equal ($p = 0.2188$). There was also no significant difference in minimum ($p = 0.2188$) or mean ($p = 0.8438$) OAR doses when comparing Gamma Knife plans produced by IP and AM.

Discussion

Developments in the field of radiosurgery seek to reduce further the doses delivered to normal tissue, and to improve efficiency of delivery. Dosimetric comparisons continue to be an important area of radiosurgical research as new systems are introduced and existing systems undergo regular upgrades. The aim of this study was to carry out a fair comparison of CyberKnife (CK) and Gamma Knife (GK), two specialist radiosurgical systems, across the range of intracranial targets treatable on both technologies. Recent GK software changes allowed the use of identical target contours in both systems in this comparison. However, the calculated volume of each contour set differed by up to 16 % across the systems. Thus in spite of the methods used, the targets under comparison were not truly identical. The same will have been true for previous comparisons between CK and GK in which "identical" targets were used (80, 83), although it has not been acknowledged in these publications.

The above observation illustrates the fact that the generation of a 3-dimensional volume from a series of 2-dimensional contour lines is open to interpretation, and different radiosurgical systems have different algorithms for deciding whether or not each individual voxel is included within the target volume. This makes it hard to carry out a truly "fair" dosimetric comparison with identical volumes. The latest MultiPlan software upgrade (version 4.5) will change the way that the CyberKnife system interprets volume from contour lines. However, it remains to be seen whether this will result in volumes closer to those seen in GammaPlan for these lesions.

However, in spite of this observation some interesting results were obtained in this study. In general, there were fewer statistically significant differences between the plan parameters from CyberKnife plans and "IP" Gamma Knife plans than in the comparison between Gamma Knife plans produced by two planners with different levels of experience (IP and AM). This means that the experience of the treatment planner has the potential to be a more important variable than which of these two systems is being used. However there were a few areas where larger differences between CK and GK plans were observed.

As discussed previously, external dose gradient and conformality are two of the most important features of a radiosurgical plan. In this study there was no significant difference between CK and GK with respect to the two different measures of dose gradient (GI and QDI) and two conformality measures (CI and nCI). However, a common pattern across all four measures was that GK values were superior when planning the smallest lesions, and CK values were better with the largest ones. Both systems tended to perform equally well for targets in the middle of the size range studied. By far the biggest difference in external dose gradient observed was for the smallest lesion (volume approximately 0.8cm^3), where GK dose fall-off was considerably steeper. Targets of even smaller volume were not studied here, due to the problems of comparing parameters such as conformality across plans of very small volume. However, it is quite possible that GK would continue to outperform CK for all targets smaller than 0.8 cm^3 volume (approximately 11 – 12 mm diameter), although this would need to be verified.

Conversely, all four of the above measures were superior on CK plans for each of the largest three targets (and both dose gradient measures were also better for the 4th largest target). It would appear, therefore, that CK starts to consistently out-perform GK for target volumes greater than about 5 cm^3 (approximately 21 – 22 mm diameter). Targets larger than 13 cm^3 volume (approximately 30 mm diameter) were not considered for comparison in this study as these volumes may not be suitable for single fraction radiosurgery. An additional advantage of CyberKnife is the ability to treat these larger volumes safely by fractionating.

The V12 was significantly smaller in the GK plans compared to the CK plans, and indeed was smaller for each of the ten targets. This result does not really fit with those obtained for both of the external dose gradient parameters. However, as previously noted, the target volume was measured as smaller in GammaPlan than MultiPlan for all ten targets. The V12 was divided by the measured PTV for each plan in order to account for this, and the resultant parameter showed results which fit more consistently with the other dose gradient results – ie Gamma Knife was superior for the smallest lesions, and CyberKnife better for the largest ones. The GI and QDI parameters were not affected by the different measured target volumes in the two systems as these two measures are already ratios of one volume to another.

The PTV minimum point dose was also significantly lower in the GK plans (median value 66 % vs 85 % of the prescription dose), and was individually lower for each of the ten targets. There have been concerns raised about the way in which GammaPlan calculates the minimum target dose value, and indeed a warning has been released by Elekta in the past, stating that this value may be inaccurate by as much as 10 %.

However, this is unlikely to account for such a large difference. Indeed, a comparison of the dose to 99 % of the PTV (D99) showed that this value was also lower in the Gamma Knife plans for 8 out of the 10 targets. In radiosurgery plan appraisal, whilst the % PTV coverage is recognised as an important parameter, far less attention has traditionally been paid to the minimum PTV dose. Gamma Knife local control rates have historically been very good, and it is not known whether changing the planning technique to ensure a higher minimum target dose may improve these rates even further.

This last point highlights one limitation of dosimetric comparison studies: it is not clear how small differences in plan quality as defined by the various radiosurgical parameters discussed here translate directly to differences in clinical outcome. However, it makes good biological sense to aim to deliver an ablative radiation dose to as much of the target as possible and to minimise the dose to normal tissue. Most of the parameters used here provide a measure of one aspect of this overall goal, and indeed some have been shown to correlate with clinical outcomes on retrospective analysis, such as V12 and the risk of post-radiosurgical complications. Together, the parameters represent a reasonable basis for treatment plan selection.

There were some other limitations of the experimental method used. The problem of differences in target volume calculation between MultiPlan and GammaPlan has already been discussed. Another difference between the two systems is the precision with which certain plan measures are displayed. For example, minimum, mean and maximum doses to target and OARs are provided to the nearest 0.01 centigray in MultiPlan, but only to the nearest 0.1 gray in GammaPlan. Also, volumes such as target volume or V12 are provided to the nearest 0.01 mm^3 in MultiPlan but only to the nearest 0.01 cm^3 in

GammaPlan (for volumes larger than 1 cm^3). This can cause problems when comparing similar values across the two systems. For example if the maximum dose to the brainstem is measured as 9.4 Gy in a Gamma Knife plan and 9.4412 Gy in a CyberKnife plan, for the purposes of this comparison the values had to be regarded as equal. This reduces the power to detect a statistically significant difference since equal values are discarded in the Wilcoxon Signed-Ranks test.

Finally, a potential problem with applying these results directly to the clinical situation is that no CTV – PTV margin was used. This was to ensure a fairer dosimetric comparison between the systems. Both systems have demonstrated sub-millimetre overall system accuracy, and common Gamma Knife practice is to use no PTV margin. However in the case of CyberKnife, for targets contoured on MRI images, there is potential for further inaccuracy in the MRI – CT image registration, which is not included in the standard tests of overall accuracy. For this reason many CyberKnife centres would add a PTV margin of 1 – 2 mm for brain lesions contoured on MRI. Thus the use of CT electron density information to calculate dose is both a strength and a weakness of the CyberKnife system. On the one hand it allows much more accurate dose calculation, but on the other hand a small PTV margin is required for intracranial targets contoured using MRI images. The latest MultiPlan version (v.4.5) has greatly improved automatic image registration algorithms, which should allow the use of smaller PTV margins, and may actually obviate the need for a PTV margin altogether.

Summary

Dosimetric comparison studies continue to be an important part of radiosurgical research as new delivery systems are developed and existing ones undergo regular upgrades. The difference between the dosimetric performance of CyberKnife and Gamma Knife over the ten targets used in this study is generally quite small, and for the majority of lesions treatable on both systems the choice of system may be less important than the experience of the treatment planner creating the plans. Nevertheless there does appear to be superior dosimetric performance with Gamma Knife for smaller targets and CyberKnife for larger ones, with this superiority being most apparent at both extremes of the treatable size range.

Chapter 8 – Discussion

Safe delivery of radiosurgery requires a steep external dose gradient outside the target, but this must be considered in conjunction with other important plan parameters such as target coverage and conformality. There will be a limit for any radiosurgical system as to how steep a dose fall-off can be produced, and this is dictated by the constraints of the hardware of the system. This limit also applies to the other plan parameters. In the CyberKnife system, the available selection of circular field sizes and the range of non-coplanar beam angles provide enormous flexibility, but ultimately also define the limits of what can be achieved. Other hardware factors such as the linac output (MU delivered per minute) may apply a further limit, for example if the overall treatment time is also a consideration. The role of MultiPlan treatment planning software is to create plans as close to these limits as possible. However, the software will only produce solutions based on the priorities and settings applied by the treatment planner. Due to the number of variables which can be adjusted, and the complexity of the optimisation algorithms, it takes considerable experience in order to interact with the software appropriately to produce the best results. The experimental work in this thesis has led to a more comprehensive understanding of these variables, so that the external dose gradient in clinically acceptable plans can be optimised in different intracranial clinical situations.

Summary of findings of the experimental chapters

It is important to verify that the dose distribution of treatment plans produced and displayed in MultiPlan accurately reflects that which is actually delivered. In-house QA checks at this centre include monthly reference dose verification, and spatial accuracy via the "End2End test". However, the opportunity was taken to perform a more detailed verification using ionisation chamber reference dose and radiochromic film spatial dose distribution analysis simultaneously on ten consecutive CyberKnife treatment plans. This study was described in Chapter 3. The ionisation chamber reference dose measured was comfortably within 3 % of the planned dose for all ten plans – in fact only one reading (2.01 %) showed > 2 % error. With regard to spatial dose distribution analysis, using the film as a measure of reference dose, all ten plans exceeded the 95 % pass rate with 5 %/1 mm Gamma Index tolerance. Unfortunately 5 % dose difference tolerance is not really strict enough for a radiosurgical plan, and therefore there is a real need to improve the reference dose accuracy of Gafchromic EBT2 film. Whilst software is now available which can apply the manufacturer's proposed correction for the intrafilm variation in active layer thickness, one centre has reported that this actually increases noise in the resulting dose images (84). On a more optimistic note, the film manufacturer acknowledges the inconsistencies of early batches of EBT2, and is working on reducing this. It may therefore be possible to perform 2-dimensional dose film analysis with a more appropriate, tighter dose difference tolerance in the near future. For the purpose of this thesis, the results from Chapter 3 demonstrated that the dose distributions shown in MultiPlan are sufficiently reliable for the subsequent analyses.

Chapters 4 and 5 explored the effect of the prescription (marginal) isodose value on the external dose gradient in the planning of solitary intracranial lesions in MultiPlan, for situations where an even dose fall-off on all sides of the target is desired. Chapter 4 used spherical "virtual" targets, and Chapter 5 used irregularly-shaped lesions from patients treated at this centre. The results were generally consistent across both chapters and were different for smaller and larger targets. For smaller targets (approximately < 20 mm diameter or < 5 cm^3 volume), there was a significant negative relationship between Gradient Index (GI) and prescription isodose value over the whole range explored. External dose gradient is therefore optimised by prescribing down to as close to the 50 % isodose as can be achieved comfortably. GI can be safely used as a sole measure of dose fall-off here. In the case of larger targets (approximately > 25 mm diameter or > 8 cm^3 volume), whilst the effect of changing the prescription isodose is not as great, nevertheless the best dose fall-off is likely to be achieved using a prescription isodose in the range 55 – 65 %. The correlation between different measures of dose fall-off was less strong here, so it may be advisable to use V12 or even Quarter Dose Index, together with GI, during plan appraisal.

A stepwise method for planning solitary intracranial lesions using MultiPlan has also been proposed, for the purpose of optimising external dose gradient without compromising on other important plan parameters. With practice, an optimised treatment plan can be produced in 1 – 3 hours (depending on target size) using this method. This has proved useful in the subsequent planning of cases at this centre, and has been shared with other CyberKnife centres. Validation of the method by different planners with a larger number of lesions would be useful to confirm the results observed here.

Chapter 6 concerned the specific clinical situation of a radiosurgical target lying close to (or abutting) the brainstem on one aspect, with cerebral cortex on all other sides. It was observed that adding a tight brainstem VOI limit produced moderate reductions in brainstem maximum dose without the need for any compromise on overall dose fall-off, coverage, conformality, and moderate dose distant to the target. Furthermore in most situations the brainstem maximum dose correlated strongly (and significantly) with the other measured brainstem dose-volume endpoints. Even further brainstem dose reductions could be achieved using this technique, but at the expense of at least one of the above plan parameters. With regard to prescription isodose, a similar picture to the previous two studies appeared to emerge: using the lowest prescription isodose value (55 %) was advantageous when planning the smaller (15 mm) target. For the larger (30 mm) target, results with the 55 and 65 % isodoses were generally better than with the 75 % isodose. Whilst the VOI limit is clearly a very useful planning tool in this situation, the latest MultiPlan software upgrade will offer the additional flexibility of DVH-based optimisation, for example the ability to constrain an OAR to a specific dose-volume value (eg kidney V12 < 25 %). Further work could look at how best to use VOI limits and DVH-based constraints together.

A dosimetric comparison of the CyberKnife and Gamma Knife systems was performed in Chapter 7, looking once again at solitary intracranial lesions. Together, the ten targets comprised a reasonable cross-section of the range of solid tumours treatable on both systems with a single fraction approach. Treatment plans were compared using a wide range of radiosurgical parameters commonly used for plan appraisal. The results showed that whilst overall performance of the two systems across the ten targets was quite similar (and largely non-significant), Gamma Knife was capable of creating

superior plans for the smallest lesions, and CyberKnife for the largest ones, with very little difference for lesions of "intermediate size". Gamma Knife plans had been produced by the author and also by a treatment planner with more than ten years' experience with Gamma Knife. Comparing these plans showed that, especially for intermediate size lesions, the effect of planning experience has the potential to be a more important factor than which of the two systems is used. Caution was raised in view of the difference in both the calculated target volume (given that identical contour sets were used) and the precision of certain calculated plan parameters across the two systems.

A possible general criticism of the experimental work in this thesis has been that numbers have been relatively small and non-parametric testing has been used throughout (the statistical reasons for which have been explained at each point). This may have resulted in the studies being underpowered to detect certain differences within the data. However, statistically significant results were obtained in each study in spite of these limitations, and it has therefore been possible to draw some important conclusions from the experimental work performed.

Radiosurgical plan parameters revisited

The 12 Gy volume (V12) is widely used in radiosurgery centres when assessing candidate treatment plans. It is not a pure measure of dose fall-off, as it is also dependent on the size of the PTV and dose prescribed. It is, however, a pure measure of the volume irradiated, and therefore it is unsurprising that it has been shown to correlate

with post-radiosurgical complications (12, 58). When comparing different plans for the same PTV, and using the same prescribed dose, then V12 can act as a relative measure of dose fall-off. This was the intention with the Gamma-Cyber comparison in Chapter 7, although unfortunately target volume was not identical on the two different systems, therefore V12 could not be used in this way.

The V12 is also intimately related to the % PTV coverage as shown in Figure 7.1 (Chapter 7), the volume decreasing as % coverage decreases for a given plan. Unsurprisingly, as % coverage decreases for a given plan, then so also does the minimum dose to the PTV. In Chapter 7 the required PTV coverage was required to be 97 % (to the nearest 1 %) for all plans in order to minimise this effect, although from a V12 perspective it was still beneficial to give eg 96.5 % coverage rather than 97.4 %. When assessing candidate plans, V12 values therefore need to be compared together with % coverage, PTV minimum dose, and other measures of dose fall-off.

Gradient Index (GI) has been used as the main measure of external dose gradient in this thesis. It has the advantage of being independent of prescribed dose and prescription isodose % value, as it is a ratio involving the prescription isodose and half-prescription isodose volumes. Also, because it is a ratio, the dose fall-off across targets of different sizes can be compared. However, the GI can be criticised for the fact that two plans for the same PTV can have the same half-prescription isodose volume, but different GI scores depending on the volume inside the prescription isodose line. This is illustrated in Figure 8.1. In this example, one plan has a “baggy” prescription isodose which conforms less well to the PTV, but which results in a lower GI score. However, if GI on

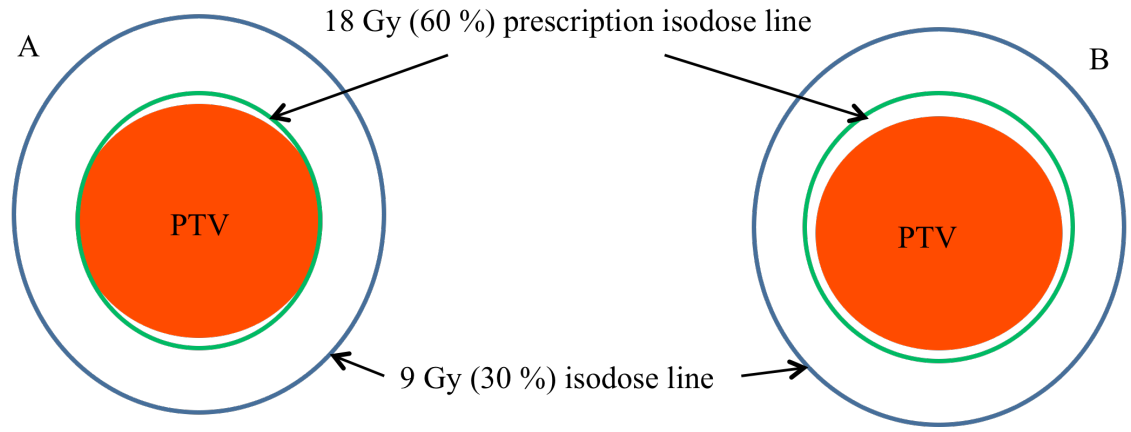

Figure 8.1 Drawing of the isodosimetry of two candidate treatment plans for the same PTV, delivering 18 Gy to the 60 % marginal isodose. Both plans have 100 % PTV coverage and identical 9 Gy volumes. Using the Gradient Index, plan B would have a lower (better) score by virtue of a more "baggy" marginal isodose line. However, plan A is more conformal, with less normal tissue inside the PTV, and this is the plan which should be selected.

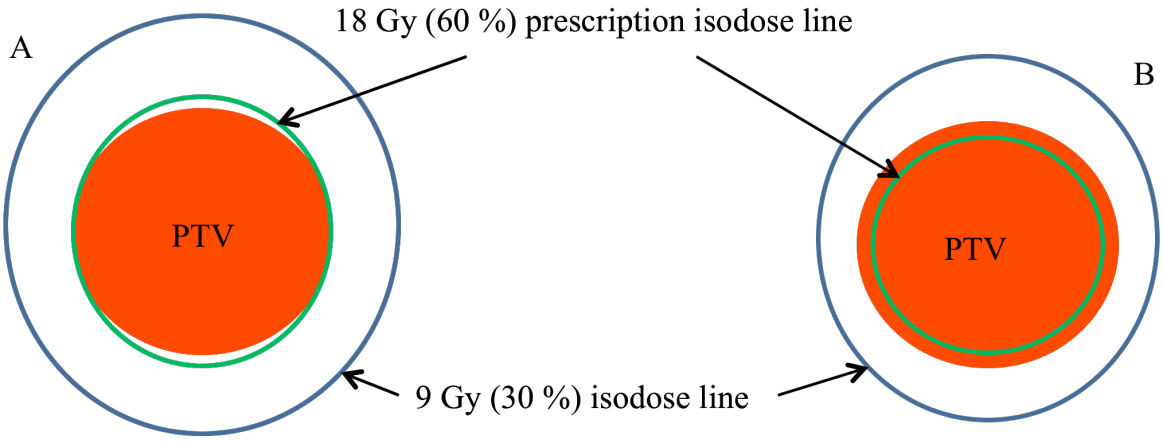

Figure 8.2 Drawing of the isodosimetry of two candidate treatment plans for the same PTV, delivering 18 Gy to the 60 % marginal isodose. Both plans would have comparable conformality as measured by nCI. Plan B has a smaller prescription isodose volume and 9 Gy volume. Using the R50 %, plan B would have a lower (better) score. However both plans have identical Gradient Index scores, and plan A has better PTV coverage. Plan A should therefore be selected.

candidate treatment plans is interpreted together with PTV % coverage and nCI values, then there is little danger of accepting the worse plan.

An alternative dose gradient measure is the R 50 %:

$$R\ 50\% = \frac{volume\ within \frac{x}{2}\%\ isodose}{planning\ target\ volume}$$

where x would be the prescription isodose. This is now used in a number of centres, having been used in the RTOG 0236 lung SBRT trial (85). Like the GI, it is independent of prescribed dose and prescription isodose % value. In the example in Figure 8.1, this dose gradient measure would be equal for both plans. However, this measure is still affected by PTV % coverage in the same way as the V12, as illustrated in Figure 8.2. The two plans in this figure have the same GI score, since the ratio of prescription isodose volume : half-prescription isodose volume is the same. However, by choosing a smaller prescription isodose line with less PTV coverage, the R 50 % is lower in the right-hand example.

It would seem, therefore, that no single measure of external dose gradient is perfect for every situation. The GI is certainly appropriate in most situations, provided that % coverage and conformality are relatively consistent across candidate plans. It is also apparent, though, that three of the most important radiosurgical plan parameters (external dose gradient, PTV % coverage and conformality) are inextricably linked together, and plan evaluation needs to take all of them into account. It would be useful to have a universal measure of plan quality which incorporates all of these measures. This would certainly make it easier to compare candidate treatment plans on one

system, and also the performance of different radiosurgical systems. However, not only do the best individual measures need to be selected, they also need to combined in an appropriate way. Wagner et al (86) proposed a Conformity Gradient Index (CGI) which illustrates some of the potential problems:

$$CGI = \frac{(CGIc + CGIg)}{2}$$

$$CGIc = \left(\frac{TV}{PIV}\right) \times 100$$

where TV = target volume, and PIV = prescription isodose volume.

$$CGIg = 100 - \{100[(R_{eff.50\%Rx} - R_{eff.Rx}) - 0.3\ cm]\}$$

where $R_{eff.50\%Rx}$ is the effective radius (in cm) of the isodose which is half the prescription, and $R_{eff.Rx}$ is the effective radius of the prescription isodose. The conformality measure is basically the reciprocal of Shaw's conformity index (CI), expressed as a percentage. It has already been demonstrated in Chapter 4 that this index can give false perfect scores. The dose gradient measure uses effective radius (the radius of a sphere with the same volume) and allows an arbitrary 3 mm dose fall-off before the measure drops below the perfect score of 100. This is certainly not a regularly-used stand-alone measure of dose gradient.

With regard to how to combine the measures, the best approach is not immediately obvious since they are measuring completely different things. For example, whilst conformality provides information about the volume of normal tissue receiving doses greater than the prescription dose, dose gradient is more concerned with the (larger) volume of normal tissue receiving doses in excess of a lower dose (eg half the prescription dose). In the above example, the authors combine the conformality and

dose gradient measures by simply adding together and dividing by 2, thus giving each equal importance in an overall score out of 100. This means that, for example, if the CI increases from 1.1 – 1.25, this can be offset if the effective radius difference between half-prescription and prescription isodoses decreases from 5 – 4 mm. It is difficult to say whether or not this is reasonable, and one can argue that reducing the plan parameters to a single measure is not useful if the resultant measure is hard to interpret. Since there is no intuitive way of combining these measures, the conclusion of this thesis would be that they should continue to be used separately in radiosurgical plan appraisal.

Suggestions for future research

This thesis has focused on the planning of intracranial lesions using the CyberKnife system. This is the traditional radiosurgical site, and most previous research into dose gradients and other plan parameters has used targets in the brain. However, a number of modern radiotherapy systems, such as CyberKnife, are able to use on-line image guidance to treat with the required accuracy to use large dose-per-fraction radiation for targets outside the skull. The use of so-called Stereotactic Body Radiotherapy (SBRT) is increasing, with the two commonest treatment sites worldwide being the lung and spine.

An extension of the work in this thesis could look at the CyberKnife planning of extracranial lesions, to see to what extent the findings can also be applied to sites outside the brain. The optimisation algorithms and range of collimator sizes are the same when treating extracranial lesions, so it is quite possible that much of this

intracranial work will be useful in the planning of body sites. However the CyberKnife treatment paths (and therefore the range of beam angles) are different for body targets. This, together with the different body skin surface contours and tissue depth (and therefore different source-target separation), means that the results from this thesis would still need to be verified for extracranial lesions.

The dose tolerance for lung tissue, as with most parallel organs, is usually expressed as a dose to a percentage of total organ volume, for example V20 < 30 % for 2 Gy/fraction radical radiotherapy, and V20 < 20 % for a three-fraction SBRT regimen (as specified in the lung cancer STARS trial). The most clinically important lung radiation toxicities are pneumonitis and fibrosis, both of which can have a significant impact on lung function. The main group of lung cancer patients treated with SBRT are those with stage I disease who are not medically fit for surgical lobectomy. Since this is often due to poor lung function, then it is critically important that in SBRT the amount of radiation-induced lung toxicity is minimised. Many lung tumours are surrounded on all sides by healthy lung parenchyma, therefore in order to minimise the V20 a steep dose fall-off on all sides of the target is usually required. Chapters 4 and 5 demonstrated that the steepest external dose gradient (as measured by Gradient Index) is achieved using a prescription isodose close to 50 % for smaller targets, and in the range 55 - 65 % for larger ones. It would be interesting to see whether the same strategy optimises dose fall-off when treating lung tumours.

In contrast, spinal tumours are located close to (or sometimes abutting) the spinal cord. As a serial organ, spinal cord tolerance in radiosurgery is described in terms of maximum point dose, or dose to a very small volume of cord, such as 0.035 or 0.1 cm^3.

Optimising dose fall-off in the direction of the cord is usually a priority in spinal radiosurgical planning. However, there may be other important OARs to consider, such as exiting nerve roots, or the oesophagus, and therefore overall external dose gradient and other plan parameters may also be important. Chapter 6 explored the effects on overall plan quality of applying a firm restriction on dose to an OAR close to an intracranial target on one aspect. Once again, a verification of whether the same relationships exist when planning spinal lesions would be useful.

Arguably the biggest difference when considering SBRT, as opposed to intracranial radiosurgery, is the presence of significant inter- and intra-fraction target and OAR movement. The ability to identify, and compensate for, target movement between fractions is critical to the safe and effective delivery of SBRT. Additionally, with CyberKnife, where the fraction time is usually between 30 and 90 minutes, this must also be done during each fraction for all targets, regardless of whether or not they move with breathing. CyberKnife uses planar imaging, and therefore relies on implanted fiducial markers in order to track the position of many extracranial tumours. The fiducials therefore act as surrogate markers for tumour position. A minimum of three fiducials are required in order for the system to determine the target position according to all six dimensions (anterior-posterior, left-right, superior-infererior, roll, pitch and yaw). Furthermore, the fiducials must be > 20 mm apart, with no overlapping in either of the two 45-degree imaging planes.

There are limitations inherent in CyberKnife fiducial tracking, and this is another possible area for future research. Firstly, there are some situations where it is not possible to insert safely at least three fiducials near/in the tumour. Examples include

patients with very poor lung function, in whom each needle pass carries the risk of life-threatening pneumothorax, and some pancreatic or abdominal nodal tumours, where major blood vessels may abut the target on most aspects. Where only one or two markers are inserted, the system can track any intra-fraction translational movements, but not the rotational ones (rotational position can only be set up at the start of the fraction, using Xsight Spine tracking). Secondly, even if the route of fiducial insertion is straightforward and safe, it may not be possible to insert three markers directly into the target, and still meet the above criteria for effective tracking. In this situation, at least some of the fiducials must be inserted around the target rather than inside it. Fiducials outside the tumour may not move in exactly the same way as the tumour itself, even if they are within the Accuray recommended maximum distance of 6 cm from the tumour.

A clearer, more quantitative understanding of these limitations would help clinicians with the appropriate use of fiducials with CyberKnife, including the size of CTV-PTV margins needed to account for any potential errors. It would also be very helpful for treatment radiographers and physicists, as decisions often have to be made during treatment regarding which (and how many) fiducials to use for tracking.

A dosimetric comparison of CyberKnife and Gamma Knife for intracranial radiosurgery (Chapter 7) has formed part of this thesis. There are a number of modern gantry-based radiosurgery systems in use, and it would interesting to extend the work in Chapter 7 to look at the ability of a gantry-based radiosurgery system to plan the same targets. It is hoped that such a collaboration will be possible in the future. Additionally, further research into the CyberKnife system in the area of extracranial treatment could also include a similar comparison with other SBRT or IMRT delivery systems. For example,

CyberKnife is designed primarily as a radiosurgical tool for treating relatively small targets. However, gantry-based IMRT delivery systems commonly deal with substantially larger targets. The most recent advances in IMRT delivery involve the use of modulated arc therapy (eg RapidArc (Varian Medical Systems, Palo Alto, CA) and VMAT (Elekta)), which confers greater target conformality and treatment efficiency, both in terms of time and monitor units used. As the target size increases there will be a point at which IMRT planning systems are capable of producing better quality plans than CyberKnife. Observations from this centre suggest that the size at which this occurs may actually be smaller than one might think. Indeed, as the maximum target diameter increases beyond approximately 6 cm the external dose fall-off in plans produced using CyberKnife appears to become less steep. This may be in part due to the fact that the largest field size available is a 60 mm diameter circle. A formal dosimetric comparison of CyberKnife and, for example, RapidArc planning would provide useful information in this area, thus helping clinicians to be better informed when deciding on the most appropriate radiotherapy system to use for each patient.

It has previously been noted that target dose inhomogeneity affects the “effective” dose delivered. This is particularly pertinent since this thesis has demonstrated that external dose gradients can be achieved in CyberKnife radiosurgery by using lower marginal idosose values than are currently favoured in centres around the world. More widespread use of generalised Equivalent Uniform Dose (gEUD) could make future comparisons of treatments across different systems (and centres) more meaningful, although unfortunately the accuracy of the gEUD calculation will tend to reduce as the degree of heterogeneity increases!

The importance of dose rate in radiotherapy has also previously been noted (32). In the experimental work in this thesis, treatment times for the clinically acceptable plans produced were not allowed to exceed 60 minutes. However, even with this restriction there could be a substantial dose rate effect when comparing, for example a 60 minute treatment with one which takes 20 minutes. There are now a number of different systems capable of delivering radiosurgery, and treatment times can vary considerably. Further work to improve understanding of the dose rate effect in radiosurgery will help to establish equivalent doses across the different systems.

Additionally, there is some evidence that for a given treatment time, the way in which the target is irradiated may have further radiobiological significance. For example, CyberKnife radiosurgical treatment usually comprises 100 – 200 beams, each of which only irradiates part of the target volume. For a given voxel within the target, the single fraction will actually consist of multiple short periods of variable dose delivery, with variable pauses in between which may allow some repair of sublethal damage. This pattern will be different for every voxel within the target. Murphy and Lin (87) have shown that the variable voxel irradiation schedules occurring during a CyberKnife fraction can translate into a spatially-variable reduction in effective dose within the target. Hopewell (88) has similarly demonstrated that in a Gamma Knife treatment, the BED can vary significantly across the different voxels in the target for the same reasons. Further work could look at methods to reduce this variability and/or optimise tumour control probability for a given radiosurgery treatment by altering the beam/shot sequence or weighting, or even simply identifying the best beam or shot with which to start the fraction.

Conclusions

Small field dosimetry is a controversial area of radiotherapy Quality Assurance, and some of the tools commonly used are in need of improvement. Ionisation chamber and radiochromic film analysis have confirmed that CyberKnife treatment plans in MultiPlan are a reasonably accurate reflection of the treatment which is actually delivered, although it would be desirable to be able to use stricter spatial dose distribution tolerances in the future.

The choice of prescription isodose affects the steepness of the external dose gradient in CyberKnife planning of solitary intracranial targets, as demonstrated with both spherical "virtual" targets and irregular lesions. The optimum prescription isodose for smaller targets is as close to 50 % as can be achieved comfortably. For larger targets, the optimum value is likely to be in the range 55 – 65 %. A stepwise method has been proposed for optimising dose fall-off in the planning of solitary intracranial lesions, where even dose fall-off on all sides is desired.

When an especially radiosensitive OAR lies near an intracranial target on one aspect, introducing a tight dose limit for this OAR during planning (using a VOI limit) can reduce the dose to this structure substantially without any real compromise on other important plan parameters. Using "eroded" target volumes may further help the optimisation process when the OAR abuts or overlaps the target.

Whilst the dosimetric performance of CyberKnife and Gamma Knife in the planning of solitary brain targets is generally similar, there is evidence to suggest that Gamma Knife dosimetry is superior for very small lesions, and CyberKnife is superior for lesions at the upper end of the single fraction target size range. The experience of the treatment planner has the potential to be a more important factor for lesions which both systems treat well.

Bibliography

1. Horsley V, Clarke RH. The structure and functions of the cerebellum examined by a new method. Brain. 1908;31(1):45-124.

2. Spiegel EA, Wycis H, Marks M, Lee A. Stereotaxic apparatus for operations on the human brain. Science. 1947;106(2754):349-50.

3. Freund L. Ein mit Röntgen-Strahlen behandelter Fall von Naevus pigmentosus piliferus. Wien Med Wochensch. 1897;10:428-33.

4. Leksell L. The stereotactic method and radiosurgery of the brain. Acta Chir Scand. 1951(102):316-9.

5. Hounsfield GN. Computerized transverse axial scanning (tomography): Part 1. Description of system. British Journal of Radiology. 1973;46(552):1016-22.

6. Betti O, Derechinsky V. Hyperselective encephalic irradiation with linear accelerator. Acta Neurochir Suppl. 1984;33:385-90.

7. Colombo F, Benedetti A, Pozza F, Avanzo RC, Marchetti C, Chierego G, et al. External stereotactic irradiation by linear accelerator. Neurosurgery. 1985;16(2):154-60.

8. Sebag-Montefiore D, Doughty D, Biggs D, Plowman P. Stereotactic multiple arc radiotherapy. I. Vascular malformations of the brain: an analysis of the first 108 patients. British journal of neurosurgery. 1995;9(4):441-52.

9. Adler Jr J, Chang S, Murphy M, Doty J, Geis P, Hancock S. The Cyberknife: a frameless robotic system for radiosurgery. Stereotactic and Functional Neurosurgery. 1997;69(1-4 Pt 2):124-8.

10. Régis J, Metellus P, Hayashi M, Roussel P, Donnet A, Bille-Turc F. Prospective controlled trial of gamma knife surgery for essential trigeminal neuralgia. Journal of neurosurgery. 2006;104(6):913-24.

11. Flickinger JC, Kondziolka D, Maitz AH, Dade Lunsford L. An analysis of the dose-response for arteriovenous malformation radiosurgery and other factors affecting obliteration. Radiotherapy and Oncology. 2002;63(3):347-54.

12. Flickinger J, Kondziolka D, Pollock B, Maitz A, Lunsford L. Complications from arteriovenous malformation radiosurgery: multivariate analysis and risk modeling. International journal of Radiation Oncology* Biology* Physics. 1997;38(3):485-90.

13. Flickinger JC, Kondziolka D, Lunsford LD, Kassam A, Phuong LK, Liscak R, et al. Development of a model to predict permanent symptomatic postradiosurgery injury for arteriovenous malformation patients. International Journal of Radiation Oncology* Biology* Physics. 2000;46(5):1143-8.

14. Lunsford LD, Niranjan A, Flickinger JC, Maitz A, Kondziolka D. Radiosurgery of vestibular schwannomas: summary of experience in 829 cases. Special Supplements. 2005;102:195-9.

15. Hansasuta A, Choi CYH, Gibbs IC, Soltys SG, Tse VCK, Lieberson RE, et al. Multi-session Stereotactic Radiosurgery for Vestibular Schwannomas: Single Institution Experience with 383 Cases. Neurosurgery. 2011;69(6):1200-9.

16. Santacroce A, Walier M, Liščák R, Motti E, Lindquist C, Kemeny A, et al. Long Term Tumour Control of Benign Intracranial Meningiomas After Radiosurgery in A Series of 4565 Patients. Neurosurgery. 2012;70(1):32-9.

17. Colombo F, Casentini L, Cavedon C, Scalchi P, Cora S, Francescon P. Cyberknife radiosurgery for benign meningiomas: short-term results in 199 patients. Neurosurgery. 2009;64(2):A7-A13.

18. Mingione V, Yen CP, Vance ML, Steiner M, Sheehan J, Laws ER, et al. Gamma surgery in the treatment of nonsecretory pituitary macroadenoma. Journal of neurosurgery. 2006;104(6):876-83.

19. Swords F, Monson J, Besser G, Chew S, Drake W, Grossman A, et al. Gamma knife radiosurgery: a safe and effective salvage treatment for pituitary tumours not controlled despite conventional radiotherapy. European Journal of Endocrinology. 2009;161(6):819-28.

20. Sperduto PW, Chao ST, Sneed PK, Luo X, Suh J, Roberge D, et al. Diagnosis-specific prognostic factors, indexes, and treatment outcomes for patients with newly diagnosed brain metastases: a multi-institutional analysis of 4,259 patients. International Journal of Radiation Oncology* Biology* Physics. 2010;77(3):655-61.

21. Patchell RA, Tibbs PA, Walsh JW, Dempsey RJ, Maruyama Y, Kryscio RJ, et al. A randomized trial of surgery in the treatment of single metastases to the brain. New England Journal of Medicine. 1990;322(8):494-500.

22. Patchell RA, Tibbs PA, Regine WF, Dempsey RJ, Mohiuddin M, Kryscio RJ, et al. Postoperative radiotherapy in the treatment of single metastases to the brain. JAMA: the journal of the American Medical Association. 1998;280(17):1485-9.

23. Soltys S, Gibbs I, Chang S, Adler J, Harsh G, Lieberson R, et al. Stereotactic Radiosurgery of the Post-operative Resection Cavity for Brain Metastases: Optimization of the Treatment Technique. International Journal of Radiation Oncology* Biology* Physics. 2010;78(3):S7.

24. Andrews DW, Scott CB, Sperduto PW, Flanders AE, Gaspar LE, Schell MC, et al. Whole brain radiation therapy with or without stereotactic radiosurgery

boost for patients with one to three brain metastases: phase III results of the RTOG 9508 randomised trial. The Lancet. 2004;363(9422):1665-72.

25. Chang EL, Wefel JS, Hess KR, Allen PK, Lang FF, Kornguth DG, et al. Neurocognition in patients with brain metastases treated with radiosurgery or radiosurgery plus whole-brain irradiation: a randomised controlled trial. The Lancet Oncology. 2009;10(11):1037-44.

26. Fowler JF. The linear-quadratic formula and progress in fractionated radiotherapy. British Journal of Radiology. 1989;62(740):679-94.

27. Withers HR. Four R's of radiotherapy. Adv Radiat Biol. 1975;5:241-7.

28. Guerrero M, Li XA. Extending the linear–quadratic model for large fraction doses pertinent to stereotactic radiotherapy. Physics in Medicine and Biology. 2004;49(20):4825-35.

29. Park C, Papiez L, Zhang S, Story M, Timmerman RD. Universal survival curve and single fraction equivalent dose: useful tools in understanding potency of ablative radiotherapy. International Journal of Radiation Oncology* Biology* Physics. 2008;70(3):847-52.

30. Fowler JF. Linear Quadratics Is Alive and Well: In Regard to Park et al.(Int J Radiat Oncol Biol Phys 2008; 70: 847–852). Respiratory Care Clinics of North America. 2008;72(3):957-8.

31. Withers HR, Taylor JMG, Maciejewski B. Treatment volume and tissue tolerance. International Journal of Radiation Oncology* Biology* Physics. 1988;14(4):751-9.

32. Steel GG, Down JD, Peacock JH, Stephens TC. Dose-rate effects and the repair of radiation damage. Radiotherapy and Oncology. 1986;5(4):321-31.

33. Aspradakis MM, Byrne JP, Palmans H, Conway J, Rosser K, Warrington JAP, et al. IPEM Report Number 103: Small Field MV Photon Dosimetry. Inst of Physics and Engineering in Medicine. 2010.

34. International Commission on Radiation Units and Measurements. ICRU Report 50. Prescribing, recording, and reporting photon beam therapy. Bethesda, MD: ICRU1993.

35. International Commission on Radiation Units and Measurements. ICRU Report 62. Prescribing, recording, and reporting photon beam therapy (Supplement to ICRU Report 50). Bethesda, MD: ICRU1999.

36. Niemierko A. A generalized concept of equivalent uniform dose (EUD). Medical Physics. 1999;26(6):1100.

37. Muacevic A, Kufeld M, Wowra B, Kreth F, Tonn J. Feasibility, safety, and outcome of frameless image-guided robotic radiosurgery for brain metastases. Journal of Neuro-Oncology. 2010;97(2):267-74.

38. Ho A, Fu D, Cotrutz C, Hancock S, Chang S, Gibbs I, et al. A study of the accuracy of Cyberknife spinal radiosurgery using skeletal structure tracking. Neurosurgery. 2007;60(2):147-56.

39. Muacevic A, Staehler M, Drexler C, Wowra B, Reiser M, Tonn J. Technical description, phantom accuracy, and clinical feasibility for fiducial-free frameless real-time image-guided spinal radiosurgery. Journal of Neurosurgery: Spine. 2006;5(4):303-12.

40. Yu C, Main W, Taylor D, Kuduvalli G, Apuzzo M, Adler Jr J, et al. An anthropomorphic phantom study of the accuracy of CyberKnife spinal radiosurgery. Neurosurgery. 2004;55(5):1138-49.

41. Coste-Maniere E, Olender D, Kilby W, Schulz R. Robotic whole body stereotactic radiosurgery: clinical advantages of the CyberKnife® integrated

system. The International Journal of Medical Robotics and Computer Assisted Surgery. 2005;1(2):28-39.

42. Antypas C, Pantelis E. Performance evaluation of a CyberKnife® G4 image-guided robotic stereotactic radiosurgery system. Physics in Medicine and Biology. 2008;53:4697-718.

43. Mack A, Mack G, Scheib S, Czempiel H, Kreiner H, Lomax N, et al. Quality assurance in stereotactic radiosurgery/radiotherapy according to DIN 6875-1. Stereotactic and Functional Neurosurgery. 2004;82(5-6):235-43.

44. Scheib S, Gianolini S, Lomax N, Mack A. High precision radiosurgery and technical standards. Acta neurochirurgica Supplement. 2004;91:9-23.

45. Mayles W, Lake R, McKenzie A, Macaulay E, Morgan H, Powley S. Physics aspects of quality control in radiotherapy: Inst. of Physics and Engineering in Medicine; 1999.

46. Saur S, Frengen J. GafChromic EBT film dosimetry with flatbed CCD scanner: A novel background correction method and full dose uncertainty analysis. Medical Physics. 2008;35:3094-101.

47. Richley L, John A, Coomber H, Fletcher S. Evaluation and optimization of the new EBT2 radiochromic film dosimetry system for patient dose verification in radiotherapy. Physics in Medicine and Biology. 2010;55:2601-17.

48. James H, Beavis A, Budgell G, Clark C, Convery D, Mott J, et al. Guidance for the Clinical Implementation of Intensity Modulated Radiation Therapy: Inst. of Physics and Engineering in Medicine.2008.

49. Low D, Harms W, Mutic S, Purdy J. A technique for the quantitative evaluation of dose distributions. Medical Physics. 1998;25:656-61.

50. Soisson E, Hardcastle N, Tomé W. Quality assurance of an image guided intracranial stereotactic positioning system for radiosurgery treatment with helical tomotherapy. Journal of Neuro-Oncology. 2010;98(2):277-85.

51. Lynch B, Kozelka J, Ranade M, Li J, Simon W, Dempsey J. Important considerations for radiochromic film dosimetry with flatbed CCD scanners and EBT gafchromic film. Medical Physics. 2006;33:4551-6.

52. Zeidan O, Stephenson S, Meeks S, Wagner T, Willoughby T, Kupelian P, et al. Characterization and use of EBT radiochromic film for IMRT dose verification. Medical Physics. 2006;33:4064-72.

53. Hartmann B, Martisiková M, Jäkel O. Homogeneity of Gafchromic EBT2 film. Medical Physics. 2010;37(4):1753-6.

54. Devic S, Wang Y, Tomic N, Podgorsak E. Sensitivity of linear CCD array based film scanners used for film dosimetry. Medical Physics. 2006;33:3993-6.

55. Shaw E, Kline R, Gillin M, Souhami L, Hirschfeld A, Dinapoli R, et al. Radiation Therapy Oncology Group: radiosurgery quality assurance guidelines. International Journal of Radiation Oncology* Biology* Physics. 1993;27(5):1231-9.

56. Knöös T, Kristensen I, Nilsson P. Volumetric and dosimetric evaluation of radiation treatment plans: radiation conformity index. International Journal of Radiation Oncology* Biology* Physics. 1998;42(5):1169-76.

57. Paddick I. A simple scoring ratio to index the conformity of radiosurgical treatment plans. Journal of Neurosurgery. 2000;93(Supplement 3):219-22.

58. Korytko T, Radivoyevitch T, Colussi V, Wessels B, Pillai K, Maciunas R. 12 Gy gamma knife radiosurgical volume is a predictor for radiation necrosis in non-AVM intracranial tumors. International Journal of Radiation Oncology* Biology* Physics. 2006;64(2):419-24.

59. Lis c ak R, Novotný Jr J, UrgoSik D, Vladyka V, Simonová G. Statistical analysis of risk factors after Gamma Knife radiosurgery of acoustic neurinomas. Radiosurgery: Karger; 1999. p. 205-13.

60. Paddick I, Lippitz B. A simple dose gradient measurement tool to complement the conformity index. Journal of Neurosurgery (Suppl). 2006;105(7):194-201.

61. Wowra B, Muacevic A, Tonn J. Quality of radiosurgery for single brain metastases with respect to treatment technology: a matched-pair analysis. Journal of Neuro-Oncology. 2009;94(1):69-77.

62. Kased N, Binder D, McDermott M, Nakamura J, Huang K, Berger M, et al. Gamma knife radiosurgery for brain metastases from primary breast cancer. International journal of Radiation Oncology* Biology* Physics. 2009;75(4):1132-40.

63. Haselsberger K, Maier T, Dominikus K, Holl E, Kurschel S, Ofner-Kopeinig P, et al. Staged gamma knife radiosurgery for large critically located benign meningiomas: evaluation of a series comprising 20 patients. Journal of Neurology, Neurosurgery & Psychiatry. 2009;80(10):1172-5.

64. Kano H, Niranjan A, Mongia S, Kondziolka D, Flickinger J, Lunsford L. The role of stereotactic radiosurgery for intracranial hemangioblastomas. Neurosurgery. 2008;63(3):443-51.

65. Lasak J, Klish D, Kryzer T, Hearn C, Gorecki J, Rine G. Gamma knife radiosurgery for vestibular schwannoma: early hearing outcomes and evaluation of the cochlear dose. Otology & Neurotology. 2008;29(8):1179-86.

66. Hara W, Tran P, Li G, Su Z, Puataweepong P, Adler Jr J, et al. Cyberknife for brain metastases of malignant melanoma and renal cell carcinoma. Neurosurgery. 2009;64(2):A26-A32.

67. Gwak H, Yoo H, Youn S, Lee D, Kim M, Rhee C. Radiosurgery for Recurrent Brain Metastases after Whole-Brain Radiotherapy: Factors Affecting Radiation-Induced Neurological Dysfunction. Journal of Korean Neurosurgical Society. 2009;45(5):275-83.

68. Ju D, Lin J, Lin M, Lee L, Tseng H, Wei C, et al. Hypofractionated CyberKnife stereotactic radiosurgery for acoustic neuromas with and without association to neurofibromatosis Type 2. Acta Neurochirurgica Supplementum. 2008;101:169-73.

69. Nedzi L, Kooy H, Alexander III E, Gelman R, Loeffler J. Variables associated with the development of complications from radiosurgery of intracranial tumors. International Journal of Radiation Oncology* Biology* Physics. 1991;21(3):591-9.

70. Valery C, Cornu P, Noel G, Duyme M, Boisserie G, Sakka L, et al. Predictive factors of radiation necrosis after radiosurgery for cerebral metastases. Stereotactic and Functional Neurosurgery. 2003;81(1):115-9.

71. Nakamura J, Verhey L, Smith V, Petti P, Lamborn K, Larson D, et al. Dose conformity of gamma knife radiosurgery and risk factors for complications. International Journal of Radiation Oncology* Biology* Physics. 2001;51(5):1313-9.

72. Luxton G, Jozsef G. Single isocenter treatment planning for homogeneous dose delivery to nonspherical targets in multiarc linear accelerator radiosurgery. International Journal of Radiation Oncology* Biology* Physics. 1995;31(3):635-43.

73. Ma L, Xia P, Verhey L, Boyer A. A dosimetric comparison of fan-beam intensity modulated radiotherapy with gamma knife stereotactic radiosurgery for treating intermediate intracranial lesions* 1. International Journal of Radiation Oncology* Biology* Physics. 1999;45(5):1325-30.

74. Dunn OJ. Multiple comparisons among means. Journal of the American Statistical Association. 1961;56(293):52-64.

75. Fuller DB, Naitoh J, Lee C, Hardy S, Jin H. Virtual HDRSM CyberKnife treatment for localized prostatic carcinoma: dosimetry comparison with HDR brachytherapy and preliminary clinical observations. International Journal of Radiation Oncology* Biology* Physics. 2008;70(5):1588-97.

76. Dhople AA, Adams JR, Maggio WW, Naqvi SA, Regine WF, Kwok Y. Long-term outcomes of Gamma Knife radiosurgery for classic trigeminal neuralgia: implications of treatment and critical review of the literature. Journal of Neurosurgery. 2009;111(2):351-8.

77. Sahgal A, Ma L, Gibbs I, Gerszten PC, Ryu S, Soltys S, et al. Spinal cord tolerance for stereotactic body radiotherapy. International Journal of Radiation Oncology* Biology* Physics. 2010;77(2):548-53.

78. Medin PM, Boike TP. Spinal Cord Tolerance in the Age of Spinal Radiosurgery: Lessons from Preclinical Studies. International Journal of Radiation Oncology* Biology* Physics. 2011;79(5):1302-9.

79. Mayo C, Yorke E, Merchant TE. Radiation associated brainstem injury. International Journal of Radiation Oncology* Biology* Physics. 2010;76(3):S36-S41.

80. Yu C, Jozsef G, Apuzzo MLJ, Petrovich Z. Dosimetric comparison of CyberKnife with other radiosurgical modalities for an ellipsoidal target. Neurosurgery. 2003;53(5):1155-63.

81. Ma L, Sahgal A, Descovich M, Cho YB, Chuang C, Huang K, et al. Equivalence in dose fall-off for isocentric and nonisocentric intracranial treatment modalities and its impact on dose fractionation schemes. International Journal of Radiation Oncology* Biology* Physics. 2010;76(3):943-8.

82. Perks JR, St George EJ, El Hamri K, Blackburn P, Plowman PN. Stereotactic radiosurgery XVI: Isodosimetric comparison of photon stereotactic radiosurgery techniques (gamma knife vs. micromultileaf collimator linear accelerator) for acoustic neuroma - and potential clinical importance. International Journal of Radiation Oncology* Biology* Physics. 2003;57(5):1450-9.

83. Ma L, Petti P, Wang B, Descovich M, Chuang C, Barani IJ, et al. Apparatus dependence of normal brain tissue dose in stereotactic radiosurgery for multiple brain metastases. Journal of Neurosurgery. 2011;15(4):1580-4.

84. Kairn T, Aland T, Kenny J. Local heterogeneities in early batches of EBT2 film: a suggested solution. Physics in Medicine and Biology. 2010;55:L37-L42.

85. Xiao Y, Papiez L, Paulus R, Timmerman R, Straube WL, Bosch WR, et al. Dosimetric evaluation of heterogeneity corrections for RTOG 0236: stereotactic body radiotherapy of inoperable stage I-II non-small-cell lung cancer. International Journal of Radiation Oncology* Biology* Physics. 2009;73(4):1235-42.

86. Wagner TH, Bova FJ, Friedman WA, Buatti JM, Bouchet LG, Meeks SL. A simple and reliable index for scoring rival stereotactic radiosurgery plans. International Journal of Radiation Oncology* Biology* Physics. 2003;57(4):1141-9.

87. Murphy MJ, Lin PS, Ozhasoglu C. Intra-fraction dose delivery timing during stereotactic radiotherapy can influence the radiobiological effect. Medical Physics. 2007;34(2):481-4.

88. Hopewell JW, Millar WT, Lindquist C. Biologically Effective Dose - Does it matter? Should we care? (Oral presentation) British Radiosugical Society 2nd Annual Meeting. 2011.

Appendix – Outputs related to this thesis

Presentations

Martin A, Cowley I, Plowman P. Choosing a value for the prescription isodose: how this affects external dose gradient in CyberKnife planning of intracranial lesions. *Oral presentation*, CyberKnife Robotic Radiosurgery Summit, San Francisco, February 2011.

Martin A, Cowley I, Hiscoke K, Plowman P. Differences in reported target volumes: are different planning systems truly comparable ? *Oral presentation*, The Radiosurgery Society SRS/SBRT Scientific Meeting, San Diego, February 2012.

Publications

Martin A, Gaya A. Stereotactic body radiotherapy: a review. *Clinical Oncology* 2010;22(3)157-172.

Martin A.G.R, Cowley I.R, Taylor B.A et al. (Stereotactic) radiosurgery XIX: spinal radiosurgery – two year experience in a UK centre. *British Journal of Neurosurgery* 2012;26(1)53-58.

Papers in preparation

Martin A, Cowley I, Plowman P. Steep external dose gradient is at the expense of target dose inhomogeneity in CyberKnife planning of solitary intracranial lesions.

Choosing a Value for the Prescription Isodose: How this Affects the External Dose Gradient in CyberKnife Planning of Intracranial Lesions

Alexander Martin, Ian Cowley, Nicholas Plowman

Objectives: In the treatment of intracranial lesions, common CyberKnife practice is to use a prescription isodose of around 65-80%. This differs from, for example, Gamma Knife radiosurgery where a prescription isodose of around 50% is often used. Further, it has been shown with the Gamma Knife system that the dose gradient outside the PTV is often steepest when using an even lower prescription isodose of around 40%. The objective of this study was to explore whether the steepness of dose fall-off outside the PTV is affected by the choice of prescription isodose when using CyberKnife, and if so, to describe this relationship further.

Methods: A spherical "virtual" target was created in a central location within the brain CT of a patient selected at random. Multiple treatment plans were generated using Multiplan v.3.5.1. Planning variables were manipulated to vary the prescription isodose of the treatment plan across the range 50-80%. For each plan the Gradient Index (GI) was calculated. For a plan prescribed to the X% isodose, GI = (volume contained within the X/2% isodose)/(volume contained within the X% isodose). All plans were setup to deliver a single fraction of 18 Gy to the target. Plans were required to be "clinically acceptable", meeting the following criteria: overall treatment time </= 60 minutes (where estimated treatment time = (Number of beams/6) + (Number of monitor units/800)); PTV coverage by the prescription isodose >95%; new conformality index (nCI) required to be within 0.03 of the best achievable nCI for the target. Planning was performed using both Simplex optimization with 3 fixed collimators, and Sequential optimization with the Iris collimator. The process was carried out on spherical targets of 3 different diameters: 15 mm, 30 mm and 50 mm. It was then repeated with five real intracranial lesions previously treated at this centre.

Results: For the 15 mm spherical target, a positive relationship was observed between prescription isodose and GI over the isodose range of 50-80%. Thus, as the prescription isodose was lowered, the dose gradient outside the PTV became steeper. For the two larger spheres, the dose fall-off was again shallowest with the 80% isodose, but there was little difference in GI scores across the 50-70% prescription isodose range. The median PTV of the five treated lesions was 5.79 cm3 (2.25-23.16 cm3). For each of the lesions, a positive relationship was once again observed between prescription isodose and GI over the isodose range of 56-80%.

Conclusions: In CyberKnife radiosurgery for intracranial targets, the steepness of dose fall-off outside the PTV is an important treatment parameter, and one which is affected by the choice of prescription isodose. Optimizing dose gradient requires the use of lower prescription isodoses than are commonly seen reported in the literature. An inevitable consequence of this strategy would be greater inhomogeneity of dose within the PTV.

Differences in Reported Target Volumes: Are Different Planning Systems Truly Comparable?

Alexander Martin, Ian Cowley, Kelvin Hiscoke, Nicholas Plowman

Presented by: Alexander Martin, BM, BCh

Objectives: Over the last twenty years there have been a number of published studies comparing dosimetric parameters, such as conformality and external dose gradient, in plans produced by different radiosurgery systems. Such studies continue to be important as new systems become available, and existing systems undergo significant upgrades. These comparisons are most informative when identical targets are planned by each system. Most modern systems are now capable of importing and exporting DICOM radiotherapy structure sets, and therefore dosimetric comparison using identical targets is theoretically possible. The purpose of this study was to compare the calculated volume of a series of imported contour sets across different radiosurgery systems.

Methods: CT and MRI scans of ten patients with intracranial solid tumours treated at this centre were selected at random. Five patients had been treated with Gamma Knife, and five with CyberKnife. Imaging from all ten patients was imported into MultiPlan v3.5 and the original target was contoured in each case. The calculated volume for each target was recorded. The primary CT dataset was then exported together with the target contour DICOM radiotherapy structure set. These were imported for analysis into the following software: MultiPlan v4.5, GammaPlan v10.1, Eclipse v8.9 and DICOMan (a third party DICOM visualisation package). The calculated volume for each target was recorded in each planning system.

Results: The calculated volume of all ten contour sets was different in each of the different planning systems and the DICOM visualisation package. The differences across all systems ranged from 6 – 20 % for the ten targets (median 10.6 %). A smaller percentage range in calculated volumes was generally seen with the larger targets. MultiPlan v3.5 reported the largest volumes for each of the ten targets, with the newer software upgrade (v4.5) reporting the second or third largest value in each case. GammaPlan v10.1 reported the smallest volume in nine out of ten cases.

Conclusions: The reported volume of a contour set can vary by as much as 20 % across different radiosurgery planning systems. This is because each system has a different method of determining whether or not each CT voxel is included within a contoured line. Work is currently underway to establish which of the above systems reports volume with the greatest accuracy. These findings have implications when comparing radiosurgical parameters from plans produced by different systems. For example, for a given external dose gradient the V12 is likely to be larger in systems which perceive the target volume to be larger. Also, conformality indices are usually better in the case of larger targets. Future work will analyse dose distributions to establish how the variation in reported volumes affects DVH-reported doses to organs at risk.

Clinical Oncology xxx (2010) 1–16

Contents lists available at ScienceDirect

Clinical Oncology

journal homepage: www.elsevier.com/locate/clon

Overview

Stereotactic Body Radiotherapy: A Review

A. Martin *, A. Gaya †

* CyberKnife Centre, The Harley Street Clinic, London, UK
† Guy's and St. Thomas' NHS Foundation Trust, London, UK

Received 3 September 2009; received in revised form 2 November 2009; accepted 30 November 2009

Abstract

Stereotactic body radiotherapy (SBRT) combines the challenge of meeting the stringent dosimetric requirements of stereotactic radiosurgery with that of accounting for the physiological movement of tumour and normal tissue. Here we present an overview of the history and development of SBRT and discuss the radiobiological rationale upon which it is based. The published results of SBRT for lung, liver, pancreas, kidney, prostate and spinal lesions are reviewed and summarised. The current evidence base is appraised and important ongoing trials are identified.

Key words: Cyberknife; radiosurgery; stereotactic body radiation therapy; stereotactic body radiotherapy

Statement of Search Strategies Used and Sources of Information

A search for the published results of stereotactic body radiotherapy for lung, liver, pancreas, kidney, prostate and spinal lesions was carried out using Ovid Online via the Athens website. Medline and Embase databases were selected, and the following terms were searched for, in all fields: 'radiosurgery', 'stereotactic radiosurgery', 'stereotactic body radiotherapy', 'stereotactic body radiation therapy' and 'cyberknife'. Appropriate publications were selected from the lists generated, and additional papers found through a manual search of the references contained in these publications. Searches were carried out in April 2009. The review also includes certain additional papers published after April 2009 that were considered to be especially pertinent to this subject, and some information obtained from oral presentations at the 2nd European Workshop on Stereotactic Radiation Therapy and Whole Body Radiosurgery, Berlin, 27–28 March 2009. Information on the history and radiobiology of stereotactic body radiotherapy was obtained from the above publications and further internet searching. Information on the stereotactic delivery systems was obtained from the manufacturers' websites, and through direct communication with the manufacturers.

Introduction

Stereotactic body radiotherapy (SBRT) refers to the precise irradiation of an image-defined extracranial lesion using a small number (one to five) of high-dose fractions. It has developed from intracranial single-fraction stereotactic radiotherapy (also known as radiosurgery), which is conceptually different from conventionally fractionated radiotherapy (CFR). In its fractionated form, SBRT shares characteristics of both radiosurgery and CFR. The high doses per fraction strive towards an ablative tumour effect, whereas the use of modest fractionation implies the need to allow some normal tissue recovery.

The safe delivery of very large doses per fraction requires effective patient immobilisation, precise target localisation (which may involve fusion of different imaging modalities), sophisticated planning software, accurate treatment delivery and the ability to produce a steep isodose gradient outside the target volume. In addition, extracranial lesions pose further challenges to treatment delivery due to inter- and intrafraction tumour and critical organ motion. Until

Author for correspondence: A. Martin, CyberKnife Centre, The Harley Street Clinic, 81 Harley Street, London W1G 8PP, UK. Tel: +44-207-034-8588.
E-mail address: agrmartin@hotmail.co.uk (A. Martin).

0936-6555/$36.00
doi:10.1016/j.clon.2009.12.003

recently this has limited the ability to deliver stereotactic radiotherapy to targets outside the brain. However, advances in image guidance have allowed treatment systems to account for such motion and, consequently, the use of SBRT is increasing.

History

Stereotactic surgery was first described by Horsley and Clarke in 1906. They developed a method of locating deep-seated brain lesions by assigning coordinates in three planes to neuroanatomical structures, based on cranial landmarks [1]. In 1947, Spiegel *et al.* [2] introduced frame-based stereotaxy using a plaster head cap known as a stereoencephalatome, and a three-dimensional coordinate system relative to this.

Lars Leksell, a Swedish neurosurgeon, was the first person to marry the two developing fields of stereotaxy and radiation therapy, and introduced the term 'radiosurgery' in 1951 [3]. He used a rigid metal stereotactic head frame fixed to the skull. Small intracranial targets were localised relative to the frame and radiation was delivered in a single high-dose fraction. The technique initially used 250 kV X-rays, but in 1967 the first Gamma Knife prototype was developed, using 179 cobalt-60 sources focused on the target. Since then, the Gamma Knife has become widely used for stereotactic radiosurgery, with sub-millimetre total system accuracy [4]. However, Gamma Knife stereotactic treatment is largely limited to intracranial targets.

The 1980s saw the adaptation of linear accelerators (linacs) for intracranial stereotactic delivery, again using rigid stereotactic head frames, and specialist dosimetry software, e.g. X-Knife (Radionics, Boston, MA, USA). In 1995, Hamilton *et al.* [5] proposed a method of delivering linac-based stereotactic radiotherapy to spinal lesions using a prototype rigid 'extracranial stereotactic frame' and associated three-dimensional coordinate system. Immobilisation was achieved by transcutaneous frame fixation to spinous processes superior and inferior to the target. They reported an overall treatment accuracy of 2 mm, but the technique was time-consuming, cumbersome and limited to the delivery of single fractions. Also, as with intracranial immobilisation methods, this approach relied upon a fixed relationship between target and bony anatomy.

Around the same time, Lax *et al.* [6] developed a stereotactic body frame, which, together with a vacuum bag, immobilised the patient from head to mid-thigh. They found the set-up reproducibility for liver and lung lesions to be within 5–8 mm for 90% of the patients. Many stereotactic radiotherapy systems today use a similar set-up with body frame immobilisation. However, for most extracranial sites the position of the tumour does not enjoy a fixed relationship relative to the external body contour, and can move both between and during each fraction of radiotherapy. An external body frame alone is therefore not sufficient to ensure accurate delivery of radiation to the target. Lax *et al.* [6] showed that diaphragmatic movements could be reduced to 5–10 mm by applying a pressure on the abdomen, and some centres have developed corsets to limit diaphragmatic movement. However, the safe delivery of large fractions of radiotherapy also requires sophisticated image guidance.

Image guidance in radiotherapy became a realistic concept with the development of the electronic portal imaging device and software to aid quantitative evaluation of patient set-up, thus allowing correction of translational errors. The next step was moving from 'off-line' to 'on-line' image guidance (i.e. adjusting the patient's position before each fraction on the basis of imaging). Accurate identification of the tumour position has improved with the use of inserted metal fiducial markers with planar images, or alternatively with the development of volumetric image guidance (e.g. cone beam computed tomography or in-room computed tomography on rails). More recently, improved software together with more sophisticated treatment couches have meant that correcting for rotational set-up errors is now possible. Finally, intrafraction image guidance is now available and is a key component of some of the stereotactic treatment systems described below.

Stereotactic systems that use planar imaging have great flexibility with respect to taking multiple intrafraction images, but largely rely on implanted fiducials. Percutaneous fiducial insertion can be technically difficult, especially in the upper abdomen, where it may be necessary to pass through other organs to reach the target lesion. In the lung, there have been concerns about the complication rates observed with percutaneous fiducial implantation. A 25–40% incidence of pneumothorax requiring drainage has been reported [7,8]. However insertion techniques are improving. In a recent series described below, Van der Voort van Zyp *et al.* [9] used either a percutaneous or a vascular approach, depending on the perceived risk of pneumothorax. Only four of 70 patients developed pneumothorax, and in only one of these cases was a chest drain necessary. 'Xsight Lung' is a feature of the CyberKnife SBRT system (see below), which allows the tracking of certain peripheral lung tumours without the need for implanted fiducials.

Fractionation and Radiobiology

In CFR, the tumour volume is irradiated together with a margin to account for tumour and organ motion, and inaccuracies of planning, set-up and delivery. The total dose is limited by the tolerance of normal tissue within, or close to, the planning target volume (PTV). The therapeutic benefit achieved with dose fractionation has been recognised for over 100 years. Conventional fractionation has emerged as a result of these early clinical observations, and subsequent changes have been driven largely by clinical outcomes. The development of radiobiological concepts, such as the linear quadratic model [10] and Withers' '4 Rs' of radiotherapy [11], has led to further understanding of the tissue effects of fractionation.

By contrast, radiosurgery exploits the potent radiobiological effect of large single doses of radiation, which transcends the considerations proposed by Withers. The aim is to

Please cite this article in press as: Martin A, Gaya A, Stereotactic Body Radiotherapy: A Review, Clinical Oncology (2010), doi:10.1016/j.clon.2009.12.003

ablate all tissue within the PTV, and the small margins used ensure that minimal normal tissue is destroyed. Considerable dose inhomogeneity within the target volume is standard practice, due to the internal dose gradient achieved by using a low prescription isodose (commonly 40–60% with Gamma Knife radiosurgery). There is some evidence to suggest that, rather than being a problem, carefully planned target dose inhomogeneity may enhance the tumoricidal effect [12].

Fractionated SBRT sits somewhere between the extremes of CFR and radiosurgery. Large doses per fraction are used and a moderate internal dose gradient achieved, with a typical prescription isodose of 60–80%. Unlike intracranial radiosurgery, inter- and intrafraction movement of tumour and organs at risk is a big problem. This increases the risk of irradiating normal tissue (and missing the tumour) during treatment. Also, the overwhelming clinical experience of treating extracranial tumours is with conventional fractionation. For these reasons, moving away from fractionation completely is a big step for many extracranial sites. The linear quadratic model and its derivatives can help clinicians to predict tissue response to altered fractionation regimens. However, there has been concern that it does not accurately predict tumour cell response at the higher doses per fraction seen with stereotactic treatment [13]. It is not clear to what extent modest fractionation (two to five fractions) differs from a single fraction with respect to tumour response and normal tissue effects.

Unsurprisingly, therefore, there has been a large variation in dose and fractionation across SBRT series published to date. Although some SBRT centres adopt a 'single large fraction' strategy for many patients, other centres would prefer to fractionate in similar cases. Current regimens have in many cases been derived empirically, often the result of cautious dose escalation, as illustrated by phase I trials in non-small cell lung cancer (NSCLC) [14], liver metastases [15] and pancreatic carcinoma [16].

Overview of Stereotactic Body Radiotherapy Systems

A number of modern linacs with on-board imaging capabilities meet the basic image guidance requirements for delivering SBRT, e.g. Varian Trilogy (Varian Medical Systems, Palo Alto, CA, USA) and Elekta Synergy (Elekta, Stockholm, Sweden). A micro multileaf collimator can be added to produce the required degree of conformality for stereotactic plans.

More recently there has been the introduction of linacs fully adapted as integrated stereotactic delivery systems. Novalis TX has a Varian Trilogy linac base with micro (2.5 mm) multileaf collimator. Other features include the BrainLAB Other features include the BrainLAB "ExacTrac X-ray 6D" system providing near real-time image guidance with six degrees of freedom, a corresponding robotic treatment couch, and associated software (BrainLAB, Munich, Germany). Elekta Axesse is a similar integrated system.

The TomoTherapy Hi-Art System (TomoTherapy, Madison, WI, USA) has a ring gantry as used in diagnostic computed tomography scanners and delivers helical intensity-modulated radiotherapy (IMRT) via thousands of small beamlets. Couch movement is continuous during radiation delivery. The system has on-board image guidance with megavoltage computed tomography.

CyberKnife (Accuray, Sunnyvale, CA, USA) is an image-guided robotic radiosurgery system. A compact 6 MV X-band linac is mounted on a six-joint robotic arm. This provides flexibility in beam pattern generation, allowing the system to produce very conformal, non-isocentric plans (Fig. 1). As with Novalis TX, a robotic couch with six degrees of freedom and near real-time kV image guidance also feature.

Lung

Lung SBRT is additionally challenging because of the problems of accounting for intrafraction target movement with breathing. Most of the published data come from centres using gantry-based linacs with vacuum and/or frame body immobilisation, and diaphragmatic pressure to reduce breathing movement.

Four-dimensional computed tomography planning allows the construction of a volume that takes into account the tumour position at all phases of the respiratory cycle. It has been shown to increase accuracy and reduce the volume irradiated in conformal radiotherapy, and is now being used in some lung SBRT centres.

Respiratory gating methods, such as active breathing control (used in some series), have sought to reduce the volume of tissue irradiated by requiring a smaller clinical target volume–PTV margin. The latest gantry-based stereotactic systems (e.g. Novalis TX) allow respiratory gating using infrared chest wall tracking and intrafraction X-ray imaging. CyberKnife uses a similar respiratory tracking system (Synchrony RTS). However, here, the predictive model that anticipates tumour movement with breathing allows the robotic arm to move the beam accordingly during radiation delivery. This obviates the need for respiratory gating.

Primary Non-small Cell Lung Cancer

Surgery remains the standard of care for early stage NSCLC. A 5-year survival rate of 65% has been reported for pathological stage I patients [17], and a recent analysis of 975 patients (85% stage I) revealed a 5-year local control of 78% [18].

However, the preferred procedure (lobectomy) results in a significant loss of functional pulmonary reserve and is associated with operative morbidity and mortality. Also, a large number of surgically resectable patients are medically inoperable (mainly due to cardiovascular or respiratory co-morbidity). CFR has traditionally been the standard alternative to surgery for these patients, but the total dose is limited by lung tolerance for peripheral tumours, and

Please cite this article in press as: Martin A, Gaya A, Stereotactic Body Radiotherapy: A Review, Clinical Oncology (2010), doi:10.1016/j.clon.2009.12.003

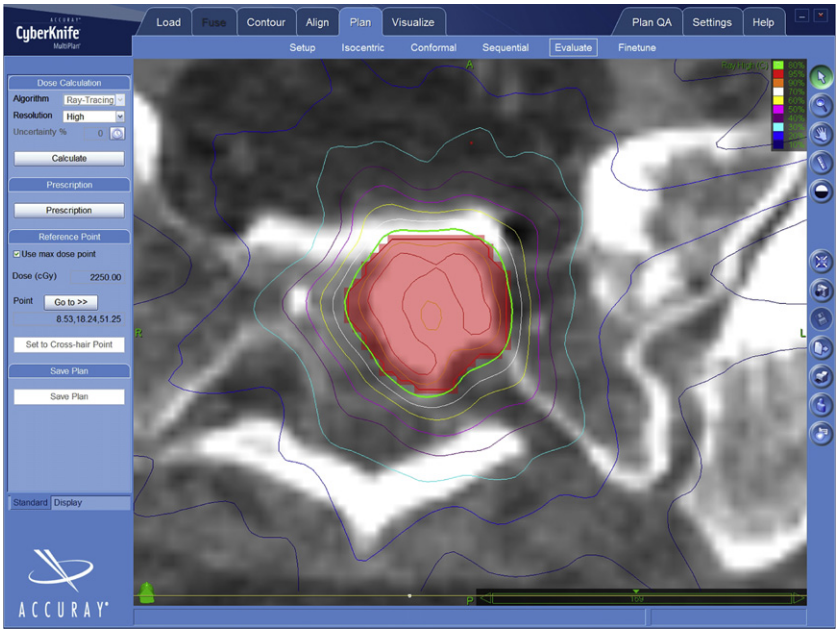

Fig. 1. Axial slice from the CyberKnife plan of a sacral metastasis. The planning target volume is shown in red overlay. The treatment is prescribed to the 80% isodose (green line). The other isodose lines shown are 95% (red), 90% (orange), 70% (white), 60% (yellow), 50% (pink), 40% (purple), 30% (light blue), 20% (blue) and 10% (dark blue).

mediastinal tolerance for central tumours. Published data have shown 5-year survival after CFR for stage I NSCLC to be in the region of 15–30% and, importantly, 5-year disease-specific survival little better at 25–30%. There does, however, seem to be a dose–response relationship [19,20]. Stereotactic radiotherapy allows safe treatment with a higher biological equivalent dose (BED) than is possible with CFR. This has led to improved local control rates.

Several important published series of lung SBRT are summarised in Table 1. The largest is a Japanese retrospective review of 257 patients from 14 institutions [21]. Patients had resectable stage I disease, but were either medically inoperable or declined surgery. There was considerable variation in immobilisation and respiratory motion management protocols, and also heterogeneity of dose and fractionation (30–84 Gy in 1–14 fractions). Five-year actuarial local control rates were 84% for patients receiving a BED of 100 Gy or more (based on assumed tumour α/β of 10) and 37% for those receiving less than 100 Gy. This dose–response relationship corroborates that seen with CFR discussed earlier. There was no difference in the recurrence rates of squamous cell carcinoma and adenocarcinoma. Five-year overall survival for medically operable patients receiving the higher dose range was 71%. This was achieved with relatively low rates of radiation toxicity.

JCOG 0403 is an ongoing Japanese multi-institutional phase II trial for medically operable or inoperable stage IA disease. On the basis of results seen in Japanese series, patients receive 4×12 Gy fractions (BED 106 Gy). The results are awaited.

There have also been a number of published series of gantry-based lung SBRT from European centres [22–26]. Two large retrospective series are summarised in Table 1, both reporting 88% local control at around 3 years [23,24]. More recently, Baumann et al. have published the results of a phase II trial of 57 non-central stage I tumours treated to a dose of 45 Gy in three fractions [26]. The tumours were small (70% T1, maximum tumour volume 51 cm^3), but the results are nevertheless very impressive. Three-year local control and overall survival were 92 and 60%, respectively. Twenty-eight per cent of patients experienced grade 3 toxicity, and there was one case of grade 4 dyspnoea in a patient who received SBRT to both lungs for metachronous primary tumours. However, there was no evidence of a decrease in FEV1 or subjective worsening of breathing capacity [26].

In the USA, McGarry et al. [14] carried out a phase I dose-escalation study with 47 medically inoperable stage I patients, with a starting dose of 3×8 Gy. The maximum tolerated dose was not reached for patients with T1 tumours, but for T2 tumours >5 cm it was reached at 66 Gy in three fractions. Local control was 79% with a median follow-up of 15 months, but nine of the 10 local failures occurred at doses of ≤ 16 Gy per fraction [14].

A subsequent phase II study from the same institution enrolled 70 inoperable stage I patients with peripheral or central (within 2 cm of the proximal bronchial tree) tumours, giving 60–66 Gy in three fractions. Two-year local control and overall survival were estimated at 95 and 54%, respectively. However, eight patients developed grade 3–4 pulmonary or skin toxicity, and there were six possible cases of grade 5 pulmonary toxicity. The risk of severe lung toxicity was 11 times higher for central tumours compared with peripheral tumours [27].

On the basis of these results, centrally located tumours, as defined above, were excluded from two subsequent

Please cite this article in press as: Martin A, Gaya A, Stereotactic Body Radiotherapy: A Review, Clinical Oncology (2010), doi:10.1016/j.clon.2009.12.003

Table 1
Selected published series of stereotactic body radiotherapy for primary non-small cell lung cancer

Reference	Type of publication	Number of patients	Accounting for tumour movement	Location	Dose	Follow-up	Local control	Overall survival	Grade ≥3 radiation toxicity
[21]	Multi-centre retrospective series	257	Varied (breath hold; respiratory gating; slow computed tomography scan)	Peripheral or central	30–84 Gy/1–14 fractions	Median 38 months (2–128)	5 year 84% for BED ≥ 100 Gy	5 year 47% (71% for medically operable, and BED ≥ 100 Gy)	5.4% lung 1% oesophagitis 1.2% dermatitis
[23]	Multi-centre retrospective series	138	Abdominal pressure if needed	Peripheral (mainly) or central	30-48 Gy/2–4 fractions	Median 33 months	88% at median 33 months	3 year 55%	10%
[26]	Multi-centre phase II	57	Abdominal pressure if needed	Peripheral	45 Gy/3 fractions	Median 35 months	3 year 92%	3 year 60%	26% grade 3 2% grade 4
[24]	Single centre retrospective series	68	Planning target volume margins guided by computed tomography assessment	Peripheral or central	24–40 Gy/3–5 fractions	Mean 17 months	3 year 88%	3 year 53%	6% pneumonitis 3% rib fracture
[14]	Single centre phase I, dose escalation	47	Abdominal pressure	Peripheral or central	24 Gy/3 fractions escalating to 72 Gy/3 fractions	Median 15 months	79% at median 15 months	–	11% lung 2% pericardial 2% dermatitis
[27]	Single centre phase II	70	Abdominal pressure	Peripheral or central	60–66 Gy/3 fractions	Median 17.5 months	2 year 95%	2 year 54%	20% (includes 6 possible grade 5 cases)
[28]	Single centre retrospective series	27	Four-dimensional computed tomography planning	Central or superior	40–50 Gy/4 fractions	Median 17 months	100% at median 17 months (50 Gy) or 57% (4 Gy)	–	11% grade 2–3 pneumonitis/ chest wall pain
[30] *	Single centre retrospective series	59	Synchrony respiratory tracking system	Peripheral or central	15–67.5 Gy/1–5 fractions	1–33 months	90% free from persistent or recurrent disease	86%	0% grade 4/5 toxicity 7% grade 1–3 pneumonitis
[9] *	Single centre retrospective series	70	Synchrony respiratory tracking system	Peripheral	45 or 60 Gy/3 fractions	Median 15 months	2 year 96% (60 Gy) or 78% (45 Gy)	2 year 62%	10% late toxicity 4% acute toxicity

BED, biological equivalent dose.
* All studies used a gantry-based linear accelerator except (CyberKnife).

phase II trials. The RTOG 0236 trial recruited medically inoperable patients with T1-3 N0 disease (and <5 cm diameter), treating with 60 Gy in three fractions. It closed in October 2006 and full results are awaited. The RTOG 0618 trial is currently underway, treating operable T1-3 N0 patients with the same dose and fractionation.

For central tumours, the maximum tolerated dose is still under investigation. Chang *et al.* [28] treated a series of 27 centrally or superiorly located lesions with a slightly more modest dose of 40–50 Gy in four fractions. At a median of 17 months, there was no local recurrence seen in the 20 patients receiving 50 Gy (BED 112.5 Gy). There were three cases of grade 2–3 skin/chest wall toxicity and one brachial plexopathy, related to a large volume of plexus receiving 40 Gy. However, there was no observed grade ≥3 pulmonary or oesophageal toxicity. RTOG 0813 is a phase I/II dose-escalation trial underway for central stage I tumours in medically inoperable patients.

There have been a number of published series of primary lung SBRT using CyberKnife [8,9,29,30]. Brown *et al.* [30] treated 59 stage I patients with peripheral tumours. Doses ranged from 15 to 67.5 Gy in one to five fractions. With follow-up ranging from 1 to 33 months, only 10% of patients had persistent or recurrent disease, and overall survival was 86%.

More recently, van der Voort van Zyp *et al.* [9] have published the results of 70 peripheral stage I tumours treated with either 45 or 60 Gy in three fractions. The estimated 2-year local control rate was 96% for the 59 patients treated with 60 Gy, and 78% for those receiving 45 Gy. Two-year overall survival was 62% for the whole group. The incidence of grade 3 late toxicity was 10%.

A specialised 'body Gamma Knife' system has been developed in China, consisting of 30 cobalt-60 sources arranged around the patient. The published results look promising [31], but the technology is not yet available outside China.

SBRT seems to be a safe and effective treatment for early stage NSCLC. With respect to local control, achieving a BED > 100 seems to be very important. Unfortunately, there are still no published randomised data comparing SBRT and surgery for operable patients with early stage disease (and no published randomised comparisons of SBRT and CFR for medically inoperable patients). However, phase III trials are now underway. ROSEL is a Dutch multicentre randomised study of gantry-based SBRT vs surgery for peripheral stage IA NSCLC. Respiratory motion is accounted for by either four-dimensional computed tomography or slow computed tomography scanning, and the radiotherapy dose is 60 Gy in three fractions (or five fractions if adjacent to the chest wall or mediastinum). The Lung Cancer STARS Trial is an international randomised trial of SBRT with CyberKnife vs surgery for stage IA or IB patients (maximum diameter <4 cm). Peripheral tumours receive 60 Gy in three fractions, and central tumours 60 Gy in four fractions. It will be some time before these trials produce mature data, and in the meantime surgery remains the standard of care. For the large number of medically inoperable patients, SBRT is emerging as the best treatment option.

Lung Metastases

The term 'oligometastases' refers to a finite small number of metastases confined to a single or limited number of organs [32]. Long-term follow-up of patients after surgical resection of lung and liver metastases has shown that some of these patients are effectively cured after surgery [33,34]. For example, in an analysis of over 5000 patients with lung metastases, survival after complete surgical resection was 36% at 5 years and 22% at 15 years [33]. Thus, in some cancers there seems to be a stable tumour state somewhere between purely localised and widely metastatic. This, together with the results of administering ablative doses of radiation to primary lung tumours (see above), has led to increasing interest in the use of SBRT for oligometastases.

The early data on SBRT for pulmonary metastases emerged as heterogeneous published series including both primary and metastatic lung lesions. Wulf *et al.* [22] published their results of gantry-based SBRT using an Elekta stereotactic body frame. Of the 61 patients, 20 had stage I/II primary NSCLC and 41 had one or two pulmonary metastases. They received 3 × 10–12.5 Gy or a single fraction of 26 Gy for small peripheral lesions. With a median follow-up of 9 months, local recurrence/progression was seen in five of the 51 metastatic lesions. Once again there was evidence of a dose–response relationship, as four of these five lesions had received the lowest dose (3 × 10 Gy). In a subsequent publication from the same centre, at a median follow-up of 18 months they reported recurrence in six of 48 metastatic lesions, giving a crude local control rate of 88%. Symptomatic pneumonitis was seen in 10% of patients, with one case of grade 3 pneumonitis [35]. Similar results have been seen in other such series [36,37].

More recently, several series of purely metastatic lung cases have been reported. Norihisa *et al.* [38] treated 35 patients with one or two lung metastases. The primary site was controlled and there were no other organs involved. The original dose of 48 Gy in four fractions was escalated to 60 Gy in five fractions for 16 patients. Two-year results for overall survival, local control and progression-free survival were 84, 90 and 35%, respectively. Local control was 100% in patients receiving 60 Gy. One case of grade 3 pulmonary toxicity was reported.

Rusthoven *et al.* [39] extended their inclusion criteria to patients with one to three lung metastases, in a multi-institutional phase I/II study. Low burden extrathoracic disease was also permitted. Again, the dose was safely escalated, from 48 to 60 Gy in three fractions. The 2-year actuarial local control rate for their 38 patients was 96%. However, 2-year overall survival was 39%, reflecting the fact that 63% had disease progression outside the treated area(s) at a median of 4 months after treatment.

Brown *et al.* [40] have published their series of 35 patients treated with SBRT using CyberKnife. All 69 metastases were technically resectable, but the patients were medically inoperable. There were no other sites of spread, although up to eight pulmonary lesions were treated for each patient. The prescribed dose varied widely

Please cite this article in press as: Martin A, Gaya A, Stereotactic Body Radiotherapy: A Review, Clinical Oncology (2010), doi:10.1016/j.clon.2009.12.003

from 5 to 60 Gy in one to four fractions, depending on the proximity to organs at risk and the number of sites treated. With a median follow-up of 18 months, 77% of patients were still alive, and 71% had local control in all treated areas. Only one patient developed ≥grade 3 acute toxicity (grade 4 pneumonitis, which settled with treatment). This occurred after retreatment of three lesions within 12 months of previous stereotactic radiotherapy to the same PTVs.

As with primary NSCLC, there are as yet no published randomised data comparing surgery and SBRT for oligometastatic lung disease, but the results seen are encouraging, and the non-invasive approach with low risk of toxicity makes it an attractive option for these patients.

Liver Metastases

As with lung metastases, surgical series of metastectomy for liver metastases have shown a proportion of long-term survivors. In a series of 1000 patients from Memorial Sloan-Kettering Cancer Center with resectable liver-only metastases from colorectal cancer, survival was 37% at 5 years and 22% at 10 years [34]. Surgery remains the gold standard for resectable disease, but many patients are unresectable, either due to the extent of metastatic disease, insufficient functional liver reserve or general medical condition. There has, therefore, been interest in potentially curative, non-surgical options for unresectable patients with oligometastatic disease. Radiofrequency ablation is widely practiced, with local control rates comparable with surgery for lesions less than 3 cm [41], but lesions close to large vessels or the diaphragm are contraindicated for this technique. Transarterial embolisation, chemoembolisation and radioembolisation are further options.

Although whole liver radiation has been used in the past for palliation [42], the radiosensitivity of normal liver tissue has limited the ability to deliver a radical dose to oligometastases in the liver using conventional radiotherapy techniques. Radiation-induced liver disease (RILD) is now well documented as a potentially life-threatening condition. SBRT offers the opportunity to deliver ablative doses, while staying within acceptable liver dose–volume histogram constraints. Table 2 summarises the main published series of SBRT for metastatic liver tumours. Longer term survival data are still awaited in the context of oligometastases.

Patients with liver metastases formed part of Blomgren *et al.*'s [43] early series of SBRT using the Elekta stereotactic body frame. Since then there have been a number of published series and early phase trials in this area. Herfarth *et al.* [44] from the University of Heidelberg published the results of a phase I/II trial of single-fraction SBRT for unresectable liver lesions. Four of the 37 patients had primary liver tumours and the remaining 33 had metastases (maximum four metastases per patient; 56 metastases in total). The dose was escalated from 14 to 26 Gy, without any incidence of grade ≥3 toxicity. Actuarial 18-month local control was 68% for all patients, but 82% for those patients receiving 20–26 Gy.

In North America there have been a number of different approaches to dose and fractionation. Stanford University has published single-fraction SBRT experience in lung [29] and pancreatic [16,45,46] cancers. From the same institution, a phase I single-fraction dose-escalation trial for unresectable liver tumours has been published in abstract form. Twenty patients were treated (of whom 16 had liver metastases), with the dose starting at 18 Gy and increasing to 30 Gy. There were two cases of grade 2 duodenal ulceration and seven cases of grade 1 toxicity, but no other side-effects. A complete or partial response was seen in 17 of the 25 sites treated, but the median follow-up was only 7 months [47].

Other centres have adopted a three-fraction approach to treating liver metastases. In a phase I study by Schefter *et al.* [15] for 18 patients with one to three metastases, the dose was escalated from 36 to 60 Gy without causing any dose-limiting toxicity. In fact, no toxicity greater than grade 1 was recorded. Patients were treated with gantry-based SBRT, using a body frame and either abdominal compression or active breathing control to account for respiratory motion. The final results of a subsequent multi-institutional phase II study from the same group have recently been published. In the phase II part, all patients received 60 Gy in three fractions. Thirty-six of the 47 patients were assessable for local control, which was estimated to be 92% at 2 years (100% for lesions <3 cm diameter). Overall survival was 30% at 2 years, although 45% patients had active extrahepatic disease at the time of treatment [48].

The University of Rochester have published the results of a more fractionated approach, treating 69 patients with 174 metastases (maximum six per patient). The dose varied considerably (Table 2), although the preferred dose was 50 Gy in 10 fractions. There was no toxicity ≥grade 3. Local control was slightly lower (57% at 20 months), but the series included lesions up to 12 cm in diameter [49]. The authors are also involved in the RTOG 0438 phase I dose-escalation trial (recently closed), in which patients with up to five lesions, <8 cm diameter, have been treated with 40–50 Gy in 10 fractions.

In a recently published phase I study from Princess Margaret Hospital, Toronto, Canada, patients were treated with a six-fraction regimen. The dose was individualised, varying between 27.7 and 60 Gy depending on the calculated risk of RILD, and a cautious dose-escalation protocol was followed. These patients had up to eight metastases, and in some cases very large treatment volumes (gross tumour volume over 3000 cm^3 in one case). Furthermore, over half of the 68 patients had extrahepatic disease. There were no cases of RILD or dose-limiting toxicity. Side-effects were more prevalent than in the other trials described above, which may well reflect the larger treatment volumes. One-year local control was 71%, with a median overall survival of 18 months [50]. A phase II trial from these investigators is currently underway.

Primary Liver Tumours

Wherever possible, surgery is the treatment of choice for primary hepatocellular carcinoma (HCC), but a significant

Please cite this article in press as: Martin A, Gaya A, Stereotactic Body Radiotherapy: A Review, Clinical Oncology (2010), doi:10.1016/j.clon.2009.12.003

Please cite this article in press as: Martin A, Gaya A, Stereotactic Body Radiotherapy: A Review, Clinical Oncology (2010), doi:10.1016/j.clon.2009.12.003

Table 2
Selected published series of stereotactic body radiotherapy for liver tumours

Reference	Type of publication	Number of patients	Primary or metastases	Maximum tumour diameter	Dose	Follow-up	Local control	Overall survival	Toxicity ≥grade 3
[44]	Phase I/II	37 (60 lesions)	4 primary, 56 metastases	6 cm	14–26 Gy/1 fraction	Mean 9.5 months	18 month 67% (81% for lesions receiving 20–26 Gy)	1 year 72%	0%
[51]	Phase I/II	25 (45 lesions)	11 primary, 34 metastases	7.2 cm	25–37.5 Gy/3–5 fractions	Median 12.9 months	2 year 82%	2 year 54%	16% acute 4% late
[47]	Phase I (abstract)	20 (26 lesions)	4 primary, 22 metastases	–	18–30 Gy/1 fraction	Median 7 months	79% crude local control	–	0%
[48]	Phase I/II	47 (63 lesions)	Metastases (1–3 lesions per patient)	5.8 cm	36–60 Gy/3 fractions	Median 16 months	2 year 92%	2 year 30%	2%
[49]	Retrospective series	69 (174 lesions)	Metastases (1–6 lesions per patient)	12.2 cm	30–55 Gy/7–20 fractions	Median 14.5 months	20 month 58%	Median 14.5 months	0%
[50]	Phase I	68	Metastases (1–8 lesions per patient)	Median tumour volume 75 cm^3	27.7–60 Gy/6 fractions	Median 10.8 months	1 year 71%	Median 17.6 months	10% acute 1% late grade 4 duodenal bleed
[53]	Phase I	41	Primary (31 HCC, 10 IHC)	Median tumour volume 173 cm^3	24–54 Gy/6 fractions	Median 17.6 months	1 year 65%	1 year 51%	44% acute 2% late gastrointestinal bleed
[54]	Retrospective series	20	Primary HCC	6.5 cm	50 Gy/5–10 fractions	Median 23 months	2 year progression-free survival 32.5%	2 year 43.1%	0%

HCC, hepatocellular carcinoma; IHC, intrahepatic cholangiocarcinoma.

number of patients are not suitable for either resection or liver transplantation [52]. Studies have shown radiofrequency ablation and transarterial chemoembolisation to be effective treatments, but again not all patients are suitable. In primary liver disease, SBRT has been used predominantly in patients in whom other local treatments are not suitable, or who have recurred after previous local treatment. Primary liver tumours have comprised a proportion of some of the SBRT publications described above (Table 2). However, there have also been exclusive published series of primary liver tumours [53,54].

Following the same individualised approach used in their treatment of liver metastases [50], Princess Margaret Hospital published a parallel phase I study of 41 patients with unresectable HCC or intrahepatic cholangiocarcinoma. Patients were required to have Child-Pugh A liver function, and $>800\ cm^3$ of uninvolved liver, but tumour sizes were large (Table 2). One-year local control was 65%, with 51% 1-year overall survival. There was no RILD or dose-limiting toxicity, but a high incidence of grade 3 liver dysfunction [53]. Once again, a phase II trial is underway.

Choi *et al.* [54] reported the results of SBRT for 20 patients with HCC. The tumours were generally smaller, with a mean diameter of 3.7 cm and 90% of patients were of Eastern Cooperative Oncology Group performance status 0–1. The patients were treated on a linac with ISOLOC image guidance and a breath-hold technique. Eighty per cent of patients had at least a partial response and 2-year overall survival was 43%, with no toxicity ≥grade 3.

In a recent oral presentation, Mirabel reported the Lille experience of treating HCC and liver metastases. Twenty-one patients with HCC received 45 Gy in three fractions. One-year progression-free survival was 94% and the median survival was estimated to be 18 months. There was one case of grade 3 late duodenal stenosis.

There have also been published series of SBRT used in combination with transarterial chemoembolisation for HCC, showing that these two modalities can be used together safely, where appropriate [55,56].

Pancreas

Surgery is the standard of care for pancreatic cancer, but unfortunately only 20% of patients are diagnosed with resectable disease [57]. Patients with metastatic disease at diagnosis proceed directly to systemic therapy. For locally advanced non-metastatic (or medically inoperable) patients, the optimum treatment is less clear. Trials have shown chemoradiotherapy to improve survival compared with radiotherapy alone [58,59], but there is conflicting evidence as to whether chemoradiotherapy is superior to chemotherapy alone, both in comparison with 5-fluorouracil-based chemotherapy [60,61] and with newer gemcitabine-based regimens [62,63].

Local failure is still a problem in patients treated with CFR. In one study, 58% of patients treated to 60 Gy with concurrent chemotherapy had local failure as the first site of progression [64]. The radiotherapy dose prescribed is limited by the small bowel and, especially, duodenal toxicity, although the latter becomes less important after palliative gastrojejunal bypass surgery, which is carried out in some centres. The development of conformal radiotherapy has led to interest in the possibility of safe dose escalation to achieve better local control. A Dutch phase II study treated patients with a dose of 70–72 Gy in 2 Gy fractions, but local control with a median follow-up of 9 months was only 56%. There were also unacceptable normal tissue effects, with 9% grade 3 acute toxicity and 18% grade 3–5 late toxicity, including three deaths due to gastrointestinal bleeding [65].

There has been hope that SBRT may succeed where CFR has failed in safe and effective dose escalation. In a phase II study of SBRT using a conventional linac, Hoyer *et al.* [66] treated 22 patients with locally advanced pancreatic cancer, with a dose of 45 Gy in three fractions. Local control at 6 months was again disappointing at 57%, and median survival only 5.4 months, with 95% developing metastatic disease at the time of recurrence. Furthermore, 64% patients experienced ≥grade 2 toxicity, including one case of non-fatal gastric ulcer perforation.

Other published results have, however, been more promising. Koong *et al.* [16] carried out a phase I dose-escalation trial of single-fraction SBRT using CyberKnife, for patients with locally advanced disease. Two of the 15 patients had received previous chemoradiotherapy to 50 Gy. The dose started at 15 Gy and was increased to 25 Gy in 5 Gy increments. No toxicity ≥grade 3 was reported, although the median follow-up was only 5 months. In the group receiving 25 Gy, local control was achieved until death or the end of follow-up. However, the median survival was only 11 months for the whole study group.

In a phase II trial from the same authors, 19 unresectable patients received 45 Gy IMRT to the pancreas and regional lymph nodes, with concurrent 5-fluorouracil chemotherapy, followed by a 25 Gy SBRT boost to the pancreas. Sixteen of the patients completed all therapy as planned. In all patients the first site of progression was distant, with a median time to progression of 4 months, and 15 of these patients continued to have local control until death. The median survival was still only 7.5 months. Also, two patients (11%) developed grade 3 gastrointestinal acute toxicity, and there were cases of medically managed late duodenal ulceration, although the precise number is not clear [45].

More recently, an updated series of 77 patients treated with a 25 Gy single fraction has been published by the same institution, with a median follow-up of 6 months [46]. Although this is the largest series of SBRT for pancreatic cancer to date, it is heterogeneous. Nineteen per cent of patients had metastatic disease and 10% had recurrent local disease. Also, 27% were resectable, with surgery not possible due to either medical reasons or metastatic disease. Nevertheless, the results confirm that this regimen provides good local control, with an estimated 84% freedom from local progression at 12 months.

Please cite this article in press as: Martin A, Gaya A, Stereotactic Body Radiotherapy: A Review, Clinical Oncology (2010), doi:10.1016/j.clon.2009.12.003

Unfortunately, the median survival was still only 6.7 months from the time of radiosurgery treatment, although only 9% of patients had received chemotherapy. Ten per cent of patients developed ≥grade 3 acute or late gastrointestinal toxicity.

Although SBRT can significantly reduce local recurrence, and may improve quality of life as a result, there is no evidence yet that it improves overall survival. It should be stressed that systemic therapy is central to the management of locally advanced patients, as most will still die of metastatic disease. With this in mind, a short course of stereotactic radiotherapy is much less likely to interfere with a patient's systemic therapy regimen, than 5–7 weeks of CFR. Patients of good performance status with at least stable disease after initial chemotherapy, and a positron emission tomography scan negative for distant disease at that time, may be the ones most likely to benefit from stereotactic radiotherapy to the primary tumour.

Kidney

Renal cell carcinoma (RCC) has traditionally been viewed as a radioresistant tumour, as the results of CFR on primary [67] and metastatic [68] lesions have been disappointing. However, published series of radiosurgery for metastatic RCC in the brain have shown that the tumour is sensitive to extreme hypofractionated treatment [69,70]. This has led to interest in the use of SBRT for primary RCC, and for extracranial oligometastatic RCC.

Beitler *et al.* [71] were the first to report an exclusive series of SBRT for non-metastatic RCC, treating nine patients who had refused surgery. The dose was 40 Gy in five fractions using a standard linac with a stereotactic body frame. The treatment volume varied from 2 to 743 cm^3 (median 97 cm^3). With a median follow-up of 27 months, overall survival was 44% and no in-field tumour recurrence was seen. All of the four surviving patients had initial tumours <3.4 cm and had follow-up of at least 4 years.

Svedman *et al.* [72] have reported on seven patients who had nephrectomy for their primary tumour, and then subsequent SBRT for metastasis to the contralateral kidney. They were able to achieve control locally in six of the patients (median 49 months of follow-up), while maintaining stable renal function in five of them. Serum creatinine rose by about 20–30% in the other two patients.

Wersall *et al.* [73] published the Karolinska Institute 5-year experience of gantry-based SBRT in 'extracranial' RCC (primary and metastatic tumours). They treated 162 lesions in 58 patients, including eight inoperable primary tumours and 117 lung metastases. The dose was heterogeneous, varying between 25 and 45 Gy in two to five fractions according to the size and location of the lesions. Overall local control was impressive at 90% with a median follow-up of 37 months. However, 40% patients experienced side-effects, and half of these registered side-effects were grade 3 in severity [73]. The authors published prospective phase II results the following year, which confirmed the impressive local control seen with their technique (98% in the 82 treated RCC lesions) [74].

Similar local control has also been reported using the Novalis stereotactic system [75]. Fourteen patients with 23 extracranial renal cell metastases were treated with a dose of 24–40 Gy in three to six fractions. Local control was 87%, albeit at 9 months of follow-up, and symptomatic relief was achieved in 93% of patients.

Although the local control seen in these series is encouraging, further prospective studies are needed in this area. In 2008, Duke University Medical Center started a phase I/II study of SBRT for patients with either locally recurrent/progressive RCC or metastatic RCC progressing on sorafenib. Unfortunately this trial has closed due to slow accrual.

In the Karolinska Institute 5-year series, 74% of patients with metastatic disease at the time of treatment developed new metastases during follow-up [73]. Given the unpredictable natural history of renal cell metastases, randomised data are needed to determine whether an aggressive management strategy, involving SBRT, significantly improves survival in oligometastatic RCC.

Prostate

There is randomised evidence showing that dose escalation in CFR for localised prostate cancer results in improved biochemical progression-free survival, at the expense of an increased risk of late rectal toxicity [76,77]. There is also increasing evidence to suggest that the α/β of prostate cancer is considerably lower than many other cancers, and indeed lower than that of the surrounding organs at risk [78]. The precise value is still uncertain, although it has been estimated to be as low as 1.2 [79]. If this is true, and if the linear quadratic model is assumed to be sufficiently accurate at very high doses per fraction, then hypofractionation should improve the therapeutic ratio of prostate radiotherapy. A number of randomised trials of hypofractionation are underway, the results of which should provide more information.

There has been a Canadian series of 30 low-risk localised prostate cancer patients treated with extreme hypofractionation (35 Gy in five daily fractions) using IMRT. At 6 months there was no grade 3 toxicity, but longer follow-up is needed to assess efficacy [80].

SBRT has been shown to produce favourable rectal dose–volume histograms when compared with IMRT and conformal three-dimensional CFR [81]. This, together with the extreme hypofractionation of stereotactic treatment, would suggest that a stereotactic approach could significantly improve the therapeutic ratio of prostate radiotherapy, in addition to the obvious convenience to patients and radiotherapy departments of shorter courses of treatment. Published series have looked at predominantly low-risk localised prostate carcinoma, as the risk of microscopic disease outside the gland is very low. There is also early interest in using SBRT as a boost after CFR for intermediate and high-risk patients.

Please cite this article in press as: Martin A, Gaya A, Stereotactic Body Radiotherapy: A Review, Clinical Oncology (2010), doi:10.1016/j.clon.2009.12.003

Madsen *et al.* [82] have published a series of 40 low-risk patients treated with SBRT using a conventional linac with stereotactic cones. The patients were treated in a 'flex-prone' position with inserted fiducial markers for on-line image guidance, and six stationary non-coplanar fields. A dose of 33.5 Gy in five fractions was used, as this is equivalent to 78 Gy in 2 Gy fractions to the tumour, assuming an α/β of 1.5. With a median follow-up of 41 months, the actuarial 4-year biochemical progression-free survival was 90% using the Phoenix definition (prostate-specific antigen nadir + 2 ng/ml rise). One case of acute grade 3 urinary toxicity was reported, and there was no late toxicity ≥grade 3.

King *et al.* [83] have reported the preliminary results of a phase II clinical trial of prostate SBRT using CyberKnife. Forty-one low-risk patients were given 36.25 Gy in five fractions either daily or on alternate days. Seventy-eight per cent of the 32 patients with a minimum follow-up of 12 months achieved a prostate-specific antigen nadir ≤0.4, and the results show that the nadir continued to fall up to and beyond 3 years. There were no cases of prostate-specific antigen failure with a median follow-up of 33 months. There were two cases of grade 3 late urinary toxicity, but no ≥grade 3 rectal toxicity.

The planning method described by King *et al.* [83] aims for a relatively homogenous dose distribution within the PTV. This differs from high dose rate (HDR) brachytherapy, a technique with proven efficacy [84,85], where there is substantial heterogeneity of dose within the target, often with a high dose in the peripheral zone of the gland. Fuller *et al.* [86] set out to mimic the dosimetry achieved with HDR brachytherapy in their patients receiving prostate SBRT. They have published the early results of 10 low- and intermediate-risk patients, using a dose of 38 Gy in four fractions – a standard HDR brachytherapy dose. For each plan, a corresponding simulated HDR brachytherapy plan was produced. Qualitatively, the external beam radiation plan achieved a similar PTV coverage, but a lower urethral dose and a sharper rectal dose falloff. Follow-up is currently too short to assess efficacy. Both homogenous and heterogeneous dosimetric approaches are under further evaluation in the USA, in multicentre phase II trials.

With the long natural history associated with low- and intermediate-risk prostate cancer, longer follow-up is necessary to confirm the efficacy (and resultant late toxicity) of SBRT. Furthermore, there are already effective treatments supported by long-term data, including surgery, permanent seed brachytherapy, HDR brachytherapy, cryotherapy and CFR. However, if longer follow-up shows at least comparable efficacy, with a continued favourable toxicity profile, then the non-invasive nature of SBRT, together with the short treatment duration, will make it a very attractive option for these patients.

Spine Metastases

Conventional radiotherapy is widely used in the management of spine metastases, for local control, palliation of pain and treatment of spinal cord compression [87–89]. However, the prescribed dose is limited by spinal cord and cauda equina radiation tolerance [87,90,91]. The steep dose falloff seen with SBRT allows the delivery of a higher dose to the tumour, while staying within cord tolerance. This will increase the probability of long-term tumour control and effective analgesia. Spinal SBRT has developed directly from intracranial radiosurgery, with heavy neurosurgical involvement. It is unsurprising, therefore, that many of the published series of spine SBRT have used single-fraction regimens (Table 3).

Chang *et al.* [92] have reported on a phase I/II trial of gantry-based, intensity-modulated SBRT for spinal metastases, using a body frame and 'near simultaneous' computed tomography image-guided treatment. Forty-six per cent of patients had had previous spinal surgery. Using a dose of 30 Gy in five fractions or 27 Gy in three fractions, 1-year local control was 84% for the 74 treated lesions, and mean pain scores were significantly reduced. There were three cases of acute grade 3 toxicity, but no significant late toxicity. There have been other reports of intensity-modulated SBRT for spinal metastases [93–98], including series using Novalis [95–97] and tomotherapy [98].

There have been a number of publications of SBRT using CyberKnife in this setting [99–105]. From Pittsburg University, Gerszten *et al.* [99] published a series of 500 metastatic spinal lesions in 393 patients. Sixty-nine per cent of lesions had received previous radiotherapy, such that any further meaningful conventional irradiation was not possible. Cervical lesions were tracked relative to skull bony landmarks; lesions at other levels required intra-osseus gold fiducial insertion for system tracking. Patients received a single fraction of 12.5–25 Gy, depending on the previous radiation dose and the proximity to cord/cauda; the median follow-up was 21 months. Local control was 90% in patients with no previous radiotherapy, and 88% overall. Long-term pain improvement was seen in 86% of patients in whom the indication for treatment was pain. There were no cases of radiation myelopathy observed in the follow-up period [99]. Smaller, more specific, series of patients with spinal metastases from primary melanoma [100], breast [101], lung [102] and RCC [103] have also been published by the same authors.

Wowra *et al.* [104] reported the Munich experience of single-fraction SBRT, using 'XSight Spine' software (Accuray), which verifies the tumour position relative to spine bony landmarks, thus allowing fiducial-free tracking of spinal lesions. They treated 102 patients with one or two malignant spinal tumours, many of which were spine metastases. One-third of patients had received previous CFR to the treatment site. With a prescribed dose of 15–24 Gy, local control for 134 treated lesions was 98% at 15 months of follow-up; median pain scores (using a 10-point visual analogue scale) were significantly lower. In a recent oral presentation, the Munich series has increased to 348 lesions in 287 patients. Forty-nine of these patients had benign spinal tumours treated. With a median follow-up of 9.6 months, local control was 94% for malignant lesions and 100% for benign lesions. There have been seven cases of late

Please cite this article in press as: Martin A, Gaya A, Stereotactic Body Radiotherapy: A Review, Clinical Oncology (2010), doi:10.1016/j.clon.2009.12.003

Table 3
Selected published series of stereotactic body radiotherapy (SBRT) for spinal tumours

Reference	Type of publication	Number of patients	Previous treatment	Primary or metastases	Prescribed dose	Follow-up	Local control	Overall survival after SBRT	Symptom improvement
[92] *	Phase I/II	63 (74 lesions)	56% radiotherapy 46% surgery	Metastases	30 Gy/5 fractions or 27 Gy/3 fractions	Median 21 months	1 year 84%	1 year 69%	Mean BPI pain score and narcotic use lower at 6 months
[96] †	Prospective series	49 (61 lesions)	0% radiotherapy	Metastases	12–16 Gy/1 fraction	6–24 months	95%	1 year 74%	Verbal/VAS pain scores lower in 85% 6% pain relapse within follow-up
[99]	Prospective series	393 (500 lesions)	69% radiotherapy	Metastases	12.5–25 Gy/1 fraction	Median 21 months	88%	–	VAS pain score improved in 86% patients where indication for radiotherapy was pain. Clinical improvement in 85% patients with progressive neurological deficit
[104]	Prospective series	102 (134 lesions)	32% radiotherapy	Metastases + sarcoma	15–24 Gy/1 fraction	15 months	98%	Median 1.4 years	Median VAS pain score significantly lower
[105]	Prospective series	200 (274 lesions)	46% radiotherapy	Primary and metastases	21–37.5 Gy/3–5 fractions	Median 12 months	–	Median 14.5 months for metastatic patients	Mean VAS pain score significantly lower and continued to improve throughout follow-up. Non-significant trend towards increased SF-12 quality of life score
[107]	Prospective series	51 (55 lesions)	8% radiotherapy 51% surgery	Primary intradural	16–30 Gy/1–5 fractions	Median 23 months	98%	96%	Significant pain reduction 70% meningioma and 50% schwannoma patients
[108]	Prospective series	73 (73 lesions)	8% radiotherapy 26% surgery	Primary intradural	12–20 Gy/1 fraction	Median 37 months	100%	–	Long-term pain improvement 73% patients (VAS pain score)

BPI, Brief Pain Inventory; VAS, visual analogue scale.
* Authors used CyberKnife except (conventional linear accelerator).
† Authors used CyberKnife except (Novalis).

toxicity: one patient with myelopathy, three with spinal instability and three with tumour haemorrhage.

There has been a recent publication from Georgetown looking specifically at pain and quality of life after SBRT for metastatic and primary spinal tumours [105]. Two hundred patients with 274 spinal lesions received 21–37.5 Gy in three to five fractions. Seventy-six per cent of patients reported pain at baseline. The mean visual analogue scale pain scores improved significantly, and continued to improve throughout the follow-up period (median 12 months). There was a non-significant trend towards improved quality of life, as measured by the SF-12 survey.

Primary Spine Tumours

Microsurgical resection is a safe and effective treatment for benign spinal tumours [106]. However, surgery may not always be possible, for example with post-surgical recurrence or medical co-morbidity. SBRT is a useful treatment in these situations.

Several series of CyberKnife SBRT for benign intradural tumours have been published [107–110]. From Stanford University, Dodd *et al.* [107] treated 55 tumours in 51 patients in whom surgery was contraindicated. Doses ranged from 16 to 30 Gy in one to five fractions, although 80% of patients were treated with one or two fractions. The median follow-up was 23 months. There was evidence of tumour growth after treatment in one patient, but local control was 100% in patients followed up for more than 2 years.

Similarly, Gerszten *et al.* [108] have reported on 73 intradural lesions treated with a single fraction of 12–20 Gy. With a median follow-up of 37 months, local control was once again 100%, and there was long-term improvement in pain scores in 73% of patients.

There have been smaller, more specific, published series of SBRT for nerve sheath tumours [111], chordomas [112] and sarcomas [113]. Stanford University have also published a series of SBRT for spinal arteriovenous malformations [114], although further work is needed here to establish efficacy and the optimum radiation dose.

Late spinal cord toxicity is one of the major concerns when planning radiotherapy to spinal lesions. In the largest published retrospective review, 1075 patients with primary or metastatic tumours were treated with SBRT at Stanford or Pittsburgh University between 1996 and 2005. Six patients developed radiation-induced late myelopathy at 2–9 months after treatment. In three of these patients, symptoms improved with intervention, and one patient progressed to paraplegia. Specific dosimetric factors associated with the development of myelopathy could not be identified [115].

The data presented for both primary and metastatic lesions show that SBRT can safely administer higher doses to spinal tumours than is possible with conventional radiotherapy. It is also a non-invasive alternative to surgery for spine metastases, both as primary treatment in unirradiated patients, and as a salvage technique for progressive disease in previously irradiated patients. It has been shown to improve disease-related pain and neurological symptoms. However, once again there are no randomised data comparing SBRT and surgery. Surgery remains the optimum strategy for intradural primary tumours and, where possible, would be the favoured option in metastatic cases where spinal stabilisation or significant neural decompression is required [116,117].

Conclusion

Advances in image guidance and radiotherapy planning software, together with improved accuracy of treatment delivery, have led to the successful use of stereotactic radiotherapy for extracranial targets. Careful patient selection is especially important. As the volume of normal tissue within the target periphery is related to the cube of the target's radius, smaller lesions are preferable. The steep dose falloff outside the target volume means that lesions with unclear, infiltrative margins should be avoided. In patients with active disease distant to the treatment site(s), SBRT is unlikely to improve survival, although may achieve good palliation through local control. Similarly, in radical treatments, the risk of distant micrometastatic disease must be carefully considered before proceeding. These qualifications aside, phase I/II data seem to be very promising, with excellent local control rates at a number of treatment sites. The results of phase III comparisons with surgery and other treatment modalities are eagerly awaited.

Conflict of Interest

A. Martin is currently employed as a research fellow at the CyberKnife Centre, The Harley Street Clinic, London, UK. There is no association with Accuray Inc.

References

[1] Horsley VA, Clarke RH. The structure and functions of the cerebellum examined by a new method. *Brain* 1908;31:45–124.
[2] Spiegel EA, Wycis HT, Marks M, *et al*. Stereotactic apparatus for operations on the human brain. *Science* 1947;106:349–350.
[3] Leksell L. The stereotactic method and radiosurgery of the brain. *Acta Chir Scand* 1951;102:316–319.
[4] Heck B, Jess-Hempen A, Kreiner HJ, *et al*. Accuracy and stability of positioning in radiosurgery: long-term results of the Gamma Knife system. *Med Phys* 2007;34(4):1487–1495.
[5] Hamilton AJ, Lulu BA, Fosmire H, *et al*. Preliminary clinical experience with linear accelerator-based spinal stereotactic radiosurgery. *Neurosurgery* 1995;36:311–319.
[6] Lax I, Blomgren H, Naslund I, *et al*. Stereotactic radiotherapy of malignancies in the abdomen: methodological aspects. *Acta Oncol* 1994;33:677–683.
[7] Kupelian PA, Forbes A, Willoughby TR, *et al*. Implantation and stability of metallic fiducials within pulmonary lesions. *Int J Radiat Oncol Biol Phys* 2007;69:777–785.
[8] Collins BT, Vahdat S, Erickson K, *et al*. Radical cyberknife radiosurgery with tumor tracking: an effective treatment for inoperable small peripheral stage I non-small cell lung cancer. *J Hematol Oncol* 2009;2:1.

Please cite this article in press as: Martin A, Gaya A, Stereotactic Body Radiotherapy: A Review, Clinical Oncology (2010), doi:10.1016/j.clon.2009.12.003

[9] van der Voort van Zyp NC, Prevost J-B, Hoogeman MS, *et al*. Stereotactic radiotherapy with real-time tumor tracking for non-small cell lung cancer: clinical outcome. *Radiother Oncol* 2009;91(3):296–300.
[10] Fowler JF. The linear quadratic formula and progress in fractionated radiotherapy. *Br J Radiol* 1989;62:679–694.
[11] Withers HR. The four R's of radiotherapy. *Adv Radiat Biol* 1975;5:241–247.
[12] Tome WA, Fowler JF. Selective boosting of tumor subvolumes. *Int J Radiat Oncol Biol Phys* 2000;48:593–599.
[13] Guerrero M, Li XA. Extending the linear-quadratic model for large fraction doses pertinent to stereotactic radiotherapy. *Phys Med Biol* 2004;49:4825–4835.
[14] McGarry RC, Papiez L, Williams M, *et al*. Stereotactic body radiation therapy of early-stage non-small-cell lung carcinoma: phase I study. *Int J Radiat Oncol Biol Phys* 2005;63(4):1010–1015.
[15] Schefter TE, Kavanagh BD, Timmerman RD, *et al*. A phase I trial of stereotactic body radiation therapy (SBRT) for liver metastases. *Int J Radiat Oncol Biol Phys* 2005;62:1371–1378.
[16] Koong AC, Le QT, Ho A, *et al*. Phase I study of stereotactic radiosurgery in patients with locally advanced pancreatic cancer. *Int J Radiat Oncol Biol Phys* 2004;58:1017–1021.
[17] Nesbitt JC, Putnam Jr JB, Walsh GL, *et al*. Survival in early-stage non-small cell lung cancer. *Ann Thorac Surg* 1995;60:466–472.
[18] Kelsey CR, Boyd JA, Hubbs JL, *et al*. Local/regional recurrence following surgery for early-stage lung cancer: a 10-year experience with 975 patients. *J Clin Oncol* 2008;26(15S):7542.
[19] Sibley GS. Radiotherapy for patients with medically inoperable stage I non-small cell lung cancer. Smaller volumes and higher doses: a review. *Cancer* 1998;82(3):433–438.
[20] Qiao X, Tullgren O, Lax I, *et al*. The role of radiotherapy in treatment of stage I non-small cell lung cancer. *Lung Cancer* 2003;41:1–11.
[21] Onishi H, Shirato H, Nagata Y, *et al*. Hypofractionated stereotactic radiotherapy (HypoFXSRT) for stage I non-small cell lung cancer: updated results of 257 patients in a Japanese multi-institutional study. *J Thorac Oncol* 2007;2(7 Suppl. 3):S94–S100.
[22] Wulf J, Haedinger U, Oppitz U, *et al*. Stereotactic radiotherapy for primary lung cancer and pulmonary metastases: a noninvasive treatment approach in medically inoperable patients. *Int J Radiat Oncol Biol Phys* 2004;60(1):186–196.
[23] Baumann P, Nyman J, Lax I, *et al*. Factors important for efficacy of stereotactic body radiotherapy of medically inoperable stage I lung cancer. A retrospective analysis of patients treated in the Nordic countries. *Acta Oncol* 2006;45(7):787–795.
[24] Zimmerman FB, Geinitz H, Schill S, *et al*. Stereotactic hypofractionated radiotherapy in stage I (T1-2 N0 M0) non-small-cell lung cancer (NSCLC). *Acta Oncol* 2006;45(7):796–801.
[25] Hof H, Muenter M, Oetzel D, *et al*. Stereotactic single-dose radiotherapy (radiosurgery) of early stage nonsmall-cell lung cancer (NSCLC). *Cancer* 2007;110(1):148–155.
[26] Baumann P, Nyman J, Hoyer M, *et al*. Outcome in a prospective phase II trial of medically inoperable stage I non-small-cell lung cancer patients treated with stereotactic body radiotherapy. *J Clin Oncol* 2009;27(20):3290–3296.
[27] Timmerman R, McGarry R, Yiannoutsos C, *et al*. Excessive toxicity when treating central tumors in a phase II study of stereotactic body radiation therapy for medically inoperable early-stage lung cancer. *J Clin Oncol* 2006;24(30):4833–4839.
[28] Chang JY, Balter PA, Dong L, *et al*. Stereotactic body radiation therapy in centrally and superiorly located stage I or isolated recurrent non-small-cell lung cancer. *Int J Radiat Oncol Biol Phys* 2008;72(4):967–971.
[29] Le QT, Loo BW, Ho A, *et al*. Results of phase I dose escalation study using single fraction stereotactic radiotherapy for lung tumors. *J Thorac Oncol* 2006;1(8):802–809.
[30] Brown WT, Wu X, Fayad F, *et al*. Cyberknife radiosurgery for stage I lung cancer: results at 36 months. *Clin Lung Cancer* 2007;8(8):488–492.
[31] Xia T, Li H, Sun Q, *et al*. Promising clinical outcome of stereotactic body radiation therapy for patients with inoperable stage I/II non-small-cell lung cancer. *Int J Radiat Oncol Biol Phys* 2006;66(1):117–125.
[32] Hellman S, Weichselbaum RR. Oligometastases. *J Clin Oncol* 1995;13:8–10.
[33] Pastorino UB, Buyse M, Friedel G, *et al*. Long-term results of lung metastasectomy: prognostic analyses based on 5206 cases: the International Registry of Lung Metastases. *J Thorac Cardiovasc Surg* 1997;113:37–49.
[34] Fong Y, Fortner J, Sun RL, *et al*. Clinical score for predicting recurrence after hepatic resection for metastatic colorectal cancer: analysis of 1001 consecutive cases. *Ann Surg* 1999;230:309–321.
[35] Guckenberger M, Heilman K, Wulf J, *et al*. Pulmonary injury and tumor response after stereotactic body radiotherapy (SBRT): results of a serial follow-up CT study. *Radiother Oncol* 2007;85(3):435–442.
[36] Lee SW, Choi EK, Park HJ, *et al*. Stereotactic body frame based fractionated radiosurgery on consecutive days for primary or metastatic tumours in the lung. *Lung Cancer* 2003;40(3):309–315.
[37] Fritz P, Kraus HJ, Muhlnickel W, *et al*. Stereotactic, single-dose irradiation of stage I non-small cell lung cancer and lung metastases. *Radiat Oncol* 2006;1:30.
[38] Norihisa Y, Nagata Y, Takayama K, *et al*. Stereotactic body radiotherapy for oligometastatic lung tumors. *Int J Radiat Oncol Biol Phys* 2008;72(2):398–403.
[39] Rusthoven KE, Kavanagh BD, Burri SH, *et al*. Multi-institutional phase I/II trial of stereotactic body radiation therapy for lung metastases. *J Clin Oncol* 2009;27:1579–1584.
[40] Brown WT, Wu X, Fowler JF, *et al*. Lung metastases treated by Cyberknife image-guided robotic stereotactic radiosurgery at 41 months. *South Med J* 2008;101(4):376–382.
[41] Mulier S, Ruers T, Jamart J, *et al*. Radiofrequency ablation versus resection for resectable colorectal liver metastases: time for a randomized trial? An update. *Dig Surg* 2008;25(6):445–460.
[42] Leibel SA, Pajak TF, Massullo V, *et al*. A comparison of misonidazole sensitized radiation therapy to radiation therapy alone for the palliation of hepatic metastases: results of a Radiation Therapy Oncology Group randomized prospective trial. *Int J Radiat Oncol Biol Phys* 1987;13:1057–1064.
[43] Blomgren H, Lax I, Naslund I, *et al*. Stereotactic high dose fraction radiation therapy of extracranial tumors using an accelerator. Clinical experience of the first thirty-one patients. *Acta Oncol* 1995;34(6):861–870.
[44] Herfarth KK, Debus J, Lohr F, *et al*. Stereotactic single-dose radiation therapy of liver tumors: results of a phase I/II trial. *J Clin Oncol* 2001;19:164–170.
[45] Koong AC, Christofferson E, Le QT, *et al*. Phase II study to assess the efficacy of conventionally fractionated radiotherapy followed by a stereotactic radiosurgery boost in patients with locally advanced pancreatic cancer. *Int J Radiat Oncol Biol Phys* 2005;63:320–323.
[46] Chang DT, Schellenberg D, Shen J, *et al*. Stereotactic radiotherapy for unresectable adenocarcinoma of the pancreas. *Cancer* 2009;115(3):665–672.

Please cite this article in press as: Martin A, Gaya A, Stereotactic Body Radiotherapy: A Review, Clinical Oncology (2010), doi:10.1016/j.clon.2009.12.003

[47] Anderson EM, Koong A, Yang G, *et al*. Phase I dose escalation study of stereotactic radiosurgery for liver malignancies (poster presentation). Proceedings of the ASCO 2007 Gastrointestinal Cancers Symposium. Orlando, Florida, USA, 19–21 January 2007.

[48] Rusthoven KE, Kavanagh BD, Cardenes H, *et al*. Multi-institutional phase I/II trial of stereotactic body radiation therapy for liver metastases. *J Clin Oncol* 2009;27:1579–1584.

[49] Katz AW, Carey-Sampson M, Muhs AG, *et al*. Hypofractionated stereotactic body radiation therapy (SBRT) for limited hepatic metastases. *Int J Radiat Oncol Biol Phys* 2007;67:793–798.

[50] Lee MT, Kim JJ, Dinniwell R, *et al*. Phase I study of individualized stereotactic body radiotherapy for liver metastases. *J Clin Oncol* 2009;27:1585–1591.

[51] Mendez Romero A, Wunderink W, Hussain SM, *et al*. Stereotactic body radiation therapy for primary and metastatic liver tumors: a single institution phase I–II study. *Acta Oncol* 2006;45(7):831–837.

[52] Llovet JM, Burroughs A, Bruix J. Hepatocellular carcinoma. *Lancet* 2003;362:1907–1917.

[53] Tse RV, Hawkins M, Lockwood G, *et al*. Phase I study of individualized stereotactic body radiotherapy for hepatocellular carcinoma and intrahepatic cholangiocarcinoma. *J Clin Oncol* 2008;26(4):657–664.

[54] Choi BO, Jang HS, Kang KM, *et al*. Fractionated stereotactic radiotherapy in patients with primary hepatocellular carcinoma. *Jpn J Clin Oncol* 2006;36:154–158.

[55] Takeda A, Takahashi M, Kunieda E, *et al*. Hypofractionated stereotactic radiotherapy with and without transarterial chemoembolization for small hepatocellular carcinoma not eligible for other ablation therapies: preliminary results for efficacy and toxicity. *Hepatol Res* 2008;38(1):60–69.

[56] Choi BO, Choi IB, Jang HS, *et al*. Stereotactic body radiation therapy with or without transarterial chemoembolization for patients with primary hepatocellular carcinoma: preliminary analysis. *BMC Cancer* 2008;8:351.

[57] Geer RJ, Brennan MF. Prognostic indicators for survival after resection of pancreatic adenocarcinoma. *Am J Surg* 1993;165:68–73.

[58] Moertel CG, Childs DS, Reitmeier RJ, *et al*. Combined 5-fluorouracil and supervoltage radiation therapy of locally unresectable gastrointestinal cancer. *Lancet* 1969;2:865–867.

[59] Moertel C, Frytak S, Hahn R, *et al*. Therapy of locally unresectable pancreatic carcinoma: a randomized comparison of high dose (6000 rads) radiation alone, moderate dose radiation (4000 rads 5-fluorouracil), and high dose radiation 5-fluorouracil: the Gastrointestinal Tumor Study Group. *Cancer* 1981;48:1705–1710.

[60] Gastrointestinal Tumor Study Group. Treatment of locally unresectable carcinoma of the pancreas: comparison of combined-modality therapy (chemotherapy plus radiotherapy) to chemotherapy alone. *J Natl Cancer Inst* 1988;80:751–755.

[61] Klaassen DJ, MacIntyre JM, Catton GE, *et al*. Treatment of locally unresectable cancer of the stomach and pancreas: a randomized comparison of 5-fluorouracil alone with radiation plus concurrent and maintenance 5-fluorouracil – an Eastern Cooperative Oncology Group study. *J Clin Oncol* 1985;3:373–378.

[62] Chauffert B, Mornex F, Bonnetain F, *et al*. Phase III trial comparing initial chemoradiotherapy (intermittent cisplatin and infusional 5-FU) followed by gemcitabine vs. gemcitabine alone in patients with locally advanced non metastatic pancreatic cancer: a FFCD-SFRO study. *J Clin Oncol* 2006;24(18S, Part I):4008.

[63] Loehrer PJ, Powell ME, Cardenes HR, *et al*. A randomized phase III study of gemcitabine in combination with radiation therapy versus gemcitabine alone in patients with localized, unresectable pancreatic cancer: E4201. abstract 4506. *J Clin Oncol* 2008;26(Suppl.):214s.

[64] Gastrointestinal Tumor Study Group. Radiation therapy combined with adriamycin or 5-fluorouracil for the treatment of locally unresectable pancreatic carcinoma. *Cancer* 1985;56:2563–2568.

[65] Ceha HM, van Tienhoven G, Gouma DJ, *et al*. Feasibility and efficacy of high dose conformal radiotherapy for patients with locally advanced pancreatic carcinoma. *Cancer* 2000;89:2222–2229.

[66] Hoyer M, Roed H, Sengelov L, *et al*. Phase-II study on stereotactic radiotherapy of locally advanced pancreatic carcinoma. *Radiother Oncol* 2005;76:48–53.

[67] Juusela H, Malmio K, Alfthan O, *et al*. Preoperative irradiation in the treatment of renal adenocarcinoma. *Scand J Urol Nephrol* 1977;11(3):277–281.

[68] Wronski M, Maor MH, Davis BJ, *et al*. External radiation of brain metastases from renal carcinoma: a retrospective study of 119 patients from the MD Anderson Cancer Center. *Int J Radiat Oncol Biol Phys* 1997;37:753–759.

[69] Sheehan JP, Sun MH, Kondziolka D, *et al*. Radiosurgery in patients with renal cell carcinoma metastasis to the brain: long-term outcomes and prognostic factors influencing survival and local tumor control. *J Neurosurg* 2003;98(2):342–349.

[70] Muacevic A, Kreth FW, Mack A, *et al*. Stereotactic radiosurgery without radiation therapy providing high local tumor control of multiple brain metastases from renal cell carcinoma. *Minim Invasive Neurosurg* 2004;47(4):203–208.

[71] Beitler JJ, Makara D, Silverman P, *et al*. Definitive, high-dose-per-fraction, conformal, stereotactic external radiation for renal cell carcinoma. *Am J Clin Oncol* 2004;27:646–648.

[72] Svedman C, Karlsson K, Rutlowska E, *et al*. Stereotactic body radiotherapy of primary and metastatic renal lesions for patients with only one functioning kidney. *Acta Oncol* 2008;47(8):1578–1583.

[73] Wersall PJ, Blomgren H, Lax I, *et al*. Extracranial stereotactic radiotherapy for primary and metastatic renal cell carcinoma. *Radiother Oncol* 2005;77(1):88–95.

[74] Svedman C, Sandstrom P, Pisa P, *et al*. A prospective phase II trial of using extracranial stereotactic radiotherapy in primary and metastatic renal cell carcinoma. *Acta Oncol* 2006;45(7):870–875.

[75] Teh BS, Bloch C, Galli-Guevara M, *et al*. The treatment of primary and metastatic renal cell carcinoma (RCC) with image-guided stereotactic body radiation therapy (SBRT). *Biomed Imaging Interv J* 2007;3(1):e6.

[76] Dearnaley DP, Sydes MR, Graham JD, *et al*. Escalated-dose versus standard-dose conformal radiotherapy in prostate cancer: first results from the MRC RT01 randomised controlled trial. *Lancet Oncol* 2007;8:475–487.

[77] Pollack A, Zagars GK, Starkschall G, *et al*. Prostate cancer radiation dose response: results of the MD Anderson phase III randomized trial. *Int J Radiat Oncol Biol Phys* 2002;53:1097–1105.

[78] Dasu A. Is the alpha/beta value for prostate tumours low enough to be safely used in clinical trials? *Clin Oncol* 2007;19:289–301.

[79] Brenner DJ, Martinez AA, Edmundson GK, *et al*. Direct evidence that prostate tumors show high sensitivity to fractionation (low alpha/beta ratio), similar to late-responding normal tissue. *Int J Radiat Oncol Biol Phys* 2002;52:6–13.

Please cite this article in press as: Martin A, Gaya A, Stereotactic Body Radiotherapy: A Review, Clinical Oncology (2010), doi:10.1016/j.clon.2009.12.003

[80] Tang CI, Loblaw DA, Cheung P, *et al*. Phase I/II study of a five-fraction hypofractionated accelerated radiotherapy treatment for low-risk localised prostate cancer: early results of pHART3. *Clin Oncol* 2008;20:729–737.
[81] Madsen BL, Pham HT, Hsi RA, *et al*. Comparison of rectal dose volume histograms for definitive prostate radiotherapy among stereotactic radiotherapy, IMRT, and 3D-CRT techniques [abstract]. *Int J Radiat Oncol Biol Phys* 2004;60:S633.
[82] Madsen BL, Hsi RA, Pham HT, *et al*. Stereotactic hypofractionated accurate radiotherapy of the prostate (SHARP), 33.5 Gy in five fractions for localized disease: first clinical trial results. *Int J Radiat Oncol Biol Phys* 2007;67(4):1099–1105.
[83] King CR, Brooks JD, Gill H, *et al*. Stereotactic body radiotherapy for localized prostate cancer: interim results of a prospective phase II clinical trial. *Int J Radiat Oncol Biol Phys* 2009;73(4):1043–1048.
[84] Grills IS, Martinez AA, Hollander M, *et al*. High dose rate brachytherapy as prostate cancer monotherapy reduces toxicity compared to low dose rate palladium seeds. *J Urol* 2004;171:1098–1104.
[85] Demanes DJ, Rodriguez RR, Schour L, *et al*. High-dose-rate intensity-modulated brachytherapy with external beam radiotherapy for prostate cancer: California endocuriether-apy's 10-year results. *Int J Radiat Oncol Biol Phys* 2005;61:1306–1316.
[86] Fuller DB, Naitoh J, Lee C, *et al*. Virtual HDR^{SM} CyberKnife treatment for localized prostatic carcinoma: dosimetry comparison with HDR brachytherapy and preliminary clinical observations. *Int J Radiat Oncol Biol Phys* 2008;70(5):1588–1597.
[87] Faul CM, Flickinger JC. The use of radiation in the management of spinal metastases. *J Neurooncol* 1995;23:149–161.
[88] Eble MJ, Eckert W, Wannenmacher M. Value of local radiotherapy in treatment of osseous metastases, pathological fractures and spinal cord compression. *Radiologe* 1995;35:47–54.
[89] Maranzano E, Latini P. Effectiveness of radiation therapy without surgery in metastatic spinal cord compression: final results from a prospective trial. *Int J Radiat Oncol Biol Phys* 1995;32:959–967.
[90] Marcus Jr RB, Million RR. The incidence of myelitis after irradiation of the cervical spinal cord. *Int J Radiat Oncol Biol Phys* 1990;19:3–8.
[91] Emami B, Lyman J, Brown A, *et al*. Tolerance of normal tissue to therapeutic irradiation. *Int J Radiat Oncol Biol Phys* 1991; 21:109–122.
[92] Chang EL, Shiu AS, Mendel E, *et al*. Phase I/II study of stereotactic body radiotherapy for spinal metastasis and its pattern of failure. *J Neurosurg Spine* 2007;7(2):151–160.
[93] Bilsky MH, Yamada Y, Yenice KM, *et al*. Intensity-modulated stereotactic radiotherapy of paraspinal tumors: a preliminary report. *Neurosurgery* 2004;54:823–830.
[94] Nelson JW, Yoo DS, Sampson JH, *et al*. Stereotactic body radiotherapy for lesions of the spine and paraspinal regions. *Int J Radiat Oncol Biol Phys* 2009;73(5):1369–1375.
[95] De Salles AA, Pedroso AG, Medin P, *et al*. Spinal lesions treated with Novalis shaped beam intensity-modulated radiosurgery and stereotactic radiotherapy. *J Neurosurg* 2004;101(Suppl. 3):435–440.
[96] Ryu S, Rock J, Rosenblum M, *et al*. Pattern of failure after single dose radiosurgery for single spinal metastasis. *J Neurosurg* 2004;101(Suppl. 3):402–405.
[97] Ryu S, Jian-Yue J, Jin R, *et al*. Partial volume tolerance of the spinal cord and complications of single-dose radiosurgery. *Cancer* 2007;109(3):628–636.
[98] Kim B, Soisson ET, Duma C, *et al*. Image-guided helical tomotherapy for treatment of spine tumors. *Clin Neurol Neurosurg* 2008;110(4):357–362.
[99] Gerszten PC, Burton SA, Ozhasoglu C, *et al*. Radiosurgery for spinal metastases: clinical experience in 500 cases from a single institution. *Spine* 2007;32(2):193–199.
[100] Gerszten PC, Burton SA, Quinn AE, *et al*. Radiosurgery for the treatment of spinal melanoma metastases. *Stereotact Funct Neurosurg* 2005;83(5–6):213–221.
[101] Gerszten PC, Burton SA, Welch WC, *et al*. Single-fraction radiosurgery for the treatment of spinal breast metastases. *Cancer* 2005;104(10):2244–2254.
[102] Gerszten PC, Burton SA, Belani CP, *et al*. Radiosurgery for the treatment of spinal lung metastases. *Cancer* 2006;107(11):2653–2661.
[103] Gerszten PC, Burton SA, Ozhasoglu C, *et al*. Stereotactic radiosurgery for spinal metastases from renal cell carcinoma. *J Neurosurg Spine* 2005;3(4):288–295.
[104] Wowra B, Zausinger S, Drexler C, *et al*. CyberKnife radiosurgery for malignant spinal tumors: characterization of well-suited patients. *Spine* 2008;33(26):2929–2934.
[105] Gagnon GJ, Nasr NM, Liao JJ, *et al*. Treatment of spinal tumors using CyberKnife fractionated stereotactic radiosurgery: pain and quality of life assessment after treatment in 200 patients. *Neurosurgery* 2009;64(2):297–306.
[106] Parsa A, Lee J, Parney I, *et al*. Spinal cord and intradural-extraparenchymal spinal tumors: current best care practices and strategies. *J Neurooncol* 2004;69:291–318.
[107] Dodd RL, Ryu MR, Kammerdsupaphon P, *et al*. CyberKnife radiosurgery for benign intradural extramedullary spinal tumors. *Neurosurgery* 2006;58:674–685.
[108] Gerszten PC, Burton SA, Ozhasoglu C, *et al*. Radiosurgery for benign intradural spinal tumors. *Neurosurgery* 2008;62(4): 887–896.
[109] Bhatnagar AK, Gerszten PC, Ozhasaglu C, *et al*. CyberKnife frameless radiosurgery for the treatment of extracranial benign tumors. *Technol Cancer Res Treat* 2005;4(5):571–576.
[110] Sahgal A, Chou D, Ames C, *et al*. Image-guided robotic stereotactic body radiotherapy for benign spinal tumors: the University of California San Francisco preliminary experience. *Technol Cancer Res Treat* 2007;6(6):595–603.
[111] Murovic JA, Gibbs IC, Chang SD, *et al*. Foraminal nerve sheath tumors: intermediate follow up after cyberknife radiosurgery. *Neurosurgery* 2009;64(2 Suppl.):A33–A43.
[112] Henderson FC, McCool K, Seigle J, *et al*. Treatment of chordomas with CyberKnife: Georgetown University experience and treatment recommendations. *Neurosurgery* 2009;64(2 Suppl.):A44–A53.
[113] Levine AM, Coleman C, Horasek S, *et al*. Stereotactic radiosurgery for the treatment of primary sarcomas and sarcoma metastases of the spine. *Neurosurgery* 2009;64(2 Suppl.): A54–A59.
[114] Sinclair J, Chang SD, Gibbs IC, *et al*. Multisession CyberKnife radiosurgery for intramedullary spinal cord arteriovenous malformations. *Neurosurgery* 2006;58(6):1081–1089.
[115] Gibbs IC, Patil C, Gerszten PC, *et al*. Delayed radiation-induced myelopathy after spinal radiosurgery. *Neurosurgery* 2009;64(2 Suppl.):A67–A72.
[116] Klimo P, Kestle JR, Schmidt MH. Treatment of metastatic spinal epidural disease: a review of the literature. *Neurosurg Focus* 2003;15(5):E1.
[117] Patchell RA, Tibbs PA, Regine WF, *et al*. Direct decompressive surgical resection in the treatment of spinal cord compression caused by metastatic cancer: a randomised trial. *Lancet* 2005;366:643–648.

Please cite this article in press as: Martin A, Gaya A, Stereotactic Body Radiotherapy: A Review, Clinical Oncology (2010), doi:10.1016/j.clon.2009.12.003

British Journal of Neurosurgery, Early Online, 1–6

ISSN: 0268-8697 print / ISSN 1360-046X online
DOI: 10.3109/02688697.2011.603857

informa
healthcare

ORIGINAL ARTICLE

(Stereotactic) radiosurgery XIX: spinal radiosurgery – two year experience in a UK centre

A.G.R. Martin[1], I.R. Cowley[1], B.A. Taylor[1,2], A.M. Cassoni[1,3], D.B. Landau[1,4], & P.N. Plowman[1,5]

[1]*The CyberKnife Centre, The Harley Street Clinic, London, UK*
[2]*The Wellington Hospital, London, UK*
[3]*University College London Hospitals NHS Foundation Trust, London, UK*
[4]*Guy's and St. Thomas' Hospital NHS Foundation Trust, London, UK*
[5]*Barts and The London NHS Trust, London, UK*

Abstract

***Introduction*. Modern radiotherapy image guidance enables the treatment of extracranial targets with the required accuracy for safe delivery of radiosurgical treatments. The first two years' experience of spinal radiosurgery in a UK radiotherapy centre is reported. *Materials and methods*. Patients with primary or metastatic spinal lesions were treated using the CyberKnife stereotactic radiotherapy system. Xsight Spine (fiducial-free) tumour tracking software was used in all cases. Treatment was delivered using either a single or a three-fraction schedule, between February 2009 and March 2011. *Results*. Fifty-three spinal lesions were treated, comprising 14 primary lesions in 12 patients, and 39 metastases in 29 patients. The prescription dose ranged from 8 to 30 Gy in 1–3 fractions. Fifty-nine percent of patients experienced no acute side effects from treatment. There were three cases of acute grade 3 back or nerve root pain, all of which responded to a short course of oral corticosteroids. At a median follow-up of 11.1 months, local control and overall survival were 91 and 65%, respectively. Pain improvement was seen in 75% of symptomatic metastases at 6 months post treatment. *Conclusions*. Early UK experience confirms that radiosurgery is well tolerated with excellent local control rates. Longer-term prospective data are needed to clarify the role of spinal radiosurgery for patients in this country.**

Keywords: CyberKnife; radiosurgery; spinal tumour; spine, stereotactic body radiotherapy.

Introduction

Radiosurgery is a well-established treatment for intracranial targets, and has changed best standard practice for many conditions that were previously solely treated by conventional surgery.[1–3] Precise patient immobilisation for intracranial radiosurgery is achieved most frequently by using a pinned stereotactic frame. For example, the Gamma Knife system (Elekta, Sweden) uses frame-based immobilisation. Unfortunately, most extracranial targets do not have a fixed relationship relative to any external frame, and traditionally this has limited the ability to deliver radiosurgery to targets outside the skull. However, modern image guidance techniques allow near 'real-time' imaging linked directly to therapy delivery. Consequently, newer treatment systems can assess, and compensate for, extracranial target motion with the required accuracy for delivering radiosurgery. Thus, stereotactic coordinates are replaced by intrafraction image-guided tracking of the actual location of the target (or a surrogate, such as implanted radiopaque 'fiducial' markers or adjacent bony landmarks). A consequence of this 'frameless' approach is the easy ability to fractionate treatment – sometimes desirable when the radiation tolerance of abutting or encompassed normal tissues is a particular concern.

CyberKnife (Accuray, Sunnyvale, CA) is one such image-guided radiosurgery system, capable of treating both intra- and extracranial targets.[4] For spinal lesions, Xsight Spine (Accuray Inc.) skeletal tracking software allows 'fiducial-free' target localisation by direct reference to the adjacent bony vertebral elements, using non-rigid image registration. The mean total system targeting error when using Xsight Spine has been measured at 0.52–0.61 mm.[5,6] This paper reports the early UK experience using this technology to treat spinal lesions.

Materials and methods

All treated patients were previously discussed at a specialist radiosurgical multidisciplinary team meeting (MDT). Most patients had a single lesion for consideration, although up to three lesions in any patient were considered. The main indications for treatment were as follows:

1. Primary spinal lesions where surgery was not considered feasible or appropriate.

Correspondence: P.N. Plowman, The CyberKnife Centre, The Harley Street Clinic, 81 Harley Street, London W1G 8PP, UK. E-mail: postmaster@pnplowman.demon.co.uk

Received 15 June 2011; accepted 4 July 2011

2. Spine metastases in the context of oligometastatic disease.
3. Symptomatic spine metastases in patients with more widespread metastatic disease, but overall prognosis estimated to be greater than 6 months.

Patients underwent CT simulation using a GE LightSpeed 16 slice scanner (GE Healthcare, Buckinghamshire, UK). They were positioned supine on a memory foam mattress with a head rest and knee supports, and arms by their sides. For lesions in the cervical spine, head and neck immobilisation was achieved using a thermoplastic shell. Axial CT slices of 1.25 mm thickness were fused with recent MR images (2.5–3 mm axial thickness) to assist target and normal tissue delineation.

Image fusion, target delineation, and treatment planning were performed using MultiPlan version 3.1.0 or 3.5.1 software (Accuray Inc.). Target and 'organ-at-risk' volumes were contoured by a clinical oncologist, often with the assistance of either a neuroradiologist or a surgeon. The prescription dose and the number of fractions (one or three) was decided on an individual patient basis, taking into account any previous radiotherapy to the treatment site, the tumour volume, and the proximity of the spinal cord/cauda equina. Where possible, the doses used were in accordance with this centre's evidence-based treatment protocol. All doses were prescribed to the marginal isodose, aiming for $>95\%$ target coverage by the prescription isodose. Treatment was delivered using a G4 CyberKnife, and Xsight Spine tracking was used in all cases. Fractionated treatments were administered on consecutive days wherever possible.

Acute toxicity was reported by the treating consultant at 1 month post treatment, and graded according to National Cancer Institute (NCI) Common Terminology Criteria for Adverse Events v3.0 (2003). Outcomes data were obtained from the referring consultant at 3, 6, 9, and 12 months after treatment and 6 monthly thereafter. Length of follow-up was defined as the time from the start of CyberKnife treatment to the date that the referring consultant last had contact with the patient, or a recorded date of death. Local treatment failure was documented on the basis of either clinical or radiological evidence of disease progression inside, or immediately adjacent to, the treatment field. For painful metastatic lesions, the referring clinician was asked to state, at each follow-up point, whether the pain was 'better', 'stable', or 'worse' than baseline levels.

Results

Treatment details

Fifty-three spinal lesions were treated. These comprised of 39 metastases in 29 patients and 14 primary spinal lesions in 12 patients. Patient and treatment details are summarised in Table I, and further information on the lesion histology/primary tumour site is shown in Table II. The prescribed dose ranged from 8 to 30 Gy in 1–3 fractions. For patients with no previous radiotherapy to the treatment area, the most common prescribed doses were 18 Gy in one fraction for smaller lesions and 30 Gy in three fractions for larger ones. The prescription isodose ranged from 52 to 80% (median 65%). Planning target volume (PTV) coverage was $>95\%$ in 44 of the 53 lesions (83%). The other nine lesions were very close to the spinal cord, and PTV coverage was compromised in order to meet spinal cord dose constraints.

Table I. Summary of patient and treatment characteristics.

Patient and treatment characteristics	No.
Age	Median 59 years (27–89 years)
Previous radiotherapy to treatment site	19/41 (46%)
Previous spinal surgery	14/41 (34%)
Location of lesions:	
Vertebral	39/53 (74%)
Paravertebral	4/53 (8%)
Intradural extramedullary	4/53 (8%)
Intramedullary	6/53 (11%)
Vertebral level of lesions	
Cervical	10/53 (19%)
Thoracic	16/53 (30%)
Lumbar	19/53 (36%)
Sacral	8/53 (15%)
Planning target volume (PTV)	Median 23.9 cm^3 (0.1–308.7 cm^3)
PTV coverage by prescription isodose	Median 96.8% (87.6–99.6%)
New conformity index (nCI)[a]	Median 1.29 (1.08–1.66)
Prescribed dose range	8–30 Gy in 1–3 fractions
Prescription isodose	Median 65% (52–80%)

[a]nCI = (PIV × TV)/TIV^2, where PIV = prescription isodose volume, TV = tumour volume, and TIV = tumour isodose volume (volume of tumour contained within the prescription isodose).

Sample cases

Case 1. A 33-year-old female with neurofibromatosis type 2 presented with a neurofibroma at the L4 left exit foramen, causing radicular pain in her left leg. Surgery was felt to be inappropriate due to the multiplicity of lesions. The patient had not undergone previous spinal radiotherapy. She received 15 Gy in one fraction, prescribed to the 69% isodose. Improved pain was seen at 1 month post treatment, and the patient was pain-free with stable imaging appearances at 12 months.

Case 2. A 34-year-old female had a cavernous angioma at the T9 vertebral level. Since 2007, the patient had two episodes of bleeding with proprioceptive loss in the lower

Table II. Details of the treated lesions by histology (primary lesions) and primary site (metastases).

Target details	No.
Metastases by primary site	
Breast	10
Kidney	8
Thyroid	6
Sarcoma	5
Prostate	3
Lung	2
Unknown primary	2
Colorectal	1
Skin (melanoma)	1
Oesophagus	1
Primary lesions by histology	
Haemangioblastoma	4
Chordoma	2
Haemangiopericytoma	2
Meningioma	2
Cavernous angioma	1
Fibrosarcoma	1
Haemangioendothelioma	1
Neurofibroma	1

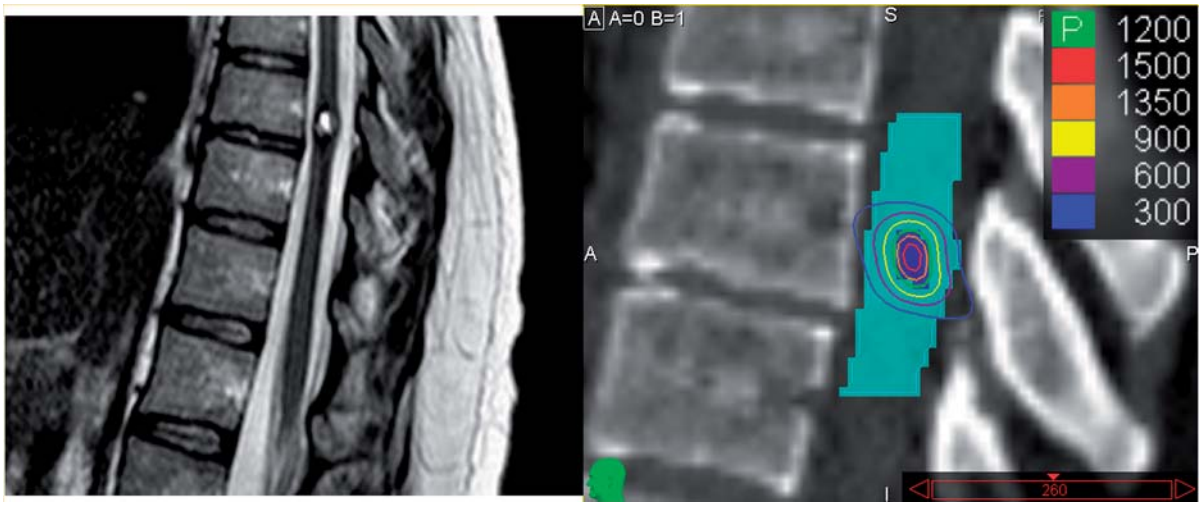

Fig 1. Cavernous angioma of the thoracic cord. Left panel shows a sagittal slice from a T2-weighted MRI; right panel shows a reconstructed sagittal CT slice with an isodose plan, and the PTV (dark blue overlay) and spinal cord (light blue overlay) contoured. Note the internal dose gradient within the PTV. The isodose key is in the top right corner; doses are shown in centigray (cGy), where 1 Gy = 100 cGy.

limbs. The patient was considered at high risk of cord damage with surgical resection. She had not undergone previous spinal radiotherapy. The patient received 12 Gy in one fraction, prescribed to the 75% isodose. Within the target, hot spots of more than 15 Gy were achieved due to the internal dose gradient (Fig. 1). At 6 months post treatment, there was stable neurology with no further bleeds.

Case 3. A 62-year-old female had a metastatic neuroendocrine tumour in the L5 vertebral body, with an unknown primary site. The tumour extended into the spinal canal, close to the cauda equina. The patient had not undergone previous spinal radiotherapy. She received 16 Gy in one fraction, prescribed to the 70% isodose, with an excellent response (Fig. 2).

Acute toxicity

Of the 41 treated patients, 24 (59%) experienced no acute side effects. The acute toxicity seen in the remaining 17 patients is summarised in Table III. There were six cases of nerve root pain, which was an exacerbation of existing symptoms in four of the six patients. In all cases, the pain responded to a short course of oral corticosteroids. There was no grade >3 toxicity and all acute toxicity had resolved by 1 month post treatment.

Local control and overall survival

Of the 41 patients treated, 5 patients were less than 3 months post treatment at the time of analysis, and 2 patients were lost to follow-up within 3 months of completing treatment (both patients moved abroad). Outcomes data are presented for the remaining 34 patients (47 lesions) with a median follow-up of 11.1 months (2.1–22.6 months). Local disease progression was documented in 4 of the 47 treated lesions, giving a crude local control figure of 91%. In three of these cases, local progression occurred inside the treated field, after treatment doses of 15 Gy in three fractions, 21 Gy in three fractions, and 16 Gy in one fraction. In the fourth case (paravertebral chordoma), progression occurred adjacent to the treated area, and the patient underwent further spinal radiosurgery to the recurrence. Of the 34 patients, 12 died (65% crude overall survival figure). Ten of these patients had been treated for metastases, and all died of their systemic

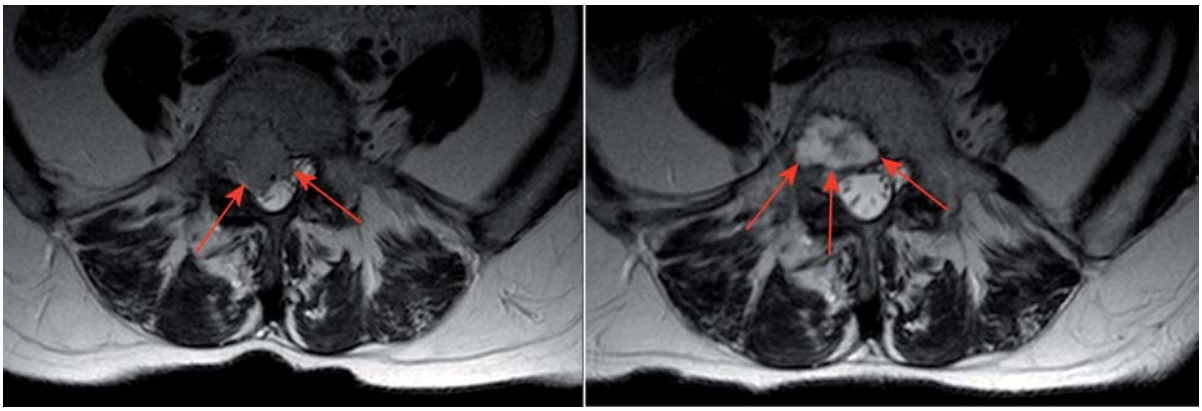

Fig 2. Axial T2-weighted MRI demonstrating the metastatic neuroendocrine tumour in the vertebral body of L5. Left panel shows the tumour appearance at baseline; right panel shows the appearance 9 months after radiosurgery. Note the tumour regression from the spinal canal, and the associated signal change.

Table III. Details of acute toxicity experienced in the first month following spinal radiosurgery.

Symptom	Grade 1 toxicity	Grade 2 toxicity	Grade 3 toxicity	Grade >3 toxicity
Abdominal pain	0	1	0	0
Back pain	2	1	1	0
Diarrhoea	0	1	0	0
Dyspepsia	1	0	0	0
Fatigue	2	5	0	0
Limb weakness	0	1	0	0
Nausea	4	2	0	0
Nerve root pain	2	2	2	0

All toxicity is graded according to NCI Common Terminology Criteria for Adverse Events v3.0 (2003).

disease. Two patients had primary spinal tumours: one died of a progressive cerebellar haemangioblastoma; the other died as a consequence of local progression of her treated spinal meningioma.

Pain relief and late toxicity

Pain information was received on 20 symptomatic metastases treated. At 3 months post treatment, pain was recorded by the referring consultant as 'better' in 13 metastases (65%) and unchanged in the remaining 7 lesions. At 6 months, pain was recorded as 'better' in an additional 3 metastases, although in 1 of the previous 13 cases, pain had returned to baseline levels. Thus, in 15 of the metastases (75%), pain was improved at 6 months post treatment. One patient developed a wedge fracture of the L3 vertebral body requiring stabilisation surgery. This occurred 2 months after receiving a single fraction of 16 Gy. There has been no myelopathy or other late treatment-related toxicity to date.

Discussion

Radiosurgery has altered practice with regard to the definitive treatment of many intracranial lesions.[1–3] Intracranial and spinal tumours comprise a similar selection of histologies, and invasive surgery to both these sites carries the risk of neurological morbidity.[3,7] It is therefore likely that the development of highly sophisticated spinal radiosurgery will have a significant impact on the management of spinal lesions. Several series of spinal radiosurgery have been published worldwide.[8–15] Table IV summarises the wider international experience.

In this series, 59% of patients tolerated treatment with no acute side effects. Exacerbation of pre-existing nerve root pain was the most common side effect, and this responded well to oral corticosteroids. A prophylactic short course of dexamethasone is now recommended for all symptomatic patients at the time of treatment. Myelopathy is a serious potential late effect of radiotherapy. In the largest published analysis of patients treated with spinal radiosurgery, 6 out of 1075 patients (0.6%) developed radiation-induced myelopathy at 2–9 months after treatment.[16] To date, there have been no cases of myelopathy in this series, but continued follow-up is necessary as this complication can develop up to a few years after treatment.

There was one case of vertebral 'collapse' following radiosurgery in a patient with a large vertebral body metastasis, who had previously received a significant dose of radiotherapy. In a published series of 71 spinal metastases, each receiving a single fraction of 18–24 Gy, a new vertebral fracture (or progression of an existing fracture) was seen in 27 vertebral bodies (38%) with a median time to event of 25 months.[17] Multivariate analysis revealed lytic radiological appearance, vertebral level below T10, and an increasing extent of vertebral body involvement as independent risk factors. This raises the issue of whether prophylactic surgery or vertebroplasty should be considered in radiosurgery patients 'at risk' of subsequent vertebral fracture. However, while there has been some progress in predicting pathological fractures based on radiological appearance, the selection of patients most likely to benefit from prophylactic intervention remains challenging. Current practice at this centre is to fractionate radiosurgery for larger vertebral metastases in an attempt to reduce the risk of fracture or collapse. Fig. 3 is a proposed flow chart for the complementary use of conventional surgery, vertebroplasty, and radiosurgery in the management of spinal tumours.

There are limitations to the data presented here. The numbers treated are modest, and follow-up is relatively short. The pain assessment is crude, but a more formal assessment was limited by poor patient compliance with

Table IV. Selected published series of radiosurgery for spinal tumours.

References	No. of patients	Primary or metastases	Previous treatment	Prescribed dose	Local control	Overall survival
Yamada *et al.*[8,b]	93 (103 lesions)	Metastases	0% RT; 0% surgery	18–24 Gy/1 F	90% at median 15 months	Median 15 months
Ryu *et al.*[9,a]	177 (230 lesions)	Metastases	0% RT	8–18 Gy/1 F	–	3 year 35%
Chang *et al.*[10,b]	63 (74 lesions)	Metastases	56% RT; 46% surgery	27 Gy/3 F or 30 Gy/5 F	1 year 84%	1 year 69%
Gerszten *et al.*[11]	393 (500 lesions)	Metastases	69% RT	Maximum dose: 12.5–25 Gy/1 F	88% at median 21 months	–
Wowra *et al.*[12]	102 (134 lesions)	Metastases and sarcoma	32% RT	15–24 Gy/1 F	98% at 15 months	Median 1.4 years
Gagnon *et al.*[13]	200 (274 lesions)	Both	46% RT	21–37.5 Gy/3–5 F	–	Median 14.5 months (metastatic patients)
Gerszten *et al.*[14]	51 (55 lesions)	Primary intradural	8% RT; 51% surgery	16–30 Gy/1–5 F	98% at median 23 months	96% at 23 months
Dodd *et al.*[15]	73 (73 lesions)	Primary intradural	8% RT; 26% surgery	12–20 Gy/1 F	100% at median 37 months	–

Authors used CyberKnife except: [a]Novalis system (BrainLAB, Germany); [b]conventional gantry-based linear accelerator with external body frame/cradle and in-room CT image guidance.
Abbreviations: RT = radiotherapy; Gy = gray; F = fraction(s).

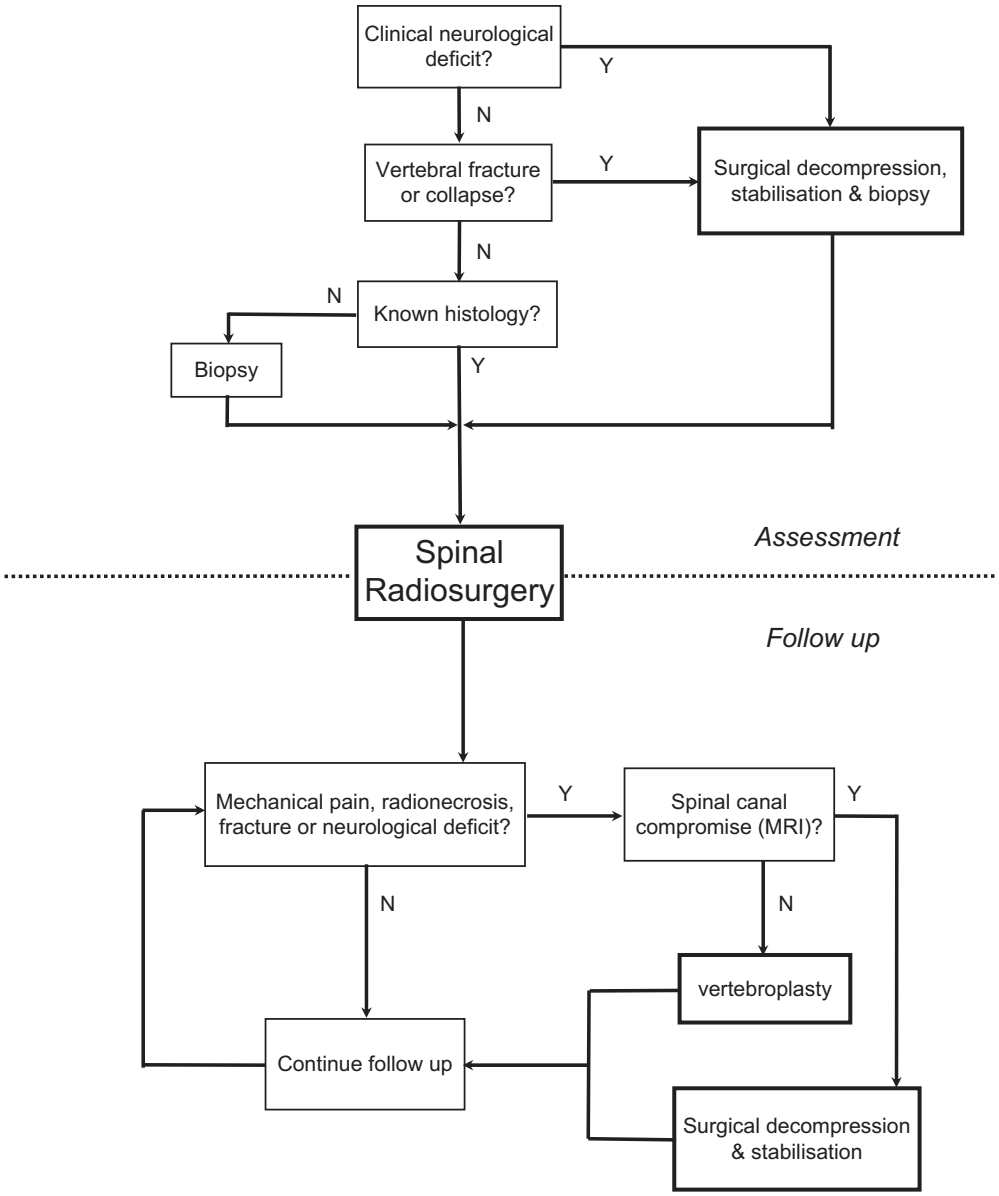

Fig 3. Proposed flow chart showing the complementary indications for conventional surgery, vertebroplasty, and radiosurgery in the management of spinal tumours. Y = Yes; N = No.

postal questionnaires. Finally, the heterogeneity of the lesions treated and doses used means that it is hard to make firm conclusions based on the local control and overall survival figures observed. Nevertheless, the data show that spinal radiosurgery is feasible and well tolerated, and the local control rate is in line with previous published series. While this treatment is now established in many countries, it is only recently available in the UK. High-quality prospective data are needed to confirm efficacy and establish spinal radiosurgery as a treatment option within the National Health Service. For unresectable primary spinal tumours, published series show excellent local control, but further data establishing long-term freedom from toxicity would still be welcome. For metastases in the context of oligometastatic disease, prospective trials with longer follow-up are needed to clarify whether the excellent local control rates translate to improved overall survival. Finally, for symptomatic metastases, there are no randomised data confirming superior rates and duration of pain relief over conventional palliative radiotherapy techniques. Systems capable of delivering spinal radiosurgery are now available in the NHS, and it is hoped that prospective trials in this area will follow shortly.

Conclusion

Modern radiotherapy technology allows treatment of extracranial lesions with 'stereotactic' accuracy, and worldwide published results of spinal radiosurgery have shown excellent local tumour control with few side effects. Early UK experience has confirmed that spinal radiosurgery is well tolerated, with local control rates similar to previous published data. Longer-term prospective data are required to confirm efficacy and toxicity profiles, and to help identify those patients most likely to benefit from this technique.

Declaration of interest

Dr. Martin and Dr. Plowman have received honoraria from Accuray Inc. for educational presentations related to the use of CyberKnife.

References

1. Pollock B, Stafford S, Link M. Gamma knife radiosurgery for skull base meningiomas. Neurosurg Clin N Am 2000;11(4):659–66.
2. Ogilvy C, Stieg P, Awad I, Brown Jr R, Kondziolka D, Rosenwasser R, Young WL, Hademenos G. AHA Scientific Statement: Recommendations for the management of intracranial arteriovenous malformations: a statement for healthcare professionals from a special writing group of the Stroke Council. American Stroke Association. Stroke 2001;32(6):1458–71.
3. Pollock B, Driscoll C, Foote R, Link M, Gorman D, Bauch C, Christopher D, et al. Patient outcomes after vestibular schwannoma management: a prospective comparison of microsurgical resection and stereotactic radiosurgery. Neurosurgery 2006;59(1):77–85.
4. Adler Jr J, Chang S, Murphy M, Doty J, Geis P, Hancock S. The Cyberknife: a frameless robotic system for radiosurgery. Stereotact Funct Neurosurg 1997;69(1–4 Pt 2):124–28.
5. Muacevic A, Staehler M, Drexler C, Wowra B, Reiser M, Tonn J. Technical description, phantom accuracy, and clinical feasibility for fiducial-free frameless real-time image-guided spinal radiosurgery. J Neurosurg: Spine 2006;5(4):303–12.
6. Ho A, Fu D, Cotrutz C, Hancock S, Chang S, Gibbs I, Maurer CR, Adler Jr. A study of the accuracy of Cyberknife spinal radiosurgery using skeletal structure tracking. Neurosurgery 2007;60(2):147–56.
7. Patil C, Lad S, Patil T, Santarelli J, Boakye M. National inpatient complications and outcomes after surgery for spinal metastasis from 1993 to 2002. Neurosurgery 2007;61(1):201–2.
8. Yamada Y, Bilsky M, Lovelock D, Venkatraman E, Toner S, Johnson J, Zatcky J, et al. High-dose, single-fraction image-guided intensity-modulated radiotherapy for metastatic spinal lesions. Int J Radiat Oncol Biol Phys 2008;71(2):484–90.
9. Ryu S, Jin J, Jin R, Rock J, Ajlouni M, Movsas B, Rosenblum M, et al. Partial volume tolerance of the spinal cord and complications of single-dose radiosurgery. Cancer 2007;109(3):628–36.
10. Chang E, Shiu A, Mendel E, Mathews L, Mahajan A, Allen P, Weinberg JS, et al. Phase I/II study of stereotactic body radiotherapy for spinal metastasis and its pattern of failure. J Neurosurg: Spine 2007;7(2):151–60.
11. Gerszten P, Burton S, Ozhasoglu C, Welch W. Radiosurgery for spinal metastases: clinical experience in 500 cases from a single institution. Spine 2007;32(2):193–9.
12. Wowra B, Zausinger S, Drexler C, Kufeld M, Muacevic A, Staehler M, Tonn JC. CyberKnife radiosurgery for malignant spinal tumors: characterization of well-suited patients. Spine 2008;33(26):2929–34.
13. Gagnon G, Nasr N, Liao J, Molzahn I, Marsh D, McRae D, Henderson FC. Treatment of spinal tumors using cyberknife fractionated stereotactic radiosurgery: pain and quality-of-life assessment after treatment in 200 patients. Neurosurgery 2009; 64(2):297–307.
14. Gerszten P, Burton S, Ozhasoglu C, McCue K, Quinn A. Radiosurgery for benign intradural spinal tumors. Neurosurgery 2008;62(4):887–96.
15. Dodd R, Ryu M, Kamnerdsupaphon P, Gibbs I, Chang Jr S, Adler Jr J. CyberKnife radiosurgery for benign intradural extramedullary spinal tumors. Neurosurgery 2006;58(4):674–85.
16. Gibbs I, Patil C, Gerszten P, Adler Jr J, Burton S. Delayed radiation-induced myelopathy after spinal radiosurgery. Neurosurgery 2009;64(2):A67–72.
17. Rose P, Laufer I, Boland P, Hanover A, Bilsky M, Yamada J, Lis E. Risk of fracture after single fraction image-guided intensity-modulated radiation therapy to spinal metastases. J Clin Oncol 2009;27(30):5075–9.